Universität der Bundeswehr München
Fakultät für Bauingenieur- und Vermessungswesen

Time dissemination and synchronization methods to support Galileo timing interfaces

Alexandre N. Moudrak

Dissertation zur Erlangung des akademischen Grades Doktor-Ingenieur

Vorsitzender des Promotionsausschusses: Univ.-Prof. Dr.-Ing. W. Reinhardt

1. Berichterstatter: Univ.-Prof. Dr.-Ing. B. Eissfeller
2. Berichterstatter: Univ.-Prof. Dr.-Ing. G. W. Hein
3. Berichterstatter: Univ.-Prof. Dr.-Ing. habil. A. Schroth (DLR)

Tag der Prüfung: 29. . Februar . 2008

Neubiberg, den ____ . _____ 200__

“Time is what a clock measures.”

A. Einstein

Abstract

Precise timing has become an important factor in the modern information-oriented society and culture. Timing is one of the key technologies for such basic and everyday things, like cellular communications, Internet, satellite navigation and many others. Satellite navigation systems offer cost-efficient and high-performance timing services, and GPS is presently the unchallenged market leader. However, GPS is under military control and does not offer availability and performance guarantees. From a user perspective, this situation will change with the advent of the European satellite navigation system Galileo which shall be operated on a commercial basis by civil entities and shall accept certain liabilities for its services providing also guaranteed service performances.

This work is motivated by the new opportunities and challenges related to Galileo timekeeping and applications, and in particular by the necessity to

- produce and maintain a stable, accurate and robust system timescale which can serve for both accurate prediction of satellite clocks and for the metrological purposes,
- establish accurate and reliable timing interface to GPS to facilitate Galileo interoperability,
- maximize user benefits from the new system features like service guarantees and support application development by enabling their certification.

The thesis starts with overview of atomic clocks, timekeeping and timing applications. Further Galileo project and system architecture are described and details on Galileo timekeeping concept are given. In addition, the state-of-the-art timekeeping and time dissemination methods and algorithms are presented.

Main findings of the thesis focus on

- Galileo timekeeping. Various options for generation of Galileo system time are proposed and compared with respect to the key performance parameters (stability and reliability). Galileo System Time (GST) stability requirements driven by its navigation and metrological functions are derived. In addition, achievable level of GST stability (considering hardware components) is analyzed. Further, optimization of the present baseline with respect to the design of Galileo Precise Timing Facility (PTF), and its redundancy and switching concepts is undertaken. Finally, performance analysis of different options for generation of the ensemble time is performed and considerations with respect to the role of the ensemble time in Galileo are provided,
- GPS Galileo timing interface. The magnitude and statistical properties of the time offset are investigated and the impact of the time offset onto the user positioning and timing accuracy is studied with the help of simulated GPS and Galileo observations. Here a novel simulation concept which is based on utilization of GPS data and their scaling for Galileo is proposed. Both GPS and Galileo baseline foresees that the GPS/Galileo time offset shall be determined and broadcast to users in the navigation messages. For this purposes, the offset shall be predicted using available measurement data. Simulations of GPS Galileo time offset determination and prediction are presented. The prediction is made relying on both traditional method and on the advanced techniques like Box-Jenkins prediction (based on the autoregressive moving average approach) and Kalman filter. The end-to-end budgets for different options of GPS Galileo time offset determination are also presented.
- Galileo interface to timing users (Galileo timing service). The relevance of GST restitution from the metrological point of view is discussed and recognition of GST as a legal time reference is proposed. Assessment of the accuracy of the Galileo timing service is presented.

Finally, recommendations for Galileo are provided based on the findings of the thesis.

Table of content

1 INTRODUCTION 18

1.1 Motivation 18

1.2 Objectives 18
1.2.1 Galileo timekeeping 18
1.2.2 Timing aspects of GPS/Galileo interoperability 19
1.2.3 Galileo interface to timing users 19

1.3 Structure of the thesis 19

1.4 Summary of results 20

2 TIME AND TIMING APPLICATIONS 22

2.1 What time is it? 22

2.2 Clocks and timescales 23
2.2.1 Clocks 23
2.2.2 Time scales and time metrology 26
2.2.3 Legal traceability of time and time transfer 28
2.2.4 Broadcasting UTC 29
2.2.5 GPS as a UTC broadcasting service 29

2.3 Applications and requirements 30

3 TIMING ASPECTS IN GALILEO 33

3.1 Galileo overview 33
3.1.1 Galileo program 33
3.1.2 Galileo and other satellite navigation systems 34
3.1.3 Galileo architecture 36
3.1.4 Navigation signals and services 40

3.2 Galileo System Time (GST) 41
3.2.1 Role of GST in Galileo operations 41
3.2.2 GST performance specification 42
3.2.3 Generation of GST 43
3.2.4 GST and GPS Time 45
3.2.5 Clocks in Galileo 46
3.2.6 Satellite clock prediction 46

3.3 Galileo time interfaces 47
3.3.1 User time interface 47
3.3.2 UTC 47
3.3.3 Relevance of UTC interface 47
3.3.4 Status of Galileo Time Service Provider activities 48
3.3.5 GTSP philosophy 48
3.3.6 Interface to GPS Time 48
3.3.7 Other time interfaces 49

4 REVIEW OF STATE-OF-THE-ART METHODS AND ALGORITHMS 50

4.1 Basics of system time generation 50
4.1.1 Weighted average algorithm for computation of ensemble time 50
4.1.2 GPS composite clock 51

4.2 Basic time restitution techniques 56
4.2.1 Overview of time restitution techniques 56
4.2.2 Satellite observations 57
4.2.3 Snap-shot position and time solution 58
4.2.4 Snap-shot position-time solution and DOP concept 61
4.2.5 Snap-shot time solution 61
4.2.6 Filtering/smoothing techniques 62

4.3 Safety and reliability in PTF design 65
4.3.1 Basic system safety concepts 65
4.3.2 Reliability calculation 66

5 OPTIONS FOR GALILEO SYSTEM TIME GENERATION 68

5.1 Considerations on Galileo time generation concept 68
5.1.1 Requirements to Galileo system time 68

5.2 Optimization of PTF design 74
5.2.1 GST failure analyses 74
5.2.2 Handling of redundancies and spares 83

5.3 Tuning the ensemble time stability 87
5.3.1 GSTR role and requirements 87
5.3.2 Analysis of the ensemble time stability 88
5.3.3 Analysis of simulation results 90

6 TIMING ASPECTS OF GPS GALILEO INTEROPERABILITY 94

6.1 General consideration 94
6.1.1 Galileo interoperability in GNSS context 94
6.1.2 Why determining GPS Galileo time offset 94
6.1.3 Structure of the section 95
6.1.4 Options for GPS Galileo time interface 95
6.1.5 Selection criteria 96

6.2 GGTO magnitude and properties 97
6.2.1 GGTO magnitude 97
6.2.2 Relative frequency instability of GGTO 97
6.2.3 Simulation of GGTO 97
6.2.4 Uncertainty of the broadcast GGTO correction 99

6.3 GGTO impact onto the user positioning accuracy 99
6.3.1 GGTO treatment scenarios 99
6.3.2 Position-time solution for users of combined navigation equipment 99
6.3.3 Studying the GGTO impact on the accuracy of standard position-time solution 102

6.4 GGTO determination at system level 104
6.4.1 GGTO determination at system level: functional overview 104
6.4.2 Impact of error in broadcast satellite orbits and clock parameters on the accuracy of GPS Time restitution 105
6.4.3 Options to measure GGTO 107
6.4.4 Galileo baseline on GGTO measurement 112
6.4.5 Error budget of GGTO measurement techniques 113

6.5 Prediction of GGTO 114
6.5.1 The purpose 114
6.5.2 GPS experience 114
6.5.3 Requirements to the GGTO prediction algorithm 115
6.5.4 Options for GGTO prediction 115

6.6 Tests of GGTO measurement 117

6.6.1 Test of GGTO measurement via link with USNO 117
6.6.2 Test of GGTO determination from reception of GPS SIS 117

6.7 Tests of GGTO prediction 117
6.7.1 Overview of test data 117
6.7.2 Test results 119

7 INTERFACE TO GALILEO USERS: TIME RESTITUTION 128

7.1 Assessing implicit specification of the accuracy of restitution of Galileo time 128
7.1.1 Relevance of GST restitution 128
7.1.2 Transformation of performance specifications 128
7.1.3 DOP simulations 129

7.2 Average accuracy of Galileo time restitution 131

8 CONCLUSIONS 134

8.1 Summary of results and conclusions 134
8.1.1 Overview 134
8.1.2 Galileo timekeeping 134
8.1.3 Timing interface to GPS (GPS Galileo Time Offset) 135
8.1.4 Timing user interface (GST dissemination) 136

8.2 Recommendations for Galileo 134

LIST OF ACRONYMS 139

NOTATION 142

REFERENCES 145

ANNEX A. ACCURACY OF COMBINED GPS/GALILEO SOLUTION 150

A .1 Worst-case HDOP and VDOP for 10° cut-off 150

A .2 Worst-case HPE for 10° cut-off 151

A .3 Worst-case VPE for 10° cut-off 152

ANNEX B. GGTO MODELING STATISTICS 154

B .1 Box-Jenkins model identification 154

B .2 Time series plots, ACF and PACF 156
B.2.1 Simulated GGTO (with steering) 156
B.2.2 Simulated GGTO (no steering) 157
B.2.3 UTC(USNO) – GPS Time 158
B.2.4 UTC(PTB) – GPS Time 159

B .3 ARIMA models for GGTO 160
B.2.1 Simulated GGTO (with steering) 160
B.2.2 Simulated GGTO (no steering) 162
B.2.3 UTC(USNO) – GPS Time 163
B.2.4 UTC(PTB) – GPS Time 164

ANNEX C. CHARACTERIZATION OF CLOCK STABILITY 168

C .1 Clock models: deterministic effects and noises 168

C .2 Time domain statistics 169
C.2.1 Allan variance 169
C.2.2 Modified Allan variance (MVAR) 169
C.2.3 Time Variance (TVAR) 169
C.2.4 Systematic effects and Allan Variance 170

C .3 Frequency domain statistics 170

ANNEX D. ATOMIC CLOCKS: AN OVERVIEW 172

D .1 Rubidium frequency standards 172

D .2 Cesium clocks 173
D.2.1 Commercial Cesium clocks 173
D.2.2 Cesium fountain 174

D .3 Hydrogen masers 174
D.3.1 Active hydrogen masers 174
D.3.2 Passive hydrogen masers 175

D .4 Galileo satellite clocks 176
D.4.1 RAFS 176
D.4.2 Passive H-maser 177

ANNEX E. NOMINAL CONSTELLATIONS 179

E .1 Galileo 179

E .2 GPS 180

ANNEX F. ENSEMBLE TIME STABILITY 181

F .1 Weighted average algorithm, satellite clocks with drift 181

F .2 Weighted average algorithm, satellite clocks without drift 182

List of figures

Figure 2-1. The first mechanical clock (Strasbourg) (left), sun clock (right, top) modern Cesium clock (right, bottom) 24
Figure 2-2. A typical clock system 25
Figure 2-3. Clock stability: historical perspective (from [HP97]) 26
Figure 2-4. Generation of TAI and UTC 27
Figure 2-5. Traceability pyramid 28
Figure 2-6. Distribution of precise time from NMI to users 28
Figure 2-7. Time scale relationships in a satellite navigation system 30
Figure 2-8. User requirements to precise timing 32
Figure 3-1. Galileo program schedule (personal best guess, September 06) 34
Figure 3-2. GPS modernization schedule (from [Cliatt03]) 36
Figure 3-3. Galileo architecture (courtesy of ESA) 37
Figure 3-4. GCS architecture (courtesy of ESA) 38
Figure 3-5. GMS architecture (courtesy of ESA) 39
Figure 3-6. GST generation overview 44
Figure 3-7. Functional scheme of GST generation 45
Figure 3-8. Interplay of PTF, GSS and OSPF 45
Figure 3-9. Test of GPS IIR RAFS prediction [Merino03] 47
Figure 4-1. GPS Composite Clock Kalman filter [Stansfield01] 55
Figure 4-2. Stability of GST and GPS Time 56
Figure 4-3 Basic principle of common view 62
Figure 4-4. Revised common view pre-processing 63
Figure 4-5. System with all elements connected in series 67
Figure 4-6. System with all elements connected in series 67
Figure 5-1. Prediction with linear (left) and quadratic (right) models (whole interval) 71
Figure 5-2. Prediction with linear (left) and quadratic (right) models (end of interval) 71
Figure 5-3. GST generation chain 72
Figure 5-4. PTF high-level architecture 74
Figure 5-5. GST generation chain: overview 75
Figure 5-6. GST generation chain: physical level 75
Figure 5-7. Propagation of AHM failures to GST 77
Figure 5-8. GST reliability logic block diagram (Configuration A) 81
Figure 5-9. GST reliability logic block diagram (Configuration B) 81
Figure 5-10. GST reliability logic block diagram (Configuration C) 82
Figure 5-11. GST reliability logic block diagram (Configuration D) 82
Figure 5-12. Baseline on switching and steering: concept 84

Figure 5-13. Change of steering links after switching between AHMs at Master PTF (left – nominal configuration; right – configuration after MC failure, changed steering links are shown in red) 84
Figure 5-14. Change of steering links after switching between PTFs (left – nominal configuration; right – configuration after switching) 85
Figure 5-15. Alternative concept of switching and steering 86
Figure 5-16. Modular architecture for the alternative switching concept 87
Figure 5-17. ADEV of Galileo clocks 89
Figure 5-18. Ensemble time ADEV at 100 min 91
Figure 5-19. Ensemble time ADEV at 8 hours 91
Figure 5-20. Ensemble time ADEV at 24 hours 91
Figure 5-21. Ensemble time ADEV at 10 days 92
Figure 6-1. Timescales relations for users of combined navigation equipment 95
Figure 6-2. Simulated GPS Time, GST and GGTO (left: non-steered, right: steered) 98
Figure 6-3. ADEV of GPS Time, GST and GGTO (left: non-steered, right: steered) 98
Figure 6-4. Galileo task to support determination of GGTO on system level 104
Figure 6-5. RMS error for zero age (left) and trend in RMS error (right) of satellite clock parameters 106
Figure 6-6. Histogram of average (left) and median (right) error for the ORB site 107
Figure 6-7. Noise pattern in averages (left) and in medians (right) for ORB site 107
Figure 6-8. The principle of GGTO measurement 108
Figure 6-9. Linking of GST with GPS Time 108
Figure 6-10. Major sources of GGTO determination uncertainty when using link with USNO 109
Figure 6-11. Major sources of GGTO determination uncertainty when using GPS time receiver at PTF 110
Figure 6-12. Major sources of GGTO determination uncertainty when using GPS and Galileo time receivers 110
Figure 6-13. Major sources of GGTO determination uncertainty when using a combined GPS/Galileo receiver 111
Figure 6-14. Box-Jenkins model building 116
Figure 6-15. Allan Deviation of GGTO test data 118
Figure 6-16. Daily prediction error vs. measurement interval (PTB data) 120
Figure 6-17. Daily prediction error vs. measurement interval (simulated data) (left: with steering, right: without steering) 121
Figure 6-18. Daily prediction error vs. measurement interval (simulated steered GGTO) (error computed vs. noisy data) 121
Figure 6-19. Prediction error vs. measurement interval (prediction vs. all data points, simulated data) (left: with steering, right: without steering) 122
Figure 7-1. Galileo maximal HDOP (left) and VDOP (right) 130
Figure 7-2. Galileo maximal TDOP 130
Figure 7-3. Average Galileo TDOP 132

Figure 7-4. Projected Galileo UERE 132
Figure 7-5. Average Galileo timing error 133
Figure A-1. Combined GPS+Galileo HDOP (left) and Galileo-only HDOP (right) 150
Figure A-2. Combined GPS+Galileo VDOP (left) and Galileo-only VDOP (right) 150
Figure A-3. GPS HDOP (left) and VDOP (right) 150
Figure A-4. GPS HPE (95%) (left) and Galileo HPE (95%) 151
Figure A-5. HPE (95%) of combined solution with GGTO (1σ) of 0 ns (left) and 2.5 ns (right) 151
Figure A-6. HPE (95%) of combined solution with GGTO (1σ) of 28 ns (left) and with 5-parameter navigation solution (right) 151
Figure A-7. HPE (95%) of combined solution with GGTO (1σ) of 28 ns (left) and with 5-parameter navigation solution (right) (both with the cut-off of 30°) (note change of the color scheme) 152
Figure A-8. GPS VPE (95%) (left) and Galileo VPE (95%) 152
Figure A-9. VPE (95%) of combined solution with GGTO (1σ) of 0 ns (left) and 2.5 ns (right) 152
Figure A-10. VPE (95%) of combined solution with GGTO (1σ) of 28 ns (left) and with 5-parameter navigation solution (right) 153
Figure A-11. VPE (95%) of combined solution with GGTO (1σ) of 28 ns (left) and with 5-parameter navigation solution (right) (both with the cut-off of 30°) (note change of the color scheme) 153
Figure B-1. Autocorrelation (top) and partial autocorrelation (down) functions of an autoregressive process of the second order 154
Figure B-2. Autocorrelation (top) and partial autocorrelation (down) functions of a moving average of process of the second order 155
Figure B-3. Steered GGTO and its first differences 156
Figure B-4. ACF and PACF for steered GGTO 156
Figure B-5. ACF and PACF for first differences of steered GGTO 156
Figure B-6. ACF and PACF for steered GGTO with added WGN (RMS 2 ns) 157
Figure B-7. ACF and PACF for first differences of steered GGTO with added WGN (RMS 2 ns) 157
Figure B-8. Non-steered GGTO and its first differences 157
Figure B-9. ACF for first and second differences of non-steered GGTO 158
Figure B-10. PACF for first and second differences of non-steered GGTO 158
Figure B-11. UTC(USNO) offset from GPS Time (left) and its first differences (right) 158
Figure B-12. ACF (left) and PACF (right) of the USNO data 159
Figure B-13. ACF (left) and PACF (right) of the USNO data 159
Figure B-14. UTC(PTB) offset from GPS Time (left) and its first differences (right) 159
Figure B-15. ACF (left) and PACF (right) of the PTB data 160
Figure B-16. ACF (left) and PACF (right) of first differences of the PTB data 160
Figure B-17. Histogram of residuals for ARIMA(1,1,1) (left) and ARIMA(1,1,4) (right) 161
Figure B-18. ACF (left) and PACF (right) of residuals for ARIMA(1,1,1) 161

Figure B-19. ACF (left) and PACF (right) of residuals for ARIMA(1,1,4) 161
Figure B-20. Histogram of residuals for ARIMA(1,1,0) (left) and ARIMA(2,1,2) (right)..... 162
Figure B-21. ACF (left) and PACF (right) of residuals for ARIMA(1,1,0) 162
Figure B-22. ACF (left) and PACF (right) of residuals for ARIMA(2,1,2) 163
Figure B-23. ACF (left) and PACF (right) of residuals for ARIMA(2,0,1) 163
Figure B-24. ACF (left) and PACF (right) of residuals for ARIMA(2,1,2) 164
Figure B-25. Histogram of residuals for ARIMA(2,0,1) (left) and ARIMA(2,1,2) (right)..... 164
Figure B-26. ACF (left) and PACF (right) of residuals for ARIMA(2,0,0) 165
Figure B-27. ACF (left) and PACF (right) of residuals for ARIMA(1,1,1) 165
Figure B-28. Histogram of residuals for ARIMA(2,0,0) (left) and ARIMA(1,1,1) (right)..... 166
Figure B-29. ACF (left) and PACF (right) of residuals for ARIMA(2,1,2) 166
Figure B-30. ACF (left) and PACF (right) of residuals for ARIMA(2,0,1) 166
Figure B-31. Histogram of residuals for ARIMA(2,0,1) (left) and ARIMA(2,1,2) (right)..... 167
Figure D-1. Commercial Rubidium standard (courtesy NIST) 172
Figure D-2. Commercial Cesium clock (courtesy NIST) 173
Figure D-3. Cesium fountain (courtesy NIST)..... 174
Figure D-4. Active H-maser (courtesy NIST) 175
Figure D-5. Passive H-maser 176
Figure D-6. Frequency stability of RAFS for Galileo [Droz03] 177
Figure D-7. Frequency stability of passive H-maser for Galileo [Mattoni02]..... 178
Figure F-1. Ensemble time stability at 100 min (left – optimization time 2 hours, right – 10 days)..... 181
Figure F-2. Ensemble time stability at 8 hours (left – optimization time 2 hours, right – 10 days)..... 181
Figure F-3. Ensemble time stability at 24 hours (left – optimization time 2 hours, right – 10 days)..... 182
Figure F-4. Ensemble time stability at 10 days (left – optimization time 2 hours, right – 10 days)..... 182
Figure F-5. Ensemble time stability at 100 min (left – optimization time 2 hours, right – 10 days)..... 183
Figure F-6. Ensemble time stability at 8 hours (left – optimization time 2 hours, right – 10 days)..... 183
Figure F-7. Ensemble time stability at 24 hours (left – optimization time 2 hours, right – 10 days)..... 183
Figure F-8. Ensemble time stability at 10 days (left – optimization time 2 hours, right – 10 days)..... 184

List of tables

Table 2-1. Applications of timing 31
Table 2-2 Summary of timing requirements 31
Table 2-3 Groups of timing applications 32
Table 3-1. Satellite navigation systems at one glance 35
Table 3-2. Mapping of Galileo services to frequencies 40
Table 3-3. Performance of Galileo navigation services 41
Table 3-4. GST frequency instability (short-term) 42
Table 3-5. GST w.r.t. TAI: baseline requirements 43
Table 3-6. GST and GPS Time 46
Table 4-1. Classification of hazard severity 66
Table 4-2. Classification of hazard likelihood 66
Table 5-1. Maximal GST instability to ensure clock prediction accuracy 71
Table 5-2. GST frequency instability (short-term) 71
Table 5-3. Events on PTF elements 76
Table 5-4. Events on GST 77
Table 5-5. Failure rates for candidate PTF equipment 80
Table 5-6. Failure rates for selected PTF configurations 82
Table 5-7. GST frequency instability (short-term) 88
Table 5-8. Scenarios for Galileo clock ensemble 89
Table 6-1. GPS Galileo time interface options 96
Table 6-2. GPS Galileo time interface options 97
Table 6-3. Simulation scenario to study user positioning accuracy 102
Table 6-4. Worst-case HPE and VPE for GPS, Galileo and their combination 103
Table 6-5. Average HPE and VPE for GPS, Galileo and their combination 103
Table 6-6. Bias, standard deviation and RMSE averaged over the GPS constellation 106
Table 6-7. Bias and standard deviation of averages and medians 107
Table 6-8. Error budget for GGTO measurements with a GPS time receiver at PTF 113
Table 6-9. Average error of GGTO determination with a GPS time receiver at PTF 113
Table 6-10 Minimal RMS of daily prediction error for simulated data 121
Table 6-11 GGTO variation around daily mean 122
Table 6-12. Minimal RMS of prediction error (all data points) for simulated data 122
Table 6-13 Selection of ARIMA models for selected test data 123
Table 6-14 GGTO prediction accuracy for selected test data 125
Table 6-15. GGTO determination budget (link with USNO) 125
Table 6-16. GGTO determination budget (GPS time receiver at PTF) 126
Table 6-17. GGTO determination budget (GPS and Galileo time receivers at PTF) 126
Table 6-18. GGTO determination budget (combined GPS/Galileo receiver) 126

Table 7-1. Galileo worst-case DOPs 130
Table B-1 Modeling error for ARIMA(N,1,M) models of steered GGTO 160
Table B-2 Modeling error for ARIMA(N,1,M) models of first differences of non-steered GGTO 162
Table B-3 Modeling error for ARIMA(N,0,M) models of USNO data 163
Table B-4 Modeling error for ARIMA(N,1,M) models of USNO data 163
Table B-5 Modeling error for ARIMA(N,0,M) models with PTB data 164
Table B-6 Modeling error for ARIMA(N,1,M) models with PTB data 165
Table C-1 Relationship between spectral density and Allan Variance 171
Table D-1 Performance of a high-quality commercial Rubidium standard 172
Table D-2 Performance of commercial Cesium standards 173
Table D-3 Performance of active H-masers 175
Table D-4 Performance of passive H-masers 176
Table D-5. Galileo RAFS specification [TEMEX03] 177
Table D-6. Galileo passive H-maser specification [Mattoni02] 178
Table D-7. Galileo SPHM test results [Dimarq04] 178
Table E-1 Nominal constellation of Galileo 179
Table E-2 Nominal constellation of GPS 180

Acknowledgements

First of all, I would like to thank my supervisors, Prof. Dr. Arno Schroth (DLR) and Prof. Dr. Bernd Eissfeller (University of German Armed Forces) for their valuable contributions and guidance on this research.

I would like to express my sincere gratitude to Prof. Dr. Arno Schroth, Dr. Johann Furthner and Jens Hammesfahr (DLR) for encouraging me to prepare this thesis and supporting my work over more than five years.

I also appreciate the generous help Dr. Andriy Konovaltsev (DLR) who provided honest and thorough feedback on my research

My sincere appreciation goes to Dr. Andreas Bauch for the lessons in the science of precise timing which he generously gave me and hours of discussions on PTF design and determination of GPS Galileo time offset.

I would like to thank Dr. Demetrios Matsakis (U.S. Naval Observatory), Dr. Carine Bruyninx and Dr. Pascale Defraigne (Royal Observatory of Belgium) for providing data for testing determination of GPS Galileo time offset and valuable discussions on this subject.

A special debt of gratitude is owed to Christophe Bourga and other colleagues at THALES Alenia Space who assisted with their broad expertise in understanding of Galileo timing aspects.

Finally, none of this work would have been possible without the love, patience, support and faith of my grandmother Claudia and my mother Ludmila.

1 Introduction

1.1 Motivation

Precise timing has become an important factor in the modern information-oriented society and culture. Timing is one of the key technologies for such basic and everyday things, like cellular communications, Internet, satellite navigation and many others. Satellite navigation systems offer cost-efficient and high-performance timing services. The US-owned and operated Global Positioning System (GPS) is presently the unchallenged market leader. However, GPS is under military control and does not offer availability and performance guarantees. From a user perspective, this situation will change with the advent of the European satellite navigation system Galileo which shall be operated on a commercial basis by civil entities and shall accept certain liabilities for its services providing also guaranteed service performances.

This work is motivated by the new opportunities and challenges related to Galileo timekeeping and applications, and in particular by the necessity to

- produce and maintain a stable, accurate and robust system timescale which can serve for both accurate prediction of satellite clocks and for the metrological purposes,
- establish accurate and reliable timing interface to GPS to facilitate Galileo interoperability,
- maximize user benefits from the new system features like service guarantees and support application development by enabling their certification.

1.2 Objectives

The objective of this work has been to develop and test methods, techniques and procedures to support Galileo time generation and optimize its interfaces to users, other navigation systems like GPS and the international reference time. These objectives are described in more details below.

1.2.1 Galileo timekeeping

Precise synchronization of satellite clocks is one of the key problems in satellite navigation system. The less the synchronization error, the higher the accuracy of positioning and timing services the system is able to offer to its users. In practice, satellite clocks are not physically manipulated to archive the synchronization, but measured against a reference timescale. The models of satellites clocks behavior are estimated from these measurements and broadcast to users in the navigation message. Satellite clock predictions (calculated with these models) are further utilized to correct user observations. Galileo will establish its own reference timescale, Galileo system time (GST). Obviously, the quality of the system time is crucial for the accuracy of satellite clock prediction. This work considers the two key quality characteristics: stability and reliability. The first is needed to ensure that the impact of the inherent noise in GST onto the accuracy of satellite clock prediction is negligible, and the second is important to minimize the probability of GST failures.

The main objectives of this work related to Galileo *timekeeping* are

- review the baseline on Galileo timekeeping approaches, and on design of time-related facilities to estimate the potential quality of GST,
- identify candidate options to improve stability and reliability of GST,
- make recommendations on Galileo timekeeping concepts. These recommendations will probably not affect the present Galileo. However, they could be useful in the frame of the work on Galileo enhancement which is expected to start shortly before the full deployment of Galileo.

1.2.2 Timing aspects of GPS/Galileo interoperability

Most users are expected to utilize Galileo in combination with other navigation (GPS) and augmentation (local and wide area differential) systems. To enable this possibility, Galileo has to be (at least) compatible or (preferably) interoperable with these systems. As concerns the *interoperability*, this work aims at the

- study of timing aspects of GPS/Galileo interoperability. One of the key interoperability aspects is broadcasting of GPS/Galileo time offset in navigation messages of Galileo and GPS,
- development of methods and algorithms for determination and prediction of the GPS/Galileo time offset,
- test of proposed approaches with representative data, and finally
- study of an alternative treatment of GPS/Galileo interoperability issues.

1.2.3 Galileo interface to timing users

Usually, under the user interface of a satellite navigation system one understands the signal-in-space (SIS) (the unity of RF signals and information broadcast through navigation satellites). Here the user interface is utilized in an extended meaning comprising the SIS and the way how users derive positioning and timing information from it (e.g. combination of different signals, implementation of specific algorithms etc.).

With respect to the *user interface*, the objectives of this work are to

- investigate the relevance of GST dissemination from the metrological point of view,
- analyze GST dissemination accuracy.

1.3 Structure of the thesis

The thesis contains eight chapters (including the introduction and conclusions) and six annexes.

Chapter 2 presents an introduction to measurement of time and applications which require precise timing information. Section 2.1 considers the definition of time. Section 2.2 deals with clocks, time metrology and dissemination of time. Finally, Section 2.3 provides an overview of timing applications and corresponding requirements on time dissemination. It is shown that for industrial and scientific applications, satellite navigation systems are one of the most important means for time dissemination enabling a cost-efficient access to precise time. However, the present market leader GPS, is under military control and provides limited service guarantees.

Galileo, the navigation system developed by the European Union, will reduce European dependence on GPS and offer new capabilities to end-users. Timing aspects and capabilities of Galileo are discussed in Section 3. Section 3.1 offers an overview of Galileo project, baseline of system architecture, and Galileo services. Brief information on other satellite navigation systems (GPS and GLONASS) is also given. The following two sections deal with timing aspects in Galileo operations: Section 3.2 describes the Galileo synchronization concept and introduces the Galileo time reference, and Section 3.3 reviews timing interfaces between Galileo and its users. Interfaces to other navigation systems (GPS), and the international time reference are also considered in the section. The rest part of the thesis concentrates on solutions to improve the quality of Galileo system time and its interfaces (including user algorithms) with the goal to ensure precise and reliable timing services for European users.

Chapter 4 presents the Galileo baseline and the state-of-the-art solutions for system time generation, time dissemination and interfaces to the international reference time and time scales of other navigation systems. The two approaches to generation of the system time, a

Master Clock and a Composite Clock solutions, are presented in Section 4.1. Section 4.2 is dedicated to time dissemination techniques and algorithms (Galileo interface to end-users). Section 4.3 addresses safety and reliability calculations with respect to the design of the Precise Time Facility (PTF).

In Chapter 5 various options for generation of Galileo system time are proposed and compared with respect to the key performance parameters (stability and reliability). Section 5.1 contains analysis of GST stability requirements driven by its navigation and metrological functions. In addition, achievable level of GST stability (considering PTF hardware components) is analyzed. Optimization of the present baseline with respect to the PTF design, and its redundancy and switching concepts is dealt with in Section 5.2. Section 5.3 contains performance analysis of different options for generation of the ensemble time. Considerations with respect to the role of the ensemble time in Galileo are also provided.

Chapter 6 deals with timing aspects of GPS/Galileo interoperability, and in particular with determination of GPS/Galileo time offset. Section 6.1 discusses the general interoperability issues and practical relevance of determination of the time offset between the two systems. The magnitude and statistical properties of the time offset are investigated in Section 6.2. The impact of the time offset onto the user positioning and timing accuracy is studied in the Section 6.3 with the help of simulated GPS and Galileo observations. Here a novel simulation concept which is based on utilization of GPS data and their scaling for Galileo is utilized. Determination of the time offset by GPS and Galileo Control Segment at system level is discussed in Section 6.4. Here a functional overview and some architecture solutions are proposed. Both GPS and Galileo baseline foresees that the GPS/Galileo time offset shall be broadcast to end-users in the navigation messages. For this purpose, the offset shall be predicted using available measurement data. Section 6.5 introduces candidate prediction techniques derived from the GPS operational experience and experience with prediction problems in other applications (the prediction technique often used for financial analysis which is based on the Autoregressive Integrated Moving Average (ARIMA) model). Sections 6.6 and 6.7 present test results for GPS/Galileo time offset determination and prediction respectively. These tests mainly rely on simulated data.

In Chapter 7 Galileo interface to timing users (Galileo timing service) is investigated. Section 7.1 discusses the relevance of GST restitution from the metrological point of view. This section also presents translation of Galileo requirements from positioning into the timing domain. Section 7.2 presents an assessment of the average accuracy of GST restitution.

1.4 Summary of results

The key results obtained during the work on this thesis are listed below.

With respect to GST, its performance and generation options:

- Analysis of the impact of GST instability to satellite clock prediction error and identification of GST performance requirements driven by its navigation and metrological functions,
- Analysis of achievable stability of GST hardware realization as produced at PTF,
- Analysis of PTF reliability and identification of an alternative redundancy concept which allow to maximize this parameter,
- Recommendations on the composition of the ensemble timescale and relevant performance analysis.

With respect to GPS Galileo time offset, its relevance and determination:

- Analysis of GPS Galileo time offset magnitude and behavior, and its impact to the positioning accuracy for users of combined GPS/Galileo equipment,
- Identification of accuracy requirements to GPS Galileo time offset determination,

- Recommendations of selection of GPS Galileo time offset determination techniques and prediction algorithms,
- Analysis of GPS Galileo time offset uncertainty budget.

With respect to dissemination of GST:

- Identification of relevance of GST dissemination and assessment of GST dissemination accuracy.

2 Time and timing applications

2.1 What time is it?

"The only reason for time is so that everything doesn't happen at once."

-- Albert Einstein

The question “What time is it?” is often to hear. The usual reaction is a look at a watch. An everyday thing that is not worth to think about. But what the watch shows and what is this “time”?

In the beginning of human history time had a distinct practical meaning which is still to hear in the modern language: “moment for something to happen, begin, or end, an opportune or suitable moment” (Merriam-Webster Online Dictionary). O’Connor and Robertson argue that timekeeping has been since the very beginning driven by very practical questions. When should crops be planted? When would rivers flood? When would the rains come? When should one harvest the crops? To answer them, some calculations were needed, and mathematics probably began through the study of time, particularly the need to record sequences of events. So the time was not a philosophical abstraction, but an “application-driven” science. Is that all about time? Merriam-Webster Online Dictionary (www.webster.com) gives also other definitions of time:

> (1) (a): the measured or measurable period during which an action, process, or condition exists or continues, (b): a non-spatial continuum that is measured in terms of events which succeed one another from past through present to future;
>
> (2): the point or period when something occurs;
>
> (3) (a): an appointed, fixed, or customary moment or hour for something to happen, begin, or end;
>
> (8) (a): a moment, hour, day, or year as indicated by a clock or calendar, (b): any of various systems (as sidereal or solar) of reckoning time;
>
> (9) (a): one of a series of recurring instances or repeated actions;
>
> (10): finite as contrasted with infinite duration;
>
> (11): a person's experience during a specified period or on a particular occasion.

Already this short dictionary article gives a feeling of the complex nature of time. So it seems that there are different kinds of it:

- time as a physical phenomenon,
- time as a philosophical category, and
- time as a personal experience.

According to W. Phipps, “basic to understanding time is recognizing the difference between real time and two ways of measuring it; real time is simply the sequence of events that happen anywhere to earthlings – to the astronaut as well as to ordinary humans who do first one thing and then another”.

So time, describes evolution of events. The direction of this evolution is governed by the thesis of “causality” – the cause shall always precede the effect. More formally, if an event A ("the cause") somehow influences an event B ("the effect") which occurs later in time, then event B cannot in turn have an influence on event A. That is, event B must occur at a later time t than event A, and further, all frames must agree upon this ordering. That is: the time shall be irreversible (at least so believes the modern physics). But that is true only for macrocosm, in microcosm governed by the laws of quantum mechanics the reversely going

time is theoretically possible. So the time is progressing by how? Straight forward or in circles or somehow else?

The antique world was did not agree on this question. Buddha (about 500 B.C.) and, later and much to the West, Pythagoras, thought time to progress in a circle whereas Zeno's Paradoxes undermined the very idea of time and motion. Plato considered as a way to "project" the divine eternity onto the creation, so to say "a moving image of eternity". Aristotle (350 BC) objected time to have no "independent" meaning, but being measured by motion (quite in the sense of Einstein's explanation formulated more then 2000 years later). However, Aristotle's time was moving itself, circling together with planets of the sky which defined its motion. The Hebrews were probably the first to introduce the idea of a "time-axis", ever progressing time. With the Christianity, this vision has been settled in the Western way of thinking.

The definition of time implies some dynamics, it assumes that events do happen, allowing thus to "feel" or "to measure" time. In this context one may ask what would happen with time in a "static" Universe, will it still exist or not. St. Augustine confessed: "What, then, is time? If no one asks me, I know what it is. If I wish to explain it to him who asks, I do not know." Later, he defined the time as a phenomenon experienced by human beings while "the creator of time existed before it began and will exist after it ends".

The modern time left the question about the meaning of time to theology and philosophy ("*there is something essential about the "now" which is outside the realm of science"*, A. Einstein) and deals, following Aristotle, mainly with the question how to measure time precisely. But what is measured? The practical answer is "time is what the clock shows" (A. Einstein).

In the earlier scientific thinking, time was an absolute category, being the same everywhere according to Newton's definition. Unlike it, Einstein's time is a subordinate value. It can be measured by counting some regular events, and it is stretchable: the special relativity theory describes the relationship between time and speed, and the general relativity theory describes it relationship with mass. In this context, to measure time would mean to select some regular event – either on the Earth or on the sky, in microcosm or in macrocosms – and then to keep counting its occurrences. Easy as it sounds, this concept is a basis for any time measurement system since more than 20,000 years.

2.2 Clocks and timescales

2.2.1 Clocks

Clock is "a device… for indicating or measuring time by means of… any periodic system by which time is measured" (Merriam Webster Online Dictionary). A similar definition can be found in [Francis02]: *"A clock consists of a device capable of counting the periods of a repeatable phenomenon, whose motion or change of state is observable and obeys a definite law"*. So the "periodic system" or "repeatable phenomenon" shall (a) move regularly (b) be (more or less) easily observed.

The word "regularly" has been many times redeemed in historical perspectives: the first time-keepers were the Sun and the Moon with their regular passages which defined the natural time units: days and months. The four seasons formed a longer unit: the year. Precisely speaking, the Sun is only a "clock-hand", it's the rotation of Earth that defines days and years.

The Sun and the Moon were good enough for quite a long time: still in the Roman time a pamphletist argued that such a nonsense as dividing a day into smaller portions – hours – would ruin its natural flow and bring only unhealthy hecticness. The early Middle Ages had also to come out with a sun clock. And sand or water clocks were sufficient to define some short intervals of minutes or hours – when it was necessary. In long-term, however, the sand and water clocks were a bad help. First the invention of the verge escapement in the 14th century allowed to build a good enough (for that time) clock independent of astronomical

events which also allowed to measure small time intervals in order of minutes or hours. The era of mechanical clocks began.

The clock development was further progressing: the “periodic systems” with more and more regular oscillations were developed: the pendulum clock of Huygens (1656), quartz oscillator (W.A. Marrison, 1928), first atomic frequency standard utilizing ammonia (1949), and, finally, the Cesium frequency standard (around 1960) which – with certain modifications – remains the most accurate commercial frequency source ever built (see Figure 2-1).

Atomic frequency standards are based on the principles of quantum mechanics which relates changes of energy of an atom to the frequency of absorbed or emitted electromagnetic radiation.

An atomic clock consists of an atomic frequency standard, divider and counter [Kamas90] (see Figure 2-2).

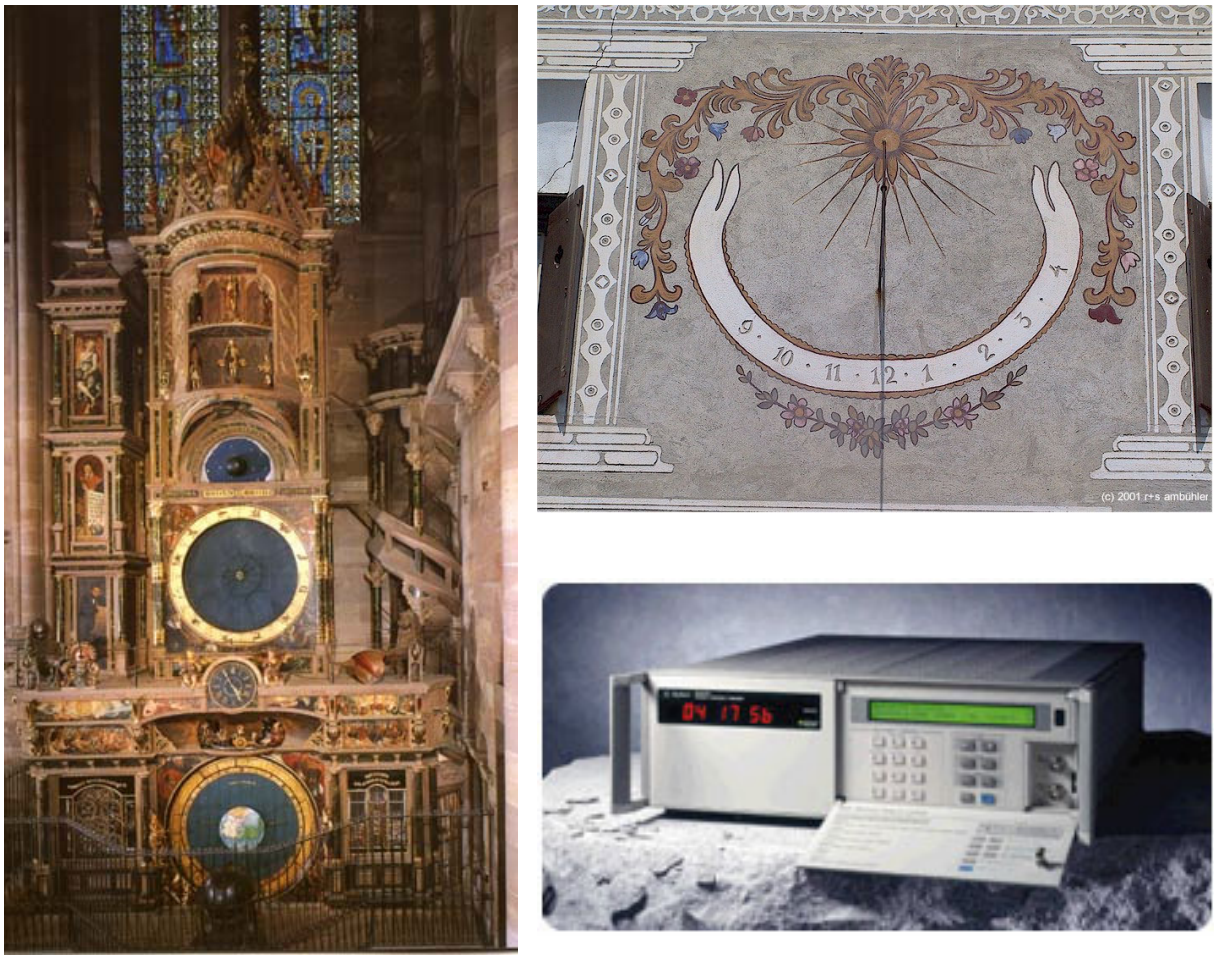

Figure 2-1. The first mechanical clock (Strasbourg) (left), sun clock (right, top) modern Cesium clock (right, bottom)

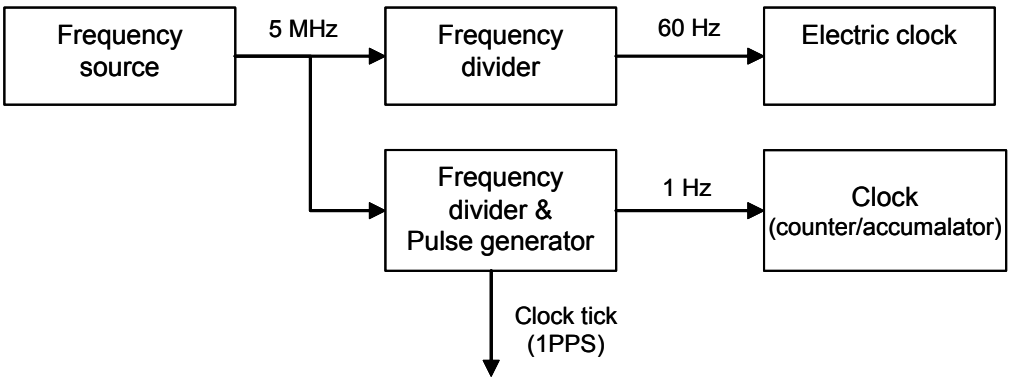

Figure 2-2. A typical clock system

More information on the principles and properties of atomic frequency standards is provided in Annex D.

At this point, a discussion on the unit of time is due. With the sun clock it was quite easy to define the time unit – it is just one day, from dusk to dusk or from dawn to dawn. So the natural period of the "period system" was the first unit of time. Oscillation period in clocks became shorter and shorter, and finally, a standard unit to measure time was defined as one second (now one of the seven base units in the International System of Units (SI)).

Until 1956, second was defined as 1/86400 of the mean solar day and was derived from astronomical observations. However, Cesium clocks appeared to be more stable than the rotation of the Earth around the Sun which defines the mean solar day, and Resolution 1, of 13th Meeting of Conférence Générale des Poids et Mesures (1967-1968), corrected in 1997 defined that *"the second is the duration of 9 192 631 770 periods of the radiation corresponding to the transition between the two hyperfine levels of the ground state of the Cesium 133 atom".* This definition refers to a Cesium atom in its ground state at a temperature of 0 K" [SI-98].

Clock quality can be characterized by two basic parameters:

- Accuracy: how closely the clock reproduces the unit of time – the second (by definition, accuracy characterizes the degree of conformity of an "is" value with a "due" value), and
- Stability (or precision): how well a clock can produce the same time offset over a given time interval. It doesn't indicate whether the time or frequency is "right" or "wrong," but only whether it stays the same (for example, a clock which runs ahead exactly one minute per day is not accurate, but stable, see Annex C for mathematical definition of stability).

With all its high performance, clock is only an instrument to measure time. Definition of time unit and keeping of time is the question of time metrology.

The historical development of clocks measuring time stability is summarized in Figure 2-3.

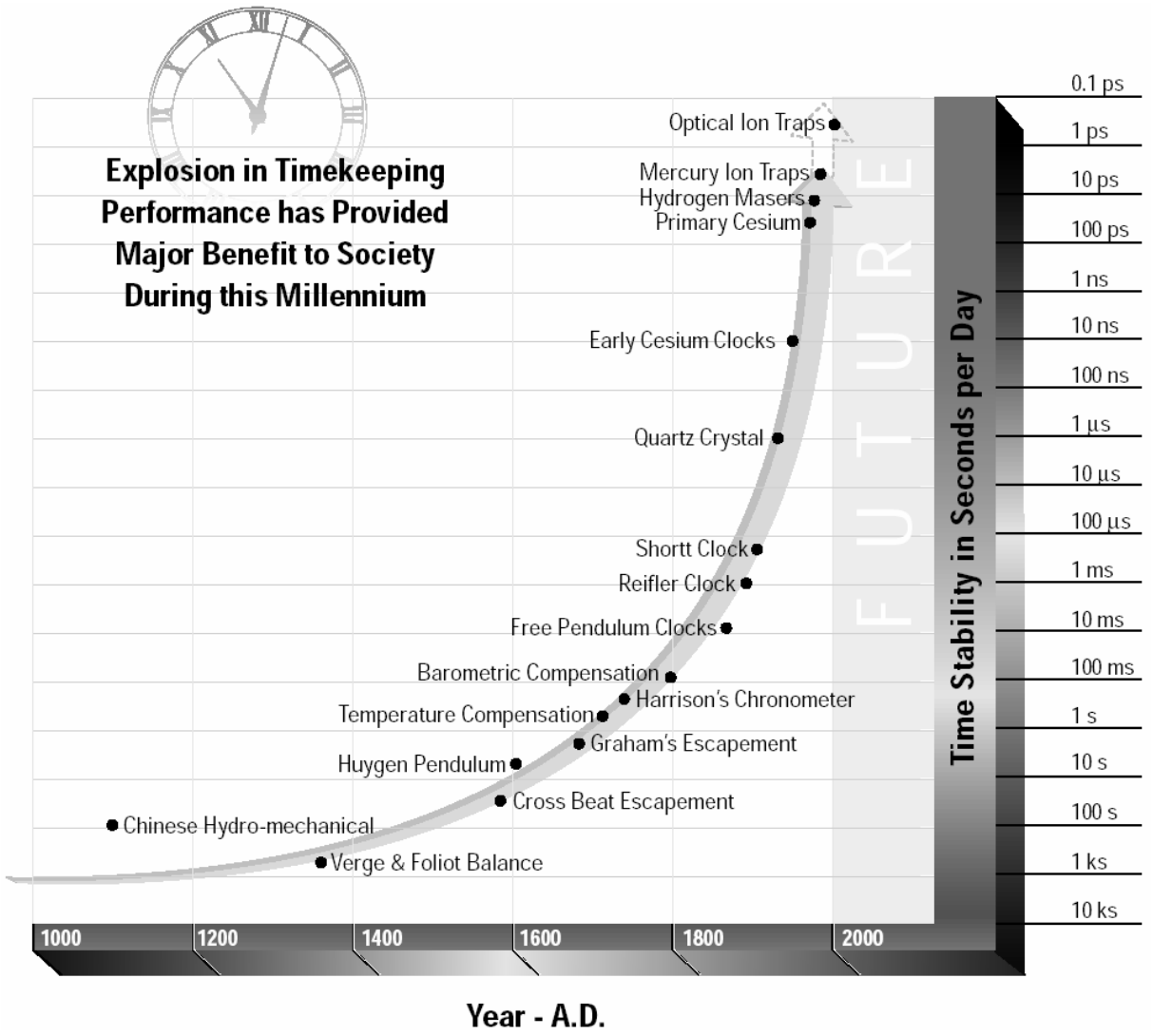

Figure 2-3. Clock stability: historical perspective (from [HP97])

2.2.2 Time scales and time metrology

According to the definition provided by the International Radio Consultative Committee (CCIR), timescale is an "ordered set of scale markers with an associated numbering". Requirements on timescales are usually formulated in terms of

- accessibility,
- stability,
- reproducibility, and
- accuracy.

The international time reference is formed by a set of timescales shortly discussed above.

Universal Time (UT1) is a time scale derived from observations of Earth rotation corrected for precession and polar variations. The time unit of this scale is the second of mean solar time defined as the fraction 1/86400 of the mean solar day. UT1 was the basis of legal time until 1972 when a timescale derived from atomic clocks acquired this function.

International Atomic Time (TAI) is derived as a weighted average of more than 200 atomic clocks operated all over the world. The unit of time in this time scale is the atomic second.

TAI was originally defined as "the time reference coordinate established by the Bureau International de l'Heure on the basis of the reading of atomic clocks operating in various establishments in accordance with the definition of the second, the unit of time of the

International System of Units" (Conference Generale des Poids et Mesures, 1971). The definition was completed in 1980 at the 9th session of the Committee Consultatif pour la Definition de la Seconde: "TAI is a coordinated time scale defined in a geocentric reference frame with the SI second as realized on the rotating geoid as the scale unit". This correction to the original definition was made to take into account relativistic effects. In 1988 the responsibility for generation of TAI was transferred to the Bureau International des Poids et Mesures (BIPM).

Coordinated Universal Time (UTC) is the basis for legal time when TAI is mainly used for scientific applications. UTC was defined in 1972 as a combination of TAI and UT1. Actually, it is a version of TAI corrected to follow UT1 by the introduction of steps equal to an integer number of seconds, so called leap seconds. The difference of UTC and UT1 shall be kept less than 0.9 s. UTC is not continuous due to these steps.

Figure 2-4 presents a general scheme of TAI/UTC generation. On the first step, atomic clocks operated in different laboratories are measured with respect to each other (the conventional comparison techniques according to BIPM recommendations are GPS Common View and Two-Way Satellite Time and Frequency Transfer). Then, the measured clock offsets are processed with a special timescale algorithm and a free-running atomic timescale EAL is produced being a weighed average of all participating clocks. EAL is corrected to follow the definition of second using a few primary Cesium standards. TAI is the result of this correction. UTC is generated as TAI coordinated to the rotation of the Earth.

UTC is produced as a paper clock, i.e. it is computed after post-processing of offsets between contributing clocks and exists in the form of corrections to these clocks.

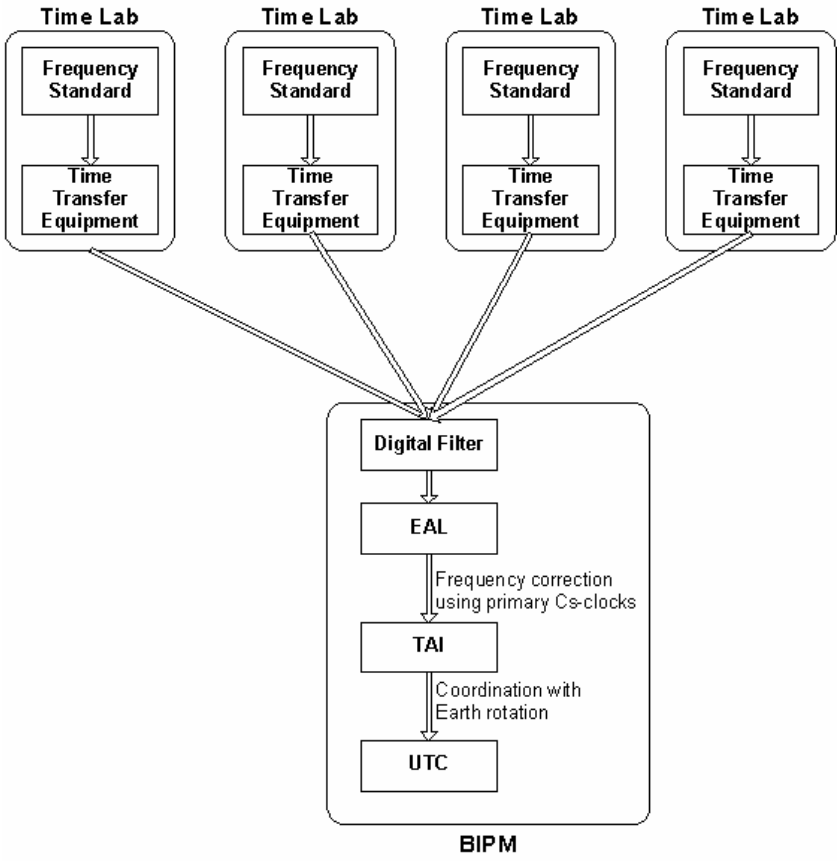

Figure 2-4. Generation of TAI and UTC

Thus, the responsibility of BIPM is to maintain a representation of the "true" second through calculation of TAI/UTC time scales. The next important task is to enable users the access to the "etalon" time.

2.2.3 Legal traceability of time and time transfer

Traceability is “the property of a result of a measurement or the value of a standard whereby it can be related to stated references, usually national or international standards, through an unbroken chain of comparisons all having stated uncertainties” [ISO93]. A good introduction to the concept of legal traceability of time is given in [Lombardi99]. The goal of the traceability concept is to ensure a link between SI and measuring unit/instruments used in everyday work. Traceability is often illustrated with a pyramid (see Figure 2-5).

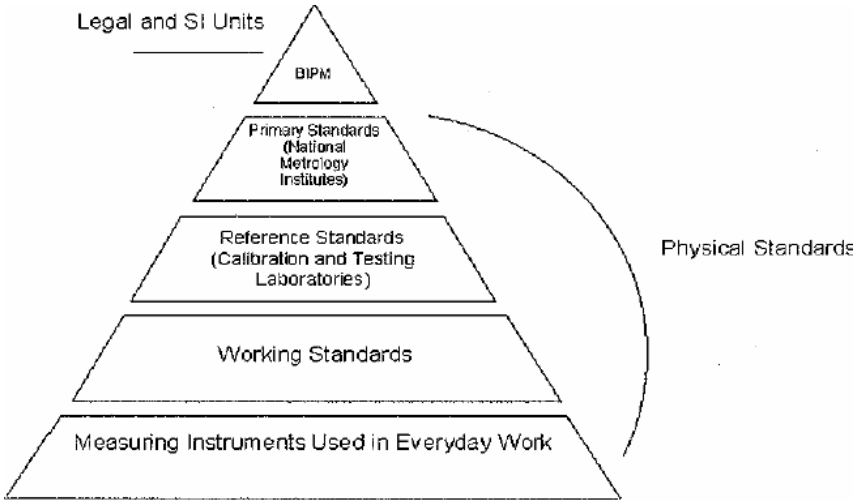

Figure 2-5. Traceability pyramid

BIPM is responsible for maintenance of the SI standard. At the national level, the National Metrology Institutes (NMIs) are responsible for maintenance and distribution of precise time. Thereto, NMIs maintain national representations of UTC, called UTC(k), and provide a number of time dissemination services.

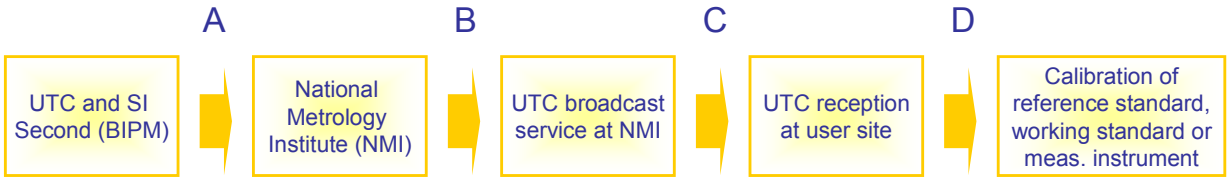

Figure 2-6. Distribution of precise time from NMI to users

Figure 2-6 illustrates the traceability chain from BIPM through NMIs to end-users. In this figure Link A is in joint control of BIPM and NMIs. It is established through regular comparisons of UTC(k) time scales produced by individual laboratories. The offset UTC(k)-UTC is published by BIPM monthly.

Link B is in the responsibility of the NMI which should provide the reference time to the broadcast system(s).

Link C is the link to the user established by or through the broadcast service. Typically, Link C is associated with the highest uncertainty of time transmission due to residual delays in propagation of signals which distribute the timing information.

Finally, Link D connects reception equipment on the user side with the clock or instrument which is to be calibrated or measured.

The scheme in Figure 2-6 is common for all time dissemination services provided by NMIs. A special case of it occurs when a user clock is monitored by NMI. Then there is an additional link to deliver timing information derived from reception of the broadcast signals on the user side back to the NMI.

2.2.4 Broadcasting UTC

There are numerous methods to realize the broadcast service, some examples of them are

(1) time and frequency transfer using radio broadcast (HF, LF and VLF bands),

(2) time and frequency transfer using TV signals,

(3) time and frequency transfer using telephone connection,

(4) time and frequency transfer via Internet,

(5) satellite time and frequency transfer: two-way time and frequency transfer through exchange of signals between two laboratories via a geostationary satellite, and time and frequency transfer through reception of signals of satellite navigation systems (GPS, GLONASS).

Methods 2 and 3 are mainly of historical interest; their description can be found e.g. in [Kart78]. Method 1 is still widely used by NMIs for links up to about 1000 km. Its description can be found in e.g. in [Kirchner93] and [Koenig93]. Method 4 – time transfer via Internet – is the "youngest", cheapest, and easiest method available for free for any user with an Internet connection. Its accuracy of some milliseconds is typically sufficient for synchronization of computer networks. An introduction to Internet-based timing service can be found in [Levine93].

The most precise method is the satellite time and frequency transfer. The two-way time and frequency transfer (see, e.g. [ITU97]) requires quite expensive equipment experienced personnel (therefore, it is mainly applied to link NMIs with each other). In the same time, the two-way technique offers the highest precision and accuracy. Time transfer via satellite navigation systems (see e.g. [Allan80] and [GPSICD]), which offers a slightly lower precision than the two-way method, has become a widely spread tool and was able to win the market with user reception devices as cheap as 100 US dollar. The US-owned and operated Global Positioning System (GPS) is today an undisputed market leader.

2.2.5 GPS as a UTC broadcasting service

De facto, GPS users establish traceability chain either to the version of UTC produced by the US Naval Observatory (USNO), UTC(USNO). From the metrological point of view, GPS can be thought of as a broadcast service of the USNO. Also, GPS itself can be thought of a provider of a time service. Its users first trace their clocks to GPS Time, the internal time scale established and maintained by GPS to support its operations, and then can correct them to UTC(USNO) using known time offset. GPS Time offset is monitored against UTC(USNO) and steered to it. The relationship between various time scales involved into the time distribution through a satellite navigation system is illustrated in Figure 2-7.

GPS has revolutionized timekeeping providing users with an easy access to a uniform precise time anywhere in the world at any moment. Nevertheless, GSP which has been designed to serve first of all military application has several important drawbacks for civil users. Some of them are

- limited commitments on system performance and availability,
- non-transparent system design and operations,
- limited liability of the system operator.

In fact, the "U.S. Space-Based Positioning, Navigation, and Timing Policy" authorized by the US president on December, 15 2004 names among others the following major policy goals:

- Provide uninterrupted access to U.S. space-based global, precise positioning, navigation, and timing services for U.S. and allied national security systems, and
- Improve capabilities to deny hostile use of any space-based positioning, navigation, and timing services.

In the same time, the policy intends to avoid unduly disruptions of the civil services and put an accent on the further promotion of GPS as a global tool for civil applications.

The European satellite navigation system Galileo which is currently under development will be under civil control, its performance is planned to be guaranteed for safety-critical services, and with its advent a redundant system for GPS will be available.

A discussion on Galileo preceded by an overview of timing applications follows.

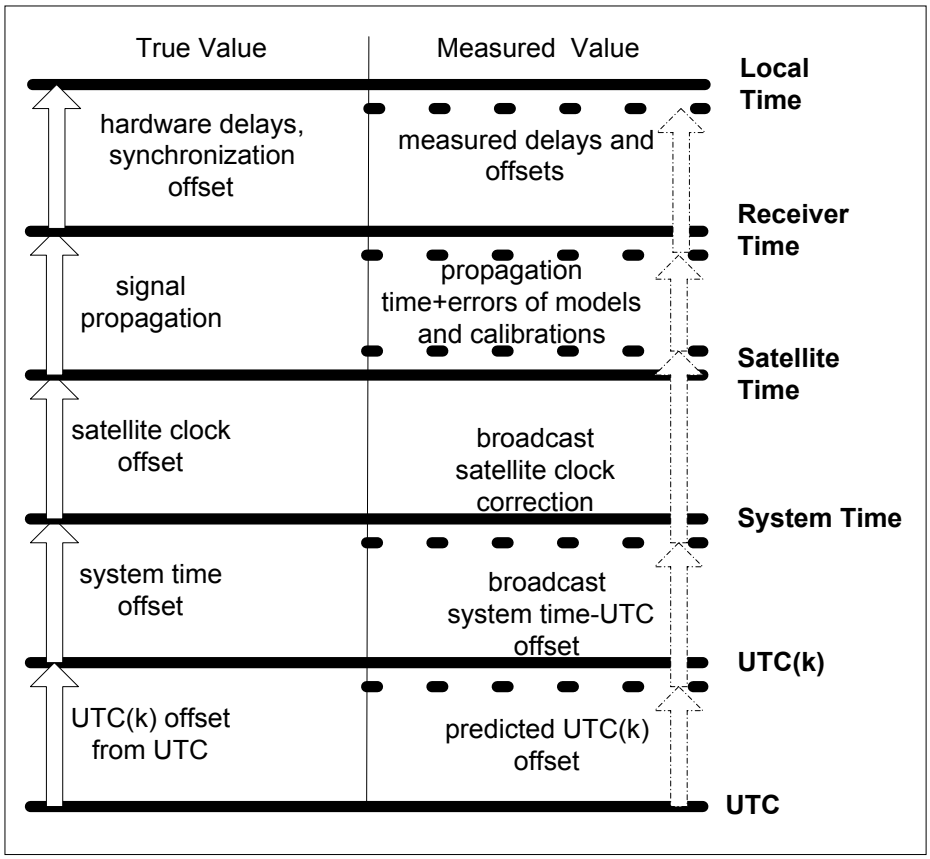

Figure 2-7. Time scale relationships in a satellite navigation system

2.3 Applications and requirements

Requirements for precise timing originate from various user applications like telecommunications, transport, power grids management, timing metrology etc. Some examples of such applications are given below.

Telecommunications is one of the most demanding commercial timing applications. Base stations in telecommunications networks shall be precisely synchronized to ensure the reliable data transmission and the required traffic density. Presently, in GMS/UMTC networks the frequency of the base stations shall be aligned within 1E-11. In future, the synchronization requirements will further increase to allow higher data traffics.

Precise timing is also of key importance for power grid management. It allows quick and exact fault localization, optimizes power distribution and management and according to latest studies could allow to detect sudden increases of power demands in-time, and thus to prevent wide-area blackouts.

In electronic banking time stamping of transactions and operations is vital for proper management of banking systems. The present demands to the accuracy of such stamping are relatively low – in order of milliseconds or hundreds of microseconds. However, electronic banking sets very high requirements to the reliability (trustworthiness) and availability of the timing services. Certification of these services and the service provider

liability are also important issues in this application. Similar requirements and problems can be found in various systems of electronic document exchange.

In transport applications (e.g. transport of goods or dangerous materials) reliable and trustworthy time stamping of vehicle locations is also an important issue. As in electronic banking service certification and service provider reliability, as well as service robustness to both intentional and unintentional jamming, are of major concern.

All applications discussed above require timing information to be available in real-time. Unlike them, timing metrology sets extremely high requirements to the accuracy of timing services, however, the results are not necessary needed in real-time. The specific processing applied in the timing metrology applications (like comparison of frequency standards) relies on relatively large sets of data collected over days or even months that allows to tolerate short service gaps or performance degradations.

Timing applications can be classified according to the markets they belong to (see Table 2-1 for some examples).

Market	***Applications***
Safety of Life and Security Market	transport of passengers and goods; emergency service (including search&rescue); security (including tracking of dangerous and valuable goods)
Mass Market	land and river navigation; personal navigation
Professional Market	timing; space; science; precise surveying; oil&gas; vehicle control and robotics; construction and civil engineering; land surveying and GIS mapping; fleet management; asset management; precise farming; fisheries; environment; mining

Table 2-1. Timing applications

The main requirements arising from applications of timing are related to

- accuracy of timing, and
- delay of access to timing information.

Figure 2-8 presents generalized requirements to precise timing in terms of accuracy and delay of access.

Thus, according to their requirements to accuracy and service latency, timing applications can be divided into several groups (see Table 2-3 and Table 2-2).

Group	***Requirements***	
	Delay of access	***Accuracy, s***
Ultra-precise	A few seconds – 1 week	10^{-10} – 10^{-8}
Delayed precise	A few seconds – one minute	10^{-7} – 10^{-4}
Real-time precise	real-time – a few seconds	10^{-6} – 10^{-3}
Non-precise	real-time – a few minutes	> 10^{-4}

Table 2-2 Summary of timing requirements

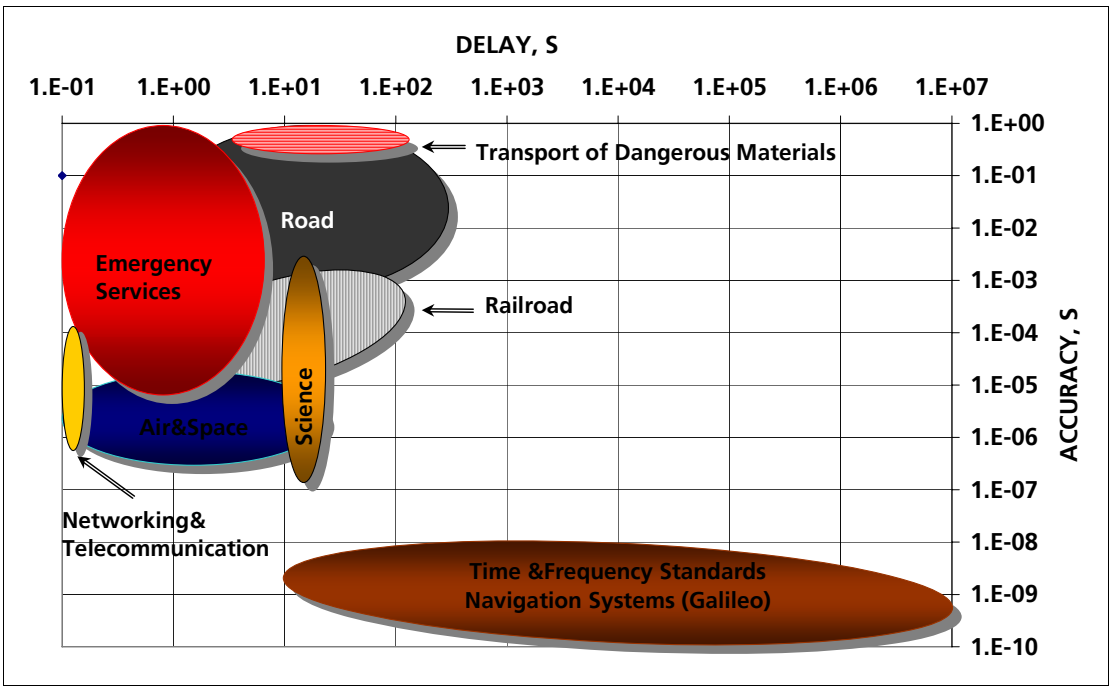

Figure 2-8. User requirements to precise timing

Group	*Applications*
High-precise	comparisons of primary frequency standards and precise time scales; timing of navigation systems; a few scientific applications like VLBI that were not included into the corresponding group
Delayed precise	scientific applications; space applications (e.g. orbit determination)
Real-time precise	networking and telecommunications; airborne applications (e.g. unmanned vehicles); space applications (e.g. launches, maneuvers); railroad (train survey)
Non-precise	other applications

Table 2-3 Groups of timing applications

3 Timing aspects in Galileo

3.1 Galileo overview

3.1.1 Galileo program

Information on Galileo program milestones, system architecture and all technical details is given as available by August 2006.

Galileo program is a European initiative aimed at building a satellite navigation system for civil needs and under civil control. The program is initiated, funded and supervised by the European Union in a close cooperation with the European Space Agency (ESA).

The main objectives of Galileo are to answer the challenge of growing user requirements and to secure a basis for civil GNSS applications. In long term Galileo shall also stimulate the European market and technology development, and secure the role of Europe as a global player in satellite navigation. Pro-Galileo arguments can be grouped into four wide categories:

- economic,
- social,
- political, and
- technological.

The idea of a European satellite navigation system was born in 90th. Its first version was the European Geostationary Overlay System (EGNOS). EGNOS is a satellite based augmentation system (SBAS) which has been developed by the European Space Agency, the European Commission and EUROCONTROL. EGNOS is mainly intended to supplement GPS. Originally, it was also planned to be capable to support GLONASS, however this option became obsolete later. EGNOS includes 3 geostationary satellites transmitting integrity information for GPS (estimates of satellite health and accuracy of their signals) and additional information (satellite orbit and clock corrections, ionospheric maps) to improve GPS accuracy. The system started its initial operations in July 2005, demonstrating the horizontal positioning accuracy better than 2 meters. EGNOS is intended to be certified for use in safety of life applications in 2008.

A global satellite navigation system under European control has become the next stage of the European navigation initiative. In 1999 a preliminary design definition study has been commissioned. The different system concepts were compared and consolidated, and the system signal and services has been preliminary defined.

On March 26, 2002 the European Council of Transport Ministers has released the first batch of Galileo program funding and agreed on the need to establish the Galileo Joint Undertaking to coordinate ESA and European Commission involvement into Galileo program. On May 26, 2003 the member states of ESA the Galileo Joint Undertaking has been finally established that paved the wave for starting the system implementation. The GNSS Supervisory Authority (established by the European Council on 12 July 2004) replaced in most concerns the Galileo Joint Undertaking. The GNSS Supervisory Authority was intended to manage the European satellite programs, control the use of corresponding funds, manage the Galileo concession issues and also take some other tasks with respect to the satellite navigation.

Interoperability with GPS has been one of the key Galileo design drivers from the very beginning of the program. In June 2004, the United States and the European Union have agreed on cooperation on satellite navigation systems and finalized the allocation of frequency bands for Galileo.

The primary contract for the presently ongoing detailed design phase C/D/E1 has been granted to Galileo Industries, a joint venture of the leading European airspace companies. This phase will be followed by the system deployment. Along with the development of the

core system infrastructure, ESA has commissioned the Galileo System Test Bed (GSTB) with two satellites, named GIOVE-A and GIOVE-B. According to the ESA definition, the objectives of GSTB-V2 are

- To secure the Galileo frequency filings allocated by the International Telecommunications Union (ITU),
- To characterize the orbits to be used by the in-orbit validation satellites,
- To test some of the critical technologies, such as the atomic clocks.

GSTB V2 will be followed by the In-Orbit Validation phase (IOV) where four Galileo satellites will be brought into orbit, Galileo Ground Segment will be fully deployed and the whole system will be validated against the key mission requirements. Finally, Galileo constellation will be extended to its nominal configuration with 27+3 satellites, the final validation will be performed and the system will achieve the Full Operational Capability (FOC). The overall schedule of the Galileo program is illustrated in Figure 3-1.

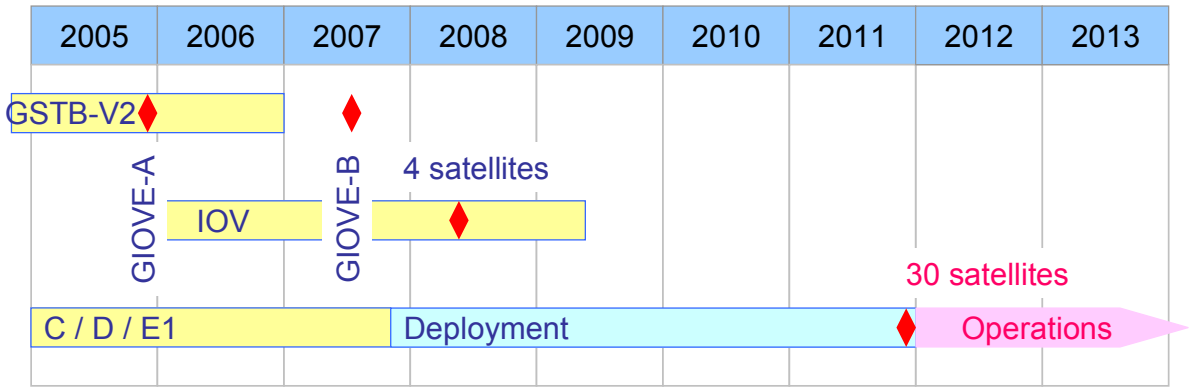

Figure 3-1. Galileo program schedule (personal best guess, September 06)

GIOVE A has been successfully launched and transmits Galileo signal. The launch took place on 28th of December 2005 at Baykonur (Russia) with a Soyuz-Fregat rocket. Since 12th of January Galileo signals are broadcast from space. GIOVE-A weighs 649 kg and is capable of transmitting navigation signals of all three frequency bands allocated for Galileo. However, only two signals can be transmitted in simultaneously: either L1+E5 or L1+E6. GIOVE-A navigation message and spreading codes differs from those of the final Galileo satellites. GIOVE-A satellite is equipped with two Rubidium frequency standards. GIOVE-B satellite will have extended functionality and will also carry the most precise clock ever flown onboard a navigation satellite, a passive Hydrogen maser.

3.1.2 Galileo and other satellite navigation systems

Presently there are active global satellite navigation systems: GPS (under US control) and GLONASS (under control of Russia) (see Table 3-1).

GPS was originally built by the U.S. to support military applications. It is still operated and controlled by the U.S. Department of Defence. However, already in the early 90th GPS has been declared as a dual-purpose, civil and military, system. Presently, GPS dominates the satellite navigation market. The US national policy on GPS, which was approved by the US President in December 2004 is to "*… provide on a continuous, worldwide basis civil space-based positioning, navigation, and timing services free of direct user fees for civil, commercial, and scientific uses … through the Global Positioning System and its augmentations, and provide open, free access to information necessary to develop and build equipment to use these services.*"

Nevertheless, due to its original objective and institutional status, GPS cannot provide firm service guarantees to civil users, furthermore the liability issues are also quite complex.

Finally, modern civil applications raise new performance requirements, especially with respect to integrity and continuity.

Like GPS, the Russian global satellite navigation system GLONASS has been originally built to support military applications. Similar to GPS, GLONASS Open Services, a free of charge service for civil users, is provided through the civil signal in L1 frequency band. However, the military signals on L1 and L2 are not decrypted. GLONASS constellation has been fully deployed by 1995. At that time Selective Availability (intentional performance degradation by manipulation of broadcast signals) in GPS was still active and GLONASS, which signals were not intentionally degraded, was an attractive alternative for the user community.

However, maintenance problems in the late 90th from which the system has not fully recovered up to now have considerably reduced the interest of users. Another issue used to be a more complicated and expensive user equipment due to utilisation of Frequency Division Multiple Access. Furthermore, presently GLONASS accuracy is considerably (four to five times) lower than that of GPS. Therefore, it will not be further considered here.

To improve the situation and encourage civil applications of GLONASS, Russia has adopted in 2001 a Federal Program aimed on completion of GLONASS satellite constellation, modernization of its Ground Segment, improvement of accuracy and facilitation of civil applications. The program has been amended in July 2006 with extra funding and increased requirements.

	GPS	***GLONASS***	***Galileo***
Operator	Department of Defense, USA	Russian Space Agency and Department of Defense, Russia	Commercial operator
Number of satellites	24 due, currently 31	24 due, currently 16	27 + 3 spares
Orbits	MEO	MEO	MEO
Number of orbital planes	6	3	3
Orbit altitude	20 350 km	19 140 km	23 616 km
Orbit eccentricity	~0	~0	~0
Orbit inclination	55°	64.8°	56°
Carrier frequencies, MHz	L1 1575.42 L2 1227.6 L5 1176.45 (planned from 2009)	G1 1592.95 - 1611.61 G2 1237.83 - 1254.61 G3 1194.45 - 1208.97	L1 1575.42 E5 1191.795 E6 1278.75
Modulation	CDMA; BPSK; BOC for PPS from Dec. 05	FDMA and CDMA (TBC); BPSK	CDMA; BPSK and BOC
Open services	Standard Positioning Service	Open Access Service	Open Service

Table 3-1. Satellite navigation systems at one glance

The GPS Standard Positioning Service (SPS) is provided via the navigation signal on the GPS L1 carrier frequency. The navigation signal includes a pseudorandom ranging code (C/A code open for civil users) and navigation message containing satellite ephemeris and clock parameters, ionospheric corrections, UTC corrections, health data and other information. The nominal performance of SPS is specified in [GPSSPSPS].

Many of dual-frequency geodetic receivers are able to make measurements using not only the C/A ranging code, but also the so called P-code, the pseudorandom ranging code intended for military users and provided on in L1 and L2 frequency bands. The P-code measurements are typically noisier than the C/A-code ones (acquisition of the P-code is

implemented in civil receiver using a kind of a “work-around” technique). However, utilization of these measurements allows calculating the ionospheric delay directly from the measurement data.

Also, geodetic receivers are capable of measuring the phase of the carrier frequency of satellite navigation signals in both L1 and L2 bands. However, both P-code and carrier frequency measurements are not made available for civil users formally.

The nominal constellation of GPS is described in [GPSSPSPS]. It includes 24 satellites (see Annex E). The actual constellation of GPS consisted of 31 active satellites (September 06).

To better serve military users of GPS and to respond to growing requirements of civil users and future concurrence from Galileo, the US government commissioned a GPS modernization program. Aside from the satellite design issues, the modernized GPS will

- Provide civil ranging code on the carrier frequency L2,
- Provide civil ranging code on the carrier frequency L5 (L5 is a new frequency in the GPS frequency plan)
- Include a number of new features for military users (BOC military ranging signals (M-code) etc).

Also, the accuracy of GPS satellite ephemeris and satellite clock parameters is planned to be improved.

A preliminary time-table of GPS modernization is shown in Figure 3-2.

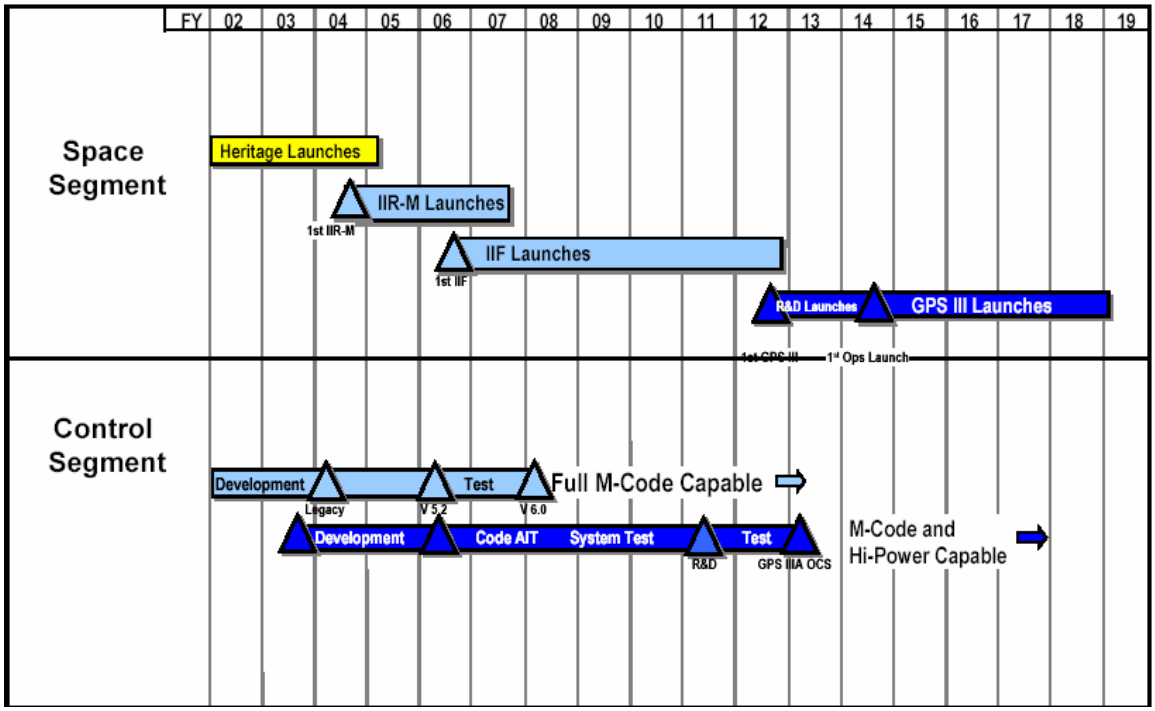

Figure 3-2. GPS modernization schedule (from [Cliatt03])

3.1.3 Galileo architecture

3.1.3.1 Overview

An overview of Galileo architecture is given in Figure 3-3. Galileo is designed as “system of systems”. It will include

- Core system,
- Reference receivers and local component demonstrator(s),
- EGNOS,

- Local components,
- User receivers.

This structure will provide three types of services:

- Satellite only services,
- EGNOS assisted services, and
- Locally assisted services.

Also, Galileo will interact with external systems:

- Navigation systems like GPS, GLONASS etc,
- Non-European SBAS like WAAS,
- Search-and-Rescue,
- Communication systems, and
- Other systems.

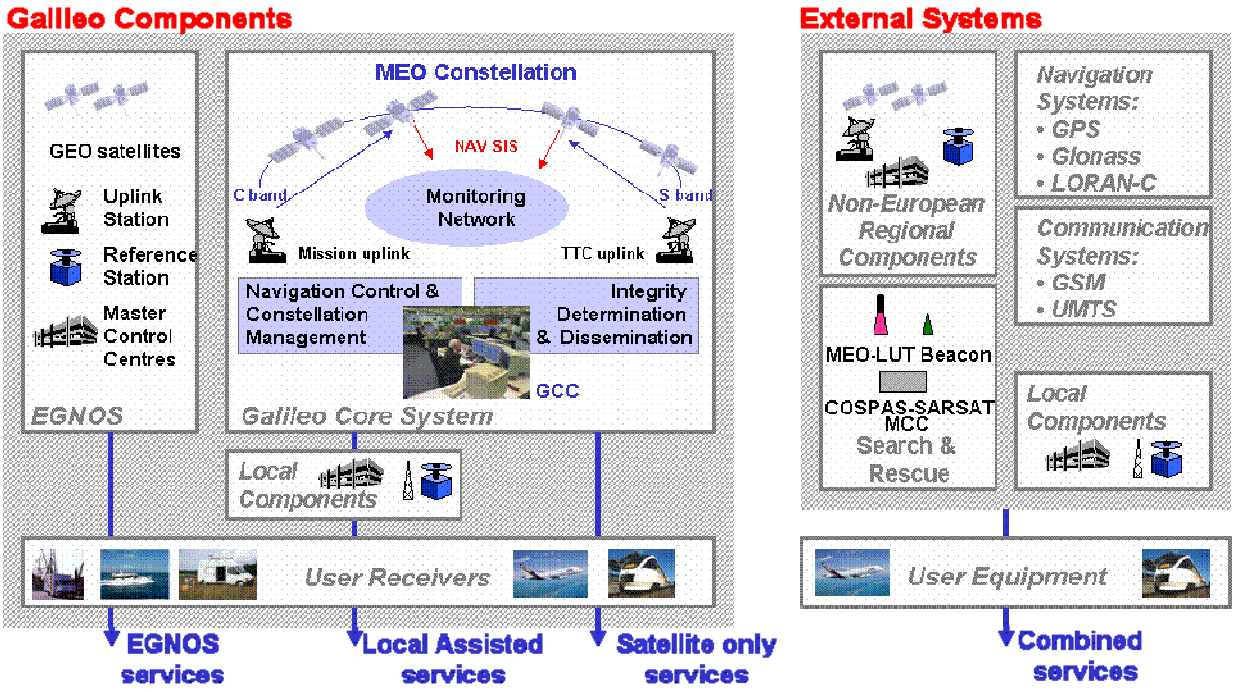

Figure 3-3. Galileo architecture (courtesy of ESA)

3.1.3.2 Galileo Core System

The Galileo Core System will include:

- Space Segment, and
- Ground Segment

The Space Segment is represented by a satellite constellation (Walker 27/3/1 pattern) of 27 satellites equally spaced in 3 orbit planes with inclination of 56° and semi-major axis of 29993.707 km. In the initial deployment the constellation will include 3 spares (1 per plane). Satellite orbit parameters for the Galileo constellation which were use in system volume simulations are summarized in Annex E (note that satellites with IDs 28-30 are the spares).

The Ground Segment will consist of two sub-segments: Ground Control Segment (GCS) and Ground Mission Segment (GMS).

GCS will be responsible for the management and monitoring (telemetry) of the Galileo satellite constellation. A preliminary GCS architecture is presented in Figure 3-4.

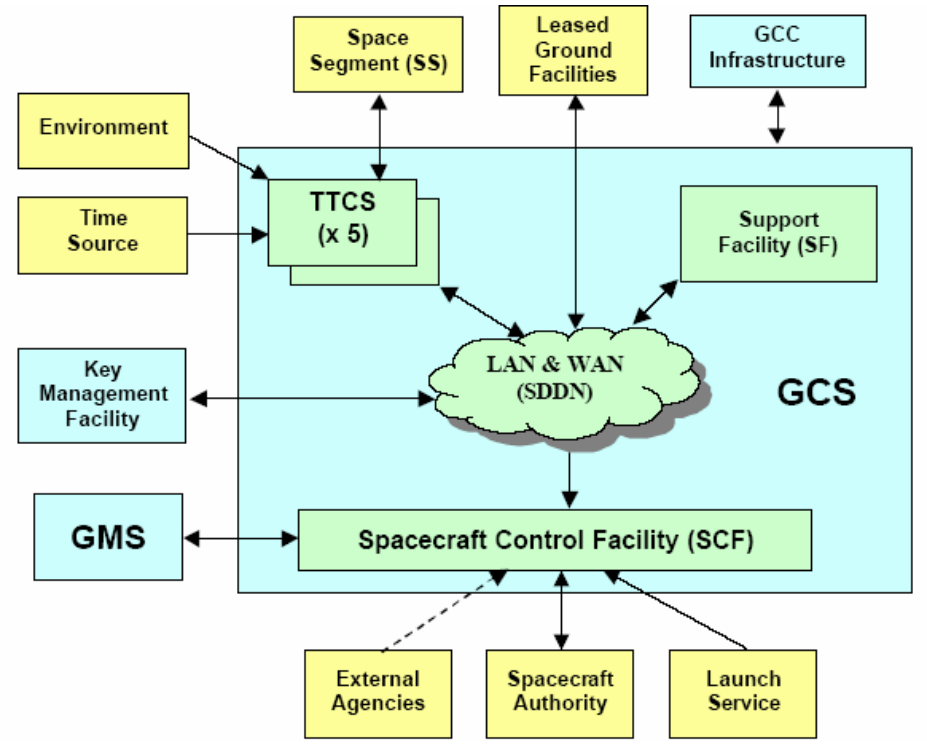

Figure 3-4. GCS architecture (courtesy of ESA)

GMS is responsible for mission planning, support (generation of navigation messages and integrity information, maintenance of Galileo system timescale etc), mission performance monitoring, and interfaces with external entities.

GMS will include:

- 9 Mission Uplink Stations (ULS) working in C-band which are in charge for uploads of navigation, integrity and SAR data to Galileo satellites,
- appr. 30 Galileo Sensor Stations (GSS) which are in charge for continuous monitoring of Galileo navigation signals through collection of satellite observations and their provision to OSPF and IPF,
- Orbit and Synchronization Processing Facility (OSPF) which is in charge for computation of satellite orbits and clock parameters, and predictions of SIS accuracy (SISA),
- Integrity Processing Facility (IPF) which is in charge for integrity processing by analyzing satellite observations collected by GSS,
- Precise Time Facility (PTF) which is in charge for generation of Galileo System Time and maintenance of time interfaces with the US Naval Observatory (USNO) and UTC laboratories affiliated to Galileo Time Service Provider (TSP),
- Mission Control Facility (MCF) which is in charge for mission performance monitoring,
- Message Generation Facility which is in charge for combining and routing data navigation and integrity data for upload to Galileo satellites,
- Mission Support Facility which represents a set of operational support facilities related to the achievement of the mission purposes,
- Service Product Facility which is responsible for management of data received or to be sent to external users (via Service Centers),

- Ground Assets Control Facility which is responsible for monitoring and control of GMS assets related to the Galileo mission purposes,
- Communication network.

A preliminary GMS architecture is presented in Figure 3-5.

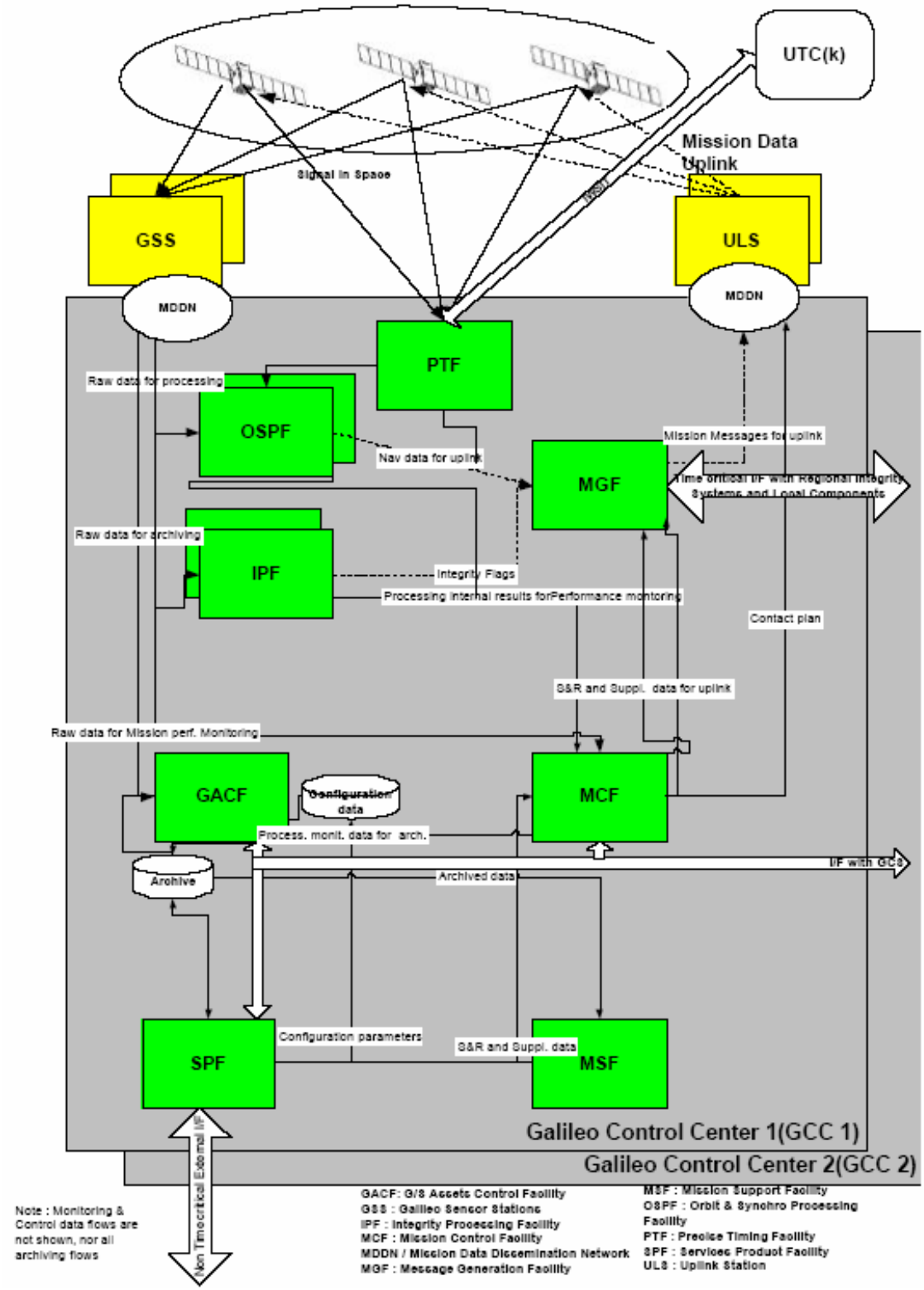

Figure 3-5. GMS architecture (courtesy of ESA)

3.1.4 Navigation signals and services

Galileo will provide four basic navigation services which are based on a certain combination of Galileo ranging signals, navigation and other broadcast information (e.g. integrity):

- *Open Service*: provides global, free-of-charge positioning and timing capabilities by means of navigation signals separated in frequency by using L1 and E5 frequency band.
- *Safety-of-Life Service*: provides integrity information by means of encrypted supplementary signals within the navigation signals of Open Service, and navigation capabilities based on the Open Service signals being provided on L1 and E5b frequency band. The performance of this service will be guaranteed.
- *Commercial Service*: provides additional data dissemination services and a third navigation signal with controlled access. Positioning capabilities (including precise carrier-phase based positioning) are provided in combination with the signals of Open Service. This service is based on the L1, E6 and E5b frequency band.
- *Public Regulated Service*: provides global positioning and timing capabilities by means of two navigation signals separated in frequency (on L1 and E6 frequency band); access to these signals will be controlled.

The following table illustrates the mapping of Galileo service to frequencies.

Band	Multiplex	Bandwidth [MHz]	Compo-nent	Modulation	Primary code	Secondary code	Symbol rate	Service
E5	AltBOC (15,10)	90x1023	E5a/I	BPSK(10)	10230	20	50	OS
			E5a/Q	BPSK(10)	10230	100	Pilot	OS
			E5b/I	BPSK(10)	10230	4	250	SoL
			E5b/Q	BPSK(10)	10230	100	Pilot	SoL
E6	CASM	40x1023	A	BOC(10,5)	Classified			
			B	BPSK(5)	5115	1	1000	CS
			C	BPSK(5)	5115	100	Pilot	CS
E1	CASM	40x1023	A	BOC(15,2.5)	Classified			
			B	CBOC	4092	1	250	OS/SoL
			C	CBOC	4092	25	Pilot	OS/SoL

Table 3-2. Mapping of Galileo services to frequencies

CBOC is a composite BOC signal which linearly combines BOC(1,1) and BOC(6,1) sub-carriers. Both sub-carriers will be transmitted continuously with 10/11 of the total signal energy in the BOC(1,1) component and 1/11 of the energy in the BOC(6,1) component, see [Hein06] for details.

Performance of Open, Safety-of-Life and Public Regulated services is defined in Galileo requirement documents is summarized (see Table 3-3). It is specified for users whose location, dynamic, environment (in terms of ionospheric effects, tropospheric effect, multipath, interference), and receiver are compatible with specifications given in Galileo System Requirements document.

Table 3-3 includes no specification of positioning and timing performance for the Commercial Service since the corresponding capabilities will be obtained through the signals of other services (e.g. Open Service). The improvement of performance due to potential use of TCAR technique is also not specified in Galileo programmatic documents.

Galileo services can be combined with those of other satellite navigation system (GPS, GLONASS), SBAS (EGNOS, WAAS, MSAS, GAGAN) or can be augmented by local elements (e.g. differential systems). Also, Galileo receiver can be used in combination with other sensors (e.g. inertial navigation systems).

Most Galileo users (at least as far as mass market applications are concerned) are expected to utilize combined GPS/Galileo equipment. In addition, in practice Galileo will be certainly combined also with navigation systems other like GLONASS. The need to support Galileo services based on combination of Galileo with other systems raises the issue of the interoperability of Galileo with these systems. The interoperability aspects include, among others, considerations on a common time reference. The GPS/Galileo timing interoperability is discussed in Section 6.

Parameter	***Open Service***		***Safety-of-Life (dual freq.)***	***Public Regulated (dual freq.)***	
	Single freq.	***Dual freq.***		***Single freq.***	***Dual freq.***
Accuracy, 95%					
- horizontal	15 m	4 m	4 m	15 m (L1) 24 m (E6)	6.5 m
- vertical	35 m	8 m	8 m	35 m	12 m
- time[1]	n/a	30 ns	n/a	n/a	n/a
- frequency	n/a	$3 \cdot 10^{-13}$	n/a	n/a	n/a
Availability					
- NOC	100%	100%	100%	100%	100%
- Average	99.5%	99.5%	99.5%	99.5%	99.5%
Integrity					
- HPL	n/a	n/a	12 m	n/a	20 m
- VPL			20 m		35 m
- TTA			6 s		10 s
- Integrity risk			$2.0 \cdot 10^{-7}$ per 150 s		$2.0 \cdot 10^{-7}$ per 150 s
Continuity	n/a	n/a	$1-\left(8 \cdot 10^{-6}\right)$ per 15 s	n/a	$1-\left(8 \cdot 10^{-6}\right)$ per 15 s

Table 3-3. Performance of Galileo navigation services

3.2 Galileo System Time (GST)

3.2.1 Role of GST in Galileo operations

Galileo System Time (GST) is the basis for the internal synchronization of all Galileo components. First of all, it has to serve to synchronize all Galileo satellite clocks through determination of their offsets to GST and broadcasting of these offsets to Galileo users.

To enable reliable system integration and tests it was proposed that GST shall have a physical representation (at least in the initial phase of Galileo operation) (see e.g. [GTWGR]).

GST will have two basic functions:

[1] The timing and frequency accuracies are specified with respect to UTC at 95% over any 24 hours for users equipped with Timing Laboratory receivers when Time Service Provider Interface is available.

- navigation support function, and
- metrological support function.

The navigation support function of GST is to support Galileo operation (synchronization of elements, computation of orbit and clock parameters) in such a manner that the Galileo Navigation Services (see Section 3.1.3.2) can be provided with the required performance. The navigation support function sets strict requirements to GST stability (see e.g. [Tjaden02], [GTWGR]).

The metrological support function of GST is to enable synchronization of Galileo users to UTC or TAI with a pre-defined accuracy (50 ns within Open Service). This function sets requirements to the GST time and frequency offset to TAI and its stability in the medium term (see e.g. [Tjaden02], [GTWGR]).

GST itself is defined as the reference for prediction of Galileo satellite clocks as utilized by OSPF. Thus, it exists in OSPF software as a result of processing of Galileo measurements from the Galileo receiver which is located at PTF which produces the physical representation of GST. This physical representation at a reference point at the PTF output is named GST(MC) where “MC” stands for “Master Clock”. The Galileo receiver at PTF is driven by the GST(MC) frequency and timing signals.

3.2.2 GST performance specification

GST performance is defined in the Galileo programmatic documents in terms of relative frequency instability (ADEV) and time and frequency accuracy with respect to TAI.

The specification of GST frequency instability as defined in the Galileo baseline is summarized in Table 3-4. The stability requirements for GST have been determined only for those the time intervals which are of interest for ODTS (100 min and 8 hours) and metrology (24 hours).

Time interval, s	*GST(MC)*	*GST*
1	3E-13	
10	4E-14	
100	7E-15	
1000	4E-15	
6000	2.1E-15	1E-14
10000	2.0E-15	
28800	2.3E-15	1.3E-14
86400	4.3E-15	6E-15

Table 3-4. GST frequency instability (short-term)

The relationship between GST and TAI is addressed in an additional set of requirements which are summarized in Table 3-5.

Parameter	*Value*
Normal operation (GTSP available)	
Offset from TAI, 95%	≤ 50 ns
Uncertainty of TAI offset, 95%	≤ 28 ns
Relative frequency offset from TAI, 95%	5.5e-14
Autonomous operation over 10 days (GTSP not available)	
Offset from TAI, 95%	≤ 50 ns
Uncertainty of TAI offset, 95%	≤ 28 ns

Table 3-5. GST w.r.t. TAI: baseline requirements

3.2.3 Generation of GST

According to the concept elaborated during the definition phase of Galileo (see [GTWGR]), the GST navigation function is essentially kept within Galileo. The GST metrology function is delegated to the Galileo Time Service Provider (GTSP), i.e. GST is generated is a free-running timescale within Galileo and further steered to TAI using GTSP products. GTSP is a third party (probably, a commercial organization) bounded to Galileo Operator by an appropriate service contract.

Thus, the responsibilities of Galileo Mission Segment are

- to generate GST,
- to provide the GTSP access to it, and
- to steer GST to TAI by implementing steering corrections computed by TSP.

Responsibilities of GTSP are

- to estimate GST offset from TAI (TAI is not available in real-time and must be predicted), and
- to compute steering correction to keep GST within specified limits from TAI.

GST, at least at the beginning, will be physically realized by an active H-maser which will be steered to TAI. PTF will also compute an average timescale from its clocks. Cs clocks at PTF would allow estimation of the inherent frequency drift of the maser. The average time scale is a “paper time” (computed value which does not have a physical equivalent), it is called GST Running (GSTR). This kind of time scales are often called “ensemble time”. In IOV, PTF will be equipped with two masers (master and hot-spare) and four Cs clocks (three clocks representing the nominal configuration and one hot-spare).

Further, the maser which signal determines GST (master H-maser or its spare in case of a failure of the primary maser) will be referred to as the Master Clock (MC). MC will be steered to TAI using GTSP corrections. Depending on the frequency drift of the maser, there are two potential options for implementation of the GST-TAI steering:

(1) to steer MC using the GTSP corrections only (assuming low-drift maser), or

(2) to steer MC to GSTR to remove the frequency drift and on top of that to implement the GTSP correction. In this case, GTSP will observe only MC with removed frequency drift.

At the time of writing, selection of an appropriate option is still under discussion.

H-maser(s) and Cs clocks participating in the generation of GST are located at PTF. Other system clocks could be also included into the GST generation after successful completion of initial tests.

An overview of GST generation is presented in Figure 3-6.

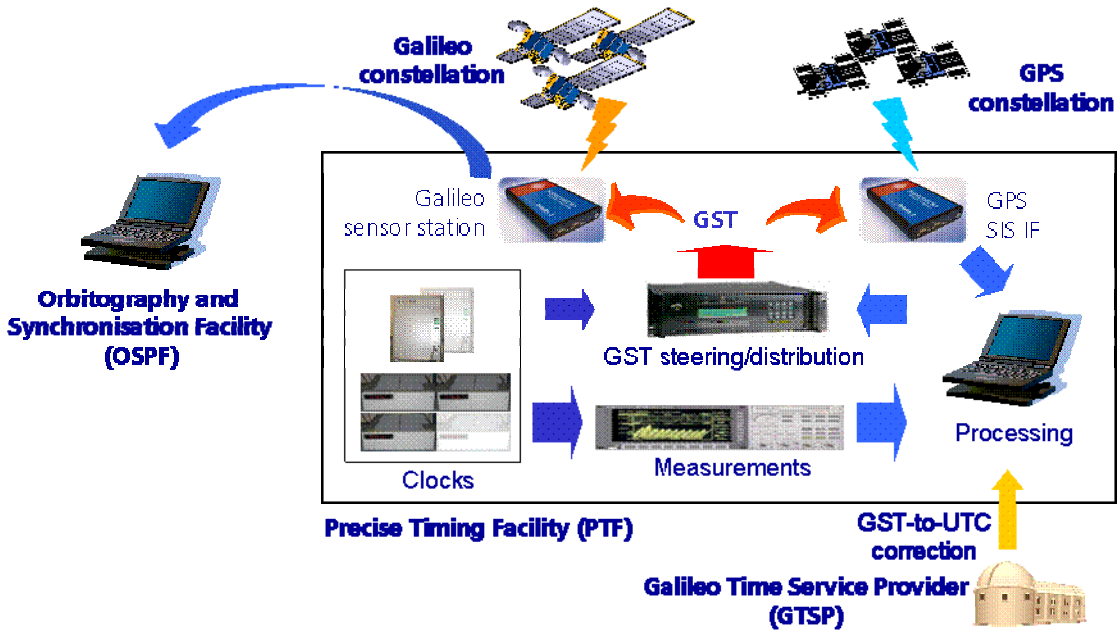

Figure 3-6. GST generation overview

The tasks of the MC steering algorithm can be summarized as follows

- to verify GST-to-TAI steering correction obtained from GTSP to prove that it will not jeopardize GST performance in short term,
- to compute a frequency correction to steer the MC to GSTR, and
- to define the steering correction value to be applied to the MC at a certain time.

A functional scheme of GST generation is given in Figure 3-7. This scheme relies on a long-term operational experience. However, it should be adopted to Galileo specifics, and in particular

- the priority of the short-term stability (up to 10 days, the time period corresponding to GST autonomy requirement) instead of the long-term goal typical for time metrology, and
- a reduced number of atomic clocks (comparing to the metrological practice) available at PTF: 3 Cesium clock (plus 1 hot-spare Cesium).

The steering correction evaluated as depicted in Figure 3-7 is applied to the phase microstepper which is connected to the master AHM. The resulting (steered) 1PPS and 10MHz signals are forwarded to 1PPS and 10MHz distribution units and constitute the physical representation of GST. These signals drive Galileo receiver collocated at PTF. Galileo observations collected by this receiver are delivered to Orbitography and Synchronization Processing Facility (OSPF) which estimates (using also the data from the whole Galileo monitoring network) satellite orbits and time offsets of both satellite and ground clocks with respect to GST. These estimates are further used to predict satellite orbits and clock offsets to GST which are uploaded to satellites and broadcast in the Galileo navigation message. The process described above is illustrated in Figure 3-8.

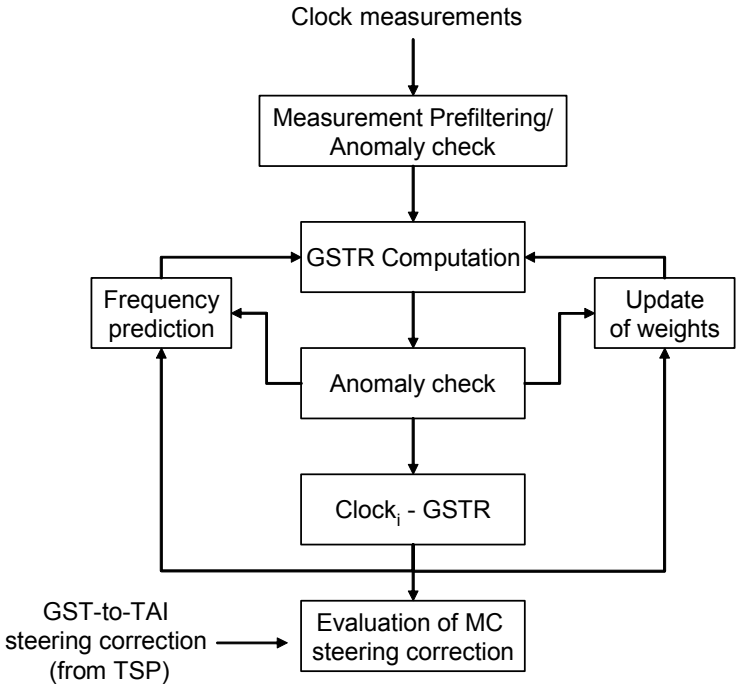

Figure 3-7. Functional scheme of GST generation

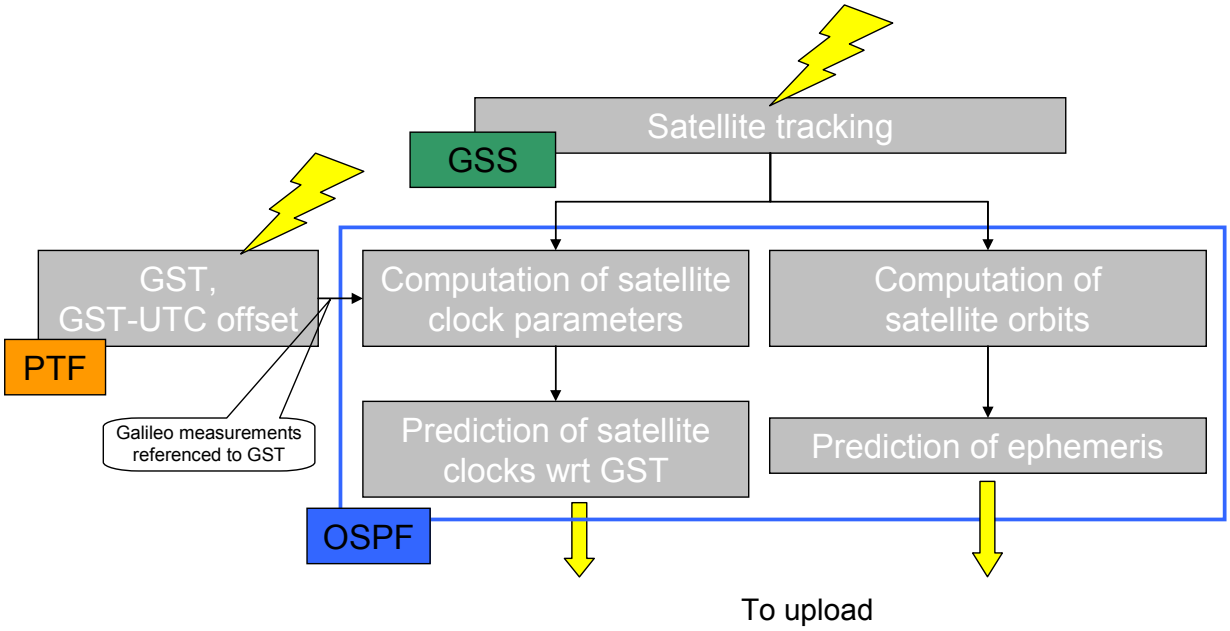

Figure 3-8. Interplay of PTF, GSS and OSPF

3.2.4 GST and GPS Time

The key characteristics of GPSTime (as presently implemented) and GST (as specified in the current Galileo baseline) are summarized in Table 3-6. There are on-going discussions on the time keeping concept for GPS-III (Master Clock or Composite Clock). On the other hand, there are considerations on utilizing a composite clock approach in future Galileo.

Property	*GPS Time*	*GST*
Type of time scale	Composite Clock: average of GPS clocks computed in a Kalman filter	Master clock: steered active H-maser
Produced at	Computations performed at the Master Control Station	Physically produced at Galileo PTF
Access outside the system	Through broadcast corrections to satellite clocks	Through direct time transfer or through broadcast corrections to satellite clocks
Steering to TAI	Through USNO	Through Time Service Provider combining several UTC laboratories
Offset from TAI	14 ns (RMS in 2004)	50 ns (95%, requirement)
Uncertainty of TAI offset	~ 9 ns (RMS in 2004)	28 ns (95%, requirement)

Table 3-6. GST and GPS Time

3.2.5 Clocks in Galileo

3.2.5.1 Ground clocks

Ground clocks in Galileo (here we consider only those clocks which will be precisely measured against each other and may be potentially used to form a Composite Clock) will be placed at

- PTFs: two active H-masers and four Cesium clocks per PTF, and
- Galileo Sensor Stations (GSS): a commercial Rubidium frequency standard.

Active H-masers are mainly produced outside the EU (US-based manufacture Symmetricom (former Datum) and Russian-based manufactures Kvarz and VREMYA-CH). The European maser manufacturer is a Swiss company T4Science, a joint venture of Temex (France), TimeTech (Germany) and VREMYA-CH. This company has taken over the H-maser activities which were formerly concentrated at the Observatory of Neuchatel (Switzerland).

A typical performance specification of active H-masers can be found in Section D.3.1.

Commercial Cesium clocks are produced only outside the EU (the US-based manufacturer Symmetricom is the one best-known, there are also many others). Typical performance specifications of Cesium clocks can be found in Section D.2.1.

Performance of commercial Rubidium frequency standard is presented in Section D .1.

3.2.5.2 Satellite clocks

According to the present baseline, Galileo satellites are to be equipped with four clocks: two space-qualified RAFS and two space-qualified passive H-masers (SPHM). Both RAFS and SPHM are European technology development specially commissioned for Galileo.

An overview of Galileo satellite clock characteristics is given in Section D .4.

3.2.6 Satellite clock prediction

Satellite clock prediction error (or simply, clock error) is one of the key factors limiting the accuracy of user positioning. This error represents the difference between the model of satellite clock deviation from the system time and the actual value of this deviation. Typically,

users utilize the clock model broadcast in the navigation message. Galileo baseline foresees the use of a quadratic model (same approach as in GPS). The requirement is to have the clock error less than 0.45 cm (~1.5 ns) (1sigma) over selected time interval (presently, 6 hours).

Galileo ODTS algorithms have been tested in the GSTB-V1 with GPS data. Prediction error for GPS IIR RAFS obtained in these tests is presented in Figure 3-9.

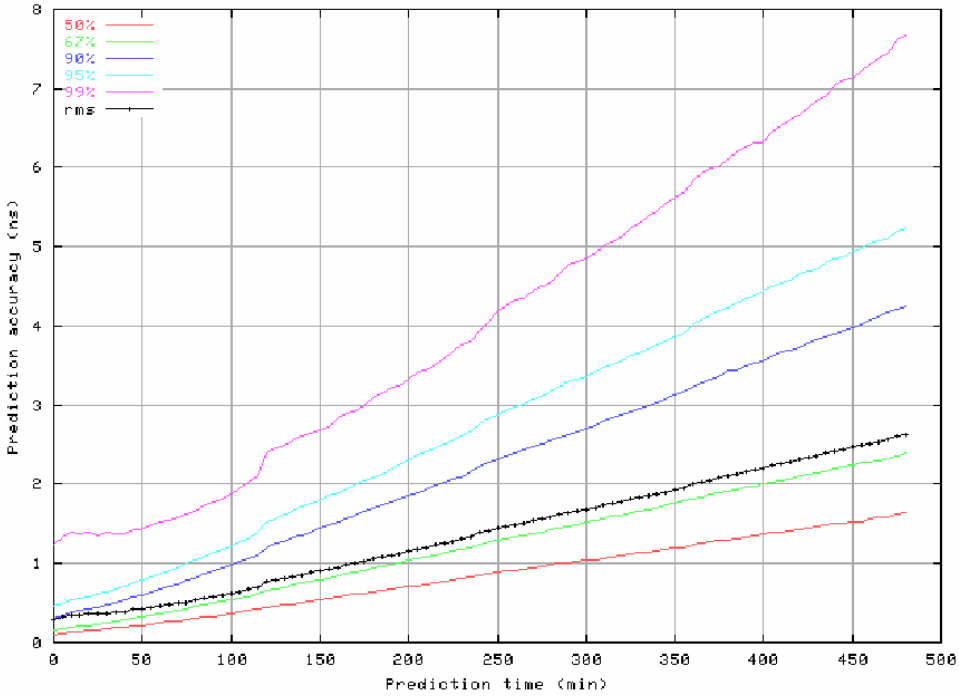

Figure 3-9. Test of GPS IIR RAFS prediction [Merino03]

The results in Figure 3-9 were obtained with a linear prediction model. Also, [Delporte01] demonstrate that a linear model gives better results than the quadratic one in case if the frequency drift is not dominating.

3.3 Galileo time interfaces

3.3.1 User time interface

The most important Galileo time interface is that to Galileo users. It will be established through provision of timing capabilities via SIS broadcast by Galileo satellites. Galileo will provide two kinds of these capabilities: user synchronization with respect to GST and with respect to TAI/UTC. In other words, in its role of a timing system, Galileo will disseminate its own reference timescale GST and the international timescale TAI/UTC. The first capability is related to the Galileo positioning service and represents a Galileo internal function. The second one is a part of the Galileo metrological function. To fulfill it Galileo will have to establish an interface to TAI/UTC. This issue is discussed below.

3.3.2 UTC

3.3.3 Relevance of UTC interface

To enable Galileo navigation function – provision of an accurate positioning capability to its users – GST has to be predictable. It does not matter if it is steered to UTC/TAI or any other time scale, also deterministic changes of GST frequency play no role as far as they can be described by some model. Knowledge of the offset between GST and UTC/TAI is also not very important for positioning. The only demand to have GST somehow linked to TAI/UTC– as far as positioning capabilities are concerned arises from the potential user wish to time-stamp his/her positions in using the legal time reference, i.e. the TAI/UTC.

However, the main argument (and the strict requirements) for linking GST to TAI/UTC is delivered by the second function of Galileo – the metrological function. Galileo will offer not only positioning but also timing capabilities to its users. In order words, Galileo will be a time dissemination system. The international practice (recommended by ITU and adopted by GPS and GLONASS) is to disseminate a representation of TAI/UTC. This calls for determination and broadcasting of the offset between GST and TAI/UTC. Theoretically, there is still no need to physically steer GST to TAI/UTC, but the excellent performance of GPS Time in the last years – and its close steering to TAI/UTC – set a bench-mark for Galileo. It makes the accuracy of GST - TAI/UTC offset determination and quality of GST steering to TAI/UTC to important commercial factors demonstrating the competence of Galileo designers and operators and, finally, contributing to commercial success of the system.

3.3.4 Status of Galileo Time Service Provider activities

The value of the timing service, and in particular of GST linkage to TAI/UTC, were early recognized by the EC/ESA and further elaborated by ESA-funded Working Group on Galileo Timing Interface which acted in 2000 – 2001. The working group has recommended to keep the navigation function in the responsibility of Galileo, but to delegate the metrological function – in the sense of establishing a link between GST and TAI/UTC – to an external body, the Galileo Time Service Provider (GSTP).

Further activities on GTSP definition were initiated by the Galileo Joint Undertaking (GJU) and accomplished in 2004 – 2005. In 2005 implementation of GSTP was started in the frame of a GJU contract. By the time of writing (September 2006), GTSP has successfully passed its Critical Design Review and its deployment has been started.

3.3.5 GTSP philosophy

As well-known, TAI/UTC are computed by the BIPM *post factum*, their real-time representations are kept by authorized laboratories/institutes. The high quality of GPS Time link to TAI/UTC is ensured by involvement of the US Naval Observatory (USNO) – the most prominent and well-equipped timing institute in the world nowadays – into the GPS operations. Presently, no individual European timing institute (ETI) is able to offer a service competitive in quality with that of the USNO. Therefore, GTSP has to become a focal point for the European timing expertise and to involve a number of ETIs.

GTSP will be a commercial entity, it has to learn to produce and offer its products in a commercial manner. On the other hand, hand having one major client – the Galileo concessionaire – GTSP has to follow the client's rules of the game and to ensure that the product performance/price is acceptable for the client.

Finally, GTSP has to evolve to track the GPS performance improvement to ensure competitive positions of Galileo.

3.3.6 Interface to GPS Time

According to [HLD], Galileo shall be interoperable with GPS. The interoperability extends over numerous system aspects, first of all, definition of navigation signals and frequency bands, and involves also coordination of GPS and Galileo system time scales.

The need for this coordination arises from the fact that users of combined GPS/Galileo receivers will observe a slowly changing offset between their GPS and Galileo measurements due to the offset between the system time scales. A similar problem occurs in combined GPS/GLONASS equipment.

Recommendations produced during the GALILEI study initiated by the European Commission include one to transmit the offset between GPS and Galileo system timescales in Galileo navigation message. It would allow users of combined equipment to correct their measurements for this offset without introduction of an additional – fifth – unknown in their navigation solution like it was done for combining GPS and GLONASS. This Galileo feature will be especially important for users with restricted sky view (e.g. urban canyons).

Two baseline options for the determination of the GPS Galileo time offset were identified by the Joint US/EU Working Group on GPS/Galileo Interoperability [Hahn04]:

- with the help of a time transfer link between PTF and USNO (primary link), and
- with the help of a combined GPS/Galileo receiver (secondary link).

Also, GGTO can be determined with the help of a GPS time receiver connected to the physical realization of GST.

The Working Group has also recommended that GPS to broadcast the GPS Galileo time offset as well. The broadcast values should be coordinated between GPS and Galileo. This decision are now included into the US-EU agreement on GPS-Galileo cooperation which was ratified by the US and EU representatives on 26th of June 2004 [USEU04].

3.3.7 Other time interfaces

No efforts or recommendations to establish an interface between the GST and the time scales of navigation systems other than GPS are known to the author. However, considering the latest developments on recovering the GLONASS constellation, determination and broadcasting of Galileo-GLONASS time offset may become of interest. This offset could be determined using a GLONASS receiver at PTF or a combined Galileo/GLONASS receiver. A direct link between GST and GLONASS Time and/or broadcast for Galileo GLONASS time offset in the GLONASS navigation message would require negotiations with the GLONASS operator(s).

4 Review of state-of-the-art methods and algorithms

4.1 Basics of system time generation

4.1.1 Weighted average algorithm for computation of ensemble time

Since no physical clock is perfect, a properly calculated combination of several physical clocks possesses better stability then any of these clocks. This combination is called "ensemble time", a fictive clock a reading of which it would represent (analogous as reading of physical clocks represent these clocks) is called "ensemble clock" or "composite clock". Set of clocks contributing to the computation of ensemble time is called "clock ensemble" or simply "ensemble".

Traditionally [see e.g. ITU recommendations], ensemble time is defined as a weighted average of corrected clocks with the ensemble. Here "corrected" stands for clock minus its prediction. Under assumptions that clock correlations and measurement noise are negligible, the ensemble time is given by the following equation:

$$\xi_e(t) = \Sigma w_i(t)\xi_i(t) \qquad \text{Eq. 4-1}$$

here

ξ_i - reading of i-th clock (i.e. the time as realized by i-th clock), note that ξ_i cannot be measured directly, only differences of clock readings are measurable,

ξ_e - reading of the ensemble clock, or ensemble time,

$w_i(t)$ - weights of individual clocks in the ensemble.

As mentioned above, ξ_i cannot be measured directly since measurements provide access only to differences $x_{i,j}$ of readings of different clocks:

$$x_{i,j}(t) = \xi_i(t) - \xi_j(t) \qquad \text{Eq. 4-2}$$

Similarly, ensemble time ξ_e exists as a correction x_i to a physical clock:

$$x_i(t) = \xi_e(t) - \xi_i(t) \qquad \text{Eq. 4-3}$$

With the definitions given by Eq. 4-2 and Eq. 4-3, Eq. 4-1 can be rewritten as

$$x_i(t) = \sum_j^N w_i(t)\left(\hat{x}_j(t) - x_{i,j}(t)\right) \qquad \text{Eq. 4-4}$$

here

$\hat{x}$ - predicted clock offset with respect to the ensemble time,

N - number of clocks in the ensemble.

Predictions $\hat{x}$ are introduced to enforce the continuity of ensemble time, i.e. to avoid steps in the ensemble time due to changes of clocks weights or to introductions/exclusions of clock to/from the ensemble. They – the predictions – are based on the analysis of clock behavior with respect to the ensemble time available from previous computations.

Typically, all clocks in the ensemble are measured with respect to one reference clock (usually, reference clock is an H-maser, and the ensemble clocks are Cesium ones). The reference clock itself does not contribute to the ensemble time. Thus, for operational implementation Eq. 4-4 can be used as follows

$$\tilde{x}_r(t) = \sum_j^N \tilde{w}_j(t)\left(\tilde{x}_{r,j}(t) - \hat{x}_j(t)\right) \qquad \text{Eq. 4-5}$$

where subscript "r" stands for the reference clock and "~" is used to indicate that we deal with estimates but not with the true values (due to measurement errors, clock correlations etc).

Predictions $\hat{x}_j$ can be obtained using an estimated frequency $\tilde{y}_j$ of j-th clock with respect to the ensemble time:

$$\hat{x}_j(t) = \tilde{x}_j(t-\tau) + \tilde{y}_j(t-\tau)\cdot\tau \qquad \text{Eq. 4-6}$$

here τ is the time step of computation of the ensemble time (typically, τ is equal to 1 day) and values of $\tilde{x}_j$ are obtained as $\tilde{x}_j = \tilde{x}_r + \tilde{x}_{r,j}$.

Frequency $\tilde{y}_j$ can be computed as

$$\tilde{y}_j(t-\tau) = \frac{\tilde{x}_j(t-\tau) - \tilde{x}_j(t-(n+1)\tau)}{n\tau} \qquad \text{Eq. 4-7}$$

here $n\tau$ is selected averaging interval (e.g. 10 days).

Weights $\tilde{w}_j$ are typically taken inverse proportional to Allan Variance of j-th clock over selected sampling time ζ:

$$\tilde{w}_j(t) = \frac{1/AVAR_j(t,\zeta)}{\sum_1^N 1/AVAR_k(t,\zeta)} \qquad \text{Eq. 4-8}$$

The Allan Deviation is determined with respect to the ensemble time using computed values of $\tilde{x}_j$.

The sampling time ζ selected for computation of Allan Variance in Eq. 4-8 is also called "optimization time" since the selection of weights will optimize the ensemble time stability for the time interval equal to ζ.

In practical implementation, it is sufficient to compute the ensemble time as a correction to the master clock from Eq. 4-5, then the offsets between each of the clocks in the ensemble and the ensemble time can be easily computed using their measured offsets with respect to the master clock:

$$\tilde{x}_j(t) = \tilde{x}_r(t) + \tilde{x}_{r,j}(t) \qquad \text{Eq. 4-9}$$

4.1.2 GPS composite clock

4.1.2.1 Theory

The so called GPS Composite Clock refers to two different phenomena:

- Concept of GPS Time generation which defines GPS Time as an implicit average of clocks (originally, only satellite clocks) that belong to the GPS system.

- Resulting timescale based on the definition above. Note that Composite Clock as a timescale is not equivalent to GPS Time, the latter being Composite Clock timescale steered to UTC(USNO).

The Composite Clock as GPS system time was introduced at June 17, 1990.

[Brown91] presents an extensive discussion on the theory of GPS Composite Clock which is computed by a Kalman filter fed with measurements from GPS Monitoring Network. This theory is based on two capstones: the idea of a "corrected clock" and the concept of "transparent variations".

Each physical clock in the system (note, that originally only satellite clocks were considered) can be thought of as a representation of an ideal (or perfect) clock:

$$\xi_i(t) = \xi_0(t) + \mathbf{x}_i(t) \qquad \text{Eq. 4-10}$$

ξ_i - state (vector) of i-th clock,

ξ_0 - state (vector) of the ideal clock,

$\mathbf{x}_i$ - deviation (vector) of the physical clock from the ideal clock ([Brown91] calls it clock bias).

Clock biases are of fundamental importance in GPS, since this is basically what user gets as satellite clock parameters in GPS navigation message.

Clock states can be represented using the usual two or three states models. The two-state model – as used in [Brown91] – is given as follows:

$$\xi_i(t_{k+1}) = \begin{bmatrix} \xi(t_{k+1}) \\ \nu(t_{k+1}) \end{bmatrix}_i = \begin{bmatrix} 1 & t_{k+1} - t_k \\ 0 & 1 \end{bmatrix} \begin{bmatrix} \xi(t_k) \\ \nu(t_k) \end{bmatrix}_i + \begin{bmatrix} w_\xi(t_k) \\ w_\nu(t_k) \end{bmatrix}_i \qquad \text{Eq. 4-11}$$

here

ξ_i and ν_i are phase and frequency of a physical clock,

w_ξ and w_ν two independent white noise process with noise densities of q_ξ and q_ν.

The state transition matrix is, thus, $\boldsymbol{F}_i = \begin{bmatrix} 1 & t_{k-1} - t_k \\ 0 & 1 \end{bmatrix}$, and the process noise vector $\mathbf{w}_i(t_k) = \begin{bmatrix} w_\xi(t_k) \\ w_\nu(t_k) \end{bmatrix}$.

The process noise covariance matrix is assumed to depend only on the time interval between consequent state estimates $\tau = t_{k+1} - t_k$ (stationary process)

$$\mathbf{Q}_i(\tau) = \begin{bmatrix} q_\xi + q_\nu \dfrac{\tau^3}{3} & q_\nu \dfrac{\tau^2}{2} \\ q_\nu \dfrac{\tau^2}{2} & q_\nu \tau \end{bmatrix}_i \qquad \text{Eq. 4-12}$$

By definition, the ideal clock has no process noise w_ξ and w_ν, and thus also q_ξ and q_ν, are essentially zeros).

A system of n clocks can be represented in terms of the state space as

$$\Xi(t_{k+1}) = \mathbf{F}(t_{k+1})\Xi(t_k) + \mathbf{w}(t_k) \qquad \text{Eq. 4-13}$$

here

$$\mathbf{\Phi}(t_k)=\begin{bmatrix}\mathbf{\Phi}_1(t_k) & 0 & \cdots & 0\\ 0 & \mathbf{\Phi}_2(t_k) & \cdots & 0\\ \cdots & \cdots & \cdots & \cdots\\ 0 & 0 & \cdots & \mathbf{\Phi}_n(t_k)\end{bmatrix},$$

$$\mathbf{\Xi}(t_k)=\begin{bmatrix}\xi_1(t_k)\\ \xi_2(t_k)\\ \cdots\\ \xi_n(t_k)\end{bmatrix}, \text{ and } \mathbf{w}(t_k)=\begin{bmatrix}\mathbf{w}_1(t_k)\\ \mathbf{w}_2(t_k)\\ \cdots\\ \mathbf{w}_n(t_k)\end{bmatrix}.$$

The process noise covariance matrix is given by

$$\mathbf{Q}(\tau)=\begin{bmatrix}\mathbf{Q}_1(\tau) & 0 & \cdots & 0\\ 0 & \mathbf{Q}_2(\tau) & \cdots & 0\\ \cdots & \cdots & \cdots & \cdots\\ 0 & 0 & \cdots & \mathbf{Q}_N(\tau)\end{bmatrix} \qquad \text{Eq. 4-14}$$

Eq. 4-10 can be also extended to a system of n clocks:

$$\mathbf{\Xi}(t_k)=\mathbf{M}\xi_0(t_k)+\mathbf{x}(t_k) \qquad \text{Eq. 4-15}$$

here

$$\mathbf{M}=\begin{bmatrix}\mathbf{I}\\ \mathbf{I}\\ \cdots\\ \mathbf{I}\end{bmatrix}, \text{ where } \mathbf{I}=\begin{bmatrix}1 & 0\\ 0 & 1\end{bmatrix}, \text{ and}$$

$$\mathbf{x}(t_k)=\begin{bmatrix}\mathbf{x}_1(t_k)\\ \mathbf{x}_2(t_k)\\ \cdots\\ \mathbf{x}_N(t_k)\end{bmatrix}.$$

The clock states cannot be measured directly, only differences of clocks are observable. In a system of N clock, N-1 differences can be measured. Measurement equation is given by

$$\mathbf{z}(t_k)=\mathbf{H}\mathbf{\Xi}(t_k)+\mathbf{v}(t_k) \qquad \text{Eq. 4-16}$$

here

$\mathbf{z}$ - vector of measured clock differences,

$\mathbf{H}$ - observation matrix which elements are defined as follows:

$$h_{i,j}=\begin{cases}1 & \text{if j - th measured clock difference includes i - th clock with "+" sign}\\ -1 & \text{if j - th measured clock difference includes i - th clock with "–" sign},\\ 0 & \text{if j - th measured clock difference does not include i - th clock}\end{cases}$$

$\mathbf{v}$ - observation noise (assumed to be white Gaussian).

Due to specific structure of the matrix $\mathbf{M}$ states of the ideal clock are not observable, i.e. measurements are independent from states of the ideal clock:

$$\mathbf{H}(t_k)\mathbf{F}(t_k)\mathbf{M}\equiv 0 \qquad \text{Eq. 4-17}$$

This property of the ideal clock leads to the concept of transparent variations. Transparent variations are defined as such changes in the states of a clock system which has no effect on measurements at any time.

A matrix of transparent variations $\mathbf{\Lambda}$ is called complete if any transparent variation can be expressed as $\mathbf{\Lambda A}$ for arbitrary $\mathbf{A}$. A complete matrix $\mathbf{\Lambda}$ is called minimal if it ceases to be complete after one of its columns is deprived. A minimal complete matrix of transparent variations is not unique. Matrix $\mathbf{M}$ is an example of such matrix.

Presence of transparent variations in the estimation problem leads to the presence of unobservable components in the covariance matrix $\mathbf{P}$ of the filter estimates:

$$\mathbf{P} = \breve{\mathbf{P}} + \mathbf{\Lambda A A \Lambda} \qquad \text{Eq. 4-18}$$

here $\breve{\mathbf{P}}$ is observable component of the covariance matrix.

The unobservable component $\mathbf{\Lambda A A \Lambda}$ of the covariance matrix has no impact on the gain of the Kalman filter. Thus, it does not represent a theoretical problem, but in practice, elements of $\mathbf{P}$ grow unbounded and the filter operations meets numerical problem (singularity of $\mathbf{P}$ to the working precision).

[Brown91] discusses to possibilities to solve this problem could be solved in two ways: either through a decomposition of the covariance matrix or through an introduction of pseudo-measurements.

Decomposition of covariance matrix aims on separating the observable and unobservable components of covariance matrix. [Brown91] proposes the following decomposition

$$\breve{\mathbf{P}} = \mathbf{P} - \mathbf{M}\left(\mathbf{M}^{\mathrm{T}}\mathbf{P}^{-1}\mathbf{M}\right)^{-1}\mathbf{M}^{\mathrm{T}} \qquad \text{Eq. 4-19}$$

Following the decomposition, $\breve{\mathbf{P}}$ should be fed into the Kalman filter instead of the original covariance matrix $\mathbf{P}$. The term $\mathbf{M}\left(\mathbf{M}^{\mathrm{T}}\mathbf{P}^{-1}\mathbf{M}\right)^{-1}\mathbf{M}^{\mathrm{T}}$ is shown to have the meaning of the combination $\mathbf{\Lambda A A \Lambda}$ discussed above. The matrix decomposition operation prevents the unbounded growth of the covariance matrix making the filtering problem numerically stable.

The overall structure of GPS Composite Clock Kalman filter is illustrated in the following figure.

The composite clock algorithm works properly provided that all contributing clocks have similar stability. In this case the frequency stability of the implicit mean (Allan Deviation) $ADEV_{im}$ can be assessed as follows:

$$ADEV_{im}(\tau) = \frac{ADEV_0(\tau)}{\sqrt{n}} \qquad \text{Eq. 4-20}$$

where $ADEV_0$ is the Allan Deviation of an individual clock in the ensemble, and n is the number of the clocks.

In case if the stability of the clocks in the ensemble is considerably different (like an order of magnitude or more), the composite clock algorithm will face numerical problems.

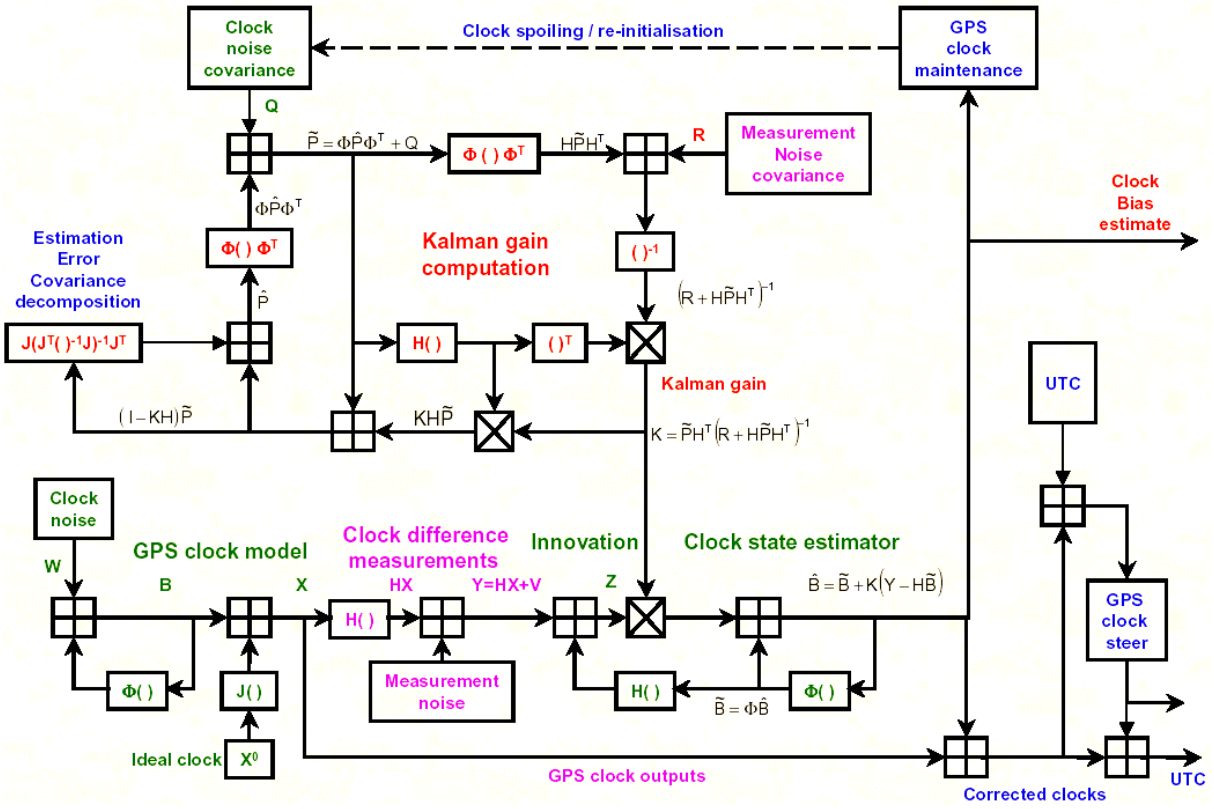

Figure 4-1. GPS Composite Clock Kalman filter [Stansfield01]

4.1.2.2 Performance

As explained in Section 4.1.2.1, GPS Time is generated as an implicit mean of clocks within the GPS system in the Kalman filter running at the GPS Master Control Station. GPS Time is available only through corrections to physical GPS clocks (satellite or ground) computed within the filter. The original paper [Brown91] assumes that all clocks in the GPS ensemble are equally weighted. However, the operational version of the Composite Clock deals with unequal clock weights and includes clocks of both GPS satellites and Monitoring Stations [Mobbs97]. GPS Time is steered to UTC(USNO) on daily basis using a "bang-bang" technique by applying relative frequency rate corrections of $\pm 1 \cdot 10^{-19}$. Over the last several years GPS Time was kept within a few tens of nanoseconds from UTC(USNO) and UTC.

Due to the lack of an explicit representation and a relatively high noise of broadcast satellite clock corrections (about 5-7 ns (1sigma)), it is not straight-forward to estimate the stability of GPS Time. USNO is continuously monitoring its offset to UTC(USNO) by collecting GPS observation with a GPS time receiver installed at USNO premises. These observations are averaged on a daily basis – that strongly reduces the effect of the measurement noise – and further used to estimate the stability of GPS Time. Such estimates are available e.g. in [Hutsell02] (the blue line in Figure 4-2). This approach, however, does not allow estimation of the short-term performance of GPS Time.

Another way to assess the performance of GPS Time – at least, approximately – is discussed in [Hutsell94] and [Brown91]. Their solution makes use of the fact that GPS Time is a weighted average of GPS clocks. Knowing the number of contributing clocks and individual clock stabilities and weights, it is easy to estimate the stability of GPS Time. We tested this approach using recent results on the GPS satellite clock stability from [Oaks03] and computed Allan Deviation (ADEV) of GPS Time under assumption that it is produced from satellite clocks only (solid green line in Figure 4-2). Further, we simulated GPS Time according to the Allan Deviation and applied a bang-bang steering (dashed green line in Figure 4-2). These results match relatively well with the measured GPS Time performance.

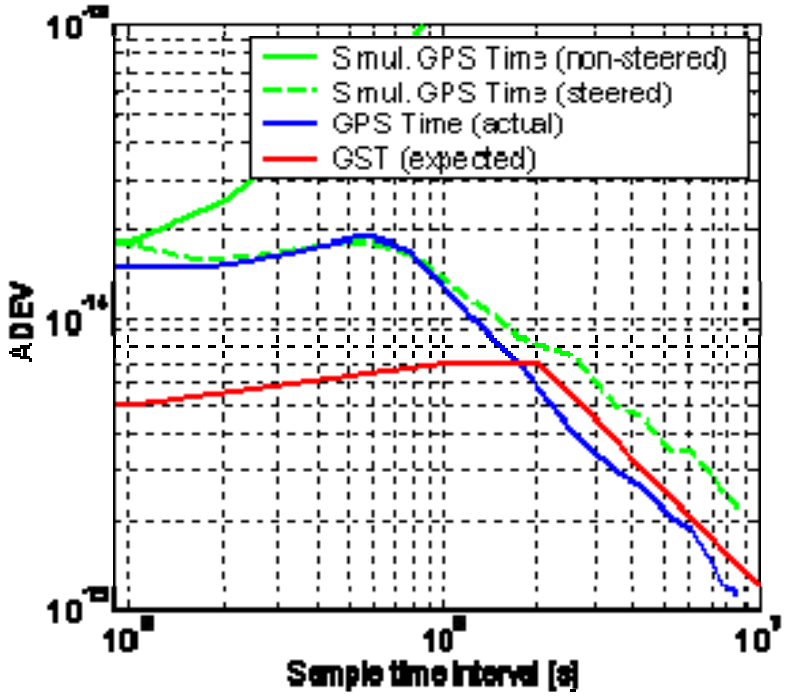

Figure 4-2. Stability of GST and GPS Time

The GPS Interface Requirements Document [GPSICD] states that GPS Time has to be steered within 1 microsecond to UTC(USNO). In practice, over the last years GPS Time was kept within a few tens of nanoseconds from it: +/- 22 ns for the period from 1 Oct 2000 until 30 Sep 2002 [Hutsell02] and +/- 18 ns in Feb-Jul 2004 [USNOWeb]). UTC(USNO) itself is steered to UTC. The residual offset was kept within +/- 19 ns in 2002, +/- 13 ns in 2003 (RMS value: 4.8 ns), and -22 – +6 ns in Jan – Jun 2004 (RMS value: 6.9 ns) according to Circular T of BIPM.

GPS Standard Positioning Service (a single-frequency service) (SPS) Performance Standard [GPSPS] defines that GPS has to provide the accuracy of user synchronization to UTC(USNO) of 40 ns (95%). This requirement refers to contributions of GPS Signal-In-Space only. [Hutsell02] demonstrates the accuracy of synchronization of UTC(USNO) for static users of the dual-frequency military GPS receiver to be 5.8 ns (1sigma).

4.2 Basic time restitution techniques

4.2.1 Overview of time restitution techniques

The term “time restitution” is utilized here with respect estimation of the offset between the user clock and the GNSS system time (or TAI/UTC as provided by this GNSS). The more common term “time dissemination” is understood as provision of information which enables user access to selected timescale. Hence, dissemination is a GNSS function, and restitution is a part of user processing.

Time restitution techniques can be classified either according to the moment when computations are performed or according to the algorithm used for the computations. Algorithms can be applied both in real-time and offline except for the case when they require specific external products (e.g. precise ephemeris from IGS) which are available only offline. Classification according to the moment of processing is as follows:

- Online (real-time) techniques, and
- Offline (post-processing) techniques.

Classification according to the algorithm:

- Snap-shot coordinate and time solution,
- Filtered or smoothed coordinate and time solution.

The snap-shot techniques are typically used in applications with high user dynamic and/or applications with environments with considerable observation obstructions. Sometimes, they are also employed in initialization mode of user operation. Another important application of snap-shot techniques is system design and analysis. Unlike filtering/smoothing techniques, snap-shot techniques utilize only the information from single observation epoch without using previous observations.

A shot review of snap-shot and filtering techniques preceded by a summary of satellite observation models follows.

4.2.2 Satellite observations

4.2.2.1 Pseudorange observations

There are two basic types of satellite measurements which are typically utilized in user applications: pseudorange and carrier phase measurements.

Pseudorange measurements are the main product offered by navigation system to its users, thus the navigation services described in GPS, GLONASS and coming Galileo Interface Control Documents (ICD) are based solely on these measurements. Pseudorange measurements are made by analyzing the correlation of two versions of the pseudorandom code: one coming from a navigation satellite and another one generate in the receiver. The time delay between these two code versions characterizes the signal propagation time and the relative time offset between the satellite and the local (receiver) clocks.

Carrier phase measurements are 10 times or even more accurate than the pseudorange ones. They are made by comparing the relative phase of the carrier of the satellite and the local (generated in the receiver) signals. Carrier phase measurements are widely used in scientific applications and surveying.

Other types of available observable (like Doppler shift measurements) are usually taken into account only for specific applications.

Generally, pseudorange measurement $d_{i,j}$ can be considered as a sum of a deterministic parameters and measurement noise. The observation equation written below is adapted for timing applications: it refers to the reference point of a laboratory timescale and not to the receiver clock as usually (i.e. the calibration biases Dly_i are also considered):

$$d_{i,j} = \left|\mathbf{r}_j - \mathbf{r}_i\right| - c \cdot \left(\Delta t_j - \Delta T_i\right) + Ion_{i,j} + Trp_{i,j} + Rel_{i,j} + Dly_i + \varepsilon_{i,j} \qquad \text{Eq. 4-21}$$

The right side of this equation includes eight terms:

- geometric distance between user and satellite (which depends on the position of satellite $\mathbf{r}_j$ and the user $\mathbf{r}_i$) ,
- time offset ΔT_i between the laboratory timescale and reference time scale (e.g. GPS-time),
- time offset Δt_j between the satellite timescale and the system timescale (e.g. GPS-time),
- ionospheric delay $Ion_{i,j}$,
- tropospheric delay $Trp_{i,j}$,
- relativistic effects Rel_i ,

- cable and hardware delays Dly_i between the reference point of the laboratory time scale and receiver antenna,
- other measurement errors (multipath, interference, receiver noise…) $\varepsilon_{i,j}$.

4.2.2.2 Phase observations

The observation equation for carrier phase measurements ϕ can be written as

$$\phi_{i,j} = \frac{1}{\lambda}\left(\left|\mathbf{r}_j - \mathbf{r}_i\right| - c\cdot\left(\Delta t_j - \Delta T_i\right) + Ion_{i,j} + Trp_{i,j} + Rel_{i,j} + Dly_i\right) + N_{i,j} + \varepsilon_{i,j} \qquad \text{Eq. 4-22}$$

where λ is the wavelength of the carrier and N is the integer ambiguity.

Effectively N is an unknown number of cycles λ since the receiver is able to measure only the fractional carrier phase offset. If no tracking problems occur, N can be taken as a constant referenced to the start of a satellite track (as observed by a user receiver), and the changes of the number of cycles since this moment will be measured by the receiver.

Estimation of N is typically called ambiguity resolution and requires advanced processing techniques and observations from at least two sites. This problem has up to now prevented wide utilization of carrier phase measurements in timing applications. Recent works of IGS on estimation of station and satellite clocks using carrier phase measurements from the IGS network pave the way to improvement of this situation.

4.2.3 Snap-shot position and time solution

Snap-shot position and time (PT) solution utilizes only of the set of measurements collected at the epoch for which this solution is made. Modern navigation algorithm in user receivers utilizes more sophisticated techniques which rely also on the measurements collected prior the epoch where the navigation solution is made. Nevertheless, the snap-shot PT solution is still important to initialize the receiver (after switching on or a loss of satellite visibility). Also, the snap-shot PT solution is widely used in system analysis, for example, Galileo and GPS programmatic documents ([GPSSPSPS] for GPS) specify accuracy, integrity, continuity and availability only for the snap-shot PT solution.

There are several versions of the snap-shot PT solution; here we consider the one based on the least-mean squares principle which makes use of only pseudorange measurements. It is also used in Galileo. The solution is basically the same for navigation users and for timing users at an unknown position.

As shown in Section 4.2.2.1, pseudorange observation can be presented as a function of eight parameters:

$$d_{i,j} = f\left(\mathbf{r}_j, \mathbf{r}_i, \Delta T_i, \Delta t_j, Ion_{i,j}, Trp_{i,j}, Rel_i, Dly_i\right) + \varepsilon_{i,j}, \qquad \text{Eq. 4-23}$$

It is assumed that ionospheric and tropospheric delays and relativistic effects are computed using suitable models (or dual-frequency data for the ionospheric delay). The satellite position and clock offset are taken as known either from broadcast navigation message (for online applications) or other sources (e.g. precise GPS ephemeris and clocks from IGS which can be used for off-line processing). Cable and hardware delays are assumed to be known – this term is not important for navigation applications, these delays are just considered to be zero. The influence of other error sources is typically not modeled and presents observation noise. Under these assumptions, we have four unknowns in Eq. 4-23: receiver coordinates and time offset, but also for these parameters some preliminary assumptions are need to be available.

Thus, for all parameters in Eq. 4-23 at least preliminary assumptions are available. It allows to model pseudorange measurements:

$$\tilde{d}_{i,j} = f\left(\tilde{\mathbf{r}}_j, \tilde{\mathbf{r}}_i, \Delta\tilde{T}_i, \Delta\tilde{t}_j, \tilde{Ion}_{i,j}, \tilde{Trp}_{i,j}, \tilde{Rel}_{i,j}, \tilde{Dly}_{i,j} \right). \qquad \text{Eq. 4-24}$$

Following the usual approach, observation residuals $l = d_{i,j} - \tilde{d}_{i,j}$ can be considered in terms of a linear transformation of the unknown parameters (user coordinates and time). The measurement model is then given by the following equation

$$\mathbf{l} = \mathbf{G}\mathbf{u} + \boldsymbol{\varepsilon}, \qquad \text{Eq. 4-25}$$

where

$\mathbf{l} = \begin{pmatrix} l_1 & l_2 & \dots & l_n \end{pmatrix}^T$ - vector of residuals (indexes correspond to the order number of residual, n is the total number of available observations),

$\mathbf{G}$ - projection matrix which defines the relationship between residuals and the state-space parameters,

$\mathbf{u}$ - user position and time vector (corrections to a priori values of coordinates and time offset),

$\boldsymbol{\varepsilon} = \begin{pmatrix} \varepsilon_1 & \varepsilon_2 & \dots & \varepsilon_n \end{pmatrix}^T$ - vector of measurement noise (in fact, it is a combination of modeling errors (e.g. ephemeris and clock errors or tropospheric correction uncertainty etc) and the actual receiver measurement noise).

User position is typically expressed in the coordinate system most natural (or convenient) for certain user application. The most popular choice is either ECEF Decart system (X, Y, Z coordinates) or ECEF geodetic system (latitude, longitude and altitude (BLH)). In the system analysis, geodetic coordinate system is used.

$\mathbf{G}$ is often called geometry matrix since its terms depend on the relative geometry satellite-user. For user position expressed in a geodetic system, $\mathbf{G}$ is given by

$$\mathbf{G} = \begin{pmatrix} \sin A_1 \cos E_1 & \cos A_1 \cos E_1 & \sin E_1 & 1 \\ \sin A_2 \cos E_2 & \cos A_2 \cos E_2 & \sin E_2 & 1 \\ \dots & \dots & \dots & \dots \\ \sin A_n \cos E_n & \cos A_n \cos E_n & \sin E_n & 1 \end{pmatrix}, \qquad \text{Eq. 4-26}$$

here A_i and E_i are azimuth and elevation of i-th satellite observed from the considered user location.

Obviously, the system of linear equations described by Eq. 4-25 has a non-trivial solution only if the number of equations n is more or equal to 4. In the case when $n = 4$ solution is unique, no least-mean squares estimator is required. If $n > 4$, a least-mean squares estimate $\hat{\mathbf{u}}$ and the corresponding covariance matrix $\mathbf{P}$ can be computed:

$$\begin{aligned} \hat{\mathbf{u}} &= \left(\mathbf{G}^T\mathbf{G}\right)^{-1}\mathbf{G}^T\mathbf{l} \\ \mathbf{P} &= \left(\mathbf{G}^T\mathbf{G}\right)^{-1} \end{aligned}, \qquad \text{Eq. 4-27}$$

Strictly speaking, $\hat{\mathbf{u}}$ give not the user position and time bias themselves but corrections to their *a priori* values $\tilde{\mathbf{u}}$. Estimates of coordinates and time are computed then as $\breve{\mathbf{u}} = \hat{\mathbf{u}} + \tilde{\mathbf{u}}$. The *a priori* vector is used to ensure that the least-mean squares procedure converges.

If, as recommended in references [DO229C] which is also recommended for Galileo users, a weighting of satellite observations is implemented, the least-mean squares estimate is given by

$$\begin{aligned}\hat{\mathbf{u}} &= \left(\mathbf{G}^T\mathbf{W}\mathbf{G}\right)^{-1}\mathbf{G}^T\mathbf{W}\mathbf{l}\\ \mathbf{P} &= \left(\mathbf{G}^T\mathbf{W}\mathbf{G}\right)^{-1}\end{aligned}, \qquad \text{Eq. 4-28}$$

here $\mathbf{W}$ is weighting matrix.

According to [DO229C], the weighting matrix is defined as follows

$$\mathbf{W} = \begin{pmatrix} 1/\sigma_1^2 & 0 & \cdots & 0 \\ 0 & 1/\sigma_2^2 & \cdots & 0 \\ \vdots & \vdots & \ddots & \vdots \\ 0 & 0 & \cdots & 1/\sigma_n^2 \end{pmatrix}, \qquad \text{Eq. 4-29}$$

where σ_i stands for the standard deviation of measurement error corresponding to i-th pseudorange measurement.

Variances (or standard deviations) of the least mean squares estimates of user position and time are given by the following equation:

$$\operatorname{trace}(\hat{\mathbf{u}}\hat{\mathbf{u}}^T) = \operatorname{trace}(\mathbf{P})[(\mathbf{l}-\mathbf{G}\hat{\mathbf{u}})^T(\mathbf{l}-\mathbf{G}\hat{\mathbf{u}})] \qquad \text{Eq. 4-30}$$

or explicitly

$$\begin{aligned}\sigma_B &= \sqrt{\mathrm{p}_{11}}\cdot\sigma_0\\ \sigma_L &= \sqrt{\mathrm{p}_{22}}\cdot\sigma_0\\ \sigma_H &= \sqrt{\mathrm{p}_{33}}\cdot\sigma_0\\ \sigma_{\Delta T} &= \sqrt{\mathrm{p}_{44}}\cdot\sigma_0\end{aligned} \qquad \text{Eq. 4-31}$$

where $\sigma_0^2 = (\mathbf{l}-\mathbf{G}\hat{\mathbf{u}})^T(\mathbf{l}-\mathbf{G}\hat{\mathbf{u}})$ is the error variance (sometimes also called variance of the weight unit).

According to the general theory of the least-mean squares estimation, the snap-shot PT solution described above provides an unbiased, optimal (minimum variance) and consistent estimate if measurement errors are white Gaussian with zero mean [Gelb74]. In other words, probability density function f_ε of measurement errors is given by

$$\mathrm{f}_\varepsilon(\varepsilon) = \frac{1}{\sqrt{2\pi}\sigma_0}e^{-\frac{\varepsilon^2}{2\sigma_0^2}}, \qquad \text{Eq. 4-32}$$

and autocorrelation function R_ε of measurement errors is of the following form

$$\mathrm{R}_\varepsilon(i,j) = \mathrm{E}(\varepsilon_i\varepsilon_j) = \sigma_0^2\,\delta(i,j), \qquad \text{Eq. 4-33}$$

here i and j are identifiers of satellites the measurement errors correspond to, and δ is delta function defined as follows

$$\delta(i,j) = \begin{cases} 1 & \text{if} \quad i = j \\ 0 & \text{if} \quad i \neq j \end{cases} \qquad \text{Eq. 4-34}$$

4.2.4 Snap-shot position-time solution and DOP concept

From the overview of the snap-shot PT solution given in Section 4.2.2 it is easy to see that variances of the least mean squares estimates in a non-weighted solution (see Eq. 4-26) depend on two parameters: a) the relative geometry satellite-user, and b) the variance of pseudorange measurements. Here the geometry dependent factor defines how the measurement error propagates into coordinate errors. Therefore, this factor is often addressed as the Dilution Of Precision (DOP). An extensive discussion on the DOP concept and its geometrical interpretation can be found, for example, in [Parkinson96]. In practice, three types of DOPs are of interest. They correspond to the horizontal, vertical, and timing errors:

$$HDOP = \sqrt{\mathrm{p}_{11} + \mathrm{p}_{22}} = \frac{\sqrt{\sigma_B^2 + \sigma_L^2}}{\sigma_0}$$

$$VDOP = \sqrt{\mathrm{p}_{33}} = \frac{\sigma_H}{\sigma_0} \qquad \text{Eq. 4-35}$$

$$TDOP = \sqrt{\mathrm{p}_{33}} = \frac{\sigma_{\Delta T}}{\sigma_0}$$

σ_0 is often called user equivalent range error (UERE).

In case if pseudorange are weighted in the user PT solution (as recommended e.g. in [DO229C]), DOP factor loose their geometrical interpretation. Typically, they are not addressed as DOPs anymore then. However, the relations given by Eq. 4-35 remain valid also in this case.

4.2.5 Snap-shot time solution

The snap-shot time solution is utilized by users at known position. Thus, unlike the PT solution described in Section 4.2.2, the snap-shot time solution has to resolve only one unknown: the receiver time offset from the GNSS system timescale. For a non-weighted solution, estimate receiver time offset and corresponding variance are given by the following equations

$$\Delta T = \frac{\sum_{i=1}^{n}\left(d_i - \tilde{d}_i\right)}{n} = \frac{\sum_{i=1}^{n} l_i}{n}, \qquad \sigma_{\Delta T}^2 = \frac{\sum_{i=1}^{n}\left(l_i - \Delta T\right)^2}{n}, \qquad \text{Eq. 4-36}$$

where n is the number of pseudorange measurements taken at the epoch for which the receiver time offset is computed.

For a weighted solution, the following equations can be used

$$\Delta T = \frac{\sum_{i=1}^{n} w_i l_i}{\sum_{i=1}^{n} w_i}$$

$$\sigma_{\Delta T}^2 = \frac{\sum_{i=1}^{n}\left[w_i\left(l_i - \Delta T\right)\right]^2}{\sum_{i=1}^{n} w_i} \qquad \text{Eq. 4-37}$$

4.2.6 Filtering/smoothing techniques

4.2.6.1 Standard BIPM technique

Since 80-th, time transfer based on simultaneous observation of GPS satellites by remote laboratories – GPS Common View – has been a de-facto standard. First described by D. Allan and J. Barns (NBS, now NIST) [Allan80], this method was further developed in the frame of metrological time transfer. Presently, BIPM is using it as the main means to link timing laboratories contributing to TAI/UTC. GPS Common View in BIPM implementation makes use of pseudorange measurements and allows reaching the accuracy of a few nanoseconds after averaging over a few days.

The essence of GPS Common View is that two labs which are going to compare their clocks should make simultaneous navigation measurements (pseudoranges) to the same GPS satellite and exchange their data. The difference of the pseudoranges measured at the two labs (corrected for geometric delays and other propagation effects) will give the offset between their clocks.

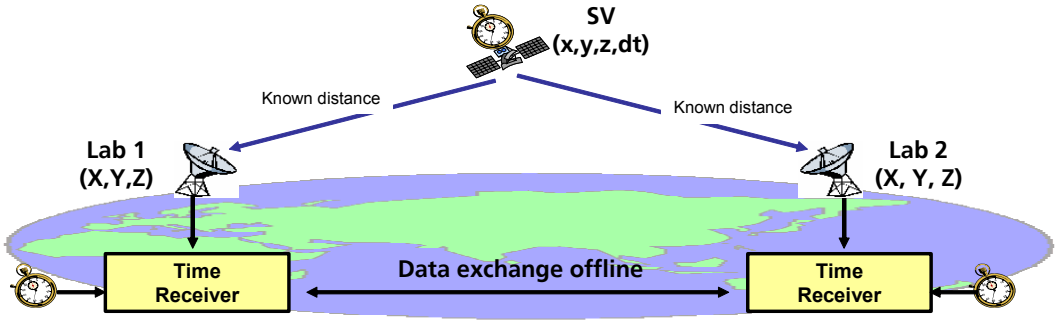

Figure 4-3 Basic principle of common view

The original measurement is the offset between the local and the satellite/system time and, and BIPM has standardized only this part of measurement and data processing which is implemented by each of the participating laboratories. Calculation of the offset between local clocks is done by the BIPM itself. Thus, the standard Common View processing can be considered as a time restitution procedure.

The original procedure described in [Allan94] was based on navigation signals provided in the frame of GPS Standard Positioning Service only (C/A-code on L1 frequency). Recent modification of GPS Common View procedure [Defraigne2003] makes also use of the signals of GPS Precise Positioning Service (P-codes on L1 and L2) which modern geodetic and timing receivers are able to utilize. However, the legal status of utilization of these signals intended for military ("authorized") users is questionable.

The revisions of the Common View procedure are described in [Defraigne03] and can be summarized as follows (see Figure 4-4):

- Data pre-processing is implemented outside receiver on a PC that collects GPS observations and satellite navigations messages (ephemeris and clock parameters) from the receiver. These data should be stored in RINEX format (daily files). The processing is implemented off-line with the help of publicly-available software (available at the FTP site of Royal Observatory of Belgium ftp://omaftp.oma.be/dist/astro/time/RINEX-CCTF).
- The classical pre-processing procedure [Allan94] is revised to adopt it for the observation rate of 30 seconds which is traditional for geodetic community. No quadratic fit to pseudoranges is used any more. The observations are corrected in the same manner as in the classical procedure, and then a linear fit to the corrected 30-second data is made. Measured ionosphere corrections computed from dual-frequency observations are used. The output data format is kept unchanged.

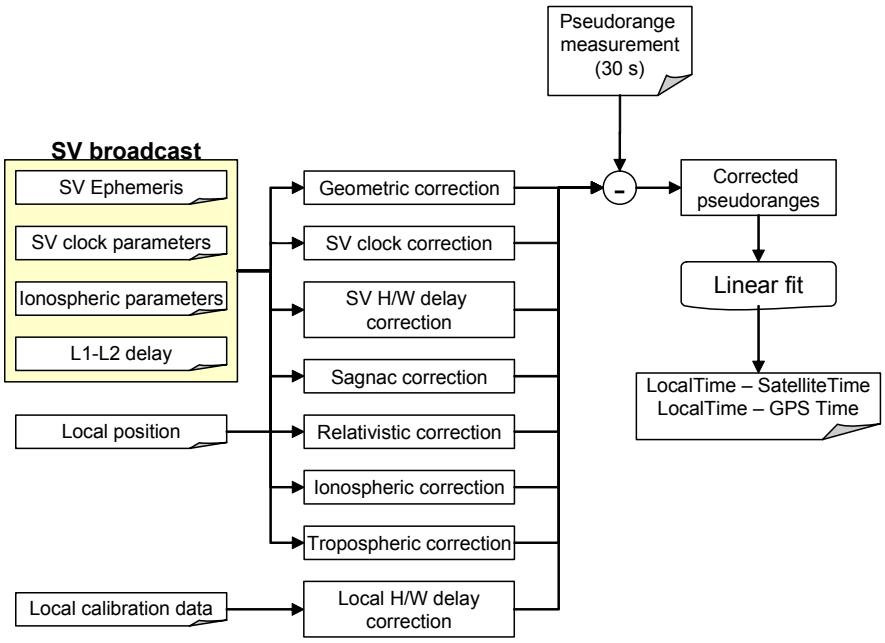

Figure 4-4. Revised common view pre-processing

The outputs of the processing are the following time offsets smoothed over 16-minute interval:

- Offsets between the local clock and the clock of the each of the observed GPS satellites,
- Offset between the local clock and the GPS system time estimated via each of the observed GPS satellites.

4.2.6.2 Kalman filter for time restitution

Implementations of Kalman filter for time restitutions have been reported by a number of authors, see e.g. [Thomas93], [Kraemer99], [Hutsell96]. This section shortly reviews these publications and presents the basic formalism of the Kalman filter.

Implementation of Kalman filter requires to describe the system being modeled (offset between two ground clocks in our case) in terms of state space and observation models. State space model is given by the following equation

$$x_k = \Phi_{k-1} x_{k-1} + w_{k-1} \qquad \text{Eq. 4-38}$$

here

x - state vector,

Φ - transition matrix,

w - process noise vector,

k and $k-1$ stand for two successive states of the system being modeled.

Observation model is given by

$$z_k = H_k x_k + v_k \qquad \text{Eq. 4-39}$$

here

z - vector of observations,

H - observation (or design) matrix,

v - observation noise.

The solution of filtering problem is given by the following equations.

$$\hat{x}_{k|k-1} = \Phi_{k-1}\hat{x}_{k-1|k-1} \quad \text{Eq. 4-40}$$

$$P_{k|k-1} = \Phi_{k-1}P_{k-1|k-1}\Phi^{T}_{k-1} + Q_{k-1} \quad \text{Eq. 4-41}$$

$$K_k = P_{k|k-1}H_k^T\left(H_k P_{k|k-1}H_k^T + R_k\right)^{-1} \quad \text{Eq. 4-42}$$

$$\hat{x}_{k|k} = \hat{x}_{k|k-1} + K_k\left(z_k - H_k\hat{x}_{k|k-1}\right) \quad \text{Eq. 4-43}$$

$$P_{k|k} = \left(I - K_{k|k}H_k\right)P_{k|k-1} \quad \text{Eq. 4-44}$$

Notation $k|k-1$ denotes estimate referring to the state k but based only on the information available at the step $k-1$. Matrices Q and R represent covariance of process and observation noise respectively

$$Q = E\left(xx^T\right)$$
$$R = E\left(zz^T\right) \quad \text{Eq. 4-45}$$

Traditionally, two (time and frequency) (see e.g. [Thomas93]) or three (time, frequency and frequency drift) (see e.g. [Hutsell96]) states are used in clock models.

Three-state model is meaningful for Rb or Quartz clocks which exhibit significant frequency drift, however its implementation calls for a more complicated form of Kalman filter. The usage of the two-state model is advisable for Cs clocks and/or H-masers and combinations of these clocks in the common view data. Further, only the filter for the latter case will be considered.

For the two-state model the transition matrix is defined as follows:

$$\Phi_k = \begin{pmatrix} 1 & t_k - t_{k-1} \\ 0 & 1 \end{pmatrix} \quad \text{Eq. 4-46}$$

Observation matrix is independent of time and is given by

$$H = \begin{pmatrix} 1 & 0 \end{pmatrix} \quad \text{Eq. 4-47}$$

At least two independent derivations of process covariance matrix exist (see [Dier84], [Brown91]). Generally, this matrix should let to account for the colored nature of the clock noise leading to non-zero correlation between process samples when the theory of Kalman filter in the form presented above assumes that both the process and the observation noises are white and Gaussian.

Processing experiments and operational experience (see e.g. [Brown91] and [Hutsell96]) has proven the implementation of the following for of process covariance matrix.

$$Q_k = \begin{pmatrix} q_1\left(t_k - t_{k-1}\right) & q_2\dfrac{\left(t_k - t_{k-1}\right)^3}{3} \\ q_2\dfrac{\left(t_k - t_{k-1}\right)^3}{3} & q_2\left(t_k - t_{k-1}\right) \end{pmatrix} \quad \text{Eq. 4-48}$$

here q_1 and q_2 are elements of the covariance matrix describing white frequency noise and frequency random walk respectively

$$\sigma_y^2(\tau) = \frac{q_1}{\tau} + \frac{q_1\tau}{3} \quad \text{Eq. 4-49}$$

Note, that for correct processing of the time transfer data which are solely differences between two clocks noise of both of them should be considered, i.e. values of Allan deviation used to compute the *q*s should referrer to the difference of the two clocks. These values can be either taken from clock specification (for new clocks) or obtained from the experience of the operation of a particular clock (e.g. from analysis of Circular T data or ensemble measurements).

Information on the observation noise (i.e. values of element of matrix R) can be taken either from practical experience or obtained from the analysis of Kalman residuals.

The filter described above can be implemented straight-forward with one channel common view receivers delivering one observation per epoch. Modern multi-channel receivers provide several (up-to-all in view) observations which allow constructing several (one per satellite in common view) differences between labs participating in the time transfer.

To solve the problem of multiple inputs, [Thomas93] proposes to compute a (weighted) average of the observations available at a certain epoch which should be further used as input (observation) for the Kalman filter.

Alternatively, [Defraigne03] proposes to skip the pre-averaging and use multi-channel observations in Kalman filter directly having observation matrix built of several rows as given in Eq. 4-47. To avoid working with variable dimensions of observation-related matrices which change depending on the number of satellites in common view [Kraemer99] proposes to fix the dimensions of H, z and R to the maximal number of observation one may expect to have (e.g. 12 if 12-channel receivers like Ashtech Z12T are used) and to use a weight matrix W in computation of Kalman gain:

$$K_k = WP_{k|k-1}H_k^T\left(H_k P_{k|k-1}H_k^T + R_k\right)^{-1} \qquad \text{Eq. 4-50}$$

Elements of W corresponding to non-existing measurements or detected outliers should be zero.

4.3 Safety and reliability in PTF design

As a provider of commercial and safety-of-life services, Galileo has to care about the quality (and especially the reliability) of its services and to take certain service guarantees. It sets high requirements to safety and reliability of the system design and individual system elements, including also PTF. To ensure these properties, the principles of the safety engineering and management should be applied to PTF design and planning of PTF operations. These principles are shortly discussed in this section. More details on system safety analysis and management can be found in [Roland90].

4.3.1 Basic system safety concepts

Safety is defined as “the condition of being free from undergoing or causing hurt, injury or loss”. *Safety in a system* can be defined according to [Roland90] as “the quality of a system that allows the system to function under predetermined conditions with an acceptable minimum of accidental loss”. In the same time, *risk* can be thought of as a measure of “the possibility of a mishap in terms of hazard severity and hazard probability”.

Early safety management programs relied on the *de facto* philosophy which included identification of accident causes and system modification to exclude them or minimize their influence. Presently, an *a priori* approach to safety management is in use which includes identification of hazards, their detailed analysis and control starting from the definition and design phases of a system life-cycle.

The primary objective of system safety is to achieve conditions when all critical hazards in the system are known and controlled to the acceptable level of harm. The term “harm” usually refers to an impact at human users and/or operators but can be also redeemed as an impact at system itself. Consequently, the objective of system safety programs is creation of

“a reasonably safe product”. The optimal or reasonable degree of safety has to be determined considering constraints like operational effectiveness, time, costs and other relevant factors. Thus, system safety is basically a balance between risks and controls.

Risks are characterized by the hazard severity and probability of their occurrence.

Category	***Name***	***Characteristic***
I	Catastrophic	Loss of system
II	Critical	Major damage to system
III	Marginal	Minor damage to system
IV	Negligible	No damage to system

Table 4-1. Classification of hazard severity

Level	***Description***	***Probability***	***Characteristics***
A	Frequent	1E-1	Likely to occur frequently
B	Probable	↕	Will occur several times
C	Occasional	> 1E-3	Likely to occur sometimes
D	Remote	> 1E-4	Unlikely but possible to occur
E	Improbable	> 1E-6	So unlikely that occurrence can be assumed no to be experienced

Table 4-2. Classification of hazard likelihood

System safety engineering employs techniques of system engineering to analyze a system as a set of interacting elements generating hazards. The goal of system safety engineering is to detect, and eliminate or control hazards.

4.3.2 Reliability calculation

The key quantities in the system reliability calculations are failure rate, mean time between failure (MTBF), reliability and availability.

Failure rate λ is “the total number of failures within an item population, divided by the total time expended by that population, during a particular measurement interval under stated conditions” [MacDiarmid]:

$$\lambda = \frac{N_{failures}}{N_{population}} \qquad \text{Eq. 4-51}$$

MTBF is the rate of the total operating time to the number of failures. MTBF has only meaning for reparable items. Assuming the failure to be constant, MTBF can be defined as

$$MTBF = \frac{1}{\lambda} \qquad \text{Eq. 4-52}$$

Reliability is defined as the probability that a component experiences no failures during a certain interval of time t given that the component was repaired to a “like new” condition or was functioning at the beginning of this time period. Reliability R is related to the failure λ rate as

$$R(t) = \int_t^\infty f(t)dt \qquad \text{Eq. 4-53}$$

where $f(t)$ is the failure probability density function.

Assuming the failure rate to be constant and the failures to be normally distributed, Eq. 4-53 can be rewritten as follows:

$$R(t) = e^{-\lambda t} = e^{-t/MTBF} \qquad \text{Eq. 4-54}$$

This equation is typically used in the practical reliability calculations.

There are two basic types of system: sequential (or serial) configuration (Figure 4-5) and parallel configuration (Figure 4-6). In practice almost all system configurations can be reduced to these two basic types by using so-called cut-sets which group sets of elements.

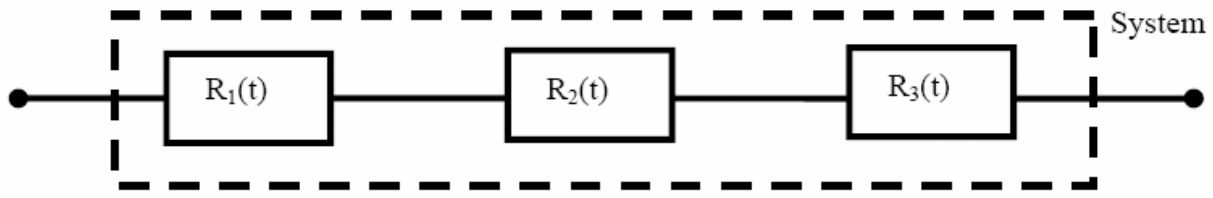

Figure 4-5. System with all elements connected in series

The reliability of the serial system in Figure 4-5 is given by the following equation:

$$R(t) = R_1(t) \times R_2(t) \times R_3(t) \qquad \text{Eq. 4-55}$$

In turn, the failure rate can be calculated as

$$\lambda = \lambda_1 + \lambda_2 + \lambda_3 \qquad \text{Eq. 4-56}$$

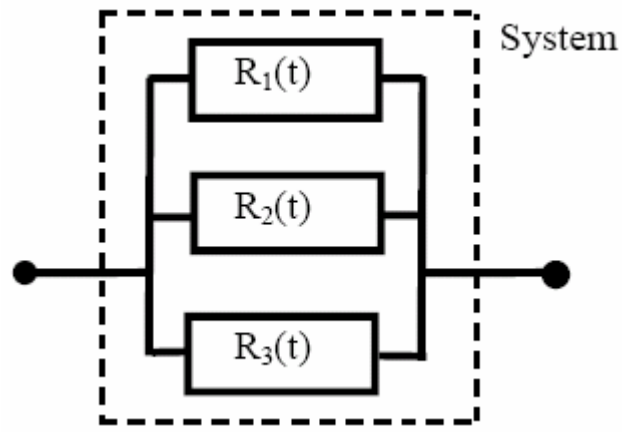

Figure 4-6. System with all elements connected in series

For the parallel configuration in Figure 4-6 reliability can be calculated as

$$R(t) = 1 - \left(\left(1 - R_1(t)\right) \times \left(1 - R_2(t)\right) \times \left(1 - R_3(t)\right)\right) \qquad \text{Eq. 4-57}$$

Eq. 4-57 can be simplified as follows

$$R(t) \triangleq R_1(t) + R_2(t) + R_3(t) + o_2 \qquad \text{Eq. 4-58}$$

here o_2 is a second order term which is typically negligible.

5 Options for Galileo system time generation

5.1 Considerations on Galileo time generation concept

5.1.1 Requirements to Galileo system time

The requirements to GST are driven by its basic functions:

- To ensure the accuracy of satellite clocks prediction,
- To ensure accuracy of UTC/TAI dissemination through Galileo.

These two types of requirements will be considered in turn.

5.1.1.1 Requirements driven by the satellite clock prediction

Galileo performance allocation foresees the uncertainty of Galileo satellite clock prediction to be less than 1.5 ns 1sigma. The update rate of broadcast navigation message shall be 100 min.

The prediction error is influenced by three main factors:

- Behavior of satellite clocks and GST,
- Selection of the prediction algorithm,
- Accuracy of determination of the offset between GST and satellite clock.

Satellite clocks and GST

The first factor, clock and time scale behavior, refers to the ability to describe evolution of the offset between the GST and a satellite clock with some (relatively simple) model. In GPS a quadratic model is in use to describe variations of the offset between GPS Time and satellite clocks corrected for relativistic effects.

The experience of GPS operations (see e.g. [Epstein03]) points out some effects on satellite clock which cannot be modeled or require careful investigations to be appropriately considered in a model:

- Steps in phase, frequency and drift,
- Relativistic effects,
- Phase excursions,
- Effects of control commands,
- Spectral (periodic) effects.

The phase, frequency and drift steps are a property of clocks. Phase steps occur extremely rare; however, frequency steps can occur with the rate of a few months or even more often and can be as large as some parts of 1E-12 on GPS-IIR Rubidiums [Epstein05]. In the same time, drift rate of GPS Rubidiums was shown to change over the clock life-time and the drift itself to exhibit random variations in some parts of 1E-14 over several days.

Some of GPS IIR Rubidiums also exhibited periodic variations of frequency and drift with the period of a few days.

Minor relativistic effects (e.g. due to satellite maneuvers) need to be corrected in the data processing (of course, first such maneuvers shall be made known to those who deal with clock predictions; however, this is a matter of operations and not of science).

Phase excursions on GPS clocks were attributed to the specific design of the phase-locked loop in the on-board time keeping system (not in the clocks themselves).

Finally, control commands, if not properly accounted in calculation of predictions, may lead to large errors.

All these errors (probably, except of phase excursions which are characteristic for GPS-IIR design) can be expected to occur also on Galileo.

Furthermore, in orbit RAFS will be subjected to variations of radiation due to satellite movement with respect to the Sun. Temperature and voltage variations can be expected to be compensated by incorporation of appropriate stabilization techniques in the RAFS design. Environmental variations and their modeling deserve a more detailed study which should rely on results of in-orbit experiments.

As for GST, since it will be defined by an output of an atomic clock (active H-maser daily steered to TAI), one may expect to observe potential anomalies of the clock behavior also in GST. Such anomalies are e.g. H-maser frequency steps which may reach the level of 1E-14 or even higher. In addition, errors due to wrong maser steering (algorithm and personnel failures) may occur.

Prediction algorithm

Selection of prediction algorithm considers mainly the model to describe the offset between a system time scale and satellite clocks and the way how the coefficients of this model are estimated.

Preliminary studies ([Delporte01], see also Section 3.2.6) have identified that a linear model allows smaller prediction uncertainty than the quadratic one. However, Allan (see [Allan87a]) has pointed out that a linear model performs better only for clocks which do not exhibit any significant drift. Typically RAFS do drift, therefore one may expect a quadratic model to be better suited for their prediction. Another alternative is still to use a linear model and to correct the RAFS drift physically (which is possible, for example, on GPS-IIR).

Of course, smarter prediction models can be employed (e.g. Chebychev polynomials tested by [Delporte01], ARIMA etc.). Selection of simple linear or quadratic model is mainly driven by the intention to make the processing at user side as easy as possible (and to avoid potential complications related to stability of more sophisticated models), and by positive GPS experiences. On top of that, preliminary structure of Galileo navigation message foresees three coefficients of a quadratic clock model to be broadcast.

Another important issue is selection of the observation period, i.e. the duration of the observation time span used to compute the coefficients of the prediction model. As shown in [Delporte01], [Allan87a] etc. optimal observation period depends on the magnitude of the observation noise, the magnitudes of different components of the clock noise (white frequency, noise, flicker noise etc.), and the selected prediction model.

Accuracy of determination of the offset between GST and satellite clock

Error of determination of the offset between satellite clocks and GST represents solely the measurement noise mentioned above. The type (spectrum) and the magnitude of this noise influence selection of the optimal prediction interval and propagate to errors in estimation of the model coefficients. Biases in the clock offset determination typically can not be corrected in the further prediction-related processing and would limit the prediction accuracy.

In Galileo the offset between satellite clocks and GST will be computed at the Orbitography and Synchronization Facility (OSPF) as a part of Orbit Determination and Time Synchronization (ODTS) procedure.

Test of the impact of GST frequency instability onto the accuracy of satellite clock prediction

A number of studies was made on prediction accuracy of Galileo RAFS during the system definition phase, see e.g. [Delporte01], [Busca03]. These studies have considered mainly prediction errors due to uncertainty of satellite clock themselves. GST requirements seem to be defined just equal to specification of an active H-maser. To test the impact of GST

instability onto the error of satellite clock prediction we simulated 50 RAFS and 50 GST representations for each of the following options:

- GST instability is the same as that of RAFS,
- GST instability is 2 times better than that of RAFS,
- GST instability is 5 times better than that of RAFS,
- GST instability is 10 times better than that of RAFS,

A prediction test with a linear and a quadratic model was made for each of the simulated pairs RAFS – GST. In addition, the case of perfectly stable GST was considered (in this case, only RAFS deviation from perfect time was to be predicted).

RAFS instability was taken according to the specification cited in Section D.4.1:

- White frequency noise: $5 \cdot 10^{-12} / \sqrt{t}$
- Flicker frequency noise: $5 \cdot 10^{-14}$
- Frequency random walk: $1 \cdot 10^{-13} \times \sqrt{t[days]}$

No frequency drift in RAFS and GST was simulated.

The simulated data covered the time span of one month with the rate of 30 s. Measurement noise of 0.3 ns (1sigma) and measurement bias of also 0.3 ns were added to the data to simulate uncertainties of the ODTS outcome. All predictions were calculated using the measurement time span of 4 hours. Two prediction intervals (6 and 12 hours) were tested.

Two kinds of prediction error (RMS) were estimated: RMS over the whole prediction interval (computed over all simulated data points which were available with the rate of 30 s), and RMS at the end of the prediction interval. The test results are presented in Figure 5-1 and Figure 5-2.

The simulation results demonstrate that the impact of GST instability onto the prediction error is negligible if GST instability is 5 or more time less than that of RAFS. It appeared to be sufficient to have GST 5 times more stable than RAFS since improvement of prediction accuracy with further increase of GST stability was found to be insignificant.

The test here was made solely with RAFS. However, its results can be also extrapolated to the passive H-maser. In general, GST has to be 5 times more stable than the most stable satellite clock to make GST impact onto the prediction accuracy insignificant. The upper thresholds for GST instability to support prediction of RAFS and SPHM are given in Table 5-1. Table 5-2 summarizes the baseline requirements on GST stability (at time intervals critical for OSPF) and stability thresholds proposed here.

As can be seen from Table 5-2, the baseline on GST stability is sufficient to enable RAFS prediction. As for SPHM, the GST stability should be somewhat improved to explore all benefits from the introduction of these clocks into the system.

The superior performance of the linear model in the prediction tests is due to absence of frequency drifts in the simulated data. In real operations of Galileo, it would be advisable to calculate the frequency drift of satellite clocks over somewhat longer time spans to reduce the uncertainty of the drift estimation, and then to subtract the drift from the clock data before the clock prediction. Preliminary, this approach seems to be feasible since as shown in [Epstein05-PTTI], drifts of GPS RAFS remained relatively stable over months with daily variations of about 1-2 parts to 10^{-14}.

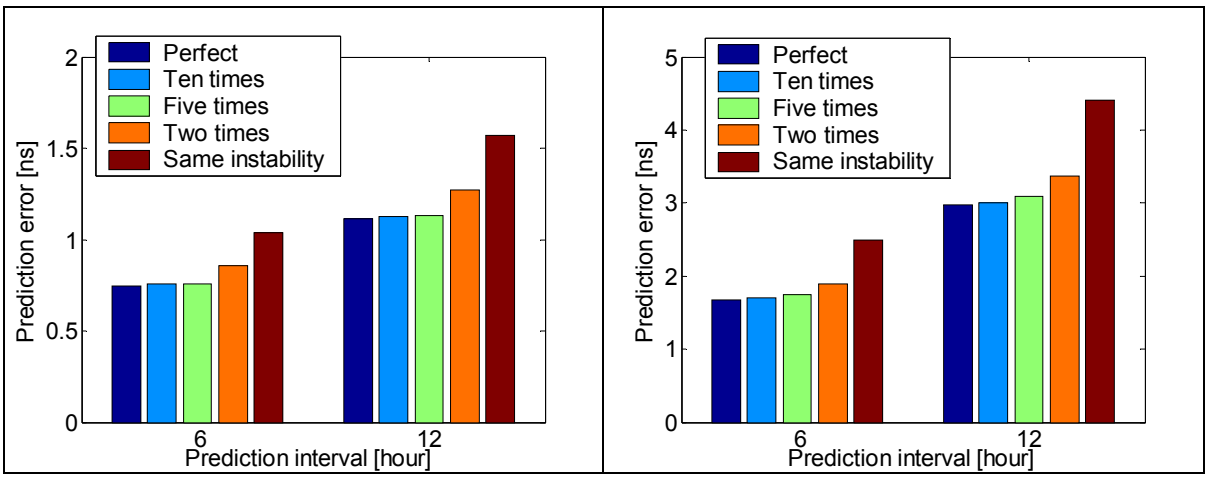

Figure 5-1. Prediction with linear (left) and quadratic (right) models (whole interval)

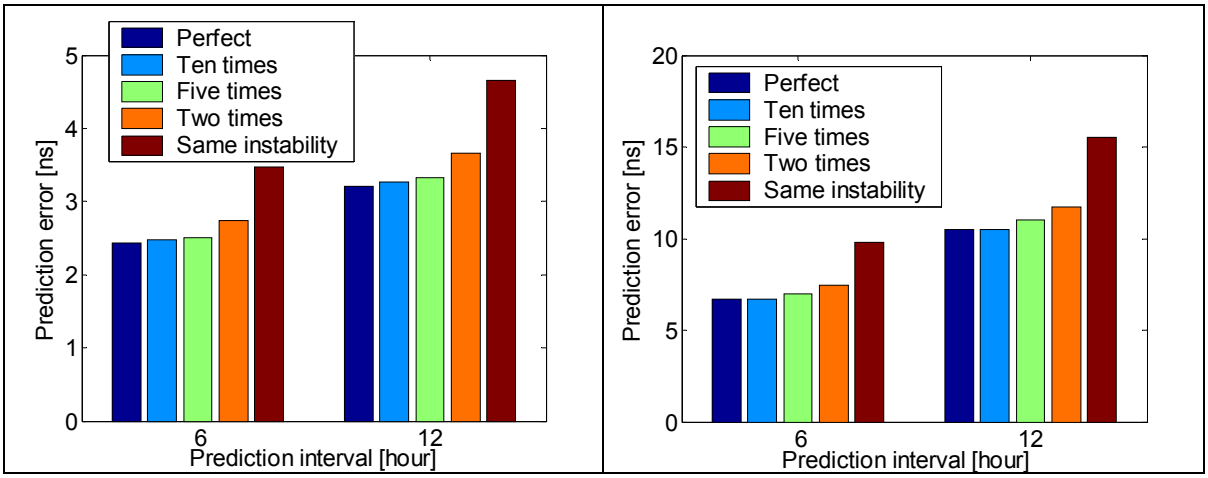

Figure 5-2. Prediction with linear (left) and quadratic (right) models (end of interval)

Process	***Maximal GST instability to ensure prediction of***	
	RAFS	***SPHM***
WFM	$1 \cdot 10^{-12} / \sqrt{t}$	$2 \cdot 10^{-13} / \sqrt{t}$
FFM	$1 \cdot 10^{-14}$	$2 \cdot 10^{-15}$
RWFM	$2 \cdot 10^{-14} \times \sqrt{t[days]}$	$2 \cdot 10^{-15} \times \sqrt{t[days]}$
Drift	$2 \cdot 10^{-14} \times t[days]$	$2 \cdot 10^{-15} \times t[days]$

Table 5-1. Maximal GST instability to ensure clock prediction accuracy

Time interval, s	***GST requirements***	***GST ADEV thresholds for***	
		RAFS	***SPHM***
100 min	1E-14	1.7E-14	3.5E-15
8 h	1.3E-14	1.2E-14	2.4E-15
24 h	6E-15	1.1E-14	2.2E-15

Table 5-2. GST frequency instability (short-term)

5.1.1.2 Requirements driven by steering to TAI/UTC

The long-term GST frequency instability shall be sufficiently low to insure its ability to meet the autonomy requirement with respect to GST-TAI offset: over 10 days of autonomous operation (GTSP not available), GST shall not accumulate more than 50 ns (95%) offset with respect to TAI and the uncertainty of GST-TAI offset shall not exceed 28 ns (95%) (see Table 3-5). This requirement is understood to refer to the additional offset accumulated over 10 days of autonomous operations over the initial value at the beginning of the autonomy period.

Following [Allan87a], in the scenario when two clocks are just freely running starting from some moment of time, their relative deviation $TDEV$ after some period of time τ would be described as follows

$$TDEV(\tau) = \tau \cdot MDEV(\tau) \qquad \text{Eq. 5-1}$$

For the averaging time of 10 days, MDEV can be considered equal to ADEV. Thus, relying on the relationship in Eq. 5-1, GST ADEV over 10 days shall not exceed 1.6E-14. This instability can be easily met assuming typical performance of a commercial Cesium clock.

The magnitude of GST-TAI offset in the nominal mode (GTSP is available) deserves a special note remark. The baseline requires it to stay under 50 ns 95% of time. In the same time the uncertainty of the offset is to be less than 28 ns (95%). Thus to ensure the offset really to stay in the specified frames, its value should be kept within 41.4 ns 95% of time (assuming Gaussian distribution of offset values). However, this performance is the responsibility of GTSP and has been demonstrated to be feasible in relevant studies.

5.1.1.3 Achievable frequency stability of GST

As was already mentioned above, the main function of GST is to provide a stable reference for prediction of satellite clocks. Therefore, it makes sense to consider GST frequency instability not inside the PTF, but at that point where GST is visible to ODTS, namely at the phase center of receiver antenna of the GSS installed at the PTF. A generalized (but a realistic) end-to-end GST generation chain is presented in Figure 5-3.

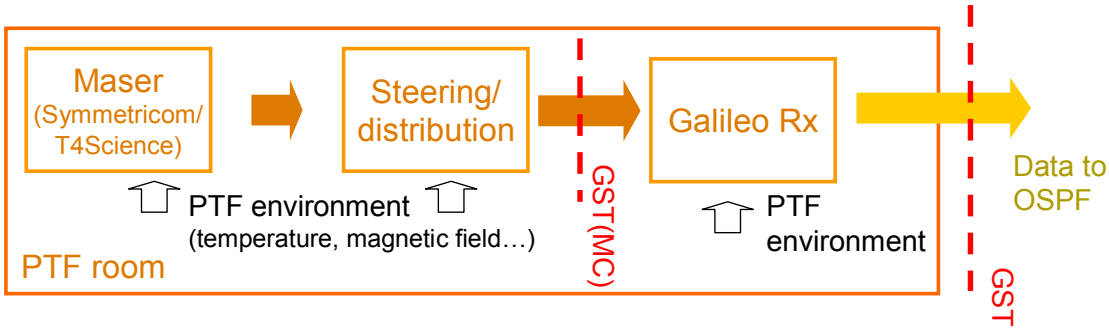

Figure 5-3. GST generation chain

Thus, GST frequency stability refers not to an individual clock, but to a time scale, which comprises the source clock, time steering and distribution equipment, cabling, receiver and antenna contributions. Also, stability of GST is affected by steering to TAI and variations of the environmental conditions at the PTF and the collocated GSS.

As shown by the practice of time laboratories, the impact of equipment in a distribution chain to the short-term stability of a timescale is typically rather low (provided that the equipment is properly selected and maintained). The impact of the distribution equipment on the short-term stability of GST was analyzed during the Galileo Phase C0 studies. The proposed short-term stability requirements are summarized in Table 5-2.

However, in Phase C0 the impact of the environmental variations in the GST distribution chain inside PTF was not investigated in details and the GSS receiver was not considered. An updated analysis of GST stability at the interval of 24 hours is presented below. Only

temperature variations at PTF and GSS are considered to significantly affect the equipment, the effect of other environmental variations (magnetic field etc.) is assumed to be negligible.

The Allan Deviation of GST at the phase center of the GSS antenna can be described by the following equation:

$$ADEV^2_{GST,antenna} = ADEV^2_{maser} + \Delta F^2 + \left(\Delta f_{maser} \cdot \Delta T_{PTF}\right)^2 + \left(\frac{\Delta d_{steeringHW} \cdot \Delta T_{PTF}}{24hours}\right)^2$$
$$+ \left(\frac{\Delta d_{distributionHW} \cdot \Delta T_{PTF}}{24hours}\right)^2 + \left(\frac{\Delta d_{PTFcabling} \cdot \Delta T_{PTF} \cdot L_{PTF}}{24hours}\right)^2 + \left(\frac{\Delta d_{Rx} \cdot \Delta T_{GSS}}{24hours}\right)^2$$
$$+ \left(\frac{\Delta d_{GSScabling} \cdot \Delta T_{GSS} \cdot L_{GSS}}{24hours}\right)^2 + \left(\frac{\Delta d_{antenna\_cabling} \cdot \Delta T_{outdoor} \cdot L_{ant}}{24hours}\right)^2$$
$$+ \left(\frac{\Delta d_{antenna} \cdot \Delta T_{outdoor}}{24hours}\right)^2 \qquad \text{Eq. 5-2}$$

here

ΔF - magnitude of the daily frequency steering correction as computed by the GTSP,

Δf_{maser} - temperature sensitivity coefficient of the maser (variation of the maser frequency depending on the temperature) (typically about 5E-15 per degree),

$\Delta d_{steeringHW}$ - temperature sensitivity coefficient of the steering hardware (variation of the hardware delay depending on the temperature) (typically negligible),

$\Delta d_{distributionHW}$ - temperature sensitivity coefficient of the distribution hardware (typically tens of picoseconds per degree),

$\Delta d_{cabling}$ - temperature sensitivity coefficient of the cabling per length unit (from 1 to 0.03 picosecond per degree per meter, here 1 ps for PTF and GSS and 0.3 ps for antenna cable),

Δd_{Rx} - temperature sensitivity coefficient of the GSS receiver (based on GPS experience, this coefficient is set to 200 picoseconds per degree),

$\Delta d_{antenna}$ - temperature sensitivity coefficient of the GSS antenna (based on GPS experience, this coefficient is set to 20 picoseconds per degree),

ΔT - magnitude of temperature variations (PTF assumption 0.2 degree, GSS assumption 1 degree, outdoor 10 degree (average)),

L – length of cabling (10 m in PTF, 10 m in GSS, 80 m outdoor antenna cable).

With the assumptions given above, the relative frequency instability of GST is 4.8E-15 per day without considering the effect of the steering corrections. Assuming the GST-to-TAI steering correction to be about 3E-15 per day (1sigma), the total GST ADEV at 1 day is 5.7E-15 which is inline with GST requirements (see Table 5-2).

Eq. 5-2 is derived under assumption that temperature continuously raises over the time span of 24 hours. In fact, the temperature will exhibit periodic variations with the average period of a few hours, so its impact on the Allan deviation will slightly differ from that described by Eq. 5-2 (see Section C.2.4 for an overview of the impact of periodic variations to the Allan deviation). However, Eq. 5-2 can be considered sufficient for preliminary analysis. Going into further details without knowing what equipment is selected for PTF and how the PTF and GSS temperature are controlled is impractical.

The analysis presented above does not consider the impact of magnetic field variations. Typically this effect is negligible, however, during the solar storms it can be considerably increased. One of the options to secure GST performance could be to use a special magnetic shielding (metal cages) to protect the H-masers.

5.2 Optimization of PTF design

5.2.1 GST failure analyses

5.2.1.1 PTF architecture

A high-level PTF architecture (see Figure 5-4) presents the major elements of the PTF. This is, however, a generalized picture which has to be transformed into a detailed PTF design which shall allow meeting the relevant requirements. One of the major challenges is to make this design robust to equipment failures to allow reliable GST generation. An example of PTF architecture is given in Figure 5-4; it does not necessarily correspond to the architecture of the operational PTF.

An analysis shows that the most critical design element is the chain AHM – GSS receiver since in this way GST is fed into the ODTS procedure. Any failure or malfunction (in general addressed further as feared events on the component level) in this chain directly affects the quality of GST and may lead to a feared event at the PTF level.

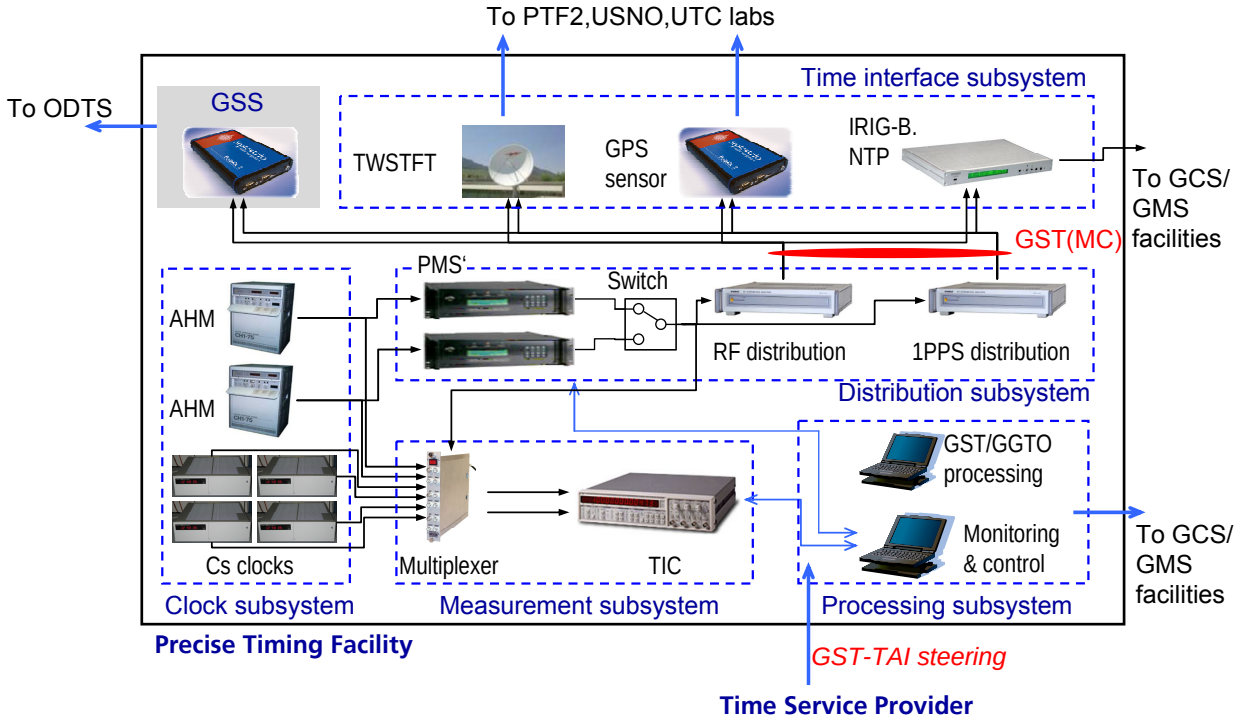

Figure 5-4. PTF high-level architecture

5.2.1.2 GST generation chain

Figure 5-5 and Figure 5-6 illustrate the GST generation chain up to the input to the GSS collocated at the PTF. Cabling, network elements and processing units are not shown in Figure 5-6. The Monitoring and Control Subsystem is also not shown in Figure 5-6 for the sake of simplicity.

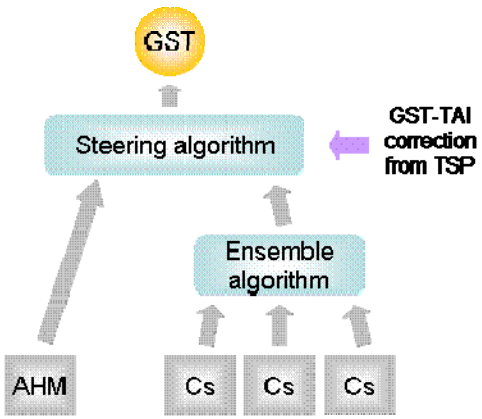

Figure 5-5. GST generation chain: overview

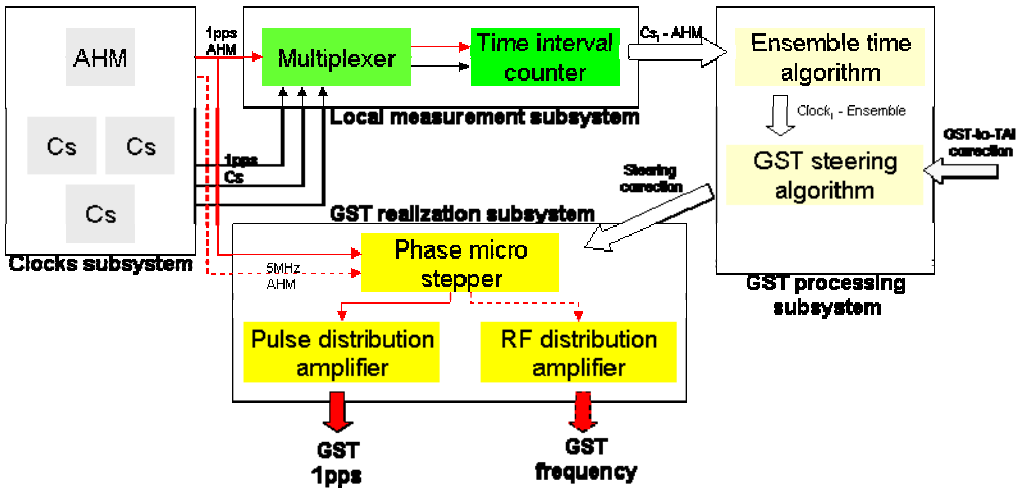

Figure 5-6. GST generation chain: physical level

5.2.1.3 *Impact of PTF component failures on GST availability and accuracy*

Here we consider a failure analysis for the PTF configuration described in Section 5.2.1.1.

Table 5-3 illustrates events on PTF elements relevant to GST generation in the context of the PTF redundancy concept (events related to Galileo and GPS receivers and TWSTFT equipment are not considered). These events were defined based on operational experience in time laboratories. The probability of events is designated as follows: “M” – medium (in order of few times a year), “L” – low (in order of one-two times during the element lifetime). The probability of certain algorithm failures cannot be presently estimated due to the lack of knowledge on failure detection procedures in these algorithms, and their verification procedure. The failures/malfunctions of the following elements are presently not considered:

- failures/malfunctions in cabling since cables typically do not produce long-lead failures if they were initially properly tested;
- data exchange interfaces between PTF hardware since we consider them to fall into the scope of AIV planning;
- data collection/device control software (needs to be included in further analysis).

Element	*ID*	*Pr*	*Event*
AHM	A1	M	Temporary malfunction (phase or frequency step), assumed to affect to both 1pps and frequency outputs
	A2	M	Degradation of performance (increase of frequency drift, increase of ADEV), assumed to effect both 1pps and frequency outputs
	A3	L	Failure of single output (one of 1pps or frequency outputs is not available)
	A4	L	Device failure (all frequency and/or 1pps outputs are not available).
Cs	C1	L	Temporary malfunction (phase or frequency step), assumed to affect to both 1pps and frequency outputs
	C2	L	Degradation of performance (increase of frequency drift, increase of ADEV), assumed to effect both 1pps and frequency outputs
	C3	L	Failure of single output (one of 1pps or frequency outputs is not available)
	C4	L	Device failure (all frequency and/or 1pps outputs are not available).
Multi-plexer		M	False switching (a wrong is connected to the device output)
		L	Degradation of performance for a single input (e.g. loose contact on the relay)
		L	Failure of single input (one of 1pps or frequency outputs is not available)
		L	Device failure (multiplexer does not function).
TIC		L	Degradation of TIC performance.
		L	Device failure (TIC does not function)
Phase micro-stepper		L	Degradation of PMS output performance (e.g. increase of noise at PMS 1pps or frequency output due to PMS hardware problems)
		L	Failure of one of PMS outputs
		L	Device failure
Pulse distributor		L	Degradation of the performance of one of pulse distributor outputs (e.g. increase or noise in terms of Allan Variance)
		L	Failure of one of pulse distributor outputs
		L	Device failure
RF distributor		L	Degradation of the performance of one of pulse distributor outputs (e.g. increase or noise in terms of Allan Variance)
		L	Failure of one of RF distributor outputs
		L	Device failure

Table 5-3. Events on PTF elements

Table 5-4 illustrates events that may occur on GST and defines their criticality for the Galileo mission (“C” – critical, “N” – non-critical).

ID	M/m	Event
GST0	-	Normal GST operation
GST 1	C	Time step more than 30 ps, relative frequency step more than 4E-15
GST 2	C	Degradation of GST short-term frequency instability in terms of ADEV
GST 3	C	Degradation of GST performance in terms of time and/or frequency offset between GST and TAI
GST 4	C	GST is not available

Table 5-4. Events on GST

5.2.1.3.1 Failure analysis

Active H-maser

Figure 5-7 illustrates the link between AHM events (as defined in Table 5-3) and the GST-level events (as per Table 5-4).

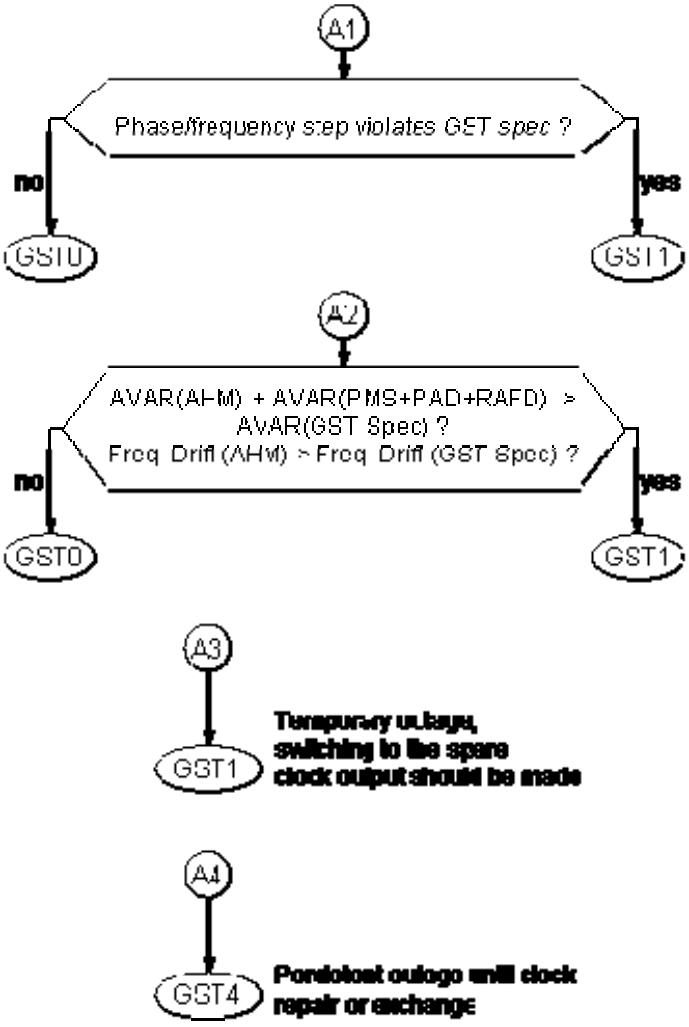

Figure 5-7. Propagation of AHM failures to GST

Phase microstepper

Any event on the phase microstepper (PMS) is directly transferred on GST physical representation in IOV configuration with one PMS. A special recovery procedure to restore

generation GST (extrapolate it from the last available data) is required for the case if PMS has to be repaired/replaced. Another option is to re-initialize GST after that. Note that to be able to detect PMS failures, both PMS output and AHM should be connected to the PTF time measurement system (multiplexer).

Degradation of PMS output performance

Depending on the type of the PMS performance degradation, this event may lead to events GST1, GST2 or GST3 (see Table 5-4) and/or a combination of these events. A phase step or a wrong frequency correction (which may be also related to a failure of personnel or PTF algorithms) can be corrected afterwards on the PMS directly or by additional steering of GST. A degradation of the output performance (e.g. increase of noise) would need the PMS to be replaced/repaired.

Failure of one of PMS outputs

A failure of either frequency or 1PPS output of PMS leads to a temporary unavailability of GST until the PMS will be repaired/replaced (event GST4).

Device failure

A complete failure of PMS leads to a temporary unavailability of GST (event GST4).

Pulse and RF distribution amplifiers

Events on pulse and/or RF distribution amplifiers directly affect the GST physical representations as distributed to PTF equipment. Recovery of GST after replacement of the pulse and/or RF amplifier would require implementation of a correction for the difference of the time delays between the new and the old (replaced) equipment.

Degradation of amplifier performance

A performance degradation may affect either a limited number of outputs (usually, it happens at one output in time) or all of the outputs. The impact of this event depends on that at which output it occurs. The following scenarios may be identified:

- Degradation of performance of the output connected to the multiplexer. Depending on the configuration of the measurement system this event may be identified as a problem on GST (PMS or AHM). To prevent it, the measurement system should be configured to be able to distinguish between AHM, PMS and distributor events: all three components should be connected to the measurement system (multiplexer). The event may become a mission critical if tests will be erroneously terminated due to a false detection of a degraded GST performance.
- Degradation of performance of the output connected to the Galileo receiver. This event will be invisible for PTF monitoring algorithms but treated by OSPF as a GST failure. A countermeasure would be either to split the signal connected to the Galileo receiver and to feed it into the measurement system, to be able to check its performance within PTF, or to organize a combined analysis of GST quality as seen by OSPF and PTF monitoring data. The event is mission critical since it will affect the performance of satellite clock parameters computed in ODTS.
- Degradation of performance of the output connected to the GPS receiver. This event will be invisible for PTF monitoring algorithms. It can be detected either by analyzing the data from the GPS receiver during computation of GGTO or by comparing GGTO computed with different techniques. As above, a countermeasure would be either to split the signal connected to the GPS receiver and to feed it into the measurement system to be able to check its performance within PTF.

Failure of one of the amplifier outputs

The impact of this failure depends on which equipment is connected to the failed output. The following scenarios may be identified:

- Failure of the output connected to the Galileo receiver

  This event leads to the situation when GST formally exists within PTF but it is not available to ODTS. The impact of this situation on generation of Galileo clock parameters depends on the time to repair for the amplifier and on the configuration of ODTS. If no spare is available at PTF "in stock", it would be a matter of weeks or at least days to obtain a new one or repair the old one. It is not known to us how ODTS can tolerate a short-term (tens of minutes to hours) interruptions of GST provision.

- Failure of the output connected to the GPS receiver

  GPS receiver at PTF will serve for time transfer (GPS Common View) with the USNO (a backup for GGTO determination) and the timing laboratories contracted by the GSTP (the backup method for linking GST to UTC). Since GPS receiver will be used for the backup time transfer method, its failure (assuming it to be repaired with the required time-to-repair) should not affect GST performance.

- Failure of the output connected to TWSTFT equipment. The failure is, probably, not critical for PTF functionality since TWSTFT links will be backed-up with other time transfer techniques. However, it could affect GST performance.

- Failure of the output connected to NTP server and IRIG-B generator. Unavailability of IRIG-B/NTP synchronization would lead to de-synchronization of GCC computers and could cause serious operational and performance problems.

A repair of an output of a distribution amplifier would require taking the whole device out of the operations leading to a temporary non-availability of GST to all PTF clients.

Device failure

Complete failure of a distribution amplifier leads to a temporary unavailability of GST to ODTS, TSP and GGTO computation procedure. NTP service will be also unavailable or will have a degraded performance.

Galileo receiver

GST will be visible to ODTS through the Galileo receiver at PTF. Degradations of receiver performance or receiver failures will be seen by ODTS as events on GST (even if the whole GST generation chain before the receiver is healthy). Therefore, we estimate failures and degradations of Galileo receiver performance to be mission critical. Note that these receiver events will be not visible to PTF monitoring function (since the processing of Galileo observation will not occur at PTF) and can be detected only in ODTS.

GPS receiver

An impact of a GPS receiver failure depends on the purpose it is used for. We assume that Common View links and GGTO computation will use the data from the same GPS receiver. A degradation of its performance will be visible at PTF since PTF makes processing of GPS data for GGTO determination and can be then detected. A degradation of the receiver performance or a receiver failure (data not available) is probably not critical since there is an independent time transfer link maintained using TWSTFT equipment. However, either failure or degradation of performance would require a receiver inspection and repair which, according to available experience, occurs at the premises of the manufactures and may take time from weeks to month.

If GPS data are used in ODTS processing (initial phase of IOV), then consideration on the failure modes of Galileo receiver will be also applicable to the GPS receiver at PTF.

5.2.1.3.2 Recommendations on PTF redundancies

The output of the Galileo receiver is of the primary interest for reliability analysis since the GST as obtained by ODTS (and as used as reference for Galileo clock prediction) refers to this point. In this section the reliability of GST will be analyzed from the point of view of ODTS considering the guidelines for reliability analysis expressed in standards MIL-STB-785B and MIL-STD-756B. Contribution of Cs clocks to the system reliability is not considered since they are used only for steering to UTC and do not directly impact the navigation function.

Equipment	***Manufacture***	***Failure rate λ [1/hour]***	
		Performance	***Availability***
H-maser	NE	1.14E-4	3.4E-5
	Symmetricom	5.7E-5	2.3E-5
	Kvarz	1.14E-4	3.4E-5
	Vremya Ch	1.14E-4	3.4E-5
	Average failure rate, λ_{maser}	1.14E-4	3.4E-5
Phase microstepper	SDI	1.14E-4	3.4E-5
	Symmetricom	5.7E-5	3.4E-5
	Average failure rate, $\lambda_{stepper}$	8.6E-5	3.4E-5
1PPS and RF distributors	Hewlett-Paccard	2.9E-5	2.3E-5
	SDI	2.3E-5	2.3E-5
	Symmetricom	2.3E-5	2.3E-5
	Kvarz	2.9E-5	2.3E-5
	Average failure rate, λ_{distr}	2.5E-5	2.3E-5
GPS Rx	Ashtech (THALES)	3.42E-4	2.3E-5
	Septentrio	1.14E-4	2.3E-5
	Average failure rate, λ_{GPSRx}	2.28E-4	2.3E-5
Galileo Rx	Average failure rate, λ_{GalRx}	2.28E-4	2.3E-5
Switch	Average failure rate, λ_{GalRx}	1.1E-5-2.3E-5 (TBC)	1.1E-5-2.3E-5 (TBC)

Table 5-5. Failure rates for candidate PTF equipment

According to the analysis of the equipment failure modes presented in Section 5.2.1.3, there are two basic types of GST failures: those affecting GST performance in terms of stability or TAI offset, and those affecting the availability of GST. This classification of failures will be also reflected in the reliability analysis. Performance failures occur during the operational life of devices as short-term or instant events, but do not require a device to be repaired/replaced (e.g. frequency steps or phase cycle-slips in H-masers). Unlike

performance failures, availability failures are related to a continuous degradation of device performance that requires the device to be replaced/repaired.

To execute the reliability analysis, equipment failure rates for each of the elements in the GST generation chain should be known. For such equipment like H-masers or phase microsteppers it is rather difficult to get a reliable value of the failure rate since only a very limited statistic is available. Also, the values differ from manufacture to manufacture. The equipment failure rates are summarized in Table 5-5. They rely to a large extent on the practical experience available in the timing community.

Based on the discussion above, several PTF configurations (with and without redundancies) can be introduced. The simplest PTF configuration with no redundancies is shown in Figure 5-8.

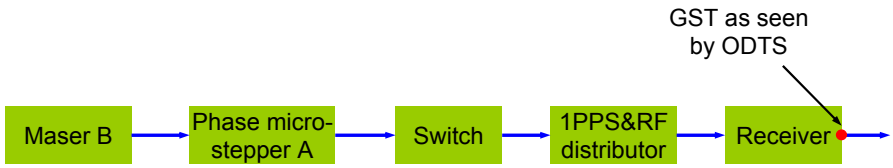

Figure 5-8. GST reliability logic block diagram (Configuration A)

Despite the fact that an estimate for the GST reliability is difficult to obtain since the reliabilities of PTF components are not well studied (see the discussion above). However, already at this point it is possible to recommend redundancies for all of the key equipment of PTF and especially for the H-maser for the following reasons:

- PTF is one of the elements on that the Galileo mission performance will depend. A failure of PTF to provide GST or a failure on GST performance may lead to an interruption of mission which may last for months since time-to-repair for some PTF equipment (e.g. H-masers) is of that order.
- A rich experience on generation of precise time is available in the timing community. However, this task is usually accomplished in manned facilities where skilled personnel is available. A lot of operations related to failure detection and handling are made to a large extent manually and rely on the experience of experts in time laboratories. In contrary, PTF will be unmanned and failure detection and handling (redundancy switching) should be made automatically. Development and implementation of such automatic procedures is a real challenge. The procedures should be thoroughly tested by reaching Galileo FOC to ensure the required level of GST performance. Thus, to collect the experience on automatic redundancy handling that is needed to ensure the proper operation of PTF and finally the ability of Galileo to fulfill its mission objective, it is strongly recommended to start the redundancy test as early as possible.
- The costs of PTF redundancies (except the clocks) are relatively low comparing with the overall Galileo costs, the procurement of redundant equipment will probably not become a critical costs factor.

Figure 5-9 presents the GST reliability logic with redundancies for the each of the key elements in the GST generation chain.

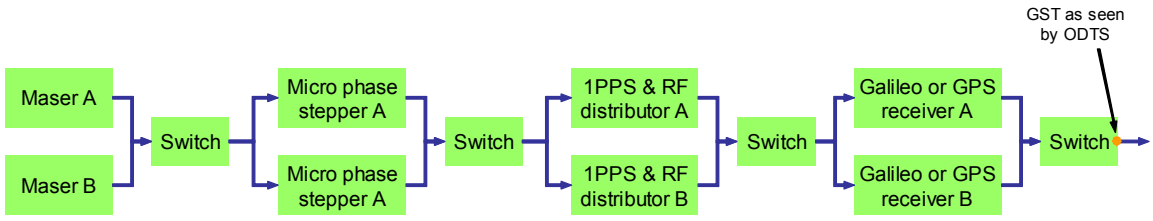

Figure 5-9. GST reliability logic block diagram (Configuration B)

The reliability logic diagram in Figure 5-9 assumes that each of the element redundancies is treated individually, i.e. there is a redundancy switch for which of the PTF elements. This approach leads to a rather complex system where the reliability of the redundancy switches themselves plays a considerable role.

Alternatively, PTF elements can be grouped in modules (logically and from the point of view of element connections), and the redundancy switching can be implemented on the level of these modules (see Figure 5-10).

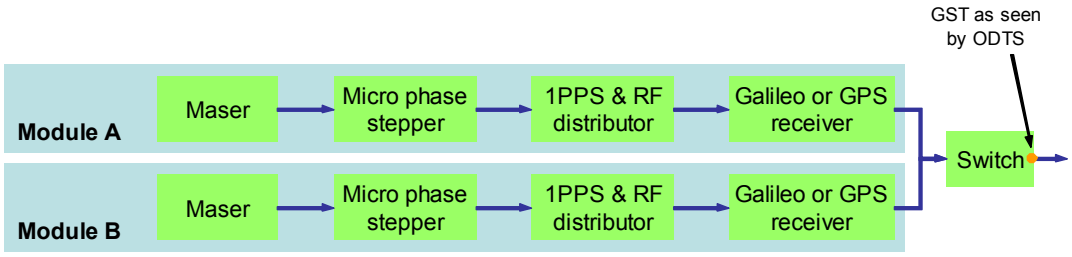

Figure 5-10. GST reliability logic block diagram (Configuration C)

Finally, the hot-spare redundancy can be implemented only for the most critical PTF elements: H-maser and phase microstepper (they also have the longest lead time). The corresponding configuration is presented in Figure 5-11. This option corresponds also to the configuration which is presently chosen in the Galileo project.

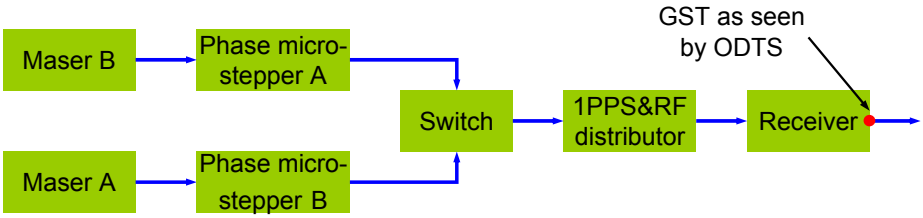

Figure 5-11. GST reliability logic block diagram (Configuration D)

Table 5-6 summarizes failure rates for performance and availability-related failures for the configurations discussed in this chapter. The failure rates are calculated under assumption of a failure-free switching between the receiver chains which is assumed to be implemented in the ODTS software.

Configuration	*Performance failure rate [1/hour]*	*Availability failure rate [1/hour]*
A	4.78E-4	1.37E-4
B	3.3E-5 - 6.9E-5	3.3E-5 - 6.9E-5
C	8E-8	6.6E-9
D	2.89E-4 - 3.01E-4	8.0E-5 - 9.2E-5

Table 5-6. Failure rates for selected PTF configurations

As can be seen from Table 5-6, configuration C is associated with the lowest failure rate. In fact, it is very much dependent on the switching mechanism implemented in ODTS (its failure rate is presently assumed to be zero). The major drawback of this configuration is shifting of the responsibility for the switching between the PTF-internal GST generation chains from the PTF itself to ODTS. This solution creates inter-dependency between the element functionalities and performance which should be carefully analyzed before this option can be chosen for implementation.

The second-best option is the configuration B. Its drawback is that switching between the PTF receivers (i.e. the detection and isolation of a receiver failure and switching to a healthy one) is still left to ODTS. Another drawback is complexity of implementation, operations and maintenance.

The failure rate associated with the configuration D is comparable with the failure rate in the configuration with no redundancies (configuration A), however, this configuration provides hot-spares for the two most critical PTF elements: H-maser and phase microstepper which time-to-repair can achieve several months. Thus, the PTF availability and mean-up-time will be also dramatically improved comparing to the “no spares” case.

In addition to the redundancies within the GST generation chain, it can be recommended to have also a redundant Local Measurement Subsystem. This is needed for the two reasons:

- a failure of the local measurement system will lead to an interruption in the program of tests on GST generation which can be in order of weeks, however, in this time GST can be generated by the H-maser directly steered to TAI which would be probably sufficient to meet the requirements to the navigation performance of Galileo;
- sometimes it is hard to distinguish between failures of local system (in terms of wrong measurements) and clock failures, simultaneous operation of two independent local measurement system would allow to unambiguously attribute these failures either to one of the measurement systems or to PTF clocks.

5.2.2 Handling of redundancies and spares

5.2.2.1 Failure handling

5.2.2.1.1 Baseline

Failure handling describes high-level measures that should be undertaken at PTF following a failure in GST generation chain (maser-stepper-distributor-receiver) to restore generation of GST and eliminate an impact on the failure on GST performance. As mentioned above, redundancy handling issues are considered to be a critical point within the GST generation scheme.

The current Galileo baseline on switching is illustrated in Figure 5-12. The switching will be executed between the outputs of the phase microsteppers. This strategy implies the PTF ability to detect a master clock failure (including the corresponding distribution chain) and to switch to the backup clock within a very short time (less than 1 ms) avoiding time and frequency steps in the PTF output.

The strict requirement to the duration of switching is driven by the consideration that the operations of the Galileo receiver collocated at the PTF shall not be disturbed. In order to avoid the deterioration of performance with respect to ODTS and the Galileo receiver at PTF, the time step after switching shall not exceed a few tens of picoseconds and the frequency step – a few parts of 1E-15.

Figure 5-12 illustrates the logic of the switching and steering involved into the GST generation. It is foreseen that one of the H-masers (AHM1a in Figure 5-12) represents GST being effectively the Master Clock for Galileo (MC). Other masers are working as hot back-ups for the MC, and the second PTF is operated on a master-slave basis with the first (or primary) one. Titles as “MC” or “primary” refer only to the role of a certain clock or PTF and do not constitute a permanent designator; these roles may change during Galileo operations as a result of switching between individual elements. The links indicating steering of AHMs to GSTR are optional, they could be used to estimate the AHM frequency drift using only PTF clocks also when GTSP is connected (link to TAI is available). The issue is still under consolidation.

Slave PTF MC will be closely steered to the master PTF MC both in time and in frequency to insure the validation of TAI parameters and GGTO following the switching between the PTFs.

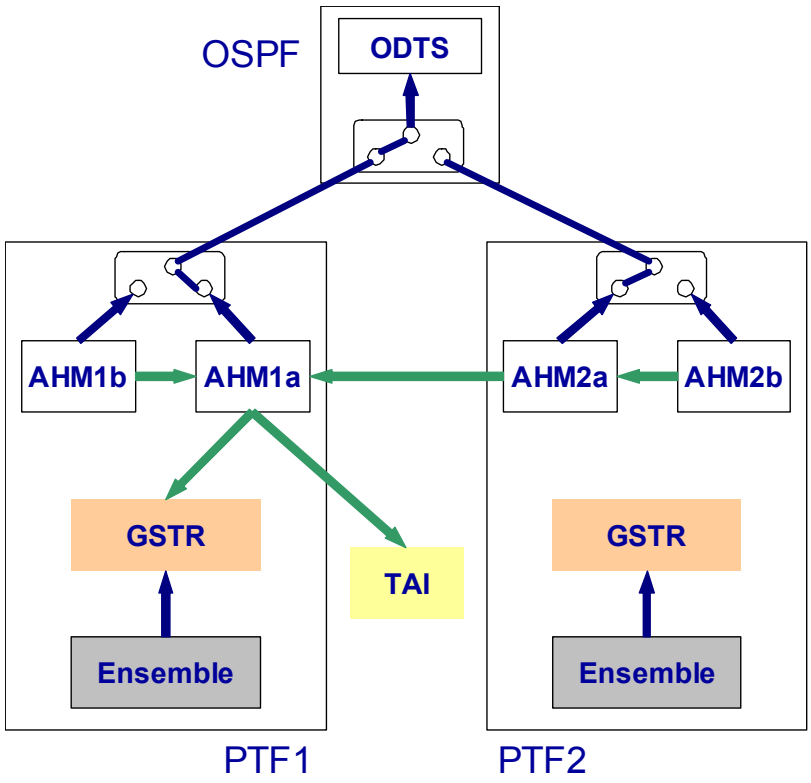

Figure 5-12. Baseline on switching and steering: concept

Minor steps in GST may still occur in this concept, since ODTS "sees" GST at the Galileo receiver, and the difference between the masers is measured at the local measurement system. To relate these two differences to the GST reference point (output of the phase microstepper), hardware delays in PTF equipment and cabling should be taken into account. As mentioned above, this step shall not exceed a few tens of picoseconds.

With the baseline design, not only hardware signals should be switched, but also a considerable amount of changes on the level of steering logic is required (see examples in Figure 5-13 and Figure 5-14).

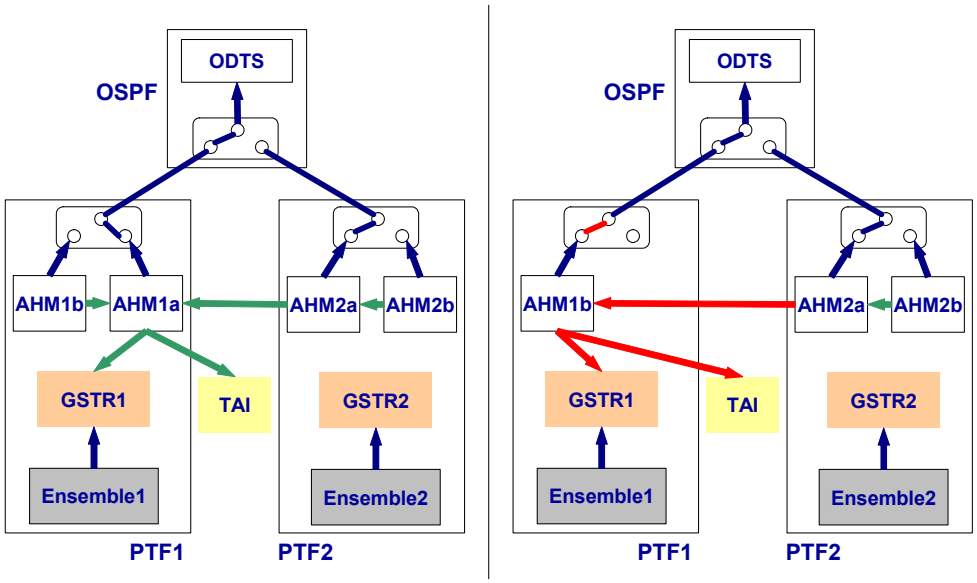

Figure 5-13. Change of steering links after switching between AHMs at Master PTF (left – nominal configuration; right – configuration after MC failure, changed steering links are shown in red)

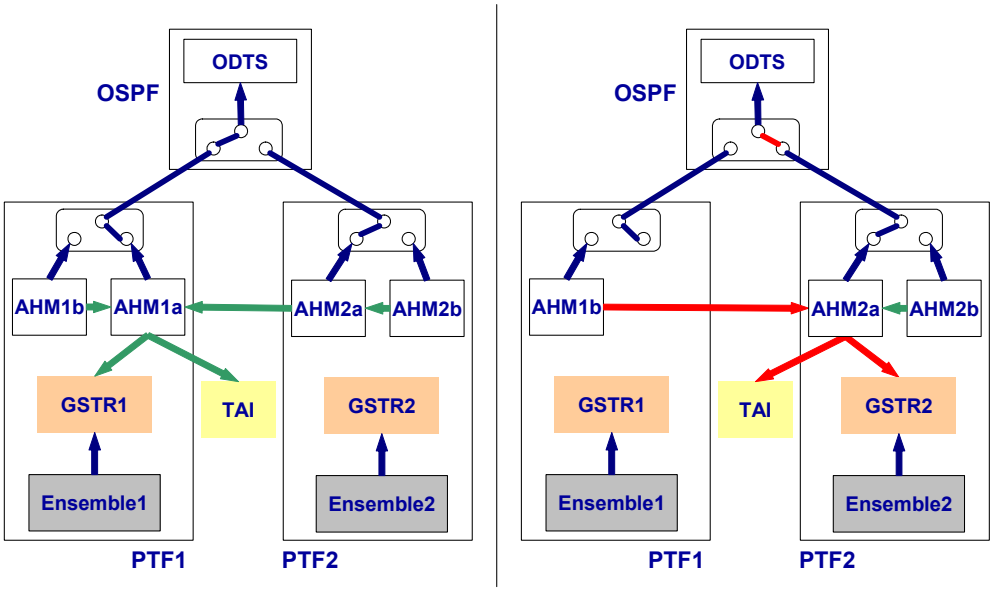

Figure 5-14. Change of steering links after switching between PTFs (left – nominal configuration; right – configuration after switching)

To avoid phase and frequency steps in GST following switching, OSPF will use a so called transition law (e.g. a third order polynomial) to correct the time and frequency offset between the GST versions produced at the two PTF. Its parameters will be determined by OSPF from the comparison of two GST versions. The software correction will be to the GST from the former slave PTF after the switching (to precisely align it with the former master). The correction will be then slowly reduced to zero according to the transition law in order to achieve that the new master PTF physically represents GST. The transition correction shall be reduced slowly enough to avoid deterioration of the clock prediction accuracy and TAI parameters (along with GGTO).

5.2.2.1.2 Alternative switching concept

The Galileo baseline concept discussed above involves two elements into the GST monitoring: PTF shall monitor the quality of GST(MC) at the PTF output, and OSPF shall monitor the quality of GST as obtained from processing of measurement from the Galileo receiver at PTF. The final GST quality (which involves the contributions of both PTF and the Galileo receiver) can be evaluated only by OSPF. In case of a receiver failure (also when the PTF at which the receiver is collocated operates normally), PTF switch needs to be executed.

To increase the GST availability, reduce the number of PTF switches and simplify PTF implementation and algorithms, the switching can be implemented at the level of modules as shown in Figure 5-10. Each module is comprised of an AHM, a phase microstepper, a 1PPS/10MHz distributor and a Galileo receiver. Thus each module effectively represents an independent GST generation chain. OSPF could process the data from all four chains (2 per PTF) designating one of them as the “master” GST. The switching can be then done in the OSPF software by moving the “master” designator to another chain (see Figure 5-15). The GST quality monitoring should be done by analyzing both the results of data processing for the PTF’s Galileo receiver and the clock monitoring information from PTFs.

Thus, the overall switching logic would become rather simple leaving individual modules and steering schemes unaffected by failures in other modules. Note that all masers are steered to GSTR as produced at the PTF where they are located, and each GSTR is individually steered to TAI.

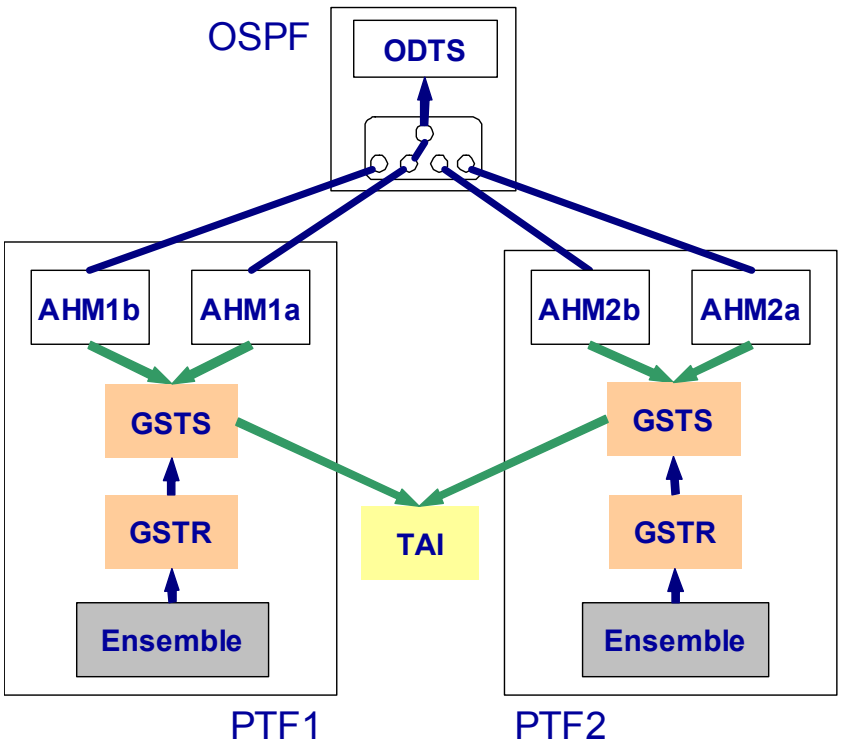

Figure 5-15. Alternative concept of switching and steering

The time and frequency offset between the GST generation chains would be somewhat higher than the offset between master and slave PTFs in the baseline (when the slave PTF MC is steered to the master PTF MC). This drawback can be compensated by dropping the transition after switching which is foreseen in the baseline concept. Only the time and frequency offset between the GST versions should be corrected after switching (to preserve the accuracy of clock prediction and TAI parameters along with GGTO). This correction should then remain unchanged. In this case all subsequent GST versions which will be put in place after the switches will be referred to the initial one (the one at the beginning of system operations). The consequence of this solution is that GST will be not directly represented by PTF and its Galileo receiver any more, but an additional phase and frequency correction should be applied to it at OSPF. This seems not to be critical for system operations. The correction is not expected to be accumulated in one direction (positive or negative) since the time and frequency offsets between the GST versions are random and can be as well positive as negative.

Hardware realization of the alternative switching scheme is illustrated in Figure 5-16 where the individual GST generation chains are marked with pink and blue. That will be no hardware switching elements on PTF, thus following a failure in one of the GST generation chain, personnel will have rather moderate time constraints for organizing repair or replacement of failed components, the overall system would than run without an impact on GST performance (but with reduced reliability until the failed chain will be repaired). Absence of hardware switching elements simplifies PTF operation and finally increases the system reliability. This design has also benefits from the verification point of view since each of the modules can be built and tested separately without disturbing the others.

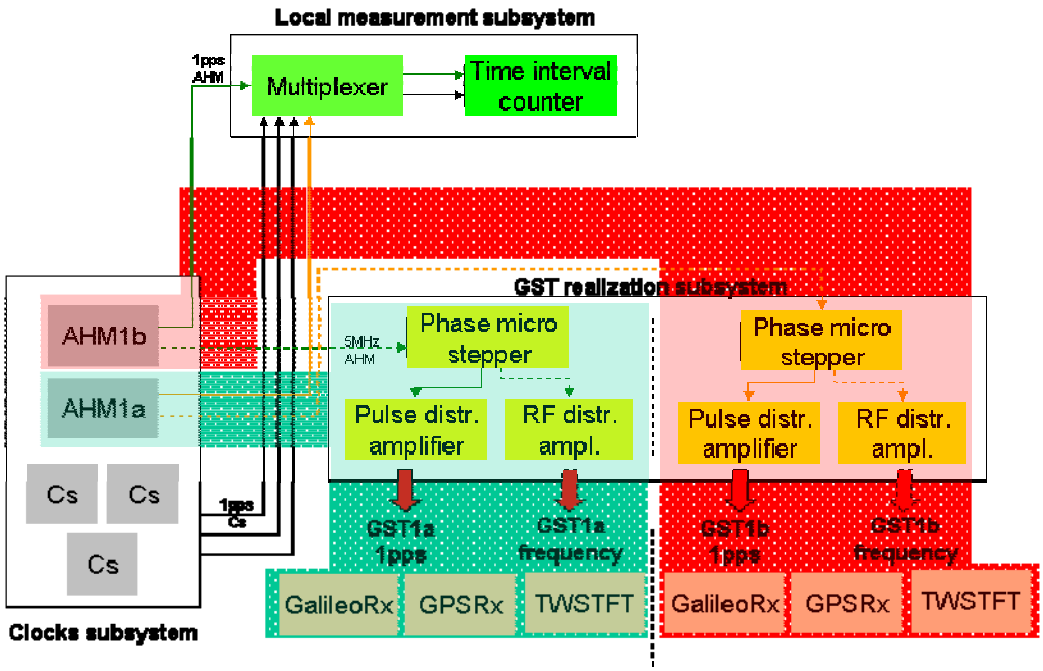

Figure 5-16. Modular architecture for the alternative switching concept

5.3 Tuning the ensemble time stability

The formalism of the weighted average algorithm is presented in Section 4.1.1. Here we look at its performance with respect to such factors as

- Stability of the ensemble time, and
- Impact of clock failures on the algorithm.

We will also try to optimize the performance of the ensemble time computed with the classis algorithm through adjustment of its parameters.

5.3.1 GSTR role and requirements

5.3.1.1 Baseline solution

In the present Galileo baseline GSTR (the paper timescale compute by PTF from its clock ensemble) is used only to ensure the ability of Galileo to provide the metrological function according to the specification in autonomous mode when GTSP is not available. Steered Master Clock is used as the reference for computation of satellite clock parameters. In other words, the short-term GST(MC) stability will be determined by the H-maser and the medium and long-term – by the stability of GSTR. This solution has been adapted since H-masers exhibit a deterministic frequency drift. The drift will be corrected using GSTR produced from Cesium clocks which frequency does not drift.

In this case the driving requirement to GSTR stability is the one coming from the metrological function of GST: the additionally accumulated uncertainty of GST-to-TAI offset shall not exceed 28 ns (2sigma) after 10 days of operations in the autonomous mode (TSP corrections are not available) (see Table 3-5). To meet this requirement GSTR ADEV shall not exceed 1.6E-14 at the averaging time of 10 days (assuming that the GST frequency is perfectly aligned with TAI at the beginning of the autonomy period).

5.3.1.2 Alternative utilization of GSTR

Alternative solution is to compute satellite clock parameters with respect to GSTR. In this case GTSR will become equal to GST which will not be determined anymore by the H-maser

output. This solution is beneficial in terms of timescale availability and robustness to clock failures. The operational scenario could be to initialize the system using the physical output of H-maser (i.e. to produce GST(MC) and GST as foreseen in the baseline), and on the next step when the system is already running to use GSTR as the basis for satellite clock prediction.

This solution would require GSTR to meet not only the long-term stability requirement discussed in the previous section, but also the GST short-term stability requirements (see Table 3-4).

5.3.1.3 Summary of GSTR requirements

GSTR requirements corresponding to the baseline and the proposed alternative are given in Table 5-7.

Time interval	*Required ADEV*	*Relevance*
100 min	1E-14	Alternative
8 hours	1.3E-14	Alternative
24 hours	6E-15	Alternative
10 days	1.6E-14	Baseline, alternative

Table 5-7. GST frequency instability (short-term)

5.3.2 Analysis of the ensemble time stability

5.3.2.1 Scenarios for ensemble time generation

There are three types of clocks which could potentially contribute to the ensemble time:

- Cesium clocks at PTF,
- Satellite Rubidium frequency standards (RAFS), and
- Satellite passive H-masers (SPHM).

H-masers at PTFs will be used are references for Cesium clock measurements and do not contribute to the ensemble time according to the logic of the weighted average algorithm (see Section 4.1.1).

Galileo Sensor Stations will be equipped with commercial Rubidium clock which contribution to the ensemble time will be negligible due to their relatively poor stability (comparing with RAFS or Cesium clocks).

Specifications of Galileo clocks (excluding the Rubidiums at sensor stations) are presented in Figure 5-17. These specifications will be further used in the analysis of ensemble time stability. For RAFS and SPHM two options are shown in the figure: with frequency drift and without it. Both RAFS' and SPHMs will exhibit the frequency drift, however, in practice it can be estimated and corrected in the ensemble time algorithm (the option without drift in the figure). Nevertheless, the drift will not be stable, its variations will limit the stability of corrected RAFS' and SPHMs. This limitation can be reliably estimated only with experimental data which are not available to the author at the time of writing this work. Therefore, the analysis will be done only for the options with frequency drift and without it, whereas the latter should be considered as optimistic.

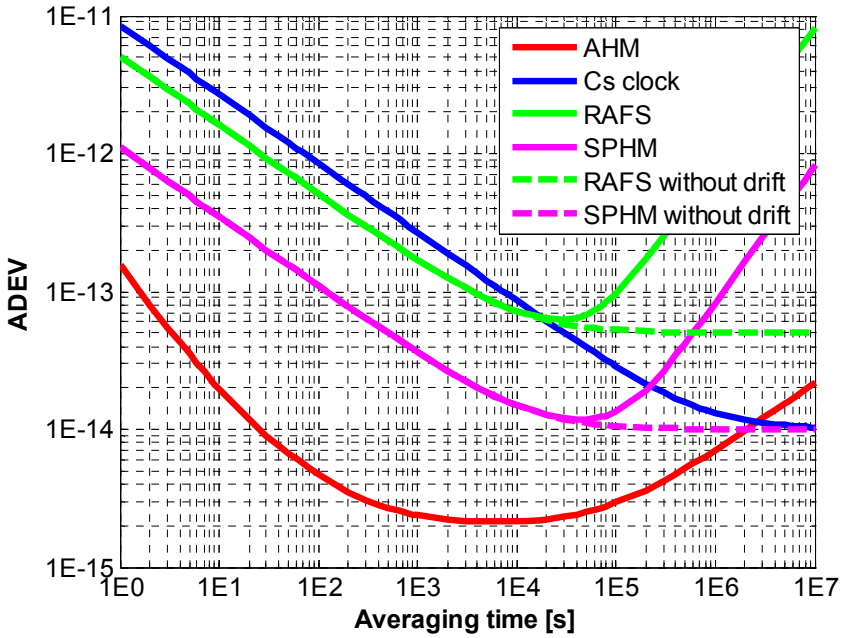

Figure 5-17. ADEV of Galileo clocks

Ensemble time stability analysis will be performed for the scenarios presented in Table 5-8.

Scenario ID	*Clocks*	*Number*
1	Cesiums of single PTF	3
2	Cesiums of both PTFs	6
3	Cesiums of both PTFs	6
	RAFS	27
4	Cesiums of both PTFs	6
	SPHM	27

Table 5-8. Scenarios for Galileo clock ensemble

Following operational modes for each of the scenarios will be considered:

- Nominal Mode: no clock failures,
- Failure mode 1: failure of one Cesium clock,
- Failure mode 2: failure of one PTF,
- Failure mode 3: failure of one PTF and one Cs clock,
- Failure mode 4: failure of all ground Cesiums.

Failure of the link to satellite clocks is equal to Scenario 1 or Scenario 2.

Another important parameter for the weighted average algorithm is the optimization time ς (see Section 4.1.1). Two values for the optimization time will be considered: 100 min and 10 day. The first value is of interest from the navigation point of view and the second one – from the metrological.

5.3.2.2 Estimation of ensemble time stability

In case the ensemble time is generated from an ensemble of N equivalent clocks (i.e. clocks with equivalent ADEV) using the weighted average algorithm (see Section 4.1.1), the relationship between the ADEV of individual clocks and the ADEV of the ensemble time is:

$$\frac{ADEV_{clock}}{ADEV_{ensemble}} = \sqrt{N} \qquad \text{Eq. 5-3}$$

Eq. 5-3 is rather simple, the situation becomes more complicated if an ensemble includes clocks with different stability (ADEV), e.g. an ensemble of Galileo clocks which includes Cesium clocks at PTFs and satellite RAFS. In this example there are two groups of clocks. For simplicity, it is assumed that the stability of clocks within each of the groups varies insignificantly. Using the formula for computation of clock weights in the ensemble time (see Eq. 4-8), the following expression for weights of clocks within group k can be obtained:

$$\tilde{w}_k = \frac{1}{\sum_{j=1}^{K} n_j \frac{ADEV_k^2(\varsigma)}{ADEV_j^2(\varsigma)}} \qquad \text{Eq. 5-4}$$

here

K - number of clock groups,

n_j - number of clocks within j-th group,

ς - optimization time (the sampling time interval at which ADEV is computed for determination of clock weights),

$ADEV_j$ - Allan Deviation of individual clocks within j-th group.

It can be shown that for any τ the stability of the ensemble time $ADEV_{ensemble}$ can be obtained as

$$ADEV_{ensemble}(\tau) = \sqrt{\sum_{j=1}^{K} n_j \cdot \tilde{w}_j^2 \cdot ADEV_j^2(\tau)} \qquad \text{Eq. 5-5}$$

5.3.3 Analysis of simulation results

Figure 5-18, Figure 5-19, Figure 5-20 and Figure 5-21 summarize the simulation results with respect to its stability. More details are presented in Annex F. The results below refer to the nominal mode (i.e. no clock failures, see Section 5.3.2.1). Two optimization time intervals are considered: 100 min and 10 days. Both cases – non-corrected and corrected frequency drift – are considered for satellite clocks. The stability requirements are shown in red. The triangles correspond to the baseline GST requirements. The alternative GST requirements derived in this work based on the stability of satellite clocks (see Section 5.1.1.1) are shown with rings. In fact, the only baseline requirements to the ensemble time stability refer to ADEV at 10 days (to support the metrological function). The short term requirements (from 100 min to 24 hours) are considered to assess the feasibility of using the ensemble time for satellite clock prediction in place of the physical representation of GST. Baseline requirements to GST stability for supporting prediction of SPHM are not known to the author. Therefore, only the alternative stability requirements derived in Section 5.1.1.1 are considered for Scenario 4 (ensemble time is generated from SPHMs and ground Cesiums).

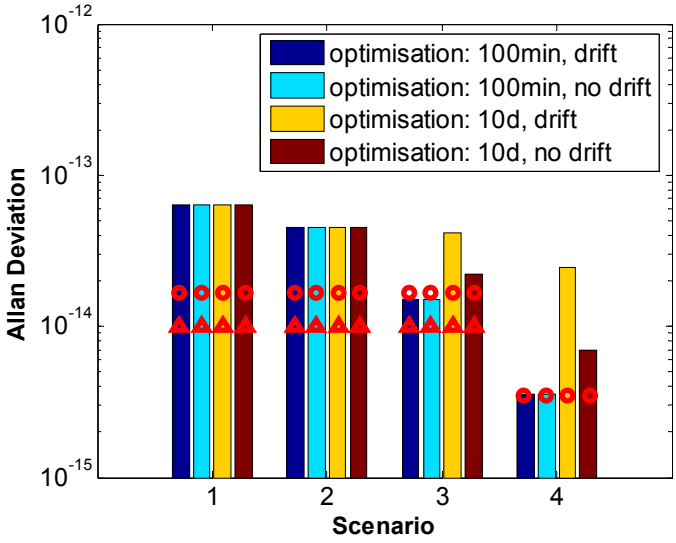

Figure 5-18. Ensemble time ADEV at 100 min

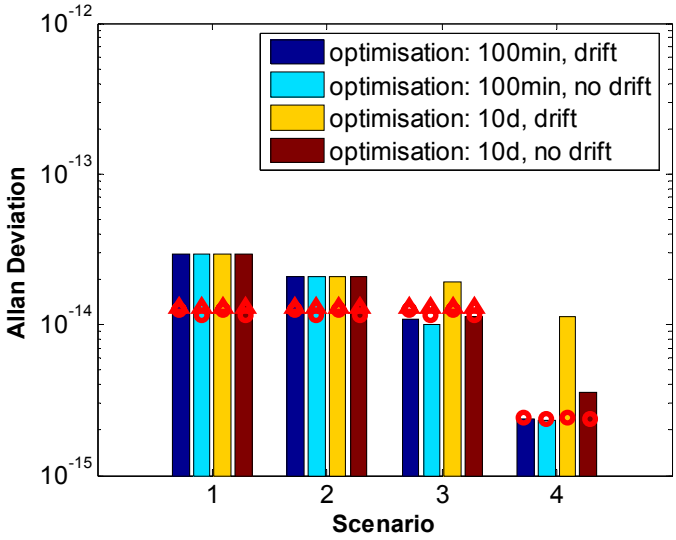

Figure 5-19. Ensemble time ADEV at 8 hours

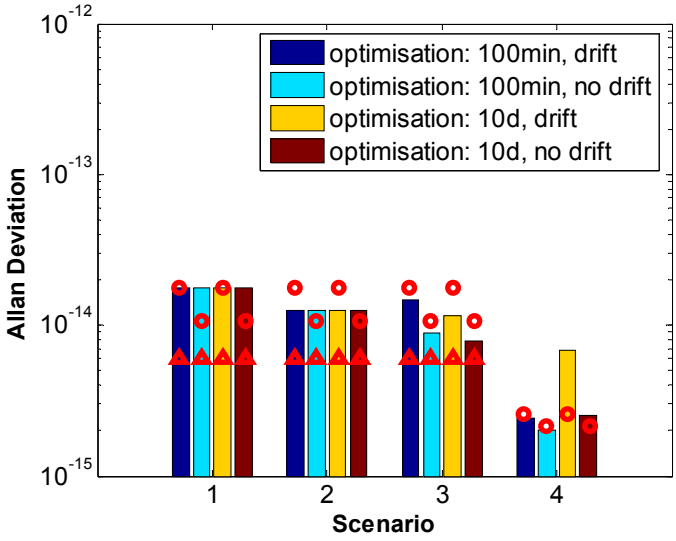

Figure 5-20. Ensemble time ADEV at 24 hours

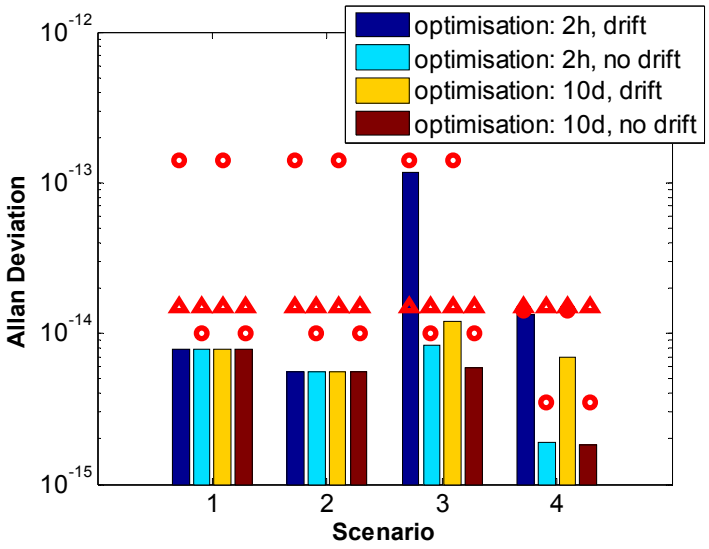

Figure 5-21. Ensemble time ADEV at 10 days

The simulation results indicate that

- The ensemble time produced from the ground clocks only (Scenario 1 and 2) is not able to fully comply with the stability requirements originating from the navigation function. Nevertheless, it fully satisfies the requirements to the metrological performance (ADEV at 10 days), both in the nominal operational mode and in the considered failure modes. Thus, the ensemble time produced from the ground clocks only should be used only for the metrological purposes. This conclusion agrees with the present Galileo baseline.
- The ensemble time produced from ground Cesiums and RAFS (Scenario 3) is closer to the baseline navigation requirements, but is also not fully compliant with them. However, with the optimization time of 100 min, the ensemble time complies with the alternative requirements navigation requirements (see Section 5.1.1.1) and, assuming the RAFS frequency drift is corrected, also with the metrological requirements. This configuration seems to be promising to use the ensemble time not only for metrological, but also for the navigation purposes. However, it should be revisited when experimental results on the stability of RAFS frequency drift are available.
- The ensemble time produced from SPHMs and ground Cesiums (Scenario 4) is compliant with both navigation and metrological requirements when the optimization time is set to 2 hours. The compliance is achieved, both in the nominal operational mode and in the considered failure modes independent on correction of SPHM frequency drift. Thus, the ensemble time produced from SPHMs and ground Cesiums could be used for both navigation and metrological purposes.

Based on the simulation results, the following recommendations on the configuration of the ensemble time can be made:

- If ensemble time is utilized only for the metrological purposes, the present baseline to produce it from the ground clocks is fully sufficient to satisfy the performance requirements. However, inclusion of SPHMs or RAFS (either with drift or de-drifted) with the timescale optimization time of 10 days would allow to increase its robustness to failures.
- If Galileo satellites utilize SPHMs, it seems to be advisable to compute the ensemble time from both satellite and PTF clocks. This timescale would be able to support both the navigation and the metrological functions.
- In case of a mixed constellation (RAFS and SPHMs) it still seems to be preferable to include satellite clocks into the ensemble time computation. Depending on the

stability of RAFS drift, such ensemble time could be able to support both precise prediction of RAFS and the metrological function. However, if the number of SPHMs in the constellation is low, this ensemble time (as well as the physical representation of GST in the present baseline) would not be able to comply with stability requirements originating from SPHM prediction. As a result, the impact of GST instability at the SPHM prediction error could become non-negligible.

6 Timing aspects of GPS Galileo interoperability

6.1 General consideration

6.1.1 Galileo interoperability in GNSS context

Since the nineties the idea of a Global Navigation Satellite System, a “system of systems” comprising several individual satellite navigation systems, has been in the air. Originally GNSS was understood mainly as GPS plus GLONASS and overlays like EGNOS. After GLONASS experienced constellation maintenance problems and GPS de facto monopolized the market, realization of the GNSS concept became somewhat distant. Now GNSS is understood mainly as GPS plus Galileo (and, of course, the overlay systems: WAAS, EGNOS etc). Being a virtual system of systems, GNSS will also offer virtual navigation services – combinations of signals and services of its individual components. These combined services are expected to have higher quality comparing to stand-alone services of individual GNSS components.

However, the “plus” in the GNSS equation stands not for a “mechanical” sum. To enable combined services and their improved quality, GNSS components shall possess the feature called “interoperability”. According to the IEEE definition, interoperability is “the ability of two or more systems or components to exchange information and to use the information that has been exchanged”. In GNSS context, interoperability is defined by the U.S.-EU “Agreement on the promotion, provision and use of Galileo and GPS satellite-based navigation systems and related applications” singed in Shannon (Ireland) on 26th of June 2004 [Shannon04]: “Interoperability at the user level is a situation whereby a combined system receiver with a mix of multiple GPS or GALILEO satellites in view can achieve position, navigation and timing solutions at the user level that are equivalent to or better than the position, navigation or timing solutions that could be achieved by either system alone.”

Obviously, the combination of GNSS signals occurs in the user receiver. Nevertheless, it is up to the systems to make this combination easy and efficient. Interoperability is a complex problem which has been extensively analyzed during Galileo definition studies (e.g. EU-funded projects GALILEI and GEM, ESA-funded GALA study). The following key interoperability aspects were identified so far:

- signal structure and frequency selection,
- geodetic and time reference frames,
- constellation configuration,
- system policies and services guarantees.

This work concentrates on the timing aspects of GPS Galileo interoperability. Technical issues will be considered so far. The institutional and political aspects were treated by US-EU working groups (see e.g. [Hahn04]); the major interoperability and cooperation issues were also addressed in the U.S.-EU agreement on GPS Galileo cooperation [Shannon04].

6.1.2 Why determining GPS Galileo time offset

This work is focused on the timing aspects of GPS Galileo interoperability. Note that geodetic reference frames of GPS and Galileo are planned to be kept in agreement on centimeter level; it makes the contribution of the corresponding error to user positioning solution negligible.

Satellite clock parameters broadcast by GPS and Galileo describe the behavior of the satellite clocks with respect to the reference time scale of the corresponding system. Thus, after correcting with their help the user pseudorange measurements (which is a part of navigation processing), the pseudorange residuals will be also referenced to different time scales (see Figure 6-1) that would lead to a bias between the GPS and Galileo residuals.

This problem is also known from the combined use of GPS and GLONASS. A similar effect will appear also when users correct pseudorange measurements to TAI using the broadcast offset between GPS and Galileo reference time scales and TAI. In this case, GGTO can be re-defined as the difference between TAI estimates derived from the Galileo and GPS broadcast (UTC_{Gal} and UTC_{GPS} respectively) since these estimates will not be perfect.

Thus, an interface between GST and GPS Time is needed. This interface can be handled at two levels: at user level and at system level. In the first case, GGTO can be calculated in the user position&time solution as an additional unknown. In the second case, GGTO have to be determined by Galileo itself and provided to user in the navigation message or in other way. The US-EU agreement on GPS Galileo cooperation states that GPS and Galileo are to broadcast GGTO in their navigation messages.

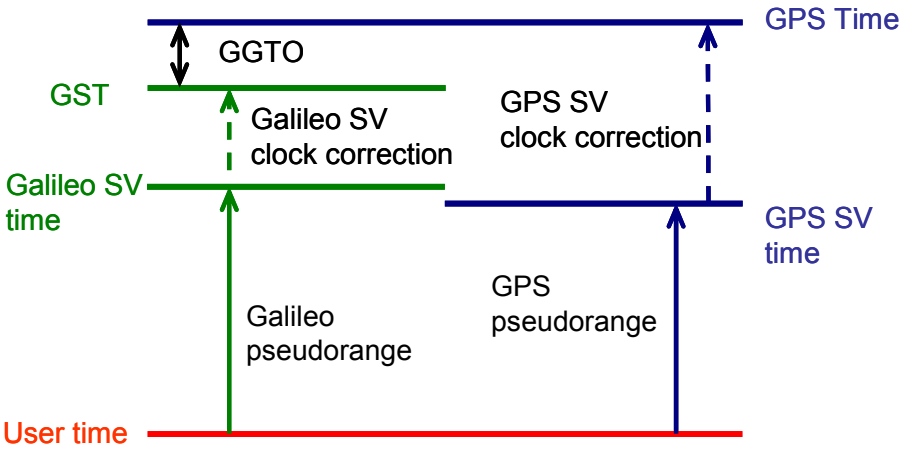

Figure 6-1. Timescales relations for users of combined navigation equipment

6.1.3 Structure of the section

The study of GPS Galileo time interface presented in this work is built as follows:

- First, we look at options for GPS Galileo time interface and define evaluation criteria aimed on supporting selection of one particular option,
- Second, we consider the potential GGTO magnitude,
- Third, we estimate the impact of GGTO onto the accuracy and availability of user positioning for different GGTO determination scenarios,
- Fourth, we consider various technical solutions for implementation of GPS Galileo time interface.
- And fifth, we summarize benefits and drawbacks of implementation options for this interface.

6.1.4 Options for GPS Galileo time interface

The three potential approaches to establishing the GPS Galileo time interface are summarized in Table 6-1. In Table 6-1 the term „standard user positioning algorithm“ stands for the user position-time solution algorithm baseline (see Section 4.2.3), and „extended user positioning algorithm“ for a position-time solution algorithm which includes GGTO as an additional unknown. This algorithm is currently not defined in Galileo documentation.

As can be seen from Table 6-1, in case GPS Galileo time interface is established at system level the major burden lies on the two systems: it should develop and implement a GGTO monitoring system and regularly broadcast GGTO values to its users. This solution is more expensive and complex from the point of view of the system design, however, it brings the benefits of „implicit“ interoperability with GPS when user should only implement a correction to GPS measurements (from Galileo broadcast).

The second solution, GPS Galileo time interface at user level, where user should determine (or ignore) GPS Galileo time offset on his own is easier for Galileo (no specific efforts are needed), but it puts the burden of GGTO determination completely on Galileo and GPS users.

Finally, it can be anticipated that some users may prefer to compute GGTO themselves when they have enough measurements to do that and use the broadcast GGTO value when not. This solution is, however, a „custom wish“, from the Galileo point of view it still means the need to establish the GPS Galileo time interface on system level.

Interface level	*Specific Galileo actions*	*Specific user actions*	*User positioning algo*
System	• continuously monitor GGTO • broadcast GGTO values in satellite navigation messages	• implement GGTO as a correction to GPS measurements	• Standard
User	-	• determine GGTO as a part of position-time solution	• Standard or extended
System & user	• continuously monitor GGTO • broadcast GGTO values in satellite navigation messages	User action depends on his observation conditions. • Less or no obstacles: determine GGTO as a part of position-time solution (or ignore it) • More obstacles: implement GGTO as a correction to GPS measurements	• Standard&extended

Table 6-1. GPS Galileo time interface options

To make reasonable recommendations on the selection of GPS Galileo time interface level, a set of selection criteria should be defined and the interface options (see Table 6-1) should be evaluated against these criteria.

6.1.5 Selection criteria

Potential selection criteria are dictated by areas of impact of GPS Galileo time interface establishment which include

- Galileo design complicity and costs and system operation costs
- Costs of user equipment
- Performance (accuracy and availability) of combined GPS Galileo positioning
- Marketing factors (or Galileo attractiveness for users).

Table 6-2 presents an evaluation of GPS Galileo time interface levels against the selection criteria mentioned above. The following impact (significance) levels are defined: major significance („M“), medium significance („m“), low significance („low“), no significance („n“) and unknown significance („?“). A positive impact is designated with the „+“ sign and a negative with the „-“ sign.

The impact of particular level of GPS Galileo time interface onto the positioning accuracy and availability of accuracy was not considered in details in Galileo studies and publications known to the author. This issue is discussed in following sections.

Factor	Significance	Interface level		
		System	User	System & user
System design complicity and costs	M	-l	n	-l
System operation costs	M	-l	n	-l
User equipment costs	M	n	-l	-l
Positioning accuracy	M	?	?	?
Availability of positioning solution	M	+M	-M	+M
Galileo attractiveness	M	+m	-m	+m

Table 6-2. GPS Galileo time interface options

6.2 GGTO magnitude and properties

6.2.1 GGTO magnitude

It is expected that at the time when Galileo becomes operational the performance of both GPS Time and GST will considerably improve compared to the values presented here (see Sections 3.2.2 and 4.1.2.2). However, to produce a preliminary GGTO estimate (which has to be considered as a kind of "worst-case" boundary), we took the values corresponding to the current performance of GPS Time and the required performance of GST.

To remind, according to Circular T, GPS Time was kept within 24.5 ns (RMS offset: 14 ns) from UTC in Jan – Sept 2004; its offset from UTC(USNO) in Feb-Jul 2004 was within +/-18 ns [USNO-Web]. Also according to Circular T, UTC(USNO) was kept within +/- 13 ns from UTC (RMS offset: 6.7 ns) in Jan – Sept 2004. The RMS error of UTC(USNO) distribution was 5.8 ns in 2002 [Hutsell02] (unfortunately, presently we do not have more recent data).

Based on these figures, one may expect GGTO of about 57 ns (95%), and the uncertainty of the offset between UTC_{Gal} and UTC_{GPS} – the UTC representations derived from Galileo and GPS (using the broadcast UTC corrections) – to be about 33 ns (95%).

6.2.2 Relative frequency instability of GGTO

GGTO is solely a difference between GPS Time and GST. Its sign is a matter of convention. Here it is assumed to be defined as follows

$$GGTO = GPSTime - GST \qquad \text{Eq. 6-1}$$

here $GPSTime$ is the GPS Time reading and GST is GST reading.

Thus, the relative frequency stability of GGTO can be expressed in terms of ADEV as

$$ADEV^2_{GGTO} = ADEV^2_{GPSTime} + GST^2_{GST} \qquad \text{Eq. 6-2}$$

The *de facto* stability of GPS Time is discussed in Section 4.1.2.2 and specification of GST is presented in Section 3.2.2. Thus, it is easy to derive the ADEV of GGTO which is an important for realistic simulations of its behavior (see Figure 6-3).

6.2.3 Simulation of GGTO

The simulation included two steps:

- Simulation of the GPS Time and GST offsets from TAI,
- Calculation of GGTO as the difference between these offsets.

To make the simulation as realistic as possible, simulated data were combined with real-world data. For GPS Time we have taken daily offsets between GPS Time and UTC available in the BIPM Circular T and "filled" the daily intervals between them with simulated

values (rate: 1 value per 15 minutes). These values were obtained with the help of DLR's clock simulator based on the frequency instability (ADEV) of GPS Time given in Section 4.1.2.2 (mixture of white frequency noise and frequency random walk).

For simulation of GST we have taken the Circular T offsets between UTC and a UTC(k) time scale whose short- and medium-term performance was considered to be representative for GST (namely, UTC(ORB)). These values were available with an interval of 5 days. Similar to GPS Time simulation, the 5-day intervals were "filled" with simulated clock data. GST specification from the Galileo baseline (see Section 3.2.2) was used for this simulation.

Due to using real GPS Time and UTC(k) data, there was no need to simulate steering of GPS Time and GST to TAI since it was already present in these data. The simulation results are presented in Figure 6-2 and Figure 6-3.

An additional GGTO simulation was made for the case GST and GPS Time were not steered to UTC. It would also correspond to the situation when the steering is known, and GPS Time and GST are corrected for it.

Simulation results for GGTO in both cases (with and without steering) are presented in Figure 6-2 and Figure 6-3.

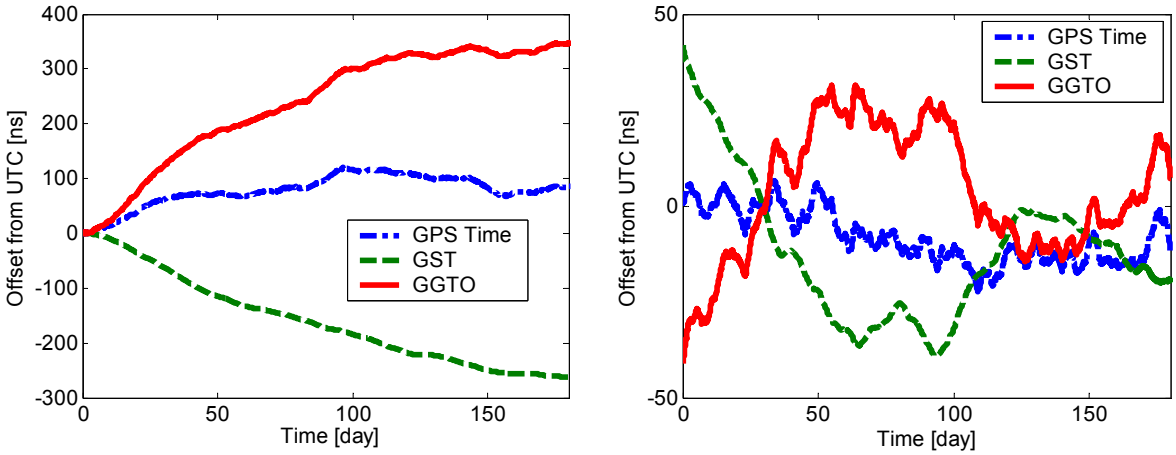

Figure 6-2. Simulated GPS Time, GST and GGTO (left: non-steered, right: steered)

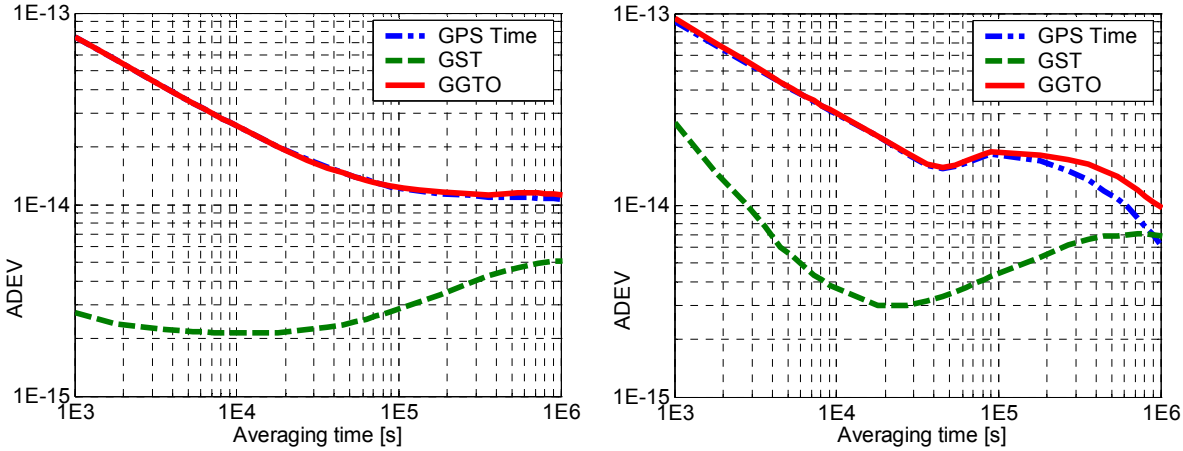

Figure 6-3. ADEV of GPS Time, GST and GGTO (left: non-steered, right: steered)

Note that up to the averaging time of 1-3 days, ADEV of GGTO and GPS Time are very close (see Figure 6-3) since contribution of GST to the GGTO instability at these time intervals is small.

6.2.4 Uncertainty of the broadcast GGTO correction

The baseline requirement to the accuracy of the GGTO correction which is to be broadcast in the GPS and Galileo navigation messages is presented in [Hahn04]: the error of the correction shall not exceed 5 ns 95% of time.

6.3 GGTO impact onto the user positioning accuracy

6.3.1 GGTO treatment scenarios

There are three possible options how user may deal with GGTO:

- Scenario 1 – Ignoring GGTO: assuming that the GGTO impact on the navigation accuracy is negligible for user application, users may compute navigation solution without considering the bias at all and treating both GPS and Galileo measurements equivalently. In this case, the position error due to GGTO will be completely included into the navigation solution.
- Scenario 2 – GGTO determination at user level (in user receiver): those users who are concerned about GGTO may compute it as an additional unknown in user navigation solution. However, in environments with limited satellite visibility (e.g. urban canyons) “spending” of an additional observation for calculation of GGTO may be critical. A sub-scenario here is to determine GGTO from the navigation solution when enough satellites are available, and when visibility conditions worsen, utilize the GGTO value cased on “historical” data.
- Scenario 3 – GGTO determination at system level: Galileo and possibly GPS operators may determine the GGTO as a part of routine system operation and distribute it to users in satellite navigation messages. In this case, user can apply GGTO as a known correction to his measurements and then make the standard position-time solution with 4 unknowns (see Section 4.2.2). The latter option is presently included into the Galileo baseline. The uncertainty of the broadcast GGTO correction may cause a residual displacement of user navigation solution.

Note that Scenario 3 is equivalent to Scenario 1 as far as the GGTO propagation into the navigation solution is considered: in both cases GPS and Galileo measurements are treated equally in the navigation solution, just in Scenario 3 they will be corrected using the broadcast GGTO value.

This section (Section 6.2) deals with preliminary estimation of the GGTO impact on user navigation accuracy considering two options:

- GGTO is either ignored or taken as known, and
- GGTO is determined in user navigation solution.

6.3.2 Position-time solution for users of combined navigation equipment

It is obviously that to assess the impact of GGTO on the accuracy of user positioning we need to define a reference algorithm for combined GPS/Galileo position-time solution.

Here (for the system analysis purpose) we consider the two options for combined user navigation accuracy:

- standard position-time solution (see Section 4.2.2) which can be used if user measurements are corrected for GGTO or GGTO is ignored, and
- extended position-time solution which can be used in case if user determines GGTO in his position-time solution.

Before proceeding with the discussion on user algorithms, let’s have a look at the measurement model for users of combined equipment.

6.3.2.1 Observation equation for users of combined navigation equipment

Obviously, the pseudorange observation equation (see Eq. 4-23 in Section 4.2.3) has the same form both for GPS and Galileo. However, while calculating pseudorange residuals, users would correct GPS pseudoranges to GPS Time and Galileo pseudoranges to GST if they utilize broadcast satellite clock parameters. Thus, there will be a bias between GPS and Galileo residuals.

In addition, the observation noise for GPS and Galileo measurements is different due to different signal structure of GPS and Galileo, different accuracy of ephemeris and clock parameters etc.

However, a combined GPS/Galileo navigation solution still can be computed from Eq. 4-27 and/or Eq. 4-28 if the following substitutions are made:

$$\mathbf{l} = \begin{bmatrix} \mathbf{l}_{GPS} \\ \mathbf{l}_{Galileo} \end{bmatrix}; \qquad \mathbf{G} = \begin{bmatrix} \mathbf{G}_{GPS} \\ \mathbf{G}_{Galileo} \end{bmatrix}; \qquad \text{Eq. 6-3}$$

6.3.2.2 Standard position-time solution for users of combined navigation equipment

The standard position-time solution algorithm for "single-system" – either GPS or Galileo – users was discussed in details in Section 4.2.3. This algorithm is also recommended in MOPS and referenced in the Galileo technical specifications. Considering the substitution defined in Eq. 6-3, the standard weighted position-time solution would be given by Eq. 4-28, and the non-weighted version of it would be given by Eq. 4-27.

Further we will consider the non-weighted solution since the accuracy improvement due to weighting in not critical for our analysis.

It can be shown that the errors of the individual components of the non-weighted position-time solution when GST and GPS Time are ideally synchronized (GGTO = 0) are

$$\begin{aligned}
\sigma_B &= \sqrt{\left(\sum_{i=1}^{n_{GPS}} \mathcal{N}_{1,i}^2\right)\cdot\sigma_{0,GPS}^2 + \left(\sum_{i=1}^{n_{Galileo}} \mathcal{G}_{1,j}^2\right)\cdot\sigma_{0,Galileo}^2} \\
\sigma_L &= \sqrt{\left(\sum_{i=1}^{n_{GPS}} \mathcal{N}_{2,i}^2\right)\cdot\sigma_{0,GPS}^2 + \left(\sum_{i=1}^{n_{Galileo}} \mathcal{G}_{2,j}^2\right)\cdot\sigma_{0,Galileo}^2} \\
\sigma_H &= \sqrt{\left(\sum_{i=1}^{n_{GPS}} \mathcal{N}_{3,i}^2\right)\cdot\sigma_{0,GPS}^2 + \left(\sum_{i=1}^{n_{Galileo}} \mathcal{G}_{3,i}^2\right)\cdot\sigma_{0,Galileo}^2} \\
\sigma_{\Delta T} &= \sqrt{\left(\sum_{i=1}^{n_{GPS}} \mathcal{N}_{4,i}^2\right)\cdot\sigma_{0,GPS}^2 + \left(\sum_{i=1}^{n_{Galileo}} \mathcal{G}_{4,j}^2\right)\cdot\sigma_{0,Galileo}^2}
\end{aligned} \qquad \text{Eq. 6-4}$$

here $\mathcal{N} = \mathbf{P}\mathbf{G}_{GPS}^T$ and $\mathcal{G} = \mathbf{P}\mathbf{G}_{GPS}^T$, $\sigma_{0,GPS}$ and $\sigma_{0,Galileo}$ are average root means square values of GPS and Galileo residuals respectively (they are often called user equivalent range error (UERE)).

Obviously, when GGTO is zero, the position-time solution is unbiased. However, also in this case, the DOP concept is not directly applicable to the combined solution as clearly shows Eq. 6-4. DOPs in their "traditional" meaning can be used to characterize the errors of the combined solution only when GPS and Galileo UERE can be considered to be equal. Otherwise, the relationship between user positioning error and UERE becomes more complex, and individual elements of the Galileo and GPS geometry matrices have to be considered (see the first two terms in equations in Eq. 6-4).

In case GGTO is non-zero (as always will be in practice), the stochastic parts of the user solution error will be still described by Eq. 6-4. In addition to that, there will be a bias caused by the GGTO which will depend on the geometry of observed GPS and Galileo constellations. We studied the accuracy of user solution in presence of GGTO with the help of Monte-Carlo simulations as described further in this section.

6.3.2.3 Modified position-time solution for users of combined navigation equipment

The standard position time solution deals with four unknowns: three components of user position vector and user time offset from the system time. For users of combined navigation equipment, inter-system time bias (i.e. GGTO for GPS/Galileo users) can be included as the fifth unknown into the position-time solution.

Assuming that user position vector is expressed in geodetic coordinates, the vector of unknowns for the modified position-time solution is given by

$$\mathbf{u} = \begin{pmatrix} B \\ L \\ H \\ \Delta T \\ GGTO \end{pmatrix} \qquad \text{Eq. 6-5}$$

The geometry matrix $\mathbf{G}$ has to be extended by one column comparing to the similar matrix of the standard solution.

$$\mathbf{G} = \begin{pmatrix} \sin A_1 \cos E_1 & \cos A_1 \cos E_1 & \sin E_1 & 1 & \frac{\partial l_1}{\partial GGTO} \\ \sin A_2 \cos E_2 & \cos A_2 \cos E_2 & \sin E_2 & 1 & \frac{\partial l_2}{\partial GGTO} \\ \cdots & \cdots & \cdots & \cdots & \cdots \\ \sin A_n \cos E_n & \cos A_n \cos E_n & \sin E_n & 1 & \frac{\partial l_n}{\partial GGTO} \end{pmatrix} \qquad \text{Eq. 6-6}$$

here $\frac{\partial l_i}{\partial GGTO}$ is the first derivative of i-th measurement with respect to GGTO. Assuming that user select GST as reference time scale, $\frac{\partial l_i}{\partial GGTO}$ is zero for Galileo measurements and one for GPS measurements (we define GGTO as GPS Time minus GST).

Here we assume that the unknowns in the position-time solution are the 3D position, user clock offset w.r.t. to GPS Time or GST and GGTO. Alternatively, other unknown set may be chosen: 3D position solution, user clock offset w.r.t. GPS Time and user clock offset w.r.t. GST.

The variances of modified solution components can be characterized by a formula similar to Eq. 6-4:

$$\sigma_k = \sqrt{\left(\sum_{i=1}^{n_{GPS}} \mathcal{N}_{k,i}^2 \right) \cdot \sigma_{0,GPS}^2 + \left(\sum_{i=1}^{n_{Galileo}} \mathcal{G}_{k,j}^2 \right) \cdot \sigma_{0,Galileo}^2} , \qquad \text{Eq. 6-7}$$

here k is the index corresponding to the position of selected unknown in the vector $\mathbf{u}$.

Obviously, the DOP concept is also not directly applicable to the modified solution.

Alternatively, the vector of unknowns could include not GGTO but two receiver time offsets, one with respect to GPS Time and one with respect to GST:

$$\mathbf{u} = \begin{pmatrix} B \\ L \\ H \\ \Delta T_{GPS} \\ \Delta T_{Gal} \end{pmatrix} \qquad \text{Eq. 6-8}$$

6.3.3 Studying the GGTO impact on the accuracy of standard position-time solution

6.3.3.1 Approach

We considered two kinds of user algorithms (see Section 6.3.2): the standard algorithm with four unknowns and the modified algorithm with five unknowns.

For the standard user algorithm in case of zero GGTO and for the modified user algorithm, we estimated the accuracy of user position-time solution from simulations of Galileo and GPS constellation geometry considering representative GPS and Galileo UERE.

For the standard user algorithm, we used the Monte-Carlo approach. We simulated GPS and Galileo geometry and errors of GPS and Galileo pseudorange measurements (from a normal distribution with variance set by the corresponding UERE), and fed this data into this algorithm. Variances of position-time solution components were estimated from the obtained series of solutions.

6.3.3.2 Simulation scenario

Simulation scenario was defined as described in Table 6-3.

Property	***Value***
Galileo constellation	constellation of 27 satellites (Walker 27/3/9)
Galileo service	Open Service (dual frequency)
GPS constellation	28 satellites (as available in April 2004)
GPS Service	SPS dual-frequency (L1+L5) (considering GPS modernization)
User range error	1.05 m for Galileo [Moudrak04a]; 1.3 m for GPS [McDonald00]
Time span/time step	72 hours / 5 minutes
Simulated locations	Grid: 3° (latitude) x 5° (longitude)
Uncertainty of broadcast GGTO parameters	0, 5, 16 ns (95%)
Elevation cut-off angle	10° and 30°
User algorithm	MOPS (4 parameter) and alternative (5 parameter)

Table 6-3. Simulation scenario to study user positioning accuracy

6.3.3.3 Simulation results

The outcome of the simulation described above was evaluated with respect to the two key parameters: accuracy and availability of navigation solution.

Both with the MOPS (four unknown parameters) and the extended MOPS (five unknown parameters) algorithms, navigation solution was available 100% of time for both 10° and 30° elevation cut-off angle assuming that user utilizes combined GPS/Galileo equipment. In the same time, the worst-case solution availability for Galileo-only users with elevation cut-off of 30° was as low as 86.3%. More results on solution availability in urban environments can be found in [Moudrak04c].

Sensitivity of the navigation solution (for the original and the modified MOPS algorithms) to the accuracy of the broadcast GGTO correction is illustrated in Table 6-4 (worst-case positioning error) and Table 6-5 (average positioning error). For comparison purposes, accuracy of Galileo-only solution (obtained with the original MOPS algorithm) with elevation cut-off of 10° is also presented in the table. No meaningful statistics were obtained for the cut-off of 30° since the geometry matrix was in many cases almost singular.

Solution	***HPE 95% [m]***		***VPE 95% [m]***	
	Cut-off 10°	*Cut-off 30°*	Cut-off 10°	*Cut-off 30°*
Galileo-only	3.3	n/a	6.6	n/a
GPS+Galileo				
Modified MOPS algorithm	2.8	570	5.4	1360
Original MOPS algorithm,				
GGTO = 33 ns (95%)	6.9	151	18	531
GGTO = 20 ns (95%)	4.4	102	11	353
GGTO = 5 ns (95%)	2.8	60	5.5	179
GGTO = 0 ns	2.8	60	5.3	162

Table 6-4. Worst-case HPE and VPE for GPS, Galileo and their combination

Solution	***HPE 95% [m]***		***VPE 95% [m]***	
	Cut-off 10°	*Cut-off 30°*	Cut-off 10°	*Cut-off 30°*
Galileo-only	2.1	n/a	3.7	n/a
GPS+Galileo				
Modified MOPS algorithm	1.6	4.8	2.8	11.9
Original MOPS algorithm,				
GGTO = 33 ns (95%)	2.5	7.3	5.7	21.6
GGTO = 20 ns (95%)	1.8	3.9	3.5	10.7
GGTO = 5 ns (95%)	1.6	3.8	2.8	11.5
GGTO = 0 ns	1.5	3.7	2.7	11.2

Table 6-5. Average HPE and VPE for GPS, Galileo and their combination

6.4 GGTO determination at system level

6.4.1 GGTO determination at system level: functional overview

In case GGTO is determined on system level, the tasks of Galileo would include

- Measurement of GGTO,
- Prediction of GGTO,
- Distribution of GGTO to users,
- Monitoring of validity of GGTO parameters provided to users.

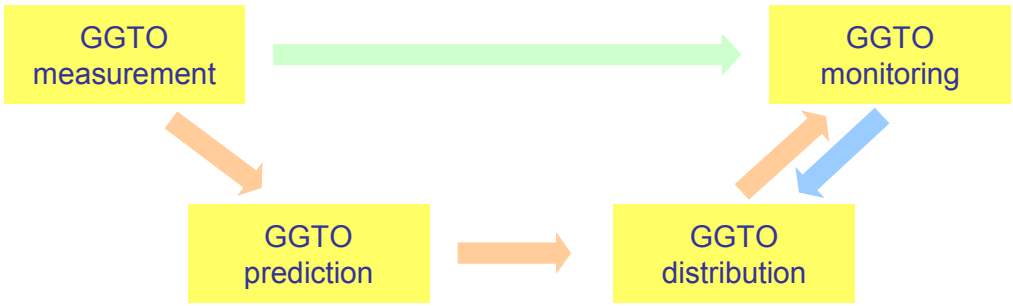

Figure 6-4. Galileo task to support determination of GGTO on system level

These tasks involve both technical and organizational issues. We will not consider the latter point and concentrate on processing methods and algorithms.

Here we discuss shortly of the tasks listed above considering them on functional level.

GGTO measurement function should acquire the information on actual GPS Galileo time offset. There are three basic options to consider:

- Measurement of GGTO making use of navigation signals of both systems,
- Measurement of GGTO making use of representations of system timescales,
- Combination of the two approaches named above.

The first option is most close to the user situation and can be implemented with the help of a combined GPS/Galileo receiver at fixed location with precisely known coordinates. A drawback here is an indirect access to the system timescale of both systems – they will be "reconstructed" from user measurements with the help of broadcast (or externally estimated) clock parameters. As a consequence, one may expect that the short-noise of the estimated will be considerably higher than of the system time itself.

The second option would potentially provide less noisy data establishing a direct link between representations of system timescales. A problem here is the lack of physical representation of GPS Time which exists as an *implicit* average of GPS clocks and "visible" only as a noisy correction to a clock within GPS system. Furthermore, it is not expected that GPS will provide access to the data these clock corrections computed by the Kalman filter at the GPS Master Control Station because of the military nature of GPS.

As a compromise the third option – a combination of the two discussed above can be considered. It may be possible to establish a link between the physical representation of GST and the timescale maintained by the U.S. Naval Observatory – UTC(USNO) – which plays an important role in GPS operation (GPS Time is steered on daily basis to UTC(USNO)). USNO determines the offset between GPS Time and UTC(USNO) from reception of GPS navigation signals with a military (keyed) receiver within its premises.

GGTO prediction function: distribution of GGTO in Galileo navigation signal implies that users will apply it after the time when the offset was computed. Thus, results of GGTO measurements (see above) should be extrapolated somewhat into the future. It is the task of the GGTO prediction function which shall provide a prediction of GGTO with required accuracy or compute parameters of GGTO model from that the prediction can be computed.

GGTO distribution function: is less a matter of algorithms than of technique, it shall ensure that the GGTO prediction computed by the GGTO prediction function will be made available to Galileo users (e.g. included into the Galileo navigation message or distributed to users by other means). This function will not be discussed in more details here.

GGTO monitoring function: shall be control the validity of GGTO parameter that Galileo provides to users through comparing the GGTO estimate which users obtain with these parameters with actual GGTO value (coming, e.g. from GGTO measurement function). If GGTO parameters are found to be invalid, an action should be undertaken to inform users about it (e.g. set a specific flag in the user navigation message). This specific type of monitoring is required since GPS Time lies outside Galileo control and its changes are in general unpredictable. The GGTO monitoring function can be implemented as a part of the overall mission performance monitoring function within Galileo.

A discussion on methods and algorithms within GGTO measurement, prediction and monitoring function follows.

6.4.2 Impact of error in broadcast satellite orbits and clock parameters on the accuracy of GPS Time restitution

Before proceeding with a study of GGTO determination techniques, we would like to discuss the accuracy of GPS Time restitution to point out the achievable level of GGTO determination accuracy.

As mentioned in Section 4.1.2, GPS Time is not available physically, it is computed by the GPS Master Station Kalman filter from clocks of GPS satellites and ground stations. GPS Time exists in the form of (noisy) corrections to individual clocks included into its computation. Outside the GPS system GPS Time is available in the form of corrections to GPS satellite clocks which are broadcast in the GPS navigation message. The corrections also contain inherent noise due to limited accuracy of measurements available from GPS ground monitoring stations. Thus, the accuracy of the broadcast clock corrections set the fundamental limit on the accuracy of access to GPS Time.

We analyzed the accuracy of broadcast GPS clock parameters over the whole year of 2003 by comparing them with precise clock products produced by IGS. The broadcast data were obtained from consolidated RINEX navigation files (data from multiple stations put together) produced by IFAG. As the reference we took IGS clock products from SP3 files (final consolidated SP3 files were used). However, clock products of IGS are referenced not to GPS Time but to an internal time scale produced by the IGS. Nevertheless, we considered them to be suitable for estimating the short-term noise of broadcast clock parameters, since IGS time scale is more stable than the GPS Time itself, and the short-term noise of the broadcast clock parameters is considerably higher than that of GPS Time. Due to the inherent sample time selected by IGS, data (i.e. the differences broadcast clock estimate minus IGS clock estimate) were available with the rate one value per 15 minutes.

The results of this analysis are presented below (see Figure 6-5 and Table 6-6).

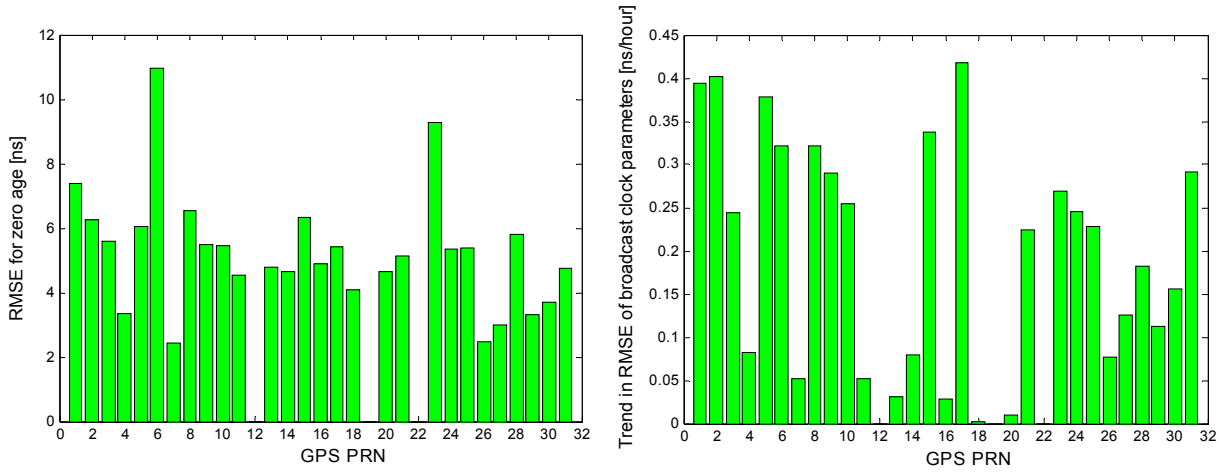

Figure 6-5. RMS error for zero age (left) and trend in RMS error (right) of satellite clock parameters

Parameter	*Average over the constellation*
Bias at zero age	3.6 ns
Trend in biases	0.094 ns/hour
Standard deviation at zero age	3.2 ns
Trend in standard deviations	0.148 ns/hour
RMSE at zero age	5.4 ns
Trend in RMSE	0.200 ns/hour

Table 6-6. Bias, standard deviation and RMSE averaged over the GPS constellation

Using the offsets between broadcast ephemeris and IGS products computed above, we estimated the GPS time dissemination error considering only the component due to errors of broadcast clock parameters. Thereto, we computed the average and the median snap-shot errors of broadcast clock parameters for two sites: the Royal Observatory of Belgium (Brussels) and the US Naval Observatory (near Washington):

$$\Delta GPSTime_{av}(t) = \frac{1}{N(t)} \sum_{i=1}^{N(t)} \left(\Delta t^i_{brd}(t) - \Delta t^i_{IGS}(t) \right)$$

$$\Delta GPSTime_{med}(t) = median\left(\Delta t^i_{brd}(t) - \Delta t^i_{IGS}(t) \right), \quad i = 1..N(t) \qquad \text{Eq. 6-9}$$

here t is observation time, N is number of observed satellites, and subscripts “brd” and “IGS” refer to broadcast and IGS data respectively. Values of t and N were extracted from observation files collected at the ORB and USNO sites in 2003.

Figure 6-6 shows histograms of the averages and the medians for the ORB site, the latter exhibiting an evident non-Gaussian behavior. Table 6-7 summarizes the biases and the standard deviations for the averages and medians for both sites.

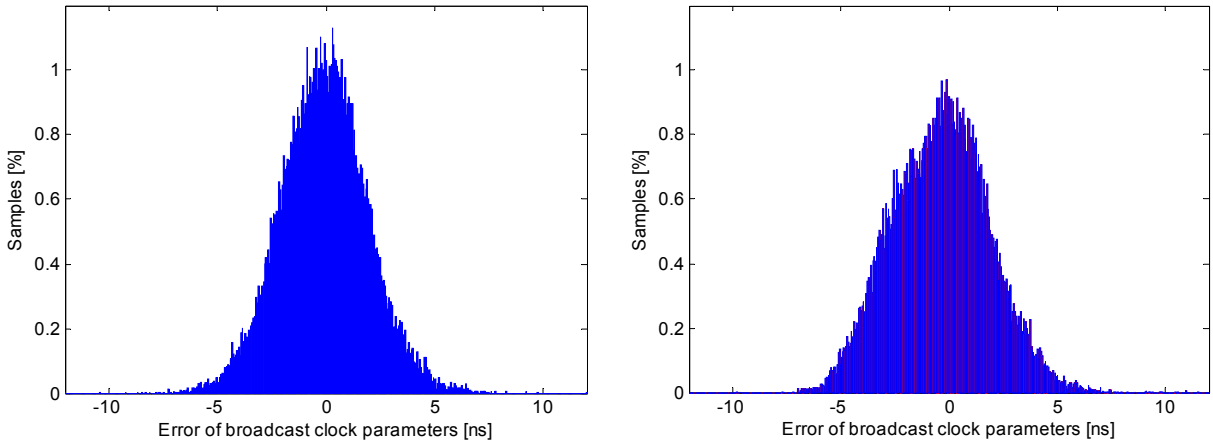

Figure 6-6. Histogram of average (left) and median (right) error for the ORB site

Parameter	*Site*	
	ORB	*USNO*
Bias in averages	-0.1 ns	0.0 ns
Standard deviation of averages	2.1 ns	2.2 ns
Bias in medians	-0.4 ns	0.0 ns
Standard deviation of medians	2.2 ns	2.4 ns

Table 6-7. Bias and standard deviation of averages and medians

A close looks at the data shows that both averages and medians have a well-visible noise pattern (see Figure 6-7).

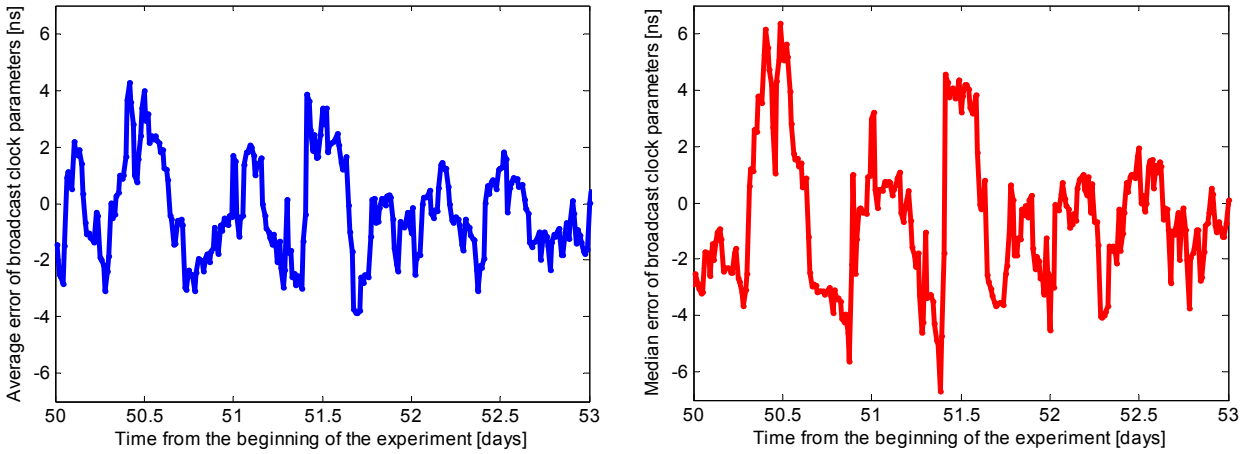

Figure 6-7. Noise pattern in averages (left) and in medians (right) for ORB site

Also, daily averages of clock error were computed. Their RMS value was below 0.1 ns.

6.4.3 Options to measure GGTO

The basic solution to link GPS Time to GST would be to establish a link between clocks with known offsets to GST and GPS Time (see Figure 6-8).

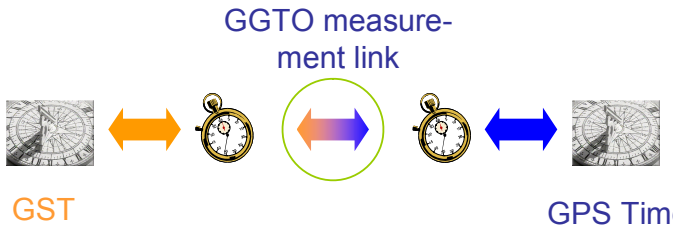

Figure 6-8. The principle of GGTO measurement

A simple way to establish such a link is to use a combined GPS/Galileo receiver. Bypassing the receiver clock, GPS and Galileo satellite clocks can be linked to each other by constructing differences between GPS and Galileo observations.

This option is close to the user situation and can be implemented with the help of a combined GPS/Galileo receiver installed at a fixed location with precisely known coordinates. A drawback here is an indirect access to the system timescales of both systems – they will be "reconstructed" from user measurements with the help of broadcast (or externally estimated) clock parameters. As a consequence, one may expect that the short-term noise of the estimation will be considerably higher than the noise of the system time itself. Another drawback of this approach is that it does not take advantage of the fact that GST is available physically and can be accessed directly.

On the other hand, a link between GST and one of the clocks of the GPS ensemble (e.g. the clocks contributing to GPS Time) can be built (see Figure 6-9). This is, however, only the first step. The second one is to get the information on the offset of the GPS clock linked to GST and the GPS Time. It is not expected that this information will be available directly from the GPS Master Control Station (MCS) where the offsets are computed. Thus, the natural solution is to build a link between GST and GPS satellite clocks for which offsets to GPS Time are available in the broadcast navigation message.

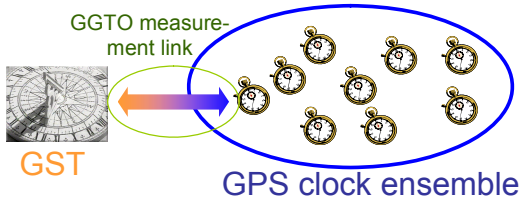

Figure 6-9. Linking of GST with GPS Time

Based on the consideration presented above and analysis of the Galileo technical documentation, four favorite options for GGTO determination can be identified

- link with the US Naval Observatory (USNO),
- reception of GPS SIS with a GPS time receiver at PTF connected to the GST realization,
- reception of GPS and Galileo SIS at PTF with separate GPS and Galileo time receivers
- reception of GPS and Galileo SIS at PTF with a combined GPS/Galileo receiver

These options are described below in more details.

6.4.3.1 GGTO determination using TWSTFT Link with USNO

USNO continuously monitors the offset between GPS Time and its Master Clock by reception of GPS signals at USNO premises using a military GPS time receiver. The GPS raw measurements are processed to compute daily values of GPS Time – UTC(USNO) time offset which are used to steer GPS Time to UTC(USNO), and to derive the GPS Time – UTC

offset parameters which are broadcast in GPS navigation message. The daily offset values can be also made available to interested users.

GGTO determination using TWSTFT link with USNO foresees involves two steps:

- Determination of GST – UTC(USNO) offset using a TWSTFT link between USNO and PTF
- Computation of GGTO using the GPS Time – UTC(USNO) offset provided by USNO (see above on determination of this offset)

The major error sources for GGTO determination using TWSTFT link to USNO are illustrated in Figure 6-10.

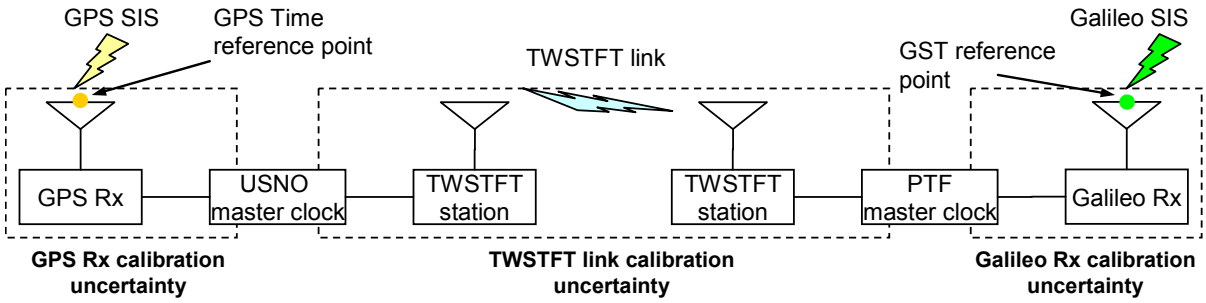

Figure 6-10. Major sources of GGTO determination uncertainty when using link with USNO

Major benefits of the method are:

- Access to USNO experience of GPS Time restitution (GPS SIS will be processed solely by USNO in the frame of their regular operations)
- Access to data from a military GPS time receiver (reduces impact of potential deterioration of civil service accuracy)
- Clear link to GPS infrastructure for exchange of GGTO determination results

Major drawbacks of the method are:

- Need to procure, maintain and operate additional equipment (TWSTFT). The equipment used for PTF-PTF time offset measurements and to link PTF to UTC laboratories can be re-used, but the need for additional operations remains.
- Need for an additional agreement with USNO on TWSTFT operations (satellite, timing, data provision)
- Dependence on USNO (operations of the USNO part of the link, provision of UTC(UNSO)-GPS Time offset)
- GGTO determination by Galileo and GPS is not independent
- Measurements from a military GPS time receiver might be not representative for civil timing service of GPS

6.4.3.2 GGTO determination using GPS SIS

This method foresees determination of GGTO from receptions of GPS SIS using a GPS time receiver collocated at PTF and operated with the time and frequency reference corresponding to GST. Reference point for GPS Time is defined at the phase center of this receiver's antenna. Reference point for GST is defined as before at the phase center of the GSS antenna.

Note that in this method, GGTO is determined independent of measurements of the Galileo SIS. In the GGTO uncertainty estimation, however, the calibration uncertainty of the GSS calibration comes into play because of the definition of GST at the GSS antenna phase centre.

The major error sources for GGTO determination from reception of GPS SIS using a GPS time receiver at PTF are illustrated in Figure 6-11.

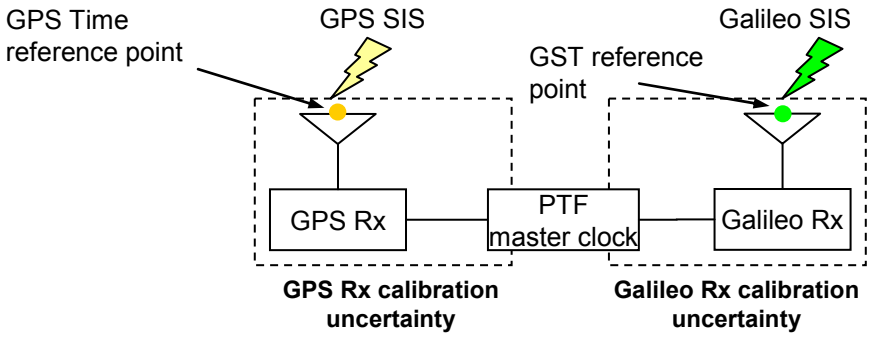

Figure 6-11. Major sources of GGTO determination uncertainty when using GPS time receiver at PTF

Major benefits of the method are:

- GGTO determination is fully under PTF (and consequently, Galileo) control
- GPS Time is accessed in the same manner as available to users

Major drawbacks of the method are:

- Additional equipment need to be procured, maintained and operated at PTF

  GPS time receiver which is used to link PTF with UTC can be re-used also for GGTO determination. In this case, probably, no additional procurements, maintenance and operations will be needed. However, some special algorithms for GGTO determination may be required.

6.4.3.3 GGTO determination using separate GPS and Galileo time receivers

This method foresees determination of GGTO from receptions of GPS and Galileo SIS using separate GPS and Galileo time receivers collocated at PTF and operated with the time and frequency reference corresponding to GST. Reference point for GPS Time is defined at the phase center of this receiver's antenna. Reference point for GST is defined as before at the phase center of the GSS antenna. The major difference to the GGTO determination from reception of GPS SIS at PTF which is described above is that in this case GST is obtained not from the PTF Master Clock but from Galileo SIS, i.e. both GPS and Galileo measurements are to be processed to estimate GGTO. This method can be implemented actually at any station (not only PTF) equipped with GPS and Galileo time receivers operating with the same time and frequency reference.

The major error sources for GGTO determination from reception of GPS and Galileo SIS using separate GPS and Galileo time receivers at PTF are illustrated in Figure 6-12.

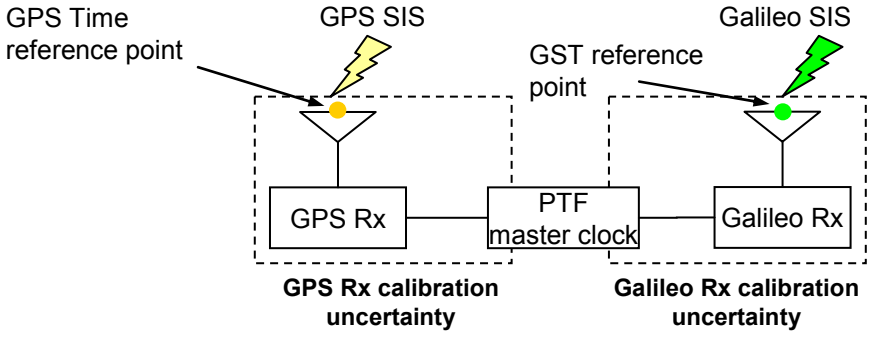

Figure 6-12. Major sources of GGTO determination uncertainty when using GPS and Galileo time receivers

Major benefits of the method are:

- GGTO determination is fully under PTF (and consequently, Galileo) control
- Both GPS Time and GST are accessed in the same manner as available to users (i.e. through the SIS)
- The method can be implemented at any station (see explanation above), also at UTC laboratories. Thus, a network of station might be utilized to increase the reliability of GGTO determination (in this case, relevant GPS and Galileo measurements should be submitted by GTSP to PTF for further processing, this option was not explored up to now). Coordination of this network is probably a task of the GTSP.

Major drawbacks of the method are:

- Reduced performance in the IOV phase due to low number of available Galileo satellites
- Additional equipment (GPS time receiver) need to be procured, maintained and operated at PTF
- GPS time receiver which is used to link PTF with UTC can be re-used also for GGTO determination. In this case, probably, no additional procurements, maintenance and operations will be needed.
- Additional interface has to be established to make Galileo measurements collected at GSS available for GGTO processing at PTF
- GGTO determination accuracy may be slightly reduced due to uncertainties of GST dissemination through Galileo SIS

6.4.3.4 GGTO determination with a combined GPS/Galileo receiver

Finally, GGTO can be also determined from reception of GPS and Galileo SIS with a combined GPS/Galileo time receiver installed at PTF. Basically, this method can be used with a combined receiver at any locations. However, since PTF is responsible for GGTO determination, it is convenient to have the receiver installed at PTF. The advantage of using this method (comparing to those involving utilization of GPS or Galileo only receivers) is that only the difference between the propagation time of GPS and Galileo signals in the receiver need to be calibrated. It can be expected that this difference will be rather small (only a few ns).

The major error sources for GGTO determination from reception of GPS and Galileo SIS using combined GPS/Galileo receiver at PTF are illustrated in Figure 6-13.

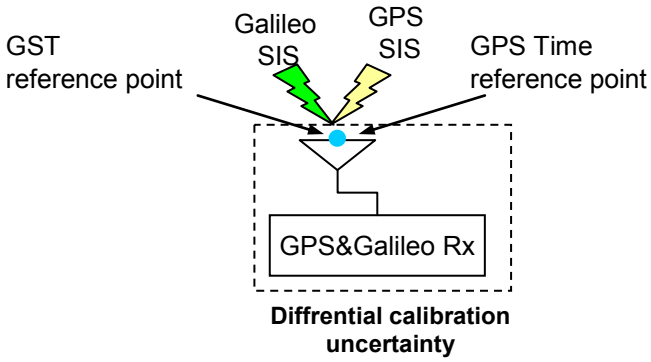

Figure 6-13. Major sources of GGTO determination uncertainty when using a combined GPS/Galileo receiver

Major benefits of the method are:

- GGTO determination is fully under PTF (and consequently, Galileo) control
- Both GPS Time and GST are accessed in the same manner as available to users

- Only the difference between the signal propagation time for GPS and Galileo signals in the receiver is to be considered (potentially, significant accuracy improvement)
- GGTO is determined using a single sensor
- The method can be implemented at any station (see explanation above), also at UTC laboratories. Thus, a network of station might be utilized to increase the reliability of GGTO determination (in this case, relevant GPS and Galileo measurements should be submitted by GTSP to PTF for further processing, this option was not explored up to now). Coordination of this network is probably a task of the GTSP.

Major drawbacks of the method are:

- Reduced performance in the IOV phase due to low number of available Galileo satellites
- Combined GPS/Galileo receiver at PTF is currently not in the Galileo baseline. It is not clear, if such receiver will be available in the due time.
- Additional equipment (GPS time receiver) need to be procured, maintained and operated at PTF

  Potentially, the GPS/Galileo receiver can be used also as a Common View receiver which serves to link PTF to UTC laboratories. In this case, the overall number of PTF equipment pieces and the complexity of PTF operations will not be increased. However, the availability of the combined GPS/Galileo receiver to support GGTO determination in the due time is not sure.

6.4.4 Galileo baseline on GGTO measurement

According to the present Galileo baseline [Hahn04], GGTO is to be measured with two techniques:

- Via a link between PTF and USNO,
- From reception of Galileo Signal-in-Space (SIS) at the PTF (with a combined GPS/Galileo time receiver).

The first technique is the primary one, the second technique is implemented for redundancy and reliability reasons.

To implement the first technique, a two way time and frequency transfer link (TWSTFT) through a geostationary satellite is planned to be implemented between Galileo PTF and USNO. The institutional issues of GGTO determination were recently addressed by a special US-EU working group (see e.g. [Hahn04]).

Also, a special attention to hardware calibration issues should be paid since the accuracy of this link will be affected by two types of calibration uncertainties: (a) calibration error in TWSTFT link (typically, about 1 ns (RMS)), (b) calibration errors in the GPS timing receiver(s) at USNO premises (about 3 ns (RMS), [White01]).

The secondary technique foresees measurement of GGTO from reception of GPS SIS and the PTF by means of a combined GPS/Galileo time receiver. However, the simplest approach is to use a GPS time receiver connected to the GST physical realization available at PTF. Here we discuss both approaches.

Also for the secondary technique, calibration issues play a key role for the GGTO determination accuracy. It can be expected that the calibration uncertainty of a GPS time receiver at PTF will be of the same order as of the similar equipment installed at USNO premises.

6.4.5 Error budget of GGTO measurement techniques

6.4.5.1 GGTO measurement with a GPS/Galileo time receiver at PTF

In case GGTO is measured with the help of a GPS time receiver at PTF, GGTO determination would become a typical problem of GPS time restitution when user wants to determine the offset between a local clock and GPS Time with the maximally possible accuracy. Further, one may assume that GGTO measurements are processed in real-time (or at least with such a short delay that precise GPS orbits and clocks (e.g. from IGS or EGNOS) are not yet available) and its estimate is based solely on pseudorange measurements processed according to the standard technique utilized in the timing community (see [Defraigne03]). Then the accuracy of GGTO determination can be assessed by analyzing Eq. 4-21. Uncertainty of GGTO determination σ_{GGTO} can written as

$$\sigma_{GGTO}^2 = \sigma_{eph}^2 + \sigma_{cl}^2 + \sigma_{trop}^2 + \sigma_{HW}^2 + \sigma_{noise}^2 \qquad \text{Eq. 6-10}$$

where the standard deviations in the right part of the equation correspond to errors of satellite ephemeris, clock parameters, tropospheric model in use, hardware calibration and measurement noise respectively. A dual-frequency GPS time receiver was assumed to be utilized for GGTO determination; therefore residual ionospheric error was expected to be negligible.

The magnitudes of uncertainties in Eq. 6-10 depend also on the selected averaging time. As a standard, averaging over 960 seconds is utilized in the timing community. Table 6-8 summarizes the error budget for GGTO determination for snap-shot (no averaging) case and averaging cases.

Error	***Snap-shot***	***960-s average***
σ_{eph} (from [Warren03])	4 ns	4 ns
σ_{cl} (from [IGSWeb])	5 ns	5 ns
σ_{trop} (from [Parkinson96])	2 ns	2 ns
σ_{HW} (from [White01])	3 ns	3 ns
σ_{noise}	2 ns	0.5 ns
Total without σ_{HW}	7.0 ns	6.7 ns
Total with σ_{HW}	7.6 ns	7.4 ns

Table 6-8. Error budget for GGTO measurements with a GPS time receiver at PTF

Assuming the average number of GPS satellites in view over Europe being about 7.5 and pseudorange errors being not correlated between different satellites, we get the following estimates for uncertainty of GGTO estimates obtained from averaging single satellite data.

Average error	***Snap-shot***	***960-s average***
Without σ_{HW}	2.6 ns	2.4 ns
With σ_{HW}	2.8 ns	2.7 ns

Table 6-9. Average error of GGTO determination with a GPS time receiver at PTF

The budgets above do not consider a presence of any kind of GPS SA modulation which was discontinued in May 2000, but may be introduced again in future.

Estimates given in Table 6-9 may appear to be slightly optimistic considering the results presented in Table 6-7 which were obtained from an analysis of broadcast clock parameters.

6.4.5.2 GGTO measurement via link with USNO

In case GGTO is measurement with a TWSTFT link between USNO and PTF and offsets between GPS Time and UTC(USNO) estimated by the USNO, the uncertainty of GGTO depends on the accuracy of calibration of the TWSTFT equipment, GPS receiver at USNO (that is used to determine the offset UTC(USNO) - GPS Time), and cabling at USNO and PTF.

The accuracy of GGTO determination via the TSWTFT link with USNO is expected to be slightly worse than via a GPS time receiver at PTF. In the first case, the link between GST and GPS Time includes two sub-links: GST – UTC(USNO) (via TWSTFT) and UTC(USNO) – GPS Time (via a GPS time receiver at USNO). In the second case, the link between GST and GPS Time is established via a GPS time receiver at PTF. We may expect that (assuming GPS Selective Availability is off) the accuracy of $UTC(USNO) - GPSTime$ and $GST - GPSTime$ determined from reception of GPS signals at USNO and PTF respectively would be similar. Thus, the usage of TWSTFT link between PTF and USNO would slightly increase the noise of the resulting GGTO estimates.

Further discussion on the error budget of GGTO determination via a link with USNO is available in Section 6.7.2.6.

6.5 Prediction of GGTO

"Prediction is very difficult, especially about the future."

-- Niels Bohr

6.5.1 The purpose

The ability to measure the GGTO is only a pre-requisite to solve the main problem: produce a precise prediction of GGTO over a certain time period that should be provided to users. Certainly, applications where it is sufficient to get results in post-processing can directly use results of GGTO determination. However, the majority of navigation users will need GGTO value in real-time. Thus, Galileo should broadcast a predicted GGTO value valid for the chosen update interval. The choice of update interval is driven by system operations trade-offs and the variability of GGTO. Galileo baseline foresees GGTO updates to be made once per day. The questions to resolve are

- how to predict the GGTO, and
- how to parameterize it for broadcasting.

6.5.2 GPS experience

Of course, GGTO determination/prediction is presently not a part of GPS operations. However, there is some relevant experience to consider – determination and prediction of GPS Time offset from UTC(USNO). As mentioned earlier, UTC(USNO) is produced from steered H-maser, and, thus, possess similar characteristics as GST.

GPS Time offset is determined with a military GPS receiver (i.e. a dual-frequency P-code receiver) installed at the USNO premises. The GPS measurements from this receiver are corrected using precise satellite ephemeris and clock estimated produced by the National Mapping Agency (NIMA). Estimates of (GPSTime-UTC(USNO)) offset are computed with the rate of 15 minutes (unlike the standard 16-minute rate recommended by BIPM). The 15-

minute points over 36 hours are used to compute a daily value of (GPSTime-UTC(USNO)) offset (by taking the mid point of a linear fit to the measurement data). The daily estimates are communicated to the GPS MCS. Two consequent values are used to compute parameters of (GPSTime-UTC(USNO)) model to be broadcast to GPS users: a_0 (time offset) and a_1 (frequency offset).

6.5.3 Requirements to the GGTO prediction algorithm

The GGTO prediction algorithm is intended for operational implementation in Galileo. It dictates some specific requirements to this algorithm and its output:

- the algorithm shall be suitable for automatic operations with minimal human interventions;
- GGTO prediction accuracy shall satisfy relevant requirements (present baseline requirements are summarized in [Hahn04]);
- it shall be possible to parameterize the GGTO predictions according to relevant requirements (the model shall be valid at least over 24 hours and shall include not more than 2 parameters – offset and drift [Hahn04]);
- the algorithm shall make use of data obtained with the baseline GGTO determination techniques (see Section 6.4.4).

These requirements helped to focus the search for an optimal GGTO prediction algorithm to the options discussed below.

6.5.4 Options for GGTO prediction

6.5.4.1 GGTO model

Galileo baseline defines that a linear model shall be used for GGTO prediction, i.e. two parameters a_0 (time offset) and a_1 (frequency offset) have to be included into the broadcast navigation message. This model is identical to the one utilized in GPS for the offset GPS Time - UTC(USNO).

Here we consider the baseline model and also its simplification: a fixed value prediction (i.e. only with a_0 parameter).

6.5.4.2 GPS-like approach

Two options for the GPS-like GGTO prediction approach would mean that GGTO parameters (either a_0 and a_1, or only a_0) are defined by fitting a line to measured GGTO values. Two kinds of measurements can be used

- "raw" GGTO measurements with there "natural" rate (1 day or 2 hours for TWSTFT data, and 16 minutes for data from GPS time receiver), and
- daily GGTO estimated obtained from pre-processing of the "raw" data mentioned above.

6.5.4.3 ARIMA approach

ARIMA stands for autoregressive integrated moving average. This modeling and prediction technique was explored by Box in Jenkins (see, e.g. [Box76], numerous editions of the book exist). The ARIMA treatment here is due to [Pankratz83].

The essence of ARIMA prediction technique is to predict the process at hand based on inherent statistical relations in it. The process model is a mixture of an autoregressive (AR) and moving average (MA) models. Such model can be successfully applied only to stationary processes. In case of non-stationary process, differencing of consequent process samples often help to achieve the stationarity (at least, in the wide sense that the mean and the

variance of the process do not depend on time). The ARMA model is then applied to the derived (differenced) process. To come to the original process which needs to be predicted, integration is used.

ARIMA process model can be presented in the so-called “compact notation”:

$$\psi(\mathrm{B})\nabla^k \tilde{z}_i = \theta(\mathrm{B})\, w_i \qquad \text{Eq. 6-11}$$

here

$\tilde{z}_t$ - deviation of the process variable from its mean,

B - backshift operator defined so that $\mathrm{B}z_i = z_{i-1}$,

∇^k - differencing operator of k-th order $\nabla^k = (1-\mathrm{B})^k$,

$$\psi(\mathrm{B}) = \left(1 - \psi_1 \mathrm{B} - \psi_2 \mathrm{B}^2 - \ldots - \psi_2 \mathrm{B}^m\right),$$

$$\theta(\mathrm{B}) = \left(1 - \theta_1 \mathrm{B} - \theta_2 \mathrm{B}^2 - \ldots - \theta_2 \mathrm{B}^n\right),$$

w - “random shock” (noise term).

Typically, ARIMA models are specified by three parameters: ARIMA(m,k,n), where m is the order of AR model, n is the order of MA model and k is the order of differencing.

ARIMA models are also able to handle periodic or seasonal effects; however this issue is not addressed here since such effects are not expected to have a significant impact on GGTO.

As soon as model parameters and coefficients of AR and MA parts of the process are estimated from analysis of experimental data, they can be used for prediction using historical data in a scrolling window manner.

However, identification of model and its coefficient is a serious problem, especially when the available set of experimental data is small. Special analysis is required to identify a suitable process model, where suitable means the model that allows to achieve the desirable prediction accuracy using smallest number of model parameters. The classical ARIMA analysis uses the 3-step iterative approach illustrated in Figure 6-14.

The first step, identification, is supported by visual analysis of the experimental data (and if necessary, their sequential differences) to check the process stationarity. The order of AR and MA models can be also guessed from visual analysis of the autocorrelation and partial autocorrelation functions. AR process exhibits peaks in the partial autocorrelation coefficients for non-zero lags. MA process leads to a similar effect in autocorrelation coefficients.

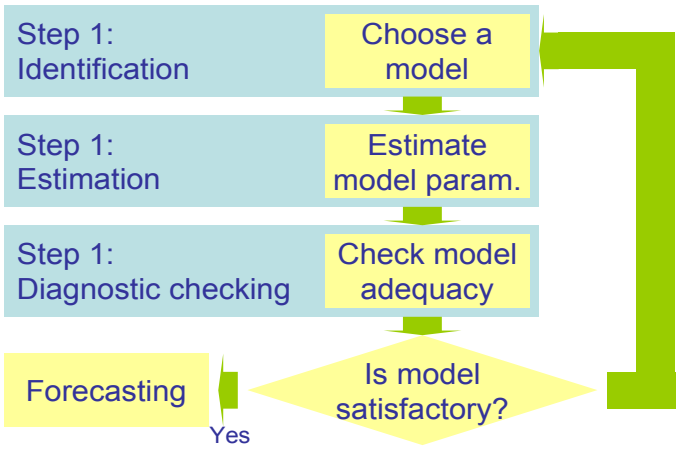

Figure 6-14. Box-Jenkins model building

The model coefficients are recommended to be estimated with a non-linear least mean squares technique (refer to [Box76] for details). The non-linear techniques are used since ARMA models lead to a set of highly non-linear equations which require an iteration technique to ensure solution convergence.

Model adequacy can be checked by analyzing the estimation residuals (deviation of the modeled values from experimental ones). The most common statistics are the square sum of residuals or their RMS value, and the autocorrelation (as well as the partial autocorrelation) function of the residuals (in general, residual should not be correlated). Another useful tool is a prediction test with the estimated model on an additional set of experimental data. The obtained prediction error should match the expectations.

6.6 Tests of GGTO measurement

6.6.1 Test of GGTO measurement via link with USNO

GGTO measurement using a link with the USNO was described in [Bauch04]. The offset between GPS Time and UTC(PTB) was computed from the TWSTFT measurements between the PTB and the USNO and the GPS measurements made at the USNO covering about 200 day in 2002 and 2003.

6.6.2 Test of GGTO determination from reception of GPS SIS

GGTO measurement from reception of GPS SIS at Galileo PTF was discussed in [Moudrak04b]. A test of GGTO determination making use of GPS observations collected at ORB was also presented there.

6.7 Tests of GGTO prediction

6.7.1 Overview of test data

We tested GGTO prediction using the following data for GGTO determination using GPS SIS:

- Offset between GPS Time and UTC(USNO)

  The data were made available by the USNO. The offset was computed by the USNO from GPS measurements made with a GPS time receiver at USNO premises. The data covered the time span between MJD 52944 and 53123, and included daily GPSTime-UTC(USNO) offset computed according to the procedure described in Section 6.4.3.1. Daily GPSTime-UTC(USNO) values and daily slopes (computed over 36-hour periods preceding the target days) were made available.

- Offset between GPS Time and UTC(PTB)

  The offset was computed from GPS measurements made at PTB premises with a dual-frequency multi-channel GPS time receiver (model Ashtech Metronom Z12T). GPS observations were processed at PTB according to the technique described in [Defraigne03] (see also Section 4.2.6.1), and made available by PTB in daily files (data rate: 16 minutes, data for all visible satellites for each observation epoch were given). Data covering the time span between MJD 52949 and 53128 were used.

  The data were additionally processed as follows. First, for each observation epoch, a median from measurements to individual satellites was computed. Then linear fits were made to the median data for each of the days. Finally, daily values (middle of each day) were computed from the linear fits.

The amount of steering applied to GPS Time and UTC(USNO) was unknown to the author. Steering of UTC(PTB) was made known by the PTB.

For all data sets, only measurement data were available. The true values were unknown. To "calibrate" the estimates of prediction accuracy obtained with the measurement data, we used simulated GGTO values.

The simulation was based on the GST specification (see Section 3.2.2) and the assumptions on GPS Time performance presented in Section 4.1.2.2. Two options were considered:

- no steering applied to GPS Time and GST (in the real world it would correspond to the situation when steering on these two time scale is known, and the collected GGTO data are corrected for it), and
- steering of GPS Time and GST is unknown, hence, GGTO data can not be corrected for it.

  To make simulation of steered GGTO as realistic as possible, simulated and real data were combined. For GPS Time daily offsets between GPS Time and UTC available in BIPM Circular T were taken. The daily intervals between them were "filled" with simulated values (rate: 1 value per 15 minutes).

  Circular T data were used also for simulation of GST: the offsets between UTC(ORB) and UTC since the short- and medium-term performance of UTC(ORB) was considered to be representative for GST. These values were available with an interval of 5 days. Similar to GPS Time simulation, the 5-day intervals were "filled" with simulated data.

  Due to using real GPS Time and UTC(k) data, steering of GPS Time and GST to TAI was not necessary to simulate: it was already present in these data.

Simulated GGTO values were produced with the interval of 15 minutes for the time span of 180 days. From these data, daily GGTO values (for the middle of each day) were computed from linear fits to daily intervals. Originally, simulated data GGTO data can be supposed to contain neither measurement noise nor biases.

Allan Deviation of all data sets mentioned above is illustrated in Figure 6-15.

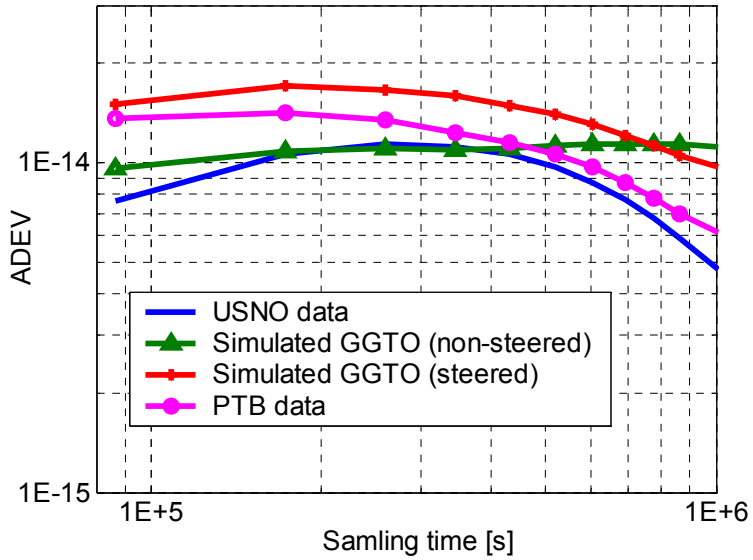

Figure 6-15. Allan Deviation of GGTO test data

A test of GGTO prediction is described in [Bauch04]. As mentioned in Section 6.6.1, in this test the offset between GPS Time and UTC(PTB) was computed from the TWSTFT measurements between the PTB and the USNO and the GPS measurements made at the USNO. The data obtained in such a way are appeared to be very similar (from the point of view of measurement noise and the underlying process dynamic) to those obtained from reception of GPS SIS at PTB (see above). Therefore, no additional tests with data for the USNO link were executed here.

6.7.2 Test results

6.7.2.1 Overview

Tests were executed for the prediction period of 24 hours that corresponded to the baseline on the validity period of broadcast GGTO model (see Section 6.5.3).

The following prediction scenarios were tested:

(1) prediction with the last daily value,

(2) prediction with the slope computed from a linear fit to the original measurement data (data rate: 15 minutes for the USNO data), 16 minutes for the PTB and simulated data, and 1 day for the two way data),

(3) ARIMA prediction,

(4) prediction with Kalman filter.

The choice of prediction techniques was driven by available GPS experience and expertise on prediction problems in other applications (see Section 6.5).

For tests with measured data (USNO, PTB and the two-way data), no reference (i.e. the true value) of GPS Time offset was available. Therefore, prediction error was estimated with respect to the measured data themselves. Only daily values were predicted (see also Section 6.7.2.2).

Furthermore, the measured data contained also measurement biases (hardware calibration uncertainties etc.). These biases do not significantly change over the selected prediction period (see Section 6.7.2.6). Therefore, estimated the prediction error estimated in these tests characterizes only the stochastic part of the prediction error in a real scenario. Expected bias values are presented in Section 6.7.2.6.

For prediction with a fixed or a linear model (techniques 1 and 2 from the list above), selection of the measurement period on which the model parameters are estimated is of the key importance. Corresponding tests are presented in Section 6.7.2.2.

6.7.2.2 Selection of optimal measurement period for GGTO determination from GPS SIS using a fixed value or a linear model

The optimal length of measurement interval on which parameters of prediction model are estimated (techniques 1 and 2, see Section 6.7.2.1) depends on two basic factors: the type of the inherent noise of the process to be predicted, and on the magnitude and type of the noise of measurement data. Theoretical considerations on selection of measurement interval can be found e.g. in [Allan87a] and [Delporte01]. They are derived for processes characterized by one noise-type: white frequency noise, flicker frequency noise or frequency random walk. However, both GPS Time and GST are affected by a combination of these noise types. Therefore, simulations were considered to be an appropriate tool to identify optimal measurement interval. They were executed on data from PTB and the simulated data sets (see Section 6.7.1) since for these data original measurements with 16-minute rate were available.

Prediction error $\Delta GGTO$ was computed as follows:

$$\Delta GGTO(t_i) = \hat{a}_0\left(t_i - \frac{\Delta t_p}{2} - \Delta t_m\right) - \hat{a}_1\left(t_i - \frac{\Delta t_p}{2} - \Delta t_m\right)\cdot \Delta t_e - \\ - GGTO(t_i) \qquad \text{Eq. 6-12}$$

here

t_i - moment of time corresponding to i-th daily value (always middle of the day),

$\hat{a}_0, \hat{a}_1$ - parameters of prediction model (offset and slope) estimated from a LMS fit to the measurement data covering the time interval $\left[t_i - \frac{\Delta t_p}{2} - \Delta t_m ; t_i - \frac{\Delta t_p}{2} \right]$,

Δt_e - extrapolation period ($\Delta t_e = \frac{\Delta t_p}{2} + \Delta t_m$ for a prediction with a linear model, and $\Delta t_e = \Delta t_m$ for fixed value prediction).

Δt_m - length of the measurement interval (several were tested: for PTB data Δt_m varied from 12 to 72 hours with 12-hour step, and for the simulated data Δt_m varied from 6 to 72 hours with 6-hour step), and

Δt_p - length of the prediction interval (fixed to 24 hours).

$GGTO$ - reference GGTO value (for PTB data – a daily value computed from the measurements, for simulated data – a daily value computed from the simulated GGTO data without measurement noise).

Finally, RMS prediction error for each of the measurement intervals under test was estimated.

Test results for the PTB data are presented in Figure 6-16. The lowest RMS (1.43 ns) was achieved with a fixed value prediction model for the measurement interval of 36 hours. In general, at all tested intervals prediction error for the fixed value prediction was lower than that for the prediction with linear model.

Prediction test was executed on the USNO data where the slopes estimated from fits to 36-hour intervals were made available by the USNO. The RMS prediction error of 0.87 ns was obtained.

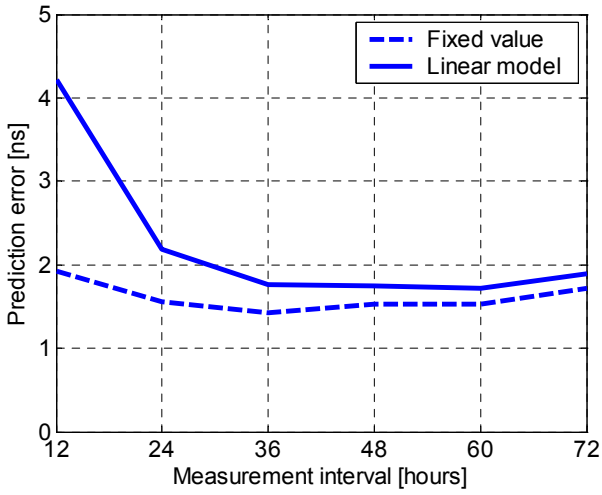

Figure 6-16. Daily prediction error vs. measurement interval (PTB data)

A similar test was made also with the simulated data of non-steered and steered GGTO. Test was executed both on the original simulated data without measurement noise and on the data where this noise was added (original simulated data plus simulated normal Gaussian noise with zero mean and standard deviation of 5 ns). Test results are presented in (see Figure 6-17), and the minimal RMS prediction error is given in Table 6-10. All values in Table 6-10 correspond to prediction with linear model which demonstrated better performance then the prediction with a fixed value.

This result contradicts with the outcome of the test with PTB data where fixed value model was performing better than the linear one. A reason for it may be utilization of measurement data (i.e. data with measurement noise, not the true values to compute prediction error). To

check this assumption, an additional test where prediction error for steered GGTO was computed against not the true GGTO value, but the value with added simulated measurement noise (see Figure 6-18). In this test as in the test with PTB data, prediction with fixed value demonstrates superior performance for all time intervals. Thus, it can be concluded that estimation of prediction error against noisy data introduces significant aberrations into the test results (compare also prediction RMS in Table 6-10 with the one estimated on PTB data, note that prediction error estimated using steered GGTO without measurement noise is close to the prediction error estimated using PTB data).

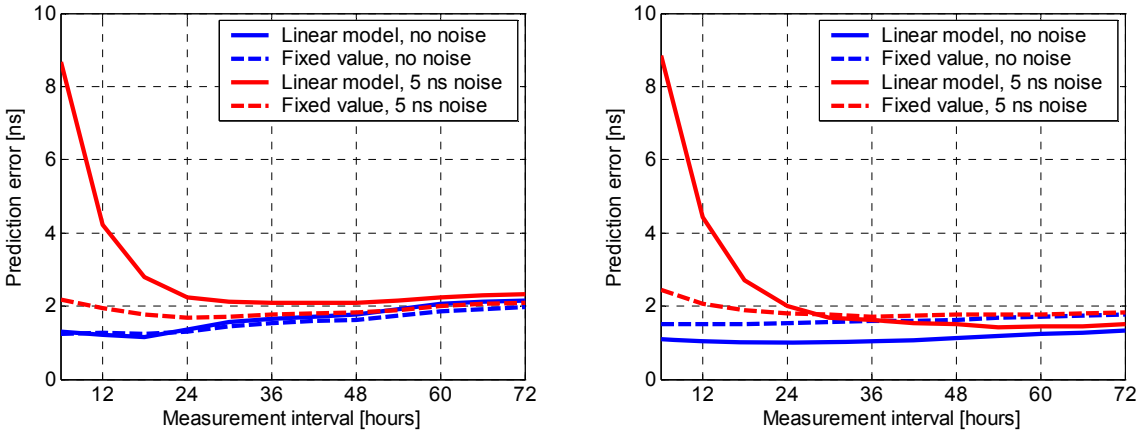

Figure 6-17. Daily prediction error vs. measurement interval (simulated data) (left: with steering, right: without steering)

Measurement noise	***Data type***	
	No steering	***With steering***
No measurement noise	1.0 (linear model, meas int 24h)	1.2 (linear model, meas int 18h)
Measurement noise	1.5 (linear model, meas int 60h)	1.7 (fixed value, meas int 36h)

Table 6-10 Minimal RMS of daily prediction error for simulated data

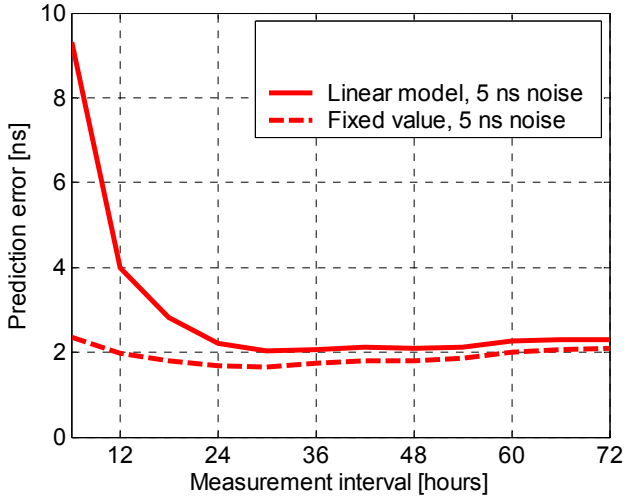

Figure 6-18. Daily prediction error vs. measurement interval (simulated steered GGTO) (error computed vs. noisy data)

Additional problem of all presented tests is that prediction error was estimated against daily value. However, GGTO varies significantly over one day (see Table 6-11).

Data type	*RMS around daily mean [ns]*	*RMS around daily linear fit [ns]*
No steering	0.9	0.2
With steering	0.7	0.2

Table 6-11 GGTO variation around daily mean

To study the impact of daily variations of GGTO onto the prediction error, a similar test as above was executed, but the prediction error was calculated not against daily average only but for all data points within the daily interval. The test was made with the simulated data for steered and non-steered GGTO (see Figure 6-15 for the GGTO performance). Test results are summarized in Figure 6-19 and Table 6-12.

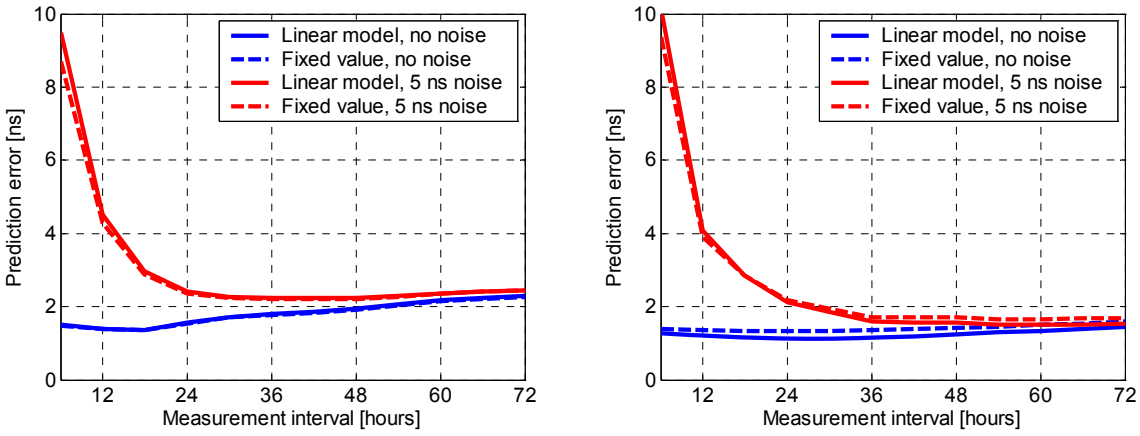

Figure 6-19. Prediction error vs. measurement interval (prediction vs. all data points, simulated data) (left: with steering, right: without steering)

Measurement noise	*Data type*	
	No steering	*With steering*
No measurement noise	1.1 (linear model, meas int 24h)	1.4 (fixed value, meas int 18h)
Measurement noise	1.5 (linear model, meas int 60h)	2.1 (fixed value, meas int 40h)

Table 6-12. Minimal RMS of prediction error (all data points) for simulated data

From the results presented in Figure 6-19 and Table 6-12, several important conclusions can be made:

- when only daily averages are used to estimate the quality of prediction (that is typically the case with real-world data since daily averages allows to suppress the measurements noise sufficiently), the estimation results are somewhat optimistic, especially in case of prediction with a fixed value using input noisy data;

- for non-steered GGTO, linear prediction performs better than the fixed value one; and for steered GGTO vice versa. However, the performance differences are practically insignificant;
- optimal measurement intervals are different for steered and non-steered data and for data with measurement noise and without it. The length of the interval would be also dependent on the magnitude of measurement noise.

Finally, a fixed-value prediction model with measurement interval of 24-48 hours could be recommended for prediction of both steered and non-steered GGTO.

It is worth to note that despite a relatively simple noise model used in simulations presented here, the results are relatively well consistent with those obtained from the elaborated simulation which incorporated real errors of GPS satellite orbits and clock parameters, and troposphere (see [Moudrak04c]). In [Moudrak04c] fixed value prediction of steered GGTO was shown to perform better than a linear model prediction. The lowest prediction RMS error was achieved for the measurement interval of 24 hours and was equal to 2.25 ns.

6.7.2.3 Identifying ARIMA models

Before proceeding with Box-Jenkins prediction (see Section 6.5.4.3 for a short review of this technique), a suitable ARIMA model for GGTO had to be identified. First of all, the order of AR and MA components had to be selected. According to [Pankratz83] a good idea on it can be obtained from studying of time series plots, ACF and PACF of experimental data. For processes exhibiting visible non-stationarity (e.g. varying mean, trends etc), sequential differencing should be applied since n-th order differences of a non-stationary processing are often stationary. This statement is in agreement with the work of D. Allan and J. Barnes who have shown that first differences of relative frequency offset between two clocks (that is equal to second differences of the relative phase offset) are usually wide sense stationary while the phase and frequency offset themselves are usually not.

Section B .1 of Annex B presents the time series plots, ACF and PACF for all data sets under test while Section B .3 shows RMS modeling errors for different orders of AR and MA processes and some statistics of modeling residuals for selected cases.

Estimation of ARIMA model using noisy data (those from USNO, PTB and two-way link) may appear to be incorrect; however, effect of the white Gaussian noise (WGN) onto the process model is well-known: WGN is essentially an MA(0) process. Nevertheless, effect of colored noise components may “bias” model selection. Therefore, results of model identification executed with simulated data can be considered as “reference”. A summary of the modeling results is given in Table 6-13.

Data set	***ARIMA model***	***RMS of modeling residuals, ns***
UTC(PTB) - GPS Time	2,0,0 1,1,1 2,1,2	2.0 2.1 2.0
UTC(USNO) - GPS Time	2,0,1 2,1,2	0.4 0.4
Simulated GGTO (no steering)	1,1,0	1.3
Simulated GGTO (with steering)	1,1,1	2.1

Table 6-13 Selection of ARIMA models for selected test data

A brief discussion on model identification for all data sets follows.

Simulated data

A look at the raw data and their first and second differences allows selection of the first differences as basis for GGTO prediction for both steered and non-steered data. This is supported by analysis of ACF and PACF (see Section B .1 of Annex B). On the other hand, [Allan87b] has shown that stationarity can be expected from second differences of a clock deviation. Nevertheless, second differences exhibit a pattern which is absent in the first differences which makes modeling more difficult and witnesses an “over-differencing” effect (see also [Pankratz83] on practical aspects of ARIMA modeling).

Analysis of ACF and PACF of first differences and modeling residuals (see Section B .3 of Annex B) allows choosing an ARIMA(1,1,0) model for non-steered GGTO and ARIMA(1,1,1) for steered GGTO. These models offered the best performance/complexity relation over tested ARIMA(n,1,m) models (both n and m varying from 0 to 4).

The additional MA(1) term in the steered GGTO model reflects the effect of (unknown) steering which represents, from the modeling point of view, a kind of frequency noise.

Modeling error for non-steered GGTO was significantly smaller than for the steered GGTO (1.3 ns and 2.1 ns respectively). This is due to a bad predictability of steering.

PTB data

First look at ACF and PACF of the original data and their first differences two models can be suggested: ARIMA(2,0,0) or ARIMA(1,1,1).

A more detailed analysis (see Section B .3 of Annex B) shows that all tested ARIMA(n,0,m) models with n varying from 2 to 4 performs very similar, thus ARIMA(2,0,0) seems to be a good choice. As for ARIMA(n,1,m) models, performance of ARIMA(2,1,2) appeared to be a good trade-off between complexity and performance.

From ACF and PACF plots of the residuals it can be seen that ACF and PACF of ARIMA(2,0,0) residuals is negligible, whereas ACF and PACF of ARIMA(1,1,1) reach the significance limits. ARIMA(2,1,2) eliminates these minor effects, its residuals become uncorrelated.

It is worth to note that utilization of non-differenced model ARIMA(2,0,0) was possible due to rigorous steering of UTC(PTB) to UTC which makes its offset from GPS Time wide sense stationary.

USNO data

Analysis of ACF and PACF of the measurement data and of ARIMA modeling results (see also Annex B) allowed to select two candidate models: ARIMA(2,0,1) and ARIMA(2,1,2) which exhibited almost equal performance. In case of USNO data it was possible to utilize a non-differenced model and to achieve higher modeling accuracy comparing to other data sets. This is due to the fact that GPS Time is closely steered to UTC(USNO).

6.7.2.4 Prediction with ARIMA

All ARIMA predictions were made using daily input data. Additional model optimization (as minimization of the prediction error) was executed.

6.7.2.5 Summary of test results

Table 6-14 summarizes prediction accuracy for different prediction scenarios for steered and non-steered data with and without measurement noise.

All Kalman predictions were executed with a two-state process model using daily input data.

Prediction scenario (see Section 6.7.1)	*Prediction error (1σ) [ns]*			
	Simulated GGTO (no steering)	*Simulated GGTO (with steering)*	*USNO data*	*PTB data*
Scenario 1 (last value)				
- no noise	2.8	2.1		
- w. noise	2.8	2.2	1.19	1.62
Scenario 2 (slope)				
- no noise	1.1 (meas int 24h)	1.4 (meas int 18h)		
- w. noise	1.5 (meas int 60h)	2.1 (meas int 40h)	0.87 (meas int 36h)	1.43 (meas int 36h)
Scenario 3 (ARIMA)				
- no noise	1.13 (ARIMA(1,1,0))	1.56 (ARIMA(1,1,1))		
- w. noise	1.52 (ARIMA(1,1,1))	1.90 (ARIMA(1,1,1))	0.67 (ARIMA(2,0,1))	1.43 (ARIMA(2,0,0))
Scenario 4 (Kalman)				
- no noise	1.17	1.87		
- w. noise	1.54	2.14	0.88	1.62

Table 6-14 GGTO prediction accuracy for selected test data

6.7.2.6 Error budget for GGTO determination and prediction

Up to now only *precision* of the GGTO prediction was considered. However, its *accuracy* will be additionally affected by the uncertainty of determination of hardware delays at involved facilities. These uncertainties are shown in Section 6.4.3. Table 6-15, Table 6-16, Table 6-17 and Table 6-18 summarize GGTO determination and prediction budgets for the four techniques introduced in Section 6.4.3. These budgets do not account for the residual delay of combined GPS/Galileo user receiver. This delay is expected to be about 2-4 ns (95%). The contribution of the switching between master and slave PTFs is also not considered.

Contribution	*Value, 1σ*
Equipment biases	
- Calibration of GPS time receiver at USNO w.r.t. GPS Time	3 ns
- Calibration of TWSTFT link USNO-PTF	2 ns
- Calibration of GSS collocated with PTF	3 ns
GPS SIS contribution to the uncertainty of GPS Time - UTC(USNO)	1 ns
Contribution of GST instability the TWSTFT uncertainty (noise) to the error of GGTO model estimation	1 ns
Uncertainty of GGTO prediction over 24 hours (including only GPS Time and GST instability)	2 ns
Total	***5.3 ns***

Table 6-15. GGTO determination budget (link with USNO)

Contribution	*Value, 1σ*
Equipment biases	
- Calibration of GPS time receiver at PTF	3 ns
- Calibration of GSS collocated with PTF	3 ns
Uncertainty of GPS Time reception via GPS SIS	2 ns
Uncertainty of GGTO prediction over 24 hours due to GPS Time and GST instability	
Contribution of GST instability and SIS reception noise to the error of GGTO model estimation	
Total	***4.7 ns***

Table 6-16. GGTO determination budget (GPS time receiver at PTF)

Contribution	*Value, 1σ*
Equipment biases	
- Calibration of GPS time receiver at PTF w.r.t. GPS Time	3 ns
- Calibration of GSS collocated with PTF	3 ns
Uncertainty of GPS Time reception via GPS SIS	1 ns
Uncertainty of GST reception via Galileo SIS	1 ns
Contribution of GST instability and SIS reception noise to the error of GGTO model estimation	1 ns
Uncertainty of GGTO prediction over 24 hours (including only GPS Time and GST instability)	1.5 ns
Total	***4.8 ns***

Table 6-17. GGTO determination budget (GPS and Galileo time receivers at PTF)

Contribution	*Value, 1σ*
Equipment biases	
- Differential calibration of GPS/Galileo receiver	2 ns
Uncertainty of GPS Time reception via GPS SIS	1 ns
Uncertainty of GST reception via Galileo SIS	1 ns
Contribution of GST instability and SIS reception noise to the error of GGTO model estimation	1 ns
Uncertainty of GGTO prediction over 24 hours (including only GPS Time and GST instability)	1.5 ns
Total	***3.0 ns***

Table 6-18. GGTO determination budget (combined GPS/Galileo receiver)

The best performance would be achieved with a combined GPS/Galileo receiver at PTF. However, the on-time availability of this receiver to install it at PTF may become an issue. The link with USNO offers a clear split of responsibilities for the performance of GGTO parameters (PTF should responsible for GST performance and its part of the link to USNO, and the USNO should be responsible for the link to GPS time and PTF). Nevertheless, this

approach does not allow independent GGTO determination by GPS and Galileo (the parameters computed at both sides are strongly correlated). As a robust baseline, GGTO determination from reception of GPS and Galileo SIS at PTF (primary method) and using a link with the USNO (secondary method) can be emphasized.

GGTO determination accuracy can be improved either by reducing the uncertainty of GPS and Galileo Rx calibration which is not yet in view today, or by undertaking a calibration campaign using a network of commercial GPS/Galileo receivers whose positions are well-determined. At each site, GGTO should be estimated over a sufficiently long time interval (preliminary, one month) from processing of GPS and Galileo observations. The estimated values should be compared with the broadcast GGTO. The difference between them would allow characterization of the bias in the broadcast GGTO parameters due to calibration uncertainties. Averaging over the network would improve the reliability of the results and mitigate the impact of residual biases of individual GPS/Galileo receivers. Such campaign should be organized at the beginning of Galileo operation and repeated from time to time (1-2 times a year) to account for aging of the PTF equipment.

7 Interface to Galileo users: time restitution

7.1 Assessing implicit specification of the accuracy of restitution of Galileo time

7.1.1 Relevance of GST restitution

The positioning performance of Galileo is explicitly specified in Galileo requirement documents and is explored in numerous publications. However, these specifications are quite lapidary when it comes to the timing performance of Galileo – despite the fact that provision of time service is one of the primary objectives of the Galileo mission.

In fact, only the accuracy of determination of time and frequency offset to UTC is specified. Moreover, this accuracy is specified only for Open Service users equipped with so called "Time laboratory receiver", i.e. for static users of dual-frequency receivers with unobstructed sky view in moderate multipath conditions (see also Section 3.1.4). Also, the Galileo specification of timing performance contains a limitation – this performance is guaranteed only when data from Galileo Time Service Provider are available for the Galileo system.

However, what users directly get from reception of Galileo signals is the GST, not UTC. Effectively, to get UTC users need to apply additional corrections available in the Galileo navigation messages. This correction will be computed with the help of information from the GTSP – an external with respect to Galileo body – which will be responsible for link between UTC and GST.

A close look on Galileo requirement documents uncovers that GST itself shall possess quite satisfactory good metrological properties: its offset from UTC will be limited to a few tens of nanoseconds (modulo 1 second) even in when GST is operated autonomously (GTSP is not available). That is similar to the performance of real-time representations of UTC – UTC(k) timescales – maintained in national metrological institutes. However, GST will have an offset of an integer number of seconds with respect to UTC. Furthermore, GST will not be subjected to introduction of new UTC leap seconds. Thus, the integer offset GST-UTC will increase with time (similarly to GPSTime-UTC offset).

After correction of the GST leap seconds, the residual GST-UTC time offset (as mentioned above, it will be order of tens of nanoseconds) will be negligible for the majority of user applications. Thus, corrected GST can be considered (technically, but not institutionally) to be similar to UTC(k) timescales generated by national timing institutes. In a way, corrected GST could be thought of as UTC(Galileo). Furthermore, Galileo shall be able to guarantee the performance of GST restitution since GST is completely under the system control.

7.1.2 Transformation of performance specifications

In fact, the performance of GST restitution is already specified (in an implicit form) in Galileo requirements. There the limits for horizontal and vertical positioning errors at 95% confidence for Galileo OS, SoL and PRS services are defined (see also Section 3.1.4). These limits shall be valid "at any time" and "at any location within the service zone". The service zone is, in this case, the whole Earth surface. To ensure that these accuracy requirements are met, it is sufficient to demonstrate that the worst-case positioning errors HPE_{ws} and VPE_{ws} stay within the specification. Eq. 4-35 defines HPE and VPE and functions of DOP and UERE. For the nominal Galileo constellation which is used in system analysis, DOP is a deterministic value changing within certain (finite) limits. Thus, we may define HPE_{ws} and VPE_{ws} as values of HPE and VPE respectively which correspond to the worst-case (the highest) DOP value.

Making use of Eq. 4-35 and assuming that measurement errors follow the normal (Gaussian) distribution, we get

$$HPE(95\%)_{ws} = 2 \cdot HPE_{ws} = 2 \cdot HDOP_{ws} \cdot UERE$$
$$VPE(95\%)_{ws} = 2 \cdot VPE_{ws} = 2 \cdot VDOP_{ws} \cdot UERE \qquad \text{Eq. 7-1}$$

where $HPE = \sqrt{\sigma_B^2 + \sigma_L^2}$ and $VPE = \sigma_H$ (see Section 4.2.4). The factor 2 in Eq. 7-1 comes from elementary statistic relating the 95-th percentile to the standard deviation for a normal distribution.

Similarly to the worst-case horizontal and vertical positioning errors, we may define the worst-case timing error TE_{ws}:

$$TE(95\%)_{ws} = 2 \cdot TE_{ws} = 2 \cdot TDOP_{ws} \cdot UERE \qquad \text{Eq. 7-2}$$

where $TE = \sigma_{\Delta T}$ (see Section 4.2.4).

Note that TE refers to synchronization to GST, not UTC.

As mentioned above, the following relationship shall be valid

$$HPE(95\%)_{ws} \le HPE(95\%)_{SRD}$$
$$VPE(95\%)_{ws} \le VPE(95\%)_{SRD} \qquad \text{Eq. 7-3}$$

where the subscript “SRD” designates the values from the Galileo requirement documents.

Thus, we get the following inequalities for TE_{ws}:

$$TE(95\%)_{ws} \le HPE(95\%)_{SRD} \frac{TDOP_{ws}}{HDOP_{ws}}$$
$$TE(95\%)_{ws} \le VPE(95\%)_{SRD} \frac{TDOP_{ws}}{VDOP_{ws}} \qquad \text{Eq. 7-4}$$

To obtain the limits for TE_{ws} we shall now assess the rates $\frac{TDOP_{ws}}{HDOP_{ws}}$ and $\frac{TDOP_{ws}}{VDOP_{ws}}$.

7.1.3 DOP simulations

DOP concept was shortly discussed in Section 4.2.4. At this stage when Galileo satellites are not yet launched, assessment of global distribution of Galileo DOP values – which is needed to transform Galileo accuracy specifications from the position domain into the time domain – can be made only from simulations. The following simulation parameters were selected

- User locations: regular grid with longitude resolution of 3° (59 slots from -87° to +87°) and latitude resolution of 5° (73 slots from 0° to 360°)
- Satellite constellation: nominal Galileo constellation (see Table E-1)
- Propagation of satellite orbits: undisturbed Kepler model (see [Mont00])
- Simulation time step: 1 minute
- Simulation time span: 3 days (the repeatability period of Galileo orbits)

The simulation was made using a software tool developed during preparation of this doctor thesis. HDOP, VDOP and TDOP were calculated.

As a result, we obtained 4320 values of HDOP, VDOP and TDOP for each of the simulated user locations. The maximum DOP values were calculated for each of the user locations (see Figure 7-1 and Figure 7-2):

$$HDOP_{\max}(B,L) = \max\left(HDOP(B,L,t_i)\right), \quad i = 1\ldots4320$$
$$VDOP_{\max}(B,L) = \max\left(VDOP(B,L,t_i)\right), \quad i = 1\ldots4320 \qquad \text{Eq. 7-5}$$
$$TDOP_{\max}(B,L) = \max\left(TDOP(B,L,t_i)\right), \quad i = 1\ldots4320$$

On the next step, the $HDOP_{ws}$, $VDOP_{ws}$ and $TDOP_{ws}$ were computed as the maximum over all user locations (see Table 7-1):

$$HDOP_{ws} = \max\left(HDOP(B_i,L_j)\right), \quad i = 1\ldots59, j = 1\ldots73$$
$$VDOP_{ws} = \max\left(VDOP(B_i,L_j)\right), \quad i = 1\ldots59, j = 1\ldots73 \qquad \text{Eq. 7-6}$$
$$TDOP_{ws} = \max\left(TDOP(B_i,L_j)\right), \quad i = 1\ldots59, j = 1\ldots73$$

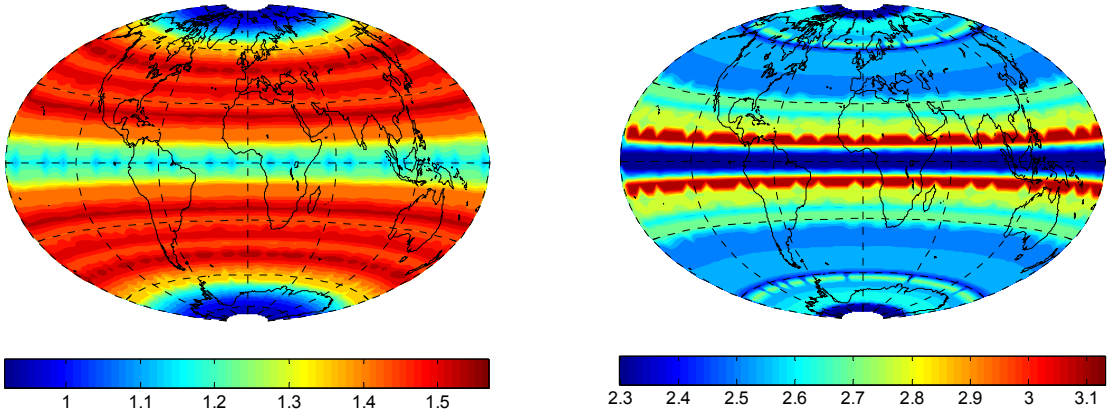

Figure 7-1. Galileo maximal HDOP (left) and VDOP (right)

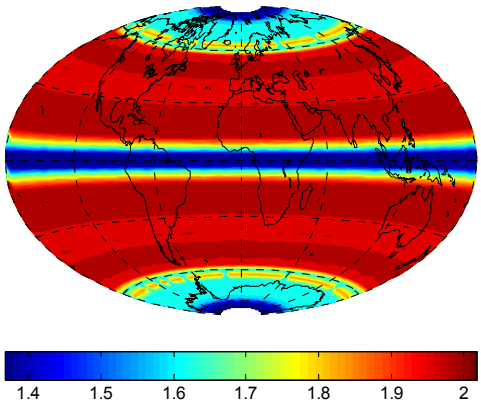

Figure 7-2. Galileo maximal TDOP

Parameter	*Location*		*Value*
	Latitude [°]	*Longitude [°]*	
$HDOP_{ws}$	-48	335	1.57
$VDOP_{ws}$	12	100	3.13
$TDOP_{ws}$	-48	335	2.02

Table 7-1. Galileo worst-case DOPs

With the values from Table 7-1 we get the following rates of the worst-case DOP values:

$$\frac{TDOP_{ws}}{HDOP_{ws}} = 1.286$$
$$\frac{TDOP_{ws}}{VDOP_{ws}} = 0.645$$

Eq. 7-7

Using Eq. 7-4 we get

$$HPE(95\%)_{SRD}\,\frac{TDOP_{ws}}{HDOP_{ws}} = 17.2\text{ns} \geq TE(95\%)_{ws}$$
$$VPE(95\%)_{SRD}\,\frac{TDOP_{ws}}{VDOP_{ws}} = 17.2\text{ns} \geq TE(95\%)_{ws}$$

Eq. 7-8

Note that transformation of the Galileo requirements to both HPE and VPE leads to the same worst-case limit for TE.

The result presented above can be also interpreted in a different manner: to satisfy the Galileo accuracy requirements Galileo UERE should be equal to or less than 1.28 m.

Finally, we would like to highlight the fact the worst-case HDOP and TDOP occur at the same location (see Table 7-1) which does not coincide with the location corresponding to the worst-case VDOP. It leads to the idea of differentiating the “worst-case” locations according to the error component we are interested in: horizontal, vertical or timing error.

7.2 Average accuracy of Galileo time restitution

The previous section dealt with the worst-case timing error for Galileo users assuming that user implement the standard PT solution algorithm (see Section 4.2.2). This error was assessed at the 95-th percentile of the user timing error for the worst user location (the global maximum of TDOP). An important underlying assumption was made: ranging error should be normally distributed or at least, there that there is a normal distribution that overbounds the actual distribution of ranging errors. Here we address the average timing error (also for the standard PT solution algorithm) making use of the same assumption. The average timing error as the 95-th percentile can be obtained from the following equation

$$TE(95\%)_{av} = 2 \cdot TE_{av} = 2 \cdot TDOP_{av} \cdot UERE$$

Eq. 7-9

here the subscript av designates average values.

Using results of the simulation described in Section 7.1.3, we calculated the values $TDOP_{av}$ for each of the simulated user locations (see Figure 7-3):

$$TDOP_{av}(B,L) = \frac{1}{n} \cdot \sum_{i=1}^{n} TDOP(B,L,t_i), \qquad n = 4320$$

Eq. 7-10

The global average value of $TDOP_{av,gl}$ was calculated as

$$TDOP_{av,gl} = \frac{1}{n_B} \cdot \frac{1}{n_L} \cdot \sum_{i=1}^{n_B} \sum_{j=1}^{n_L} TDOP_{av}(B_i, L_j), \qquad n_B = 59, n_L = 73$$

Eq. 7-11

The global average was equal to 1.10

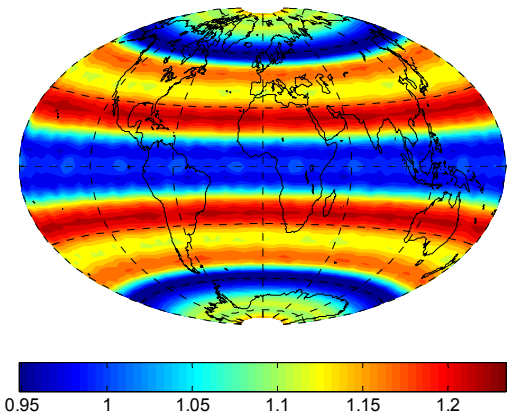

Figure 7-3. Average Galileo TDOP

The error budget of pseudorange measurements for Galileo users (UERE components) was analyzed during the definition phase of the Galileo program. A finalized error budget for users of the dual-frequency Open and Safety-of-Life Service is given in [Ehret03]. There UERE is represented as a function of satellite elevation (red dots in Figure 7-4).

In practical usage, we need to interpolate UERE between the discrete elevation values given in [Ehret03]. Empirically, we constructed the following function describing UERE as a function of satellite elevation E (see blue line in Figure 7-4):

$$UERE(E) = 0.01408 \cdot E^{-1.695} + 0.99 \quad [m] \qquad \text{Eq. 7-12}$$

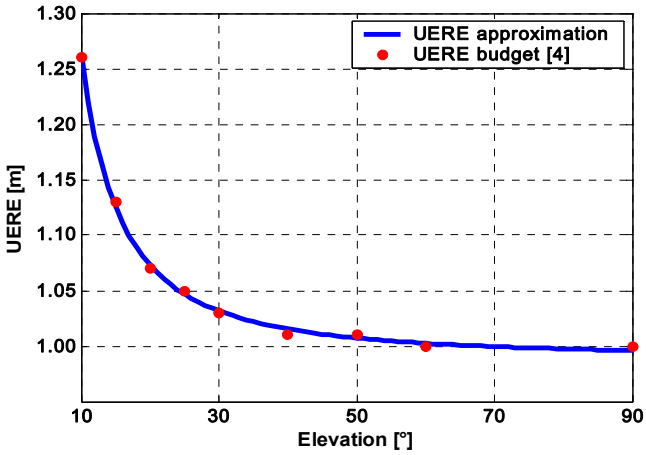

Figure 7-4. Projected Galileo UERE

From the Galileo simulation described in Section 7.1.3, we assessed the distribution of Galileo satellites at different elevation angles (i.e. calculated number of Galileo satellites n(E) visible at different elevation angles E), and then computed the weighted average value of UERE over the span of elevations from 10° to 90° (Galileo requirement documents foresees that only satellites over the elevation of 10° should be taken into the user positioning solution):

$$UERE = \frac{\sum UERE(E)n(E)}{\sum n(E)} \qquad \text{Eq. 7-13}$$

The weighted average UERE was equal to 1.05 m. With the weighted average UERE and the average Galileo TDOPs (see Figure 7-3) we calculated average values of TE(95%) for each of the simulated user locations (see Figure 7-5, the scale on the figure is in nanoseconds). The global average of TE(95%) was 5.8 ns.

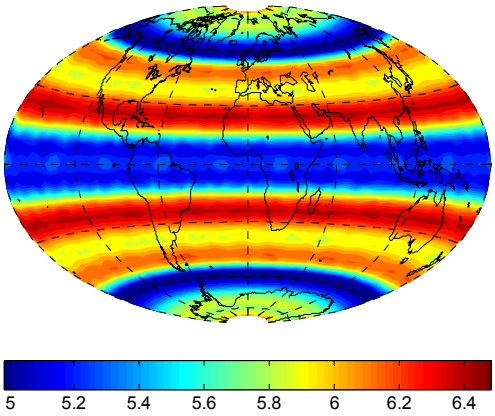

Figure 7-5. Average Galileo timing error

Note that the timing error addressed here is the error of user synchronization to GST. The synchronization error w.r.t. TAI – considering the baseline specification of TAI offset uncertainty broadcast by Galileo – would be 28.6 ns (95%).

8 Conclusions

8.1 Summary of results and conclusions

8.1.1 Overview

This thesis has addressed the timing aspects in the design and operations of the European navigation system Galileo:

- Galileo timekeeping in terms of requirements, stability and generation of Galileo System Time (GST). Hardware implementation aspects such as the design and reliability of the Galileo Precise Time Facility (PTF) have been also addressed. In addition, the role, the composition and the stability of the ensemble timescale have been investigated;
- Determination of GPS Galileo Time Offset (GGTO) with respect to its magnitude and behavior, impact to the positioning accuracy, determination and prediction techniques. Detailed performance budgets for various GGTO termination techniques have been also produced;
- GST restitution in terms of its relevance from the metrological point of view and accuracy.

8.1.2 Galileo timekeeping

GST will serve as the reference for the overall Galileo operations and in particular for prediction of satellite clocks. Accuracy of the clock prediction is of vital importance for the overall accuracy of Galileo positioning and timing services. The clock prediction error is affected by the instability of both satellite clocks and GST. Thus, requirements to GST stability should be driven by the need to minimize the corresponding contribution to the clock prediction. Extensive clock simulations (see Section 5.1.1.1) have allowed to identify that GST shall be about 5 times more stable than the satellite clocks. In this case the impact of its instability to the prediction error would be negligible. In fact, the Galileo baseline foresees GST to be even more than 5 times stable than satellite Rubidium standards (RAFS).

GST will be physically produced at PTF from an active H-maser which will be steered to TAI. OSPF will observe GST through the Galileo receiver collocated at PTF. Thus, from ODTS point of view, GST stability will include the contributions of the complete GST generation chain at PTF (H-maser, phase microstepper, 1PPS and 10MHz distributors, cabling) and the Galileo receiver (e.g. variations of the receiver group delays due to temperature changes). Hardware performance analysis in this thesis (see Section 5.1.1.3) has identified that the baseline GST stability requirements (which support precise prediction of RAFS) can be met considering the baseline PTF design and specification of its environmental conditions. However, the baseline GST stability is not quite sufficient for precise characterization of satellite passive H-masers (SPHM).

In addition to the navigation function which is discussed above (satellite clock prediction), GST shall support the metrological function (dissemination of UTC). The link to UTC is established though the Galileo Time Service Provider. However, also in the autonomy mode (the service provider is not available), GST offset to TAI shall be limited that sets requirements not only to the short term, but also to the long term stability of GST.

Galileo baseline foresees that to support the metrological function, an ensemble timescale from PTF Cesium clocks will be computed. This timescale will be stable in long-term that would allow correction of the frequency drift of the PTF active H-maser and, thus, to meet the long-term stability targets. Alternatively, satellite clocks could also contribute to the ensemble time and the resulting ensemble timescale could be used also as the reference for satellite clock prediction.

Different options with respect to the composition of the ensemble time are considered in Section 5.3. The corresponding stability analysis has indicated that the Galileo baseline on the ensemble time generation is fully able to satisfy the long-term stability requirements (for the metrological function), but not the short- and medium-term ones (for the navigation function). Thus, the ensemble time from PTF Cesiums can be used (as foreseen now) only to support the metrological function. In case the frequency drift of satellite Rubidium clocks will be corrected in the ensemble time software and the optimization time is set to 100 min, inclusion of RAFS into the ensemble time calculation would allow to produce a timescale which is able to support both the navigation (for RAFS prediction) and the metrological requirements. Thus, the ensemble time with de-drifted RAFS and PTF Cesiums could be utilized at place of the physical representation of GST. Similarly, the ensemble time based on SPHMs and PTF Cesiums is able to support both SPHM prediction and the metrological function.

The reliability of GST hardware realization is another important issue in the baseline on Galileo timekeeping. GST reliability and PTF redundancy management are investigated in Section 5.2. As mentioned above, GST from the OSPF point of view will include contributions of both PTF and its collocated Galileo receiver. Thus, the complete view of GST performance and feared events could be achieved only within the OSPF since PTF will not monitor the Galileo receiver. Present baseline foresees that PTF shall monitor its performance up to the output and switch between the master and slave H-masers in case if a malfunction is detected.

In turn, OSPF will monitor the overall GST performance and switch to the slave PTF in case a malfunction is detected at the master one. To avoid time and frequency steps in GST after the PTF switching (the GST versions at the master and slave PTFs are not perfectly aligned), a so-called transition law will be implemented in OSPF, i.e. after the switching, OSPF will correct time and frequency of the GST from the slave PTF. To insure that GST has a physical realization the correction will be slowly reduced to zero.

Reliability analysis in Section 5.2 indicates that the present baseline on H-maser and PTF switching is a reasonably good choice. However, an alternative solution to increase the overall GST reliability and simplify PTF operations could be proposed: the switching could be made in the OSPF software. In this case each of the four masers (two per PTF) should be connected to an individual Galileo receiver, and all four sets of data should be sent to OSPF. Further, OSPF will execute the quality monitoring using the receiver measurements and additional clock monitoring data from PTF. Based on the quality monitoring, one of the chains (H-maser – receiver) will be selected to represent GST. Thus, there will be no need in hardware switching between the masers at PTF.

8.1.3 Timing interface to GPS (GPS Galileo Time Offset)

GPS and Galileo will utilize different, independently generated reference timescales: GPSTime and GST respectively. Both timescales will be steered to UTC, therefore, their mutual offset (GPS Galileo Time Offset (GGTO) will be limited. A detailed study of GGTO magnitude and properties is presented in Section 6.2. According to the estimates obtained their, GGTO magnitude can reach as much as 57 ns (95%). If the users implement the broadcast UTC corrections, the offset will be reduced to about 33 ns (95%).

GGTO will introduce a bias between GPS and Galileo measurements in combined GPS/Galileo user equipment. This bias, in turn, will offset user position and time estimates. To cope with this problem, both Galileo and GPS will estimate and broadcast GGTO in their navigation messages. Alternatively, GGTO can be determined as an additional (fifth) unknown in the user navigation solution as it is done in GPS/GLONASS combined equipment. Section 6.3 discusses the impact of GGTO at the user positioning accuracy considering the option to use the broadcast GGTO value, to estimate GGTO in the user receiver, and to use uncorrected measurements Galileo and GPS measurements (i.e. to ignore GGTO).

The results of extensive simulations indicate that in case GGTO is not corrected at all, worst-case error of the GPS/Galileo positioning solution is about 2 times higher than that of Galileo only solution. The accuracy achieved when the broadcast GGTO value is utilized or GGTO is estimated in the user receiver is very similar, and it is better than the accuracy of Galileo-only equipment. However, in urban conditions, the situation is quite different. Considering the limited satellite visibility which results in deteriorated geometry of the observed constellation, determination of GGTO in user receiver seems to be the worst choice; and ignoring of GGTO could results in errors of some hundred meters. Thus, in urban conditions it seems to be advisable for user to utilize the broadcast GGTO value.

Galileo baseline defines several methods for GGTO determination: a link between PTF and the U.S. Naval Observatory (which continuously monitors the offset between its timescale and GPSTime), a GPS time receiver at PTF connected to the physical realization of GST, and a combined GPS/Galileo time receiver.

Section 6.7 presents test results for GGTO prediction for the cases when GGTO is determined via a link with USNO or with a GPS time receiver at PTF. Along with the well-known techniques which rely on GPS experience, to advanced approached have been tested: Box-Jenkins prediction based on the autoregressive moving average (ARIMA) and prediction with Kalman filter. The tests have been executed with both simulated and real measurement data. To achieve realistic modeling of GGTO measurements, the simulated data have been produced using real GPS orbits and clocks from IGS. For Galileo, the orbit and clock errors have been scaled according to the relevant performance specification. In addition, GPSTime and GST steering to UTC have been also simulated. The representative measurement data to emulate PTF-USNO link were taken from Physikalisch-Technische Bundesanstalt and Royal Observatory of Belgium. For each of the data types, a specific ARIMA model has been empirically identified.

The Box-Jenkins method has demonstrated the best performance in these tests. The prediction error has been estimated to 1.9 ns (1sigma) with simulated data and from 0.7 to 1.4 ns (1sgima) with real measurement data. The prediction with Kalman filter was only slightly worse.

Finally, the overall GGTO performance budget (considering also hardware calibration uncertainties) has been produced. The budgets are presented in Section 6.7.2.6. Hardware calibration seems to be the limiting factor for GGTO determination accuracy. The best accuracy is expected when GGTO is determined with a combined GPS/Galileo time receiver (since the calibration errors in this method seem to be the lowest). GGTO uncertainty has been estimated to reach about 3 ns (1sigma) which is only 20% over the baseline requirement.

Utilization of a combined GPS/Galileo receiver also allows determination of GGTO without additional time transfer links (e.g. to USNO) and corresponding data exchanges. It may potentially constitute a more robust design solution and simplify the operational implementation.

8.1.4 Timing user interface (GST dissemination)

According to the recommendations of the International Telecommunications Union, global satellite navigation systems should disseminate the international reference timescale, UTC. The link between GST and UTC will be established by the Galileo Time Service Provider. The corresponding time and frequency offset will be broadcast in the Galileo navigation message. Thus, the users (who originally get access to GST through their measurements) will be able to synchronize their equipment to UTC by applying this correction.

According to its specifications, GST itself will possess remarkable metrological properties. It will be steered to UTC within 50 ns (95%) (modulo 1 second) that is two times better than what is required by the Bureau Internationale des Poids et Mesures (BIPM) from the metrological institutes. Therefore, GST could be considered as a real-time representation of UTC with a similar status as the timescales produced by the national metrological institutes.

It would allow utilization of GST as another legal reference for synchronization of user equipment. This decision would pave the way to provision of guaranteed timing services and timing services for Safety-of-Life applications since the responsibility for GST performance is solely with Galileo.

The accuracy of GST dissemination is not specified in Galileo requirements explicitly (specification refer rather to UTC). However, it is present in an implicit form in the requirements to Galileo positioning accuracy – the accuracy of positioning and timing are closely related. The corresponding transformation (based on simulated Galileo geometry) is presented in Section 7.1. The implicit requirement to the worst-case world-wide error of GST dissemination is estimated to be 17.2 ns (95%).

Section 7.2 deals with the average accuracy of GST dissemination. This parameter has been also estimated from simulated Galileo geometry using the specification of Galileo user range error. The average value depends on the user location and varies from 5 to 6.5 ns (95%).

Both the worst-case and the average accuracy of GST dissemination is far beyond user application requirements (expect of the metrological, geodetic and some of scientific applications).

8.2 Recommendations for Galileo

A number of recommendations on Galileo improvement may be derived from the findings of this thesis.

With respect to Galileo timekeeping concept:

- As long as the present master clock concept is kept and GST is physically generated at PTF, the switching concept with four independent GST generation chains (H-maser – receiver) seems to provide better reliability and simplify the operations comparing to the present baseline. The responsibility for switching should be completely shifted to ODTS. To improve the performance, the transition law could be dropped, i.e. the initial GST time and frequency correction implemented after switching to avoid time and frequency steps could be left unchanged instead of reducing it to zero.
- De-trended RAFS and especially SPHMs should be included into the computation of the ensemble time. With these clocks, the ensemble time should be used for both satellite clock prediction and the metrological purposes (now it is utilized only for metrology). In this case, the reliability and robustness of the Galileo time reference would be increased. The physical realization of GST could be dropped. Modern ensemble time algorithms that allow optimal combination of clocks with different metrological characteristics (RAFS and Cesiums, or SPHM and Cesiums) should be considered as a better option than the weighted average algorithm which has been considered here.

With respect to GPS Galileo Time Offset:

- Since the combined GPS/Galileo time receiver promises the best accuracy in determination of GPS/Galileo time offset, Galileo project should undertake necessary actions on development and verification of such receiver. The accuracy and reliability of the receiver should make it suitable for utilization in the core Galileo infrastructure.
- Box-Jenkins (ARIMA based) technique should be considered for prediction of GPS Galileo time offset since it provides the best performance in the comparison with other known approaches. Additional study on operational implementation and robustness of ARIMA could be undertaken.
- Establishment of the time interface to other navigation systems like GLONASS or the coming Chinese system should be considered to improve Galileo interoperability. The

interface could be established by utilizing (similar to the GPS interface) combined receivers.

With respect to GST dissemination:

- Galileo project may undertake necessary actions to acquire for GST a legal status similar to the real-time UTC representations produced by the national metrology institutes. On the base of this status, guaranteed timing services should be defined. Necessary technical information to support development of Safety Cases for timing applications should be made available to users.

List of Acronyms

1PPS	One Pulse Per Second Signal
ADEV	Allan Deviation
AMC	Alternative Master Clock
AOC	Advanced Operational Capability
AOG	Auxiliary Output Generator
AR	Autoregressive
ARIMA	Autoregressive Integrated Moving Average
AT	Acceptance Tests
BIPM	Bureau International des Poids et Mesures
BNM SYRTE	Laboratoire des Systèmes des Références Temps-Espace du Bureau National de Métrologie
CCTF	Comité Consultatif du Temps et Fréquence
CDR	Critical Design Review
CGGTTS	CCTF Group on Global navigation satellite systems Time Transfer Standards
CIPM	Comité International des Poids et Mesures
CV	Common View
DD&AIV	Design, Development, Integration, Assembly and Verification
DKP	Development Key Point
DLR	Deutsches Zentrum für Luft- und Raumfahrt
DOP	Dilution of Precision factor
EAL	Echelle Atomique Libre
EC	European Commission
EGNOS	European Global Navigation Overlay System
E-GST	Experimental Galileo System Time
E-PTS	Experimental Precise Timing Stations
ESA	European Space Agency
EU	European Union
FOC	Full Operational Capability
FTP	File Transfer Protocol
GEM	Galileo Mission Implementation
GGC	Galileo Global Component
GJU	Galileo Joint Undertaking
GLONASS	GLObal Navigation Satellite System
GMS	Galileo Ground Mission Segment
GNSS	Global Navigation Satellite System
GOC	Galileo Operating Company

GPS	Global Positioning System
GST	Galileo System Time
GSTB	Galileo System Test Bed
GSTR	Galileo System Time Running
GTSP	Galileo Time Service Provider
HDOP	Horizontal Dilution of Precision factor
HPE	Horizontal Positioning Error
I/F	Interface
IEN	Istituto Elettrotecnico Nazionale
IERS	International Earth Rotation and Reference Systems Service
IERS	International Earth Rotation Service
IOV	In-Orbit Validation
KF	Kalman Filter
KO	Kick Off
LMS	Least Mean Squares
MA	Moving Average
MC	Master Clock
NIST	National Institute of Standards
NMI	National Metrology Institute
NPL	National Physical Laboratory
NTP	Network Time Protocol
ORB	Royal Observatory of Belgium
ORR	Operational Readiness Review
PMS	Phase microstepper
PPS	GPS Precise Positioning Service
PTB	Physikalisch-Technische Bundesanstalt
PTF	Precise Time Facility
RAMS	Risk Availability Maintainability Safety
RINEX	Receiver Independent Exchange Format
RMS	Root Mean Square
SPS	GPS Standard Positioning Service
TAI	International Atomic Time
TAI	Temps Atomique International (International atomic time)
TBC	To Be Confirmed
TDOP	Time Dilution of Precision factor
TRR	Test Readiness Review
TWSTFT	Two Way Satellite Time and Frequency Transfer
TWSTFT	Two Way Satellite Time and Frequency Transfer
UK	United Kingdom

US	United States
USNO	US Naval Observatory
UTC	Universal Coordinated Time
UTC	Coordinated Universal Time
UTC(k)	Representation of UTC provided by laboratory “k”
VDOP	Vertical Dilution of Precision factor
VKP	Validation Key Point
VPE	Vertical Positioning Error
w.r.t.	with respect to
OS	Galileo Open Service
SoL	Galileo Safety of Life Service
PRS	Galileo Public Regulated Service

Notation

$\bar{}$	designator of an average value
~	when placed over a symbol: designator of an estimated value (in 4.2): change it to “hat” sign) when placed before a symbol: designator of an approximate value
$\langle\ \rangle$	sum of elements
∇	differencing operator (in Box-Jenkins models)
$\mathbf{A}$	arbitrary matrix
A	azimuth
$ADEV$	Allan Deviation
B	backshift operator
BLH	geodetic longitude, latitude and altitude
a	regression parameters
c	speed of light
d	pseudorange
Dly	hardware delay
E	elevation
E	expectation
f	Fourier frequency
f	probability density function
f	arbitrary function
$\mathbf{F}$	state transition matrix
$\mathbf{G}$	projection matrix for GPS/Galileo observation model
$GPSTime$	reading of GPS Time
GST	reading of GST
h	amplitudes of individual terms in a power spectral density model (in Section 4.3 element of observation matrix $\mathbf{H}$)
HPE	horizontal positioning error (standard deviation)
$\mathbf{H}$	observation (projection) matrix in Section 4.3
$\mathbf{I}$	identity matrix
i, j, k	indices
Ion	ionospheric delay
l	pseudorange residual
$\mathbf{l}$	vector of pseudorange residuals
$\mathbf{M}$	vector of identity matrices used in the theory of GPS Composite Clock

n, N, m	upper limits of indices for a data series
p	element of the covariance matrix
$\mathbf{P}$	covariance matrix (for Kalman estimates)
$\mathbf{Q}$	process covariance matrix
q	elements of covariance matrix or covariance of individual parameters
$\mathbf{r}$	position vector
R	autocorrelation function
Rel	relativistic correction (sum of relativistic effects)
S	power spectral density
t	time (as independent argument in equations)
T	reading of a user (receiver) clock
TE	timing error (standard deviation)
Trp	tropospheric delay
$\mathbf{u}$	user position and time vector
$\mathbf{v}$	vector of observation noise
VPE	vertical positioning error (standard deviation)
w	weight coefficient
w	Gaussian white noise term
$\mathbf{w}$	vector of Gaussian white noises
$Variable_{ws}$	worst-case value of an arbitrary variable $Variable$ (the highest or the lowest value depending on the context)
x	relative time deviation of two clocks
y	relative frequency deviation of two clocks
XYZ	Decart coordinates in an Earth-centered reference frame
$\mathbf{z}$	vector of measurements (for Kalman filter)
α	index by terms of power spectral density function model
δ	delta function
$\mathbf{\Delta}$	GPS Galileo time offset vector
Δ	discrete difference operator (first order)
Δ^2	discrete difference operator (second order)
ΔT	user (receiver) time offset
Δt	satellite time offset
ε	sum of residual pseudorange measurement errors (multipath, receiver noise, modeling errors etc.)
φ	absolute phase of a clock
$\mathbf{\Xi}$	state space of a clock ensemble

ν	absolute frequency of a clock
ϕ	relative phase deviation of two clocks or carrier phase measurement (in the context of satellite observations)
$\mathbf{\Lambda}$	matrix of transparent variations
λ	failure rate (in the context of reliability analysis) or wave length (in the context of satellite observations)
ρ	true geometrical distance
θ	moving average coefficients
θ	moving average function
σ	standard deviation
σ_B	standard deviation of the latitude component of user positioning error
σ_L	standard deviation of the longitude component of user positioning error
σ_H	standard deviation of the altitude component of user positioning error
$\sigma_{\Delta T}$	standard deviation of the error of determination of receiver clock offset
σ_y	relative frequency instability (AVAR or MVAR)
Σ	sum of elements
τ	sample time or a certain time interval
ξ	clock reading
$\boldsymbol{\xi}$	state (vector) of a clock
ψ	autoregressive coefficients
ψ	autoregressive function

References

[Allan78] D. Allan and H. Hellwig: *Time Deviation and Time Prediction Error for Clock Specification, Characterization, and Application*, Proc. IEEE PLANS Conference, 1978, pp. 29-36

[Allan80] D. Allan and M. Weiss: *Accurate Time and Frequency Transfer during Common-View of a GPS Satellite*, Proc. 34th Ann. Symp. on Frequency Control, 1980, pp. 334-346

[Allan87a] D. Allan: *Time and Frequency (Time-Domain) Characterization, Estimation, and Prediction of Precision Clocks and Oscillators*, IEEE Transactions on Ultrasonics and Ferroelectronics, Vol. 43, 1987, pp. 647-654

[Allan87b] D. Allan: *Should the Classical Variance Be Used as a Basic Measure in Standards Metrology?* IEEE Transactions on Instrumentation and Measurements, Vol. 36, 1987, pp. 646-654

[Allan94] D. Allan and C. Thomas: *Technical Directives for Standardization of GPS receiver Software to be Implemented for Improving the Accuracy of Common View Time Transfer*, Metrologia, Vol. 31, N. 1, 1994, pp. 69-79

[Baeriswyl95] P. Baeriswyl et al.: *Frequency and Time Transfer with Geodetic GPS Receivers: First Results*, Proceedings of 9th EFTF Meeting, 1995, pp. 46-51.

[Barnes66] J. Barnes: *Atomic Timekeeping and the Statistics of Precision Signal Generators*, Proceedings of IEEE Vol. 54, No. 2, 1966, pp. 207-220

[Bauch04] A. Bauch et al.: *Time Comparisons between USNO and PTB: A Model for the Determination of the Time Offset between GPS time and the Future Galileo System Time*, Proceedings of 2004 IEEE Intl. Frequency Control Symposium, Aug. 2004

[Bauch05] A. Bauch et al.: *Time Scale Prediction Using Information from External Sources*, Proceedings of EFTF, 2005, CD-ROM

[BERNWeb] http://www.aiuv.unibe.ch

[Brown91] K. Brown: *The Theory of the GPS Composite Clock*, Proceedings of ION-GPS, 1991, pp.223-242

[Brown97] R. Brown and P. Hwang: Introduction to Random Signals and Applied Kalman Filtering, 3-rd edition, J.Wiley&Sons, 1997

[Bruyninx99] C. Bruyninx et al.: *Time and frequency Transfer Using GPS Codes and Carrier Phases: Onsite Experiments*, GPS Solutions, Vol. 3, No. 2, 1999, pp. 1-10

[Busca03] G. Busca et al.: *Time prediction accuracy for a space clock*, Metrologia, Vol. 40, pp. 265-269

[Cliatt03] S. Cliatt: *GPS Modernization*, Proceedings of GNSS2003, 2003

[Davis01] J. Davis et al.: *Least-squares Analysis of Two-Way Satellite Time and Frequency Transfer Measurements*, Proceedings of PTTI, 2001

[Defraigne03] P. Defraigne and G. Petit: *Time Transfer to TAI Using Geodetic Receivers*, Metrologia (40), August 2003, pp. 184-188.

[Delporte01] J. Delporte et al.: *Modellisation and Extrapolation of Time Deviation : Application to the Estimation of the Datation Stability of a Navigation Payload*, Proceeding of 15th EFTF, 2001

[MacDiarmid] P. MacDiarmid et al.: Reliability Toolkit: Commercial Practices Edition, Reliability Analysis Center and Rome Laboratory, Rome, New York, (no date), pp. 35-39

[Dier84] A. Van Dierendonck and R. Brown: *Relationship between Allan Variances and Kalman Filter Parameters*, Proceeding of PTTI, 1984

[Dimarq04] N. Dimarq: *Horloges Atomiques Embarquees*, Presentation made at the meeting "Galileo et la Science", CNES, 11 Jun 2004

[DO229C] Minimum operational performance standards for GPS/WAAS airborne equipment, RTCA/DO-229C, Prepared by SC-159, RTCA, 28.11.2001

[Droz03] F. Droz et al.: *On-Board Galileo RAFS, Current Status and Performances*, Proceedings of the 2003 IEEE International Frequency Control Symposium and PDA Exhibition Jointly with the 17th EFTF, 2003, pp. 105-108

[Ehret03] W. Ehret et al.: *Comparison of GALILEO Integrity Approaches w.r.t. Performanc*e, Proceedings of 11-th IAIN World Congress, Berlin, 2003

[Epstein03] M. Epstein et al.: *GPS IIR Rubidium Clocks: In-orbit Performance Aspects*, Proceeding of 35th PTTI, 2003, CD-ROM

[Epstein05] M. Epstein et al.: *GPS Block IIR Clocks in Space: Current Performance and Plans for the Future*, Proceeding of 37th PTTI, 2005, CD-ROM

[ESAWeb] www.esa.int/galileo

[Francis02] S. Francis et al.: *Time keeping and time dissemination in a distributed space-based clock ensemble*, Proceedings of PTTI, 2002

[Giffard96] R.Giffard et al.: *Continuous Multi-channel Common-view L1-GPS Time Comparison over a 4,000 km Baseline*, Proceedings of Frequency Control Symposium, 1996

[GPSICD] GPS-ICD-200c, 10.10.1993

[GPSPS] Global Positioning System Standard Positioning Service Performance Standard, Oct 2001

[GPSSPSPS] Global Positioning System Standard Positioning Service Performance Standard, Oct. 2001.

[Greenhall88] C. Greenhall: *Frequency Stability Review*, TDA Progress Report, 42-88, 1988, pp. 200-212

[GTWGR] J. Laverty et al.: Report of Galileo Time Interface Working Group, ESA, 2001

[Hahn04] J. Hahn and E. Powers: *GPS and Galileo Timing Interoperability*, Proceedings of GNSS 2004 (CD-ROM), 2004

[Harris97] R. Harris: *Direct Resolution of Carrier-Phase Ambiguity by 'Bridging the Wavelength Gap'*, ESA Publication TST/60107/RAH/Word, 2/97

[Hein06] G. Hein et al.: *MBOC: The New Optimized Spreading Modulation Recommended for Galileo L1 OS and GPS L1C,* Proceedings of 2006 IEEE/ION PLANS, San Diego, USA, 24-27.04.2006

[HP97] Hewlett-Paccard (authors: D. Allan et al.): *The Science of Time Keeping*, Application Note 1289, 1997

[Hutsell02] S. Hutsell and C. McFarland: *One-Way GPS Time Transfer: 2002 Performance*, Proceedings of 34-th PTTI Meeting, 2002, pp. 69-76

[Hutsell94] S. Hutsell: *Recent MCS Improvements to GPS Timing*, Proceeding of the ION GPS-94 Meeting, 1994, pp. 261-273

[Hutsell96] S. Hutsell: *Kalman Filtering USNO's GPS Observations for Improved Time Transfer Predictions*, Proceedings of 27-th PTTI Meeting, 1996, pp. 269-278

[IGSWeb] http://igscb.jpl.nasa.gov

[ISO93] International Vocabulary of Basic and General Terms in Metrology, second edition, International Organization for Standardization (ISO), 1993.

[ITU97] International Communication Union (ITU) Radiocommunications Study Group 7, Operational Use of Two-Way Satellite Time and Frequency Transfer Employing PN Codes, Recommendation ITU-R TF.1153-1, 1997

[Jaldehag99] K. Jaldehag and J. Johansson: *Kalman-Smoothed Estimates of GPS Common View Data*, Proceedings of EFTF, 1999

[Kamas90] G. Kamas and M. Lombardi: *Time and Frequency Users Manual*, NIST Special Publication #559, Revised in 1990

[Kart78] P. Kartaschoff: Frequency and Time, London, England: Academic Press, 1978.

[Kirchner93] D. Kirchner and H. Ressler: *Zeitübertragung über Telefonmodems*, in „Funkuhren, Zeitsignale, Frequenznormale", Verlag Sprache und Technik, Gross-Bieberau, 1993.

[Kraemer99] R.Kraemer, J.Hahn and L.Schmidt: *Results in GPS Time Restitution with Kalman Filters*, Proceedings of EFTF, 1999

[Koenig93] G. Koenig: *Das Implussystem zur fernsehtechnischen Taktversorgung des ZDF-Sendezentrums*, in „Funkuhren, Zeitsignale, Frequenznormale", Verlag Sprache und Technik, Gross-Bieberau, 1993.

[Larson98] K. Larson and J. Levine: *Time Transfer Using the Phase of the GPS Carrier*, IEEE Transactions on Ultrasonics, Ferroelectronics, and Frequency Control, Vol. 45, No. 3, May 1998, pp. 539-540

[Larson99] K. Larson and J. Levine: *Carrier-Phase Time Transfer*, IEEE Transactions on Ultrasonics, Ferroelectronics, and Frequency Control, Vol. 46, No. 4, July 1999, pp. 1001-1012

[Lombardi99] M. Lombardi: *Traceability in Time and Frequency Metrology*, Cal Lab Magazine, Sept-Oct 1999

[Lucas04] R. Lucas: *GalileoSat and EGNOS Development Status*, Presentation made at the Second Galileo Conference for an Enlarged Europe (Budapest, Hungary, 27-28 May 2004)

[Mattioni02] L. Mattioni et al.: *The Development of a Passive Hydrogen Maser Clock for the Galileo Navigation System*, Proceedings of 34-th Annual PTTI Meeting, 2002, pp. 161-170.

[Mattoni02] L. Mattoni et al.: *The Development of a Passive Hydrogen Maser Clock for the Galileo Navigation System*, Proceedings of the 34-th Annual Precise Time and Time Interval (PTTI) Meeting, pp. 161-170, 2002

[McDonald00] K. McDonald and C. Hegarty: *Post-Modernization GPS Performance Capabilities*, Proceedings of ION 56-th Annual Meeting, June 2000, pp. 242-249.

[Merino03] M. Romay-Merino et al.: *Orbit Determination and Time Synchronization Experimentation in GSTB V1*, Proceedings of the European navigation conference GNSS 2003, 2003

[Mobbs97] S. Mobbs and T. Hutsell: *Refining Monitor Station Weighting In the GPS Composite Clock*, Proceedings of the 29-th Annual Precise Time and Time Interval (PTTI) Meeting, 1997, pp. 131-142

[Mont00] O. Montenbruck and E. Gill: Satellite Orbits: Models, Methods, and Applications, Springer Verlag, Berlin, 2000

[Moudrak04a] A. Moudrak et al.: *Time Dissemination and Synchronisation for Galileo Users*, Proceedings of ION NTM 04, 2004, CD-ROM

[Moudrak04b] A. Moudrak et al.: *Determination of GPS/Galileo time offset to support system interoperability*, Proceedings of the 8th European Navigation Conference GNSS 2004, May 2004, CD-ROM.

[Moudrak04c] A. Moudrak et al.: *GPS Galileo Time Offset : How It Affects Positioning Accuracy and How to Cope with It*, Proceedings of ION GNSS 04, 2004, CD-ROM

[Oaks03] J. Oaks et al.: *Global Positioning System Constellation Clock Performance*, Proceedings of 35-th Annual PTTI Meetings, 2003, CD-ROM

[OConnor81] P. D. T. O'Connor, Practical Reliability Engineering, Heyden & Son, East Kilbride, 1981

[Parkinson96] B. Parkinson and J. Spilker (editors): Global Positioning System: Theory and Applications, American Institute of Aeronautics and Austronautics, Washington, 1996.

[Petit04] Private communication with Gerard Petit (BIPM), Jan 2004.

[Petit00] G. Petit et al. : *Differential calibration of Ashtech Z12-T receivers for accurate time comparisons*, Proceedings of 14th EFTF Meeting, 2000, pp. 40-44.

[Roland90] H. Roland and B. Moriarty, System Safety Engineering and Management, 2nd edition, John Wiley and Sons, 1990

[Schild90] T. Schildknecht et al.: *Towards Subnanosecond GPS Time Transfer Using Geodetic Processing Techniques*, Proceedings of 4th EFTF Meeting, March 1990, pp. 335-346

[Schmaliy01] Y. Schmaliy et al.: *Studies of an Optimally Unbiased MA Filter Intended for GPS-based Timekeeping*, Proceedings of PTTI 2001, 2001

[Senior01] K. Senior and J. Ray: *Accuracy and Precision of GPS Carrier-Phase Clock Estimates*, Proceedings of 33-rd PTTI Meeting, 2001, pp. 199-220.

[Shannon04] Agreement on the promotion, provision and use of Galileo and GPS satellite-based navigation systems and related applications, Shannon (Ireland), 26.06.2004, http://pnt.gov/public/docs/2004-US-EC-agreement.pdf

[Stansfield01] E. Stansfield: *Kalman Filters: A Tutorial*, Materials of Meeting of IEE/DERA/ASPC Adaptive Signal Processing Club, 7.03.2001

[Taris00] F. Taris et al.: *The BNM-LPTF Software for the Frequency Comparison of Atomic Clocks by the Carrier Phase of the GPS Signal*, IEEE Transactions on Ultrasonics, Ferroelectronics, and Frequency Control, Vol. 47, No. 5, Sept 2000, pp. 1140-1146

[TEMEX03] TEMEX Time and ASTRIUM, iSource+ Space Qualified RAFS Spec, Revised 3 Feb 2003

[Thomas93] C.Thomas: *Real-Time Restitution of GPS Time*, Proceedings of 7-th EFTF, 1993

[Tjaden02] J. Tjaden and C. Fagan: *GNSS Applications to Transportation and Timing, Draft Summary and Synthesis Report*, UN/USA International Meeting of Experts on the Use and Applications of GNSS, Nov 2002, Vienna (publicly available in Web at http://www.oosa.unvienna.org/SAP/gnss)

[USEU04] Agreement on the Promotion, Provision and Use of Galileo and GPS Satellite-Based Navigation Systems and Related Applications, 26th of June 2004, Shannon, Ireland.

[USNOWeb] http://tycho.usno.navy.mil

[Vollath98] U. Vollath et al.: *Analysis of Three-Carrier Ambiguity Resolution (TCAR) Technique for Precise Relative Positioning in GNSS-2*, Proceedings of ION GPS 98, Sept. 1998

[Vondrak69] J. Vondrak: *A Contribution to the Problem of Smoothing Observational Data*, Bull. Astron. Inst. Czechoslovakia, vol. 20, pp. 349-355, 1969

[Warren03] D. Warren and J. Raque: *Broadcast vs. Precise GPS Ephemerides: A Historical Perspective*, GPS Solutions, 7 (3), 2003, pp. 151-156.

[White01] J. White et al.: *Dual Frequency Absolute Calibration of a Geodetic GPS Receiver for Time Transfer*, Proceedings of 15th EFTF, 2001, pp. 167-170.

[Wolf99] P. Wolf and G. Petit: *Use of IGS Ionosphere Products in TAI*, Proceedings of 31st Annual PTTI Meeting, 1999, pp. 419-430

[Box76] G. P. E. Box and G. M. Jenkins: Time Series Analysis: Forecasting and Control, 2nd edition, Holden-Day, San Francisco, 1976

[Pankratz83] A. Pankratz: Forecasting with Univariate Box-Jenkins Models: Concepts and Cases, John Wiley & Sons, New York, 1983

Annex A. Accuracy of combined GPS/Galileo solution

A .1 Worst-case HDOP and VDOP for 10° cut-off

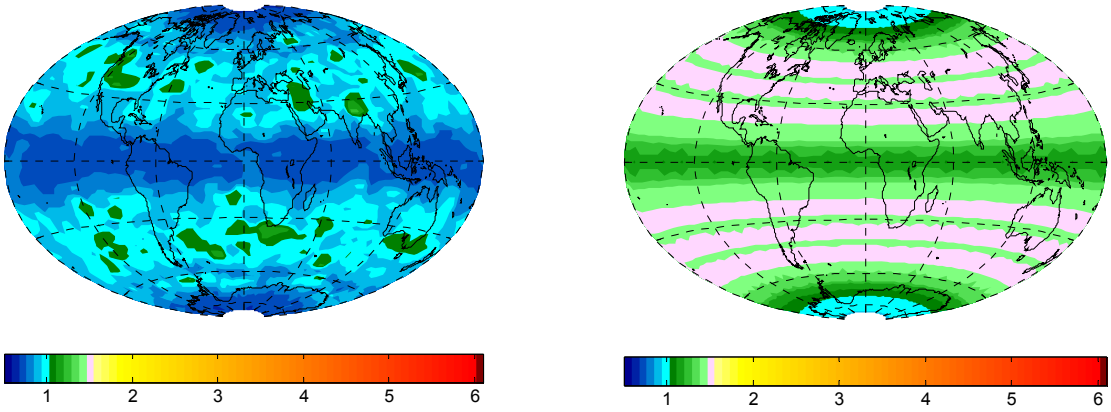

Figure A-1. Combined GPS+Galileo HDOP (left) and Galileo-only HDOP (right)

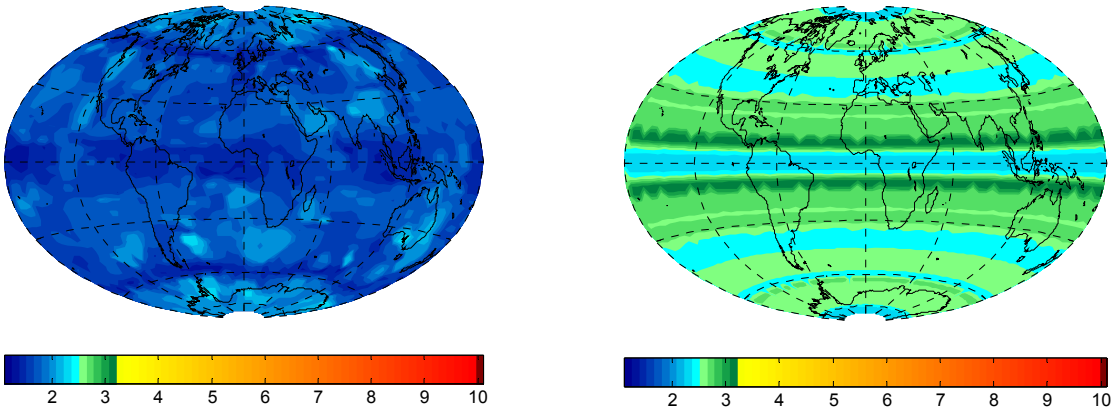

Figure A-2. Combined GPS+Galileo VDOP (left) and Galileo-only VDOP (right)

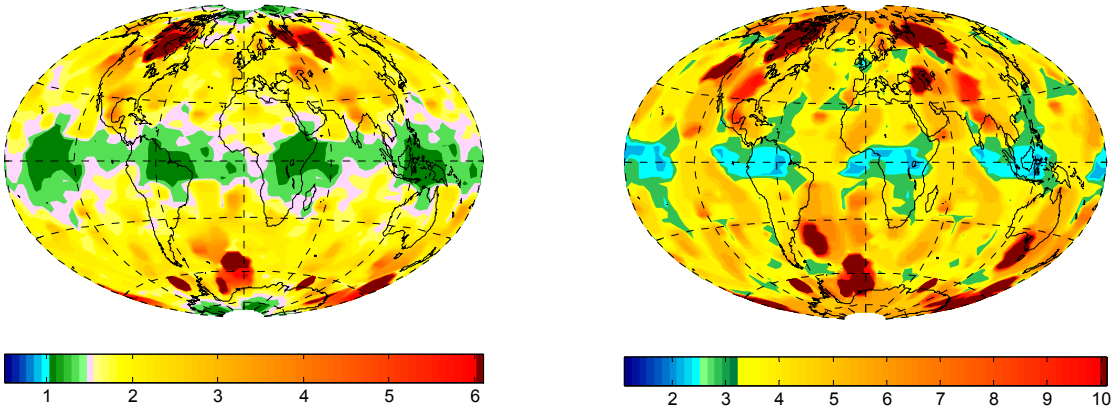

Figure A-3. GPS HDOP (left) and VDOP (right)

A .2 Worst-case HPE for 10° cut-off

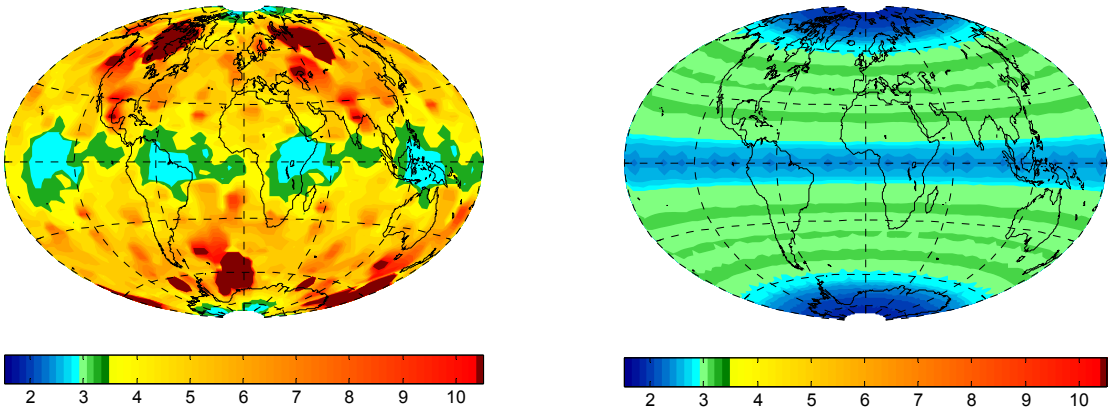

Figure A-4. GPS HPE (95%) (left) and Galileo HPE (95%)

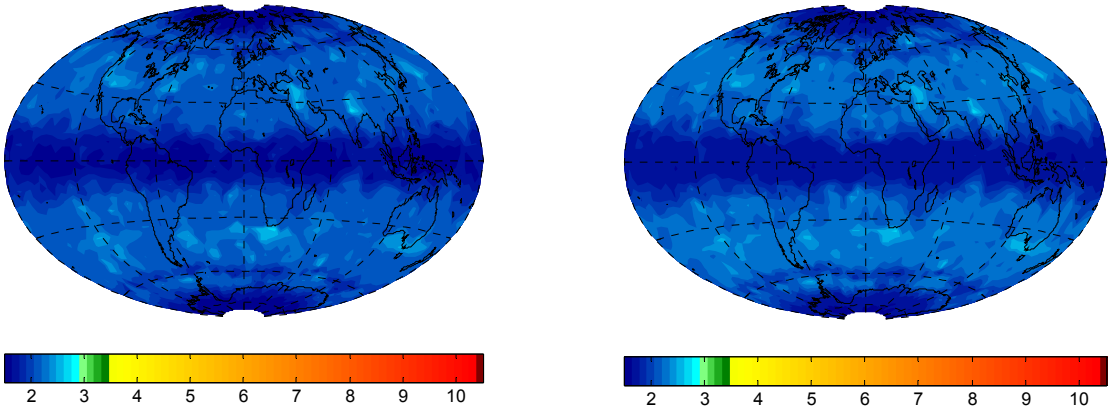

Figure A-5. HPE (95%) of combined solution with GGTO (1σ) of 0 ns (left) and 2.5 ns (right)

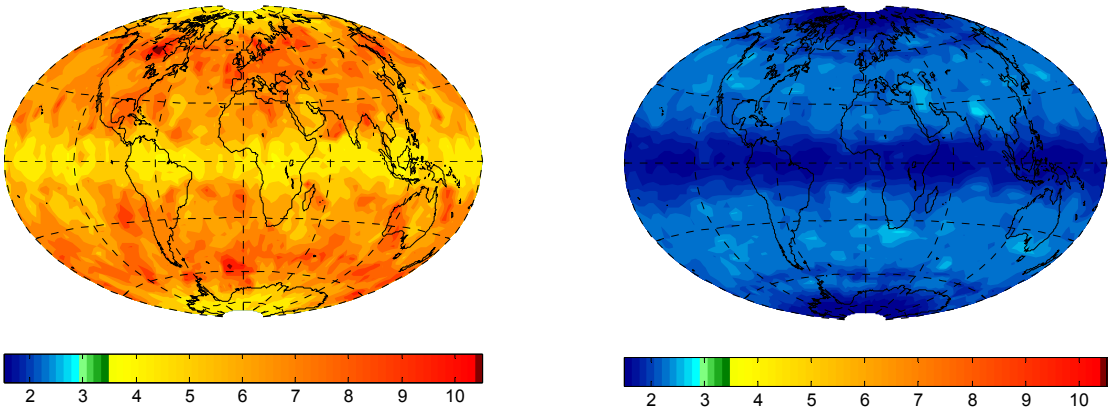

Figure A-6. HPE (95%) of combined solution with GGTO (1σ) of 28 ns (left) and with 5-parameter navigation solution (right)

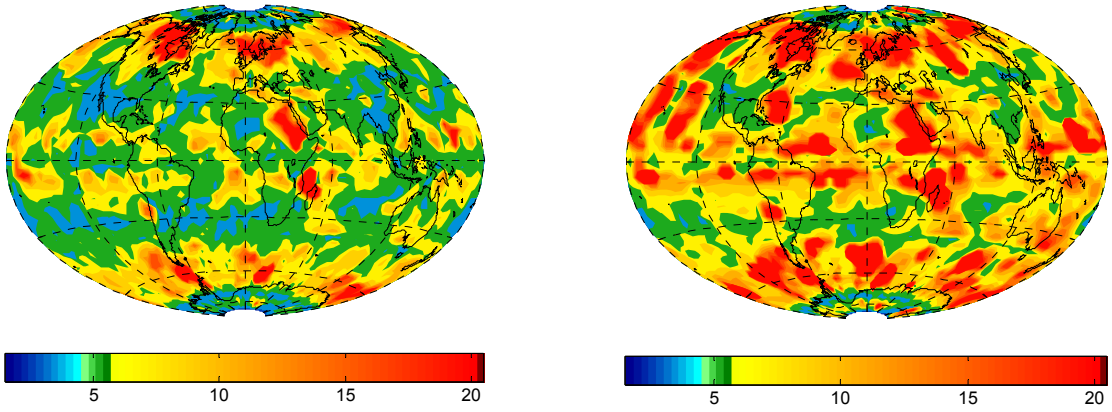

Figure A-7. HPE (95%) of combined solution with GGTO (1σ) of 28 ns (left) and with 5-parameter navigation solution (right) (both with the cut-off of 30°) (note change of the color scheme)

A .3 Worst-case VPE for 10° cut-off

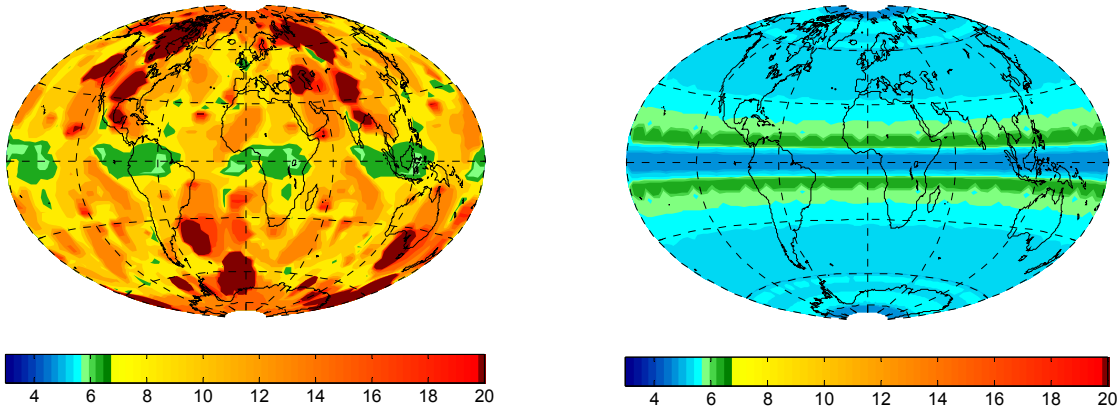

Figure A-8. GPS VPE (95%) (left) and Galileo VPE (95%)

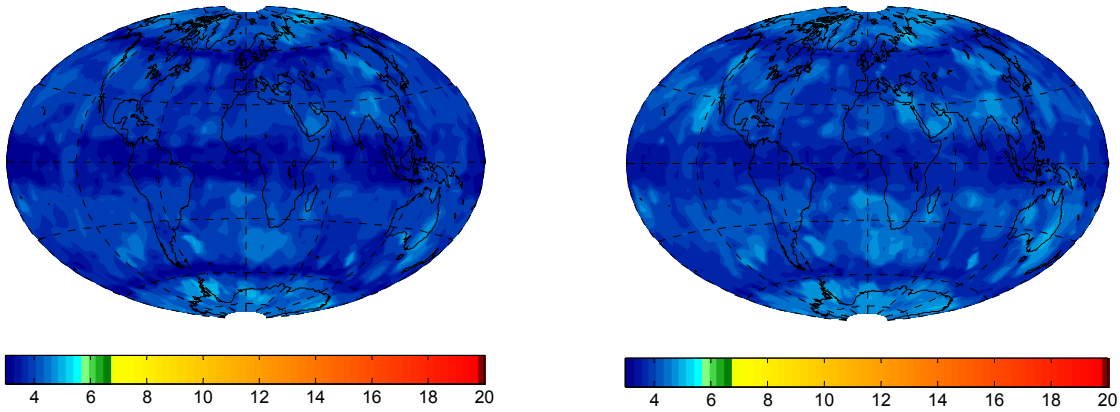

Figure A-9. VPE (95%) of combined solution with GGTO (1σ) of 0 ns (left) and 2.5 ns (right)

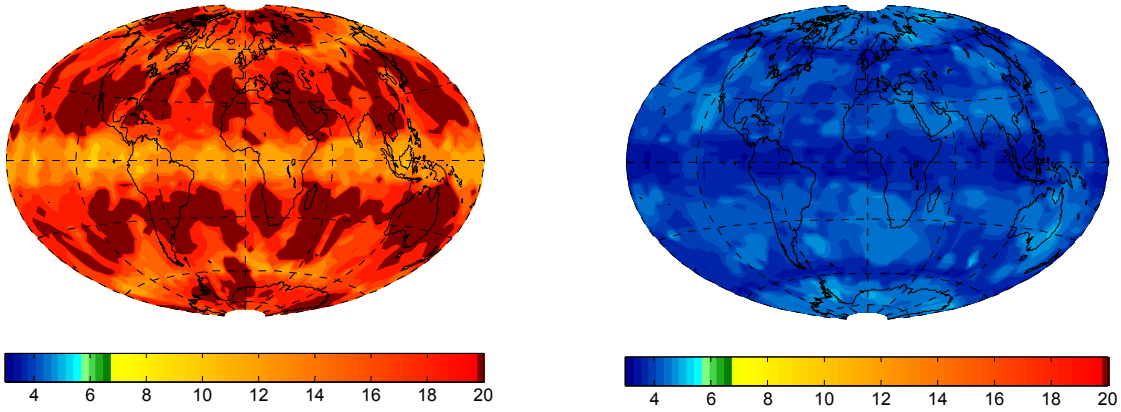

Figure A-10. VPE (95%) of combined solution with GGTO (1σ) of 28 ns (left) and with 5-parameter navigation solution (right)

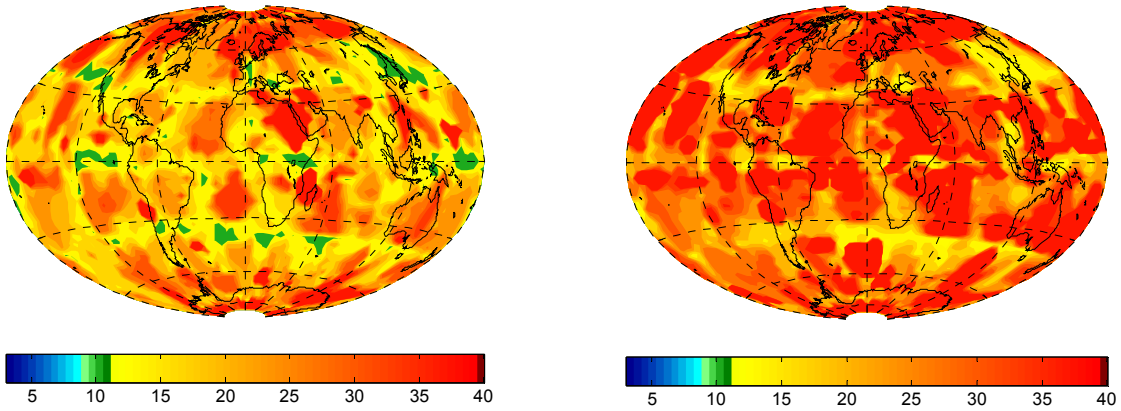

Figure A-11. VPE (95%) of combined solution with GGTO (1σ) of 28 ns (left) and with 5-parameter navigation solution (right) (both with the cut-off of 30°) (note change of the color scheme)

Annex B. GGTO modeling statistics

B .1 Box-Jenkins model identification

The identification of an optimal Box-Jenkins model is described below.

Step 1. Stationarity test

Stationarity can be tested by the analysis of the time series plot: the mean and the variance of the process should not change significantly with time. Another indicator is the plot of autocorrelation function. Non-stationary processes typically exhibit a very slow decay.

If non-stationarity is detected, data are differenced until an acceptable level of stationarity is achieved.

Step 2. Identifying the order of the autoregressive and moving average processes.

Stationary autoregressive processes have the autocorrelation function that decay to zero. The partial autocorrelation function of such a process drops to zero after a few spikes. The number of spikes is equal to the order of the autoregressive process.

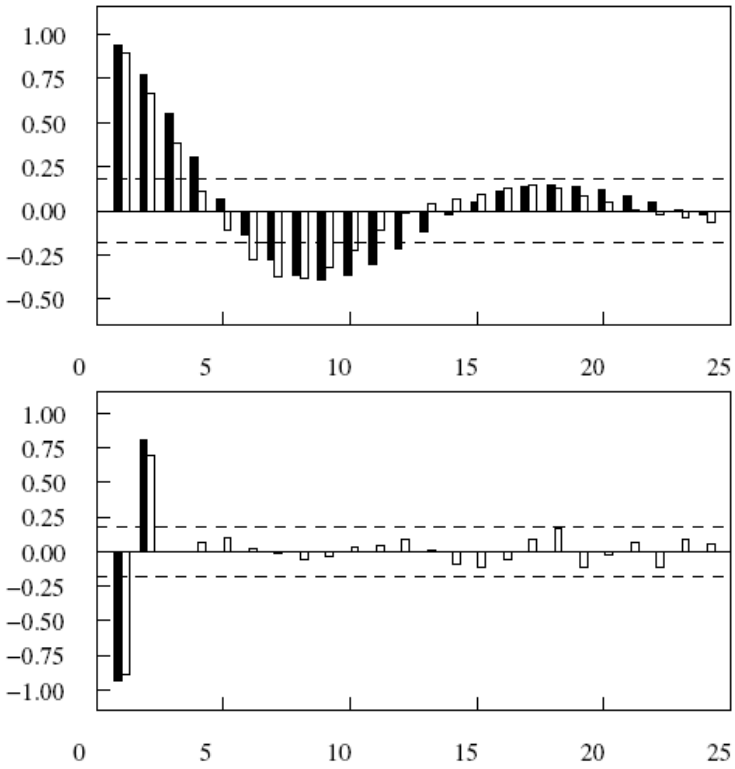

Figure B-1. Autocorrelation (top) and partial autocorrelation (down) functions of an autoregressive process of the second order

Moving average processes have the autocorrelation function that drops to zero after a few spikes. The number of spikes is equal to the order of the moving average process. The partial autocorrelation function of a moving average process decays to zero.

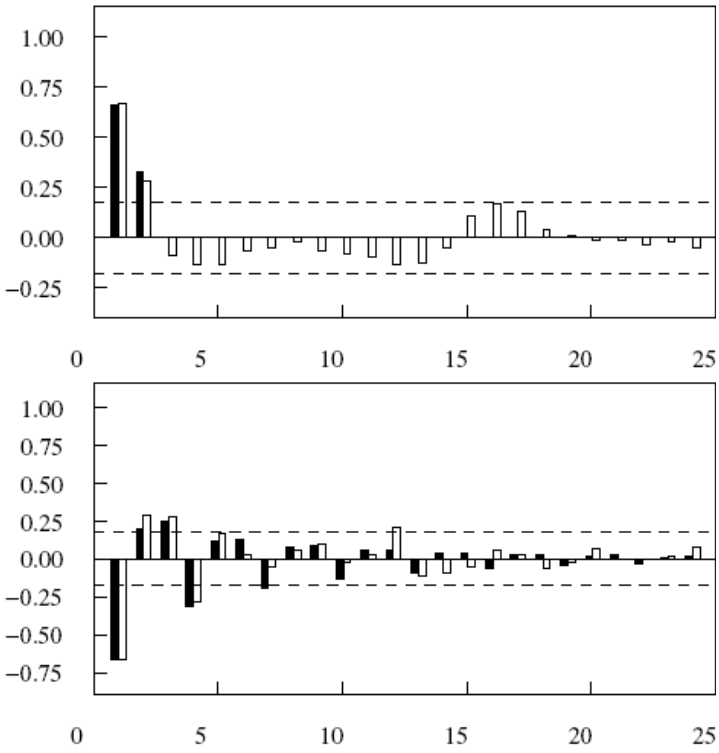

Figure B-2. Autocorrelation (top) and partial autocorrelation (down) functions of a moving average of process of the second order

The partial autocorrelation function at certain lag, one of the most important tools for the Box-Jenkins model identification, is the correlation between the two sets of residuals obtained from regressing the elements x_i and x_{i-lag} on the set of intervening elements $x_1, x_2, ..., x_{i-lag+1}$. Thus, the partial autocorrelation measures the dependence between x_i and x_{i-lag} after the effect of the intervening values has been removed. The sample partial autocorrelation is equal to the estimated coefficient at lag k obtained by fitting an autoregressive model of order k to the data:

$$x_i = a_{k,1}x_{i-1} + a_{k,2}x_{i-2} + ... + a_{k,k-1}x_{i-k+1} + a_{k,k}x_{i-k} + a_i .$$

B .2 Time series plots, ACF and PACF

B.2.1 Simulated GGTO (with steering)

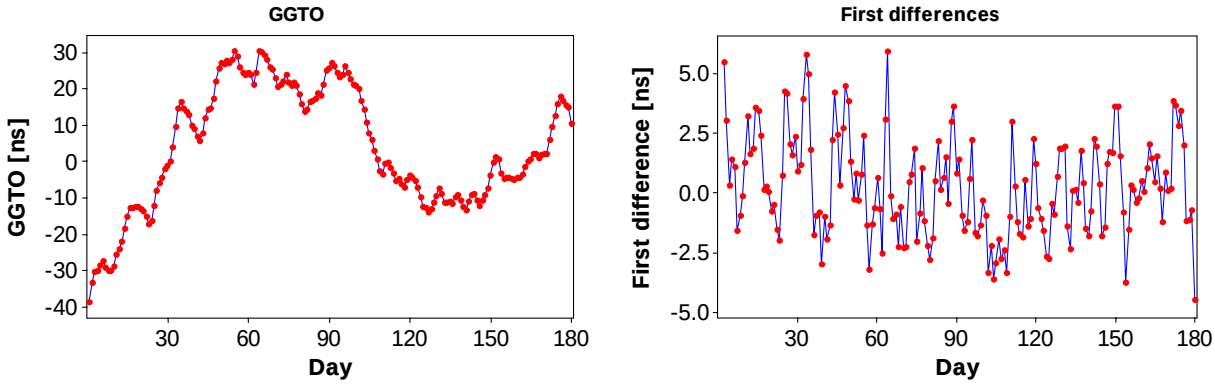

Figure B-3. Steered GGTO and its first differences

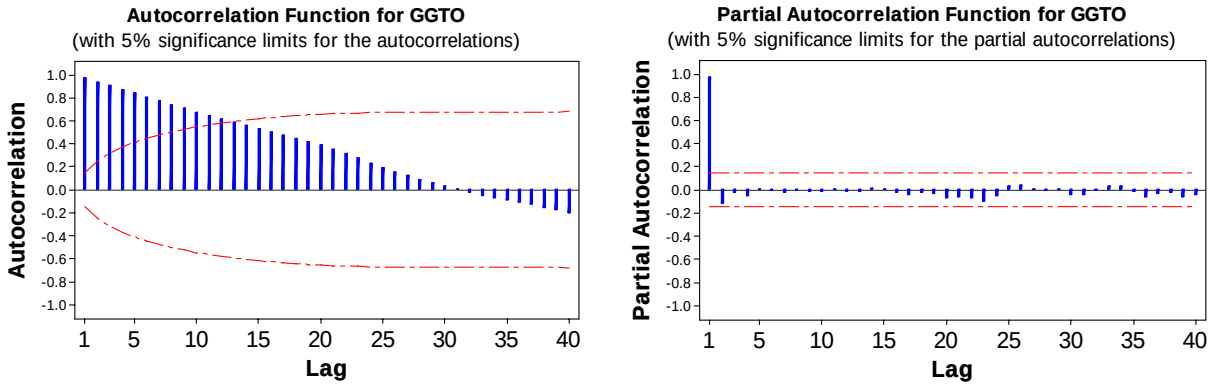

Figure B-4. ACF and PACF for steered GGTO

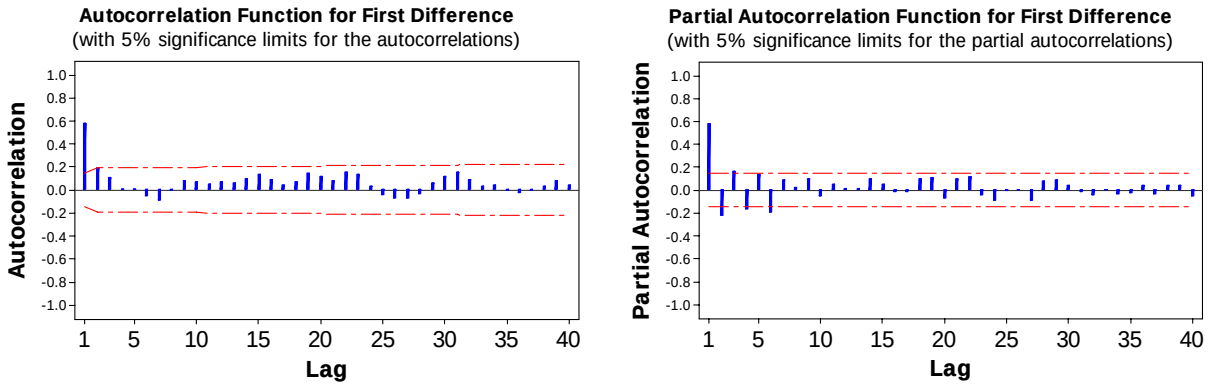

Figure B-5. ACF and PACF for first differences of steered GGTO

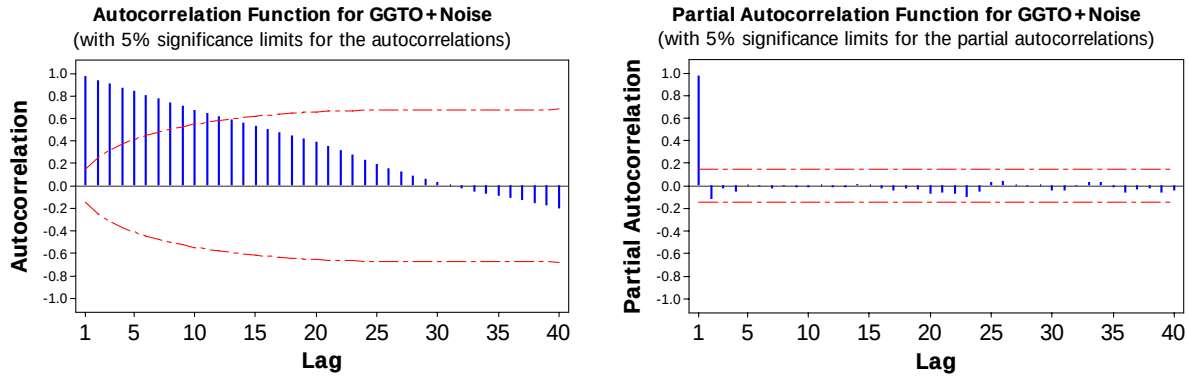

Figure B-6. ACF and PACF for steered GGTO with added WGN (RMS 2 ns)

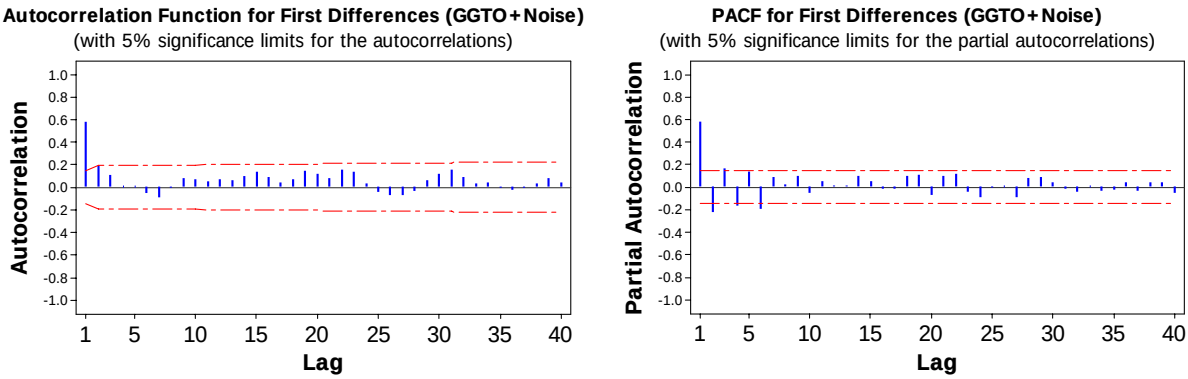

Figure B-7. ACF and PACF for first differences of steered GGTO with added WGN (RMS 2 ns)

B.2.2 Simulated GGTO (no steering)

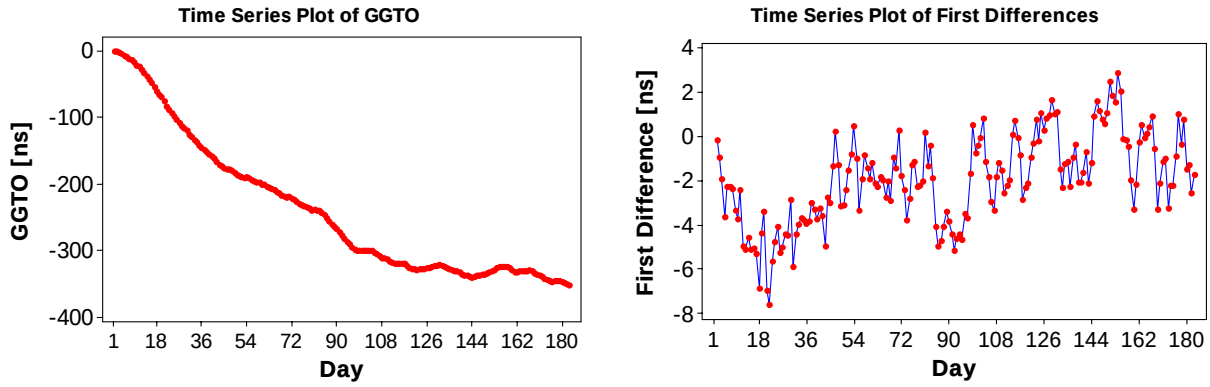

Figure B-8. Non-steered GGTO and its first differences

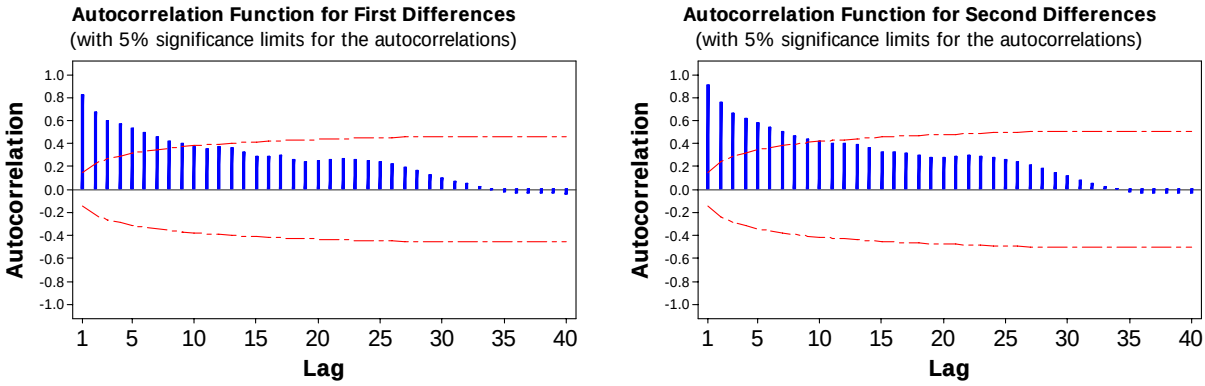

Figure B-9. ACF for first and second differences of non-steered GGTO

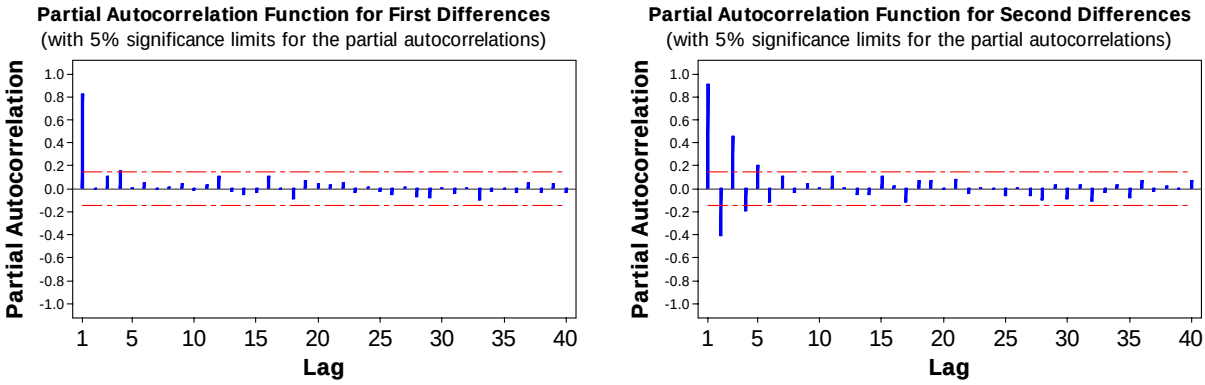

Figure B-10. PACF for first and second differences of non-steered GGTO

B.2.3 UTC(USNO) – GPS Time

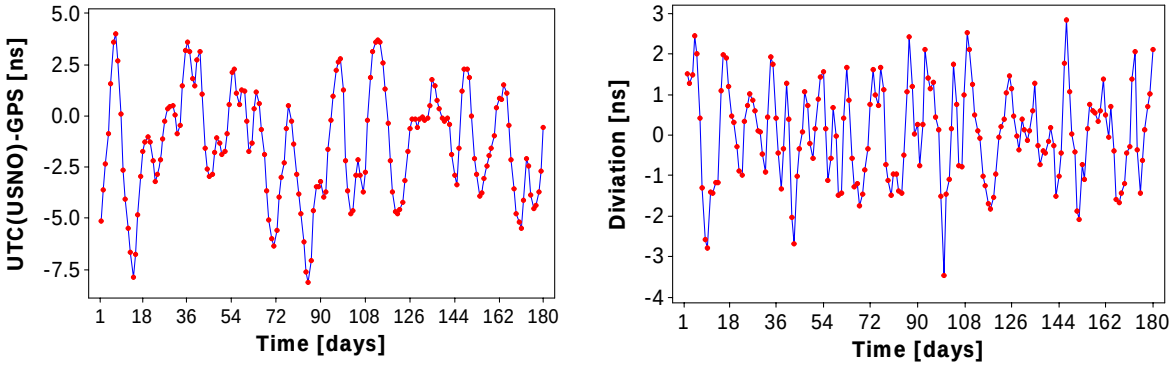

Figure B-11. UTC(USNO) offset from GPS Time (left) and its first differences (right)

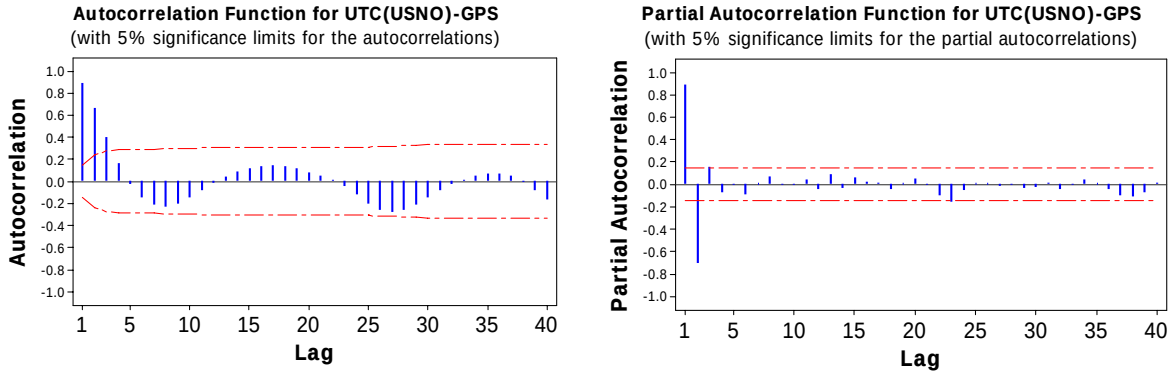

Figure B-12. ACF (left) and PACF (right) of the USNO data

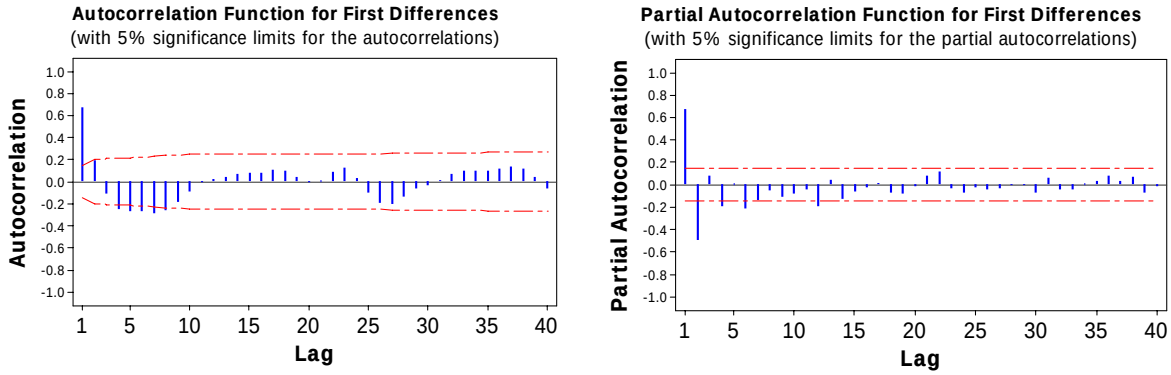

Figure B-13. ACF (left) and PACF (right) of the USNO data

B.2.4 UTC(PTB) – GPS Time

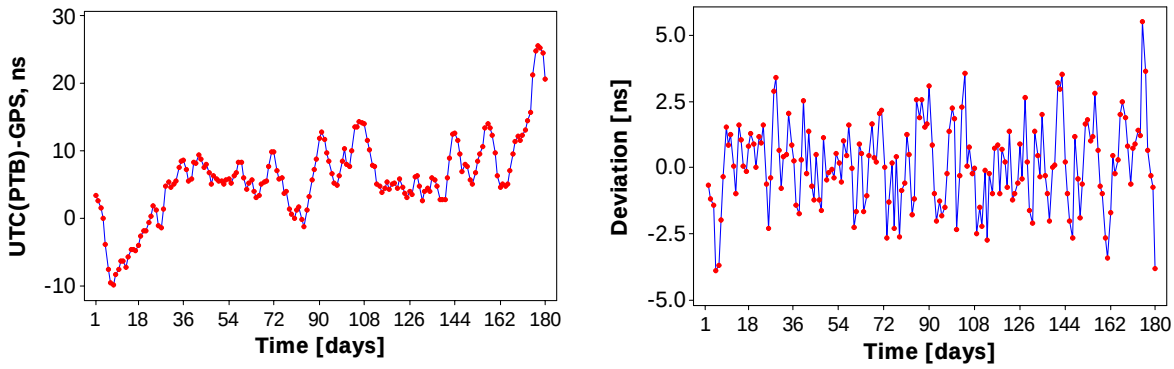

Figure B-14. UTC(PTB) offset from GPS Time (left) and its first differences (right)

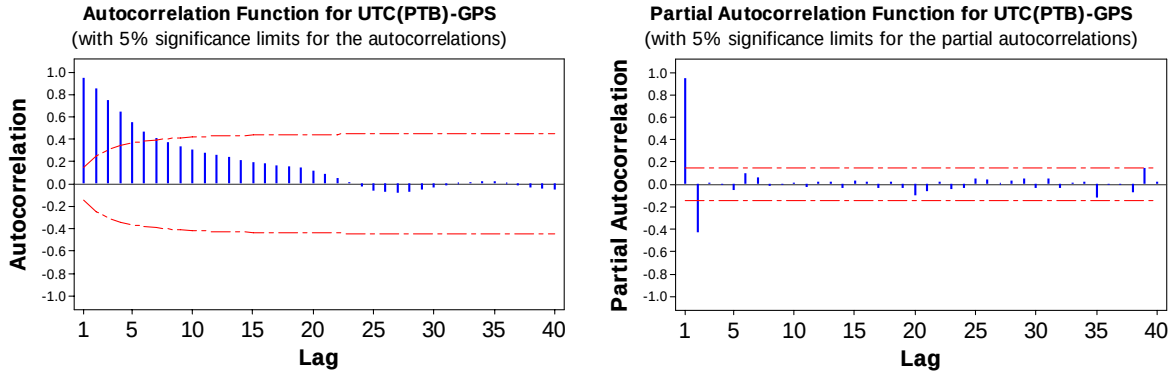

Figure B-15. ACF (left) and PACF (right) of the PTB data

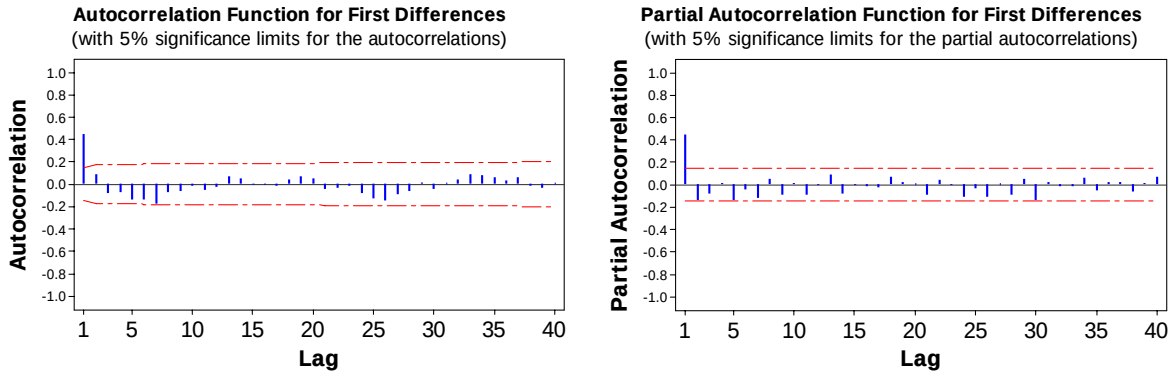

Figure B-16. ACF (left) and PACF (right) of first differences of the PTB data

B .3 ARIMA models for GGTO

B.2.1 Simulated GGTO (with steering)

Order of MA model	*RMS of model residuals [ns]*				
	Order of AR model				
	0	***1***	***2***	***3***	***4***
0	n/a	2.767	2.603	2.518	2.437
1	2.107	2.080	n/a	2.068	2.554
2	2.087	2.070*	2.087	2.074	n/a
3	2.075	2.098	2.112	2.078	n/a
4	2.059	2.075	2.078	1.964*	n/a

** conversion criterion was not met after 25 iterations*

Table B-1 Modeling error for ARIMA(N,1,M) models of steered GGTO

In the table above “n/a” stands for combinations for which ARIMA model either does not exist or failed to be estimated.

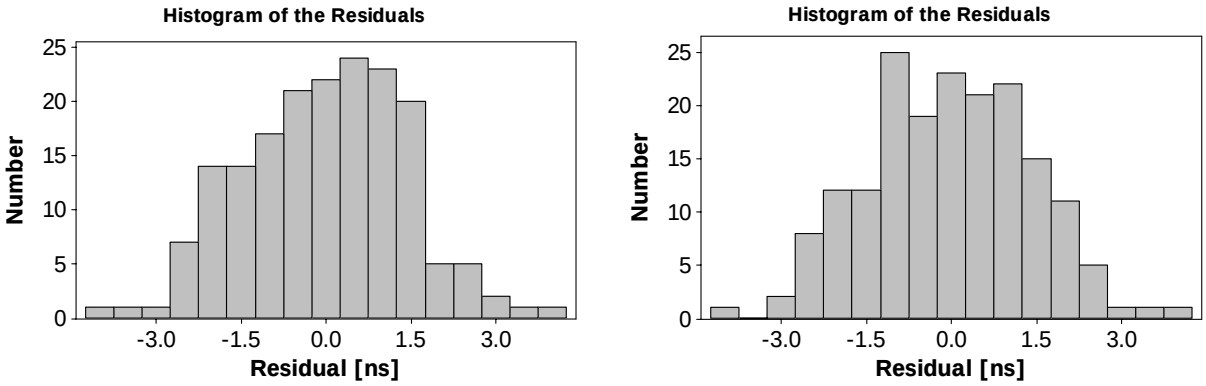

Figure B-17. Histogram of residuals for ARIMA(1,1,1) (left) and ARIMA(1,1,4) (right)

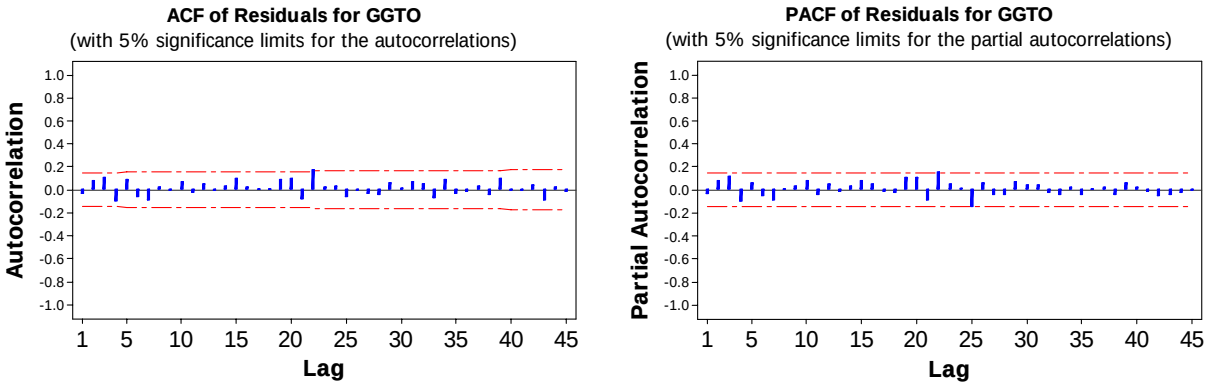

Figure B-18. ACF (left) and PACF (right) of residuals for ARIMA(1,1,1)

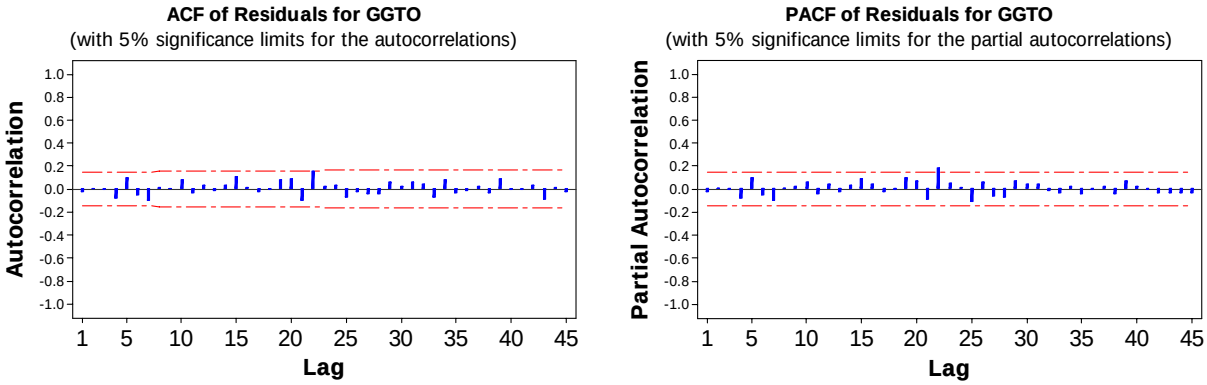

Figure B-19. ACF (left) and PACF (right) of residuals for ARIMA(1,1,4)

B.2.2 Simulated GGTO (no steering)

Order of MA model	*RMS of model residuals [ns]*				
	Order of AR model				
	0	***1***	***2***	***3***	***4***
0	n/a	1.283	1.290	1.283	1.264
1	2.103	1.290	1.275	1.286	1.271
2	1.596	1.279	1.270	1.274	1.275
3	1.498	1.262*	n/a	1.275	1.282*
4	1.428	1.268	1.274	1.282	1.289

** conversion criterion was not met after 25 iterations*

Table B-2 Modeling error for ARIMA(N,1,M) models of first differences of non-steered GGTO

In the table above "n/a" stands for combinations for which ARIMA model either does not exist or failed to be estimated.

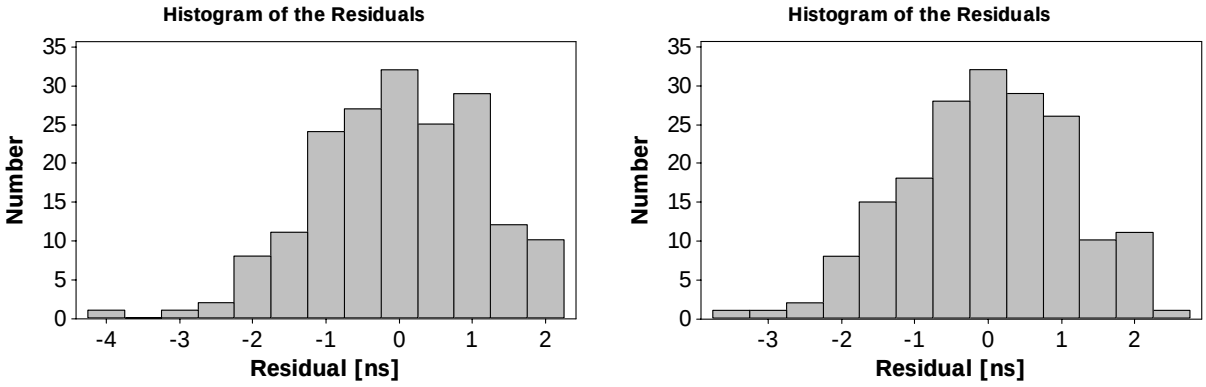

Figure B-20. Histogram of residuals for ARIMA(1,1,0) (left) and ARIMA(2,1,2) (right)

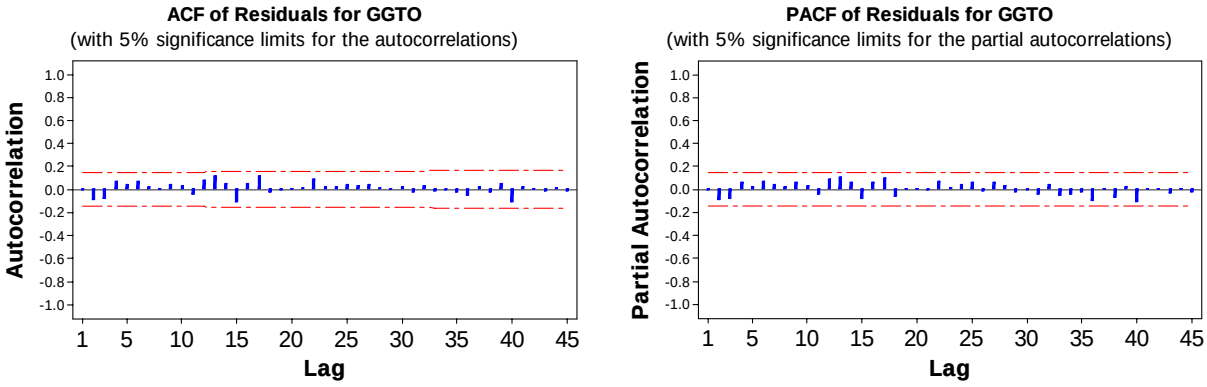

Figure B-21. ACF (left) and PACF (right) of residuals for ARIMA(1,1,0)

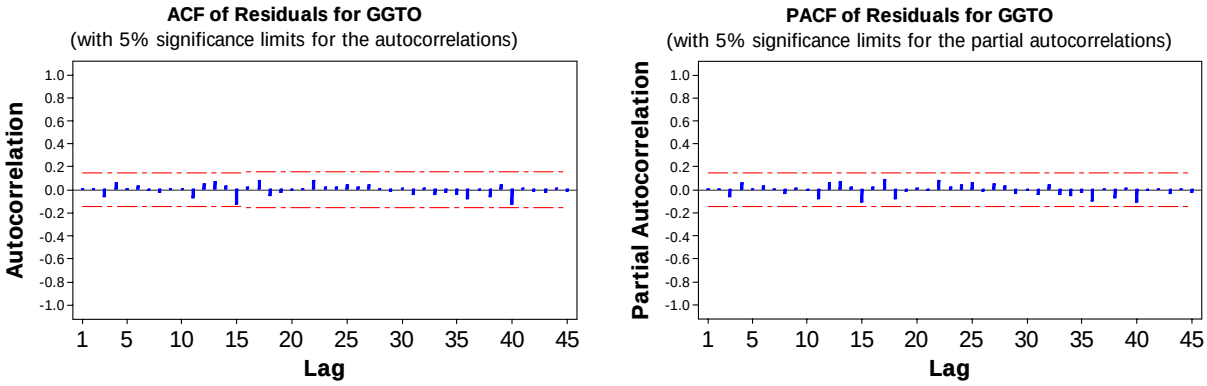

Figure B-22. ACF (left) and PACF (right) of residuals for ARIMA(2,1,2)

B.2.3 UTC(USNO) – GPS Time

Order of MA model	*RMS of model residuals [ns]*	
	Order of AR model	
	2	*3*
0	0.549	0.488
1	0.442	0.443
2	0.443	n/a

Table B-3 Modeling error for ARIMA(N,0,M) models of USNO data

Order of MA model	*RMS of model residuals [ns]*		
	Order of AR model		
	2	*3*	*4*
0	0.556	0.550	0.524
1	0.562	0.524	0.522
2	0.441	n/a	n/a
3	0.455	n/a	0.498*

Table B-4 Modeling error for ARIMA(N,1,M) models of USNO data

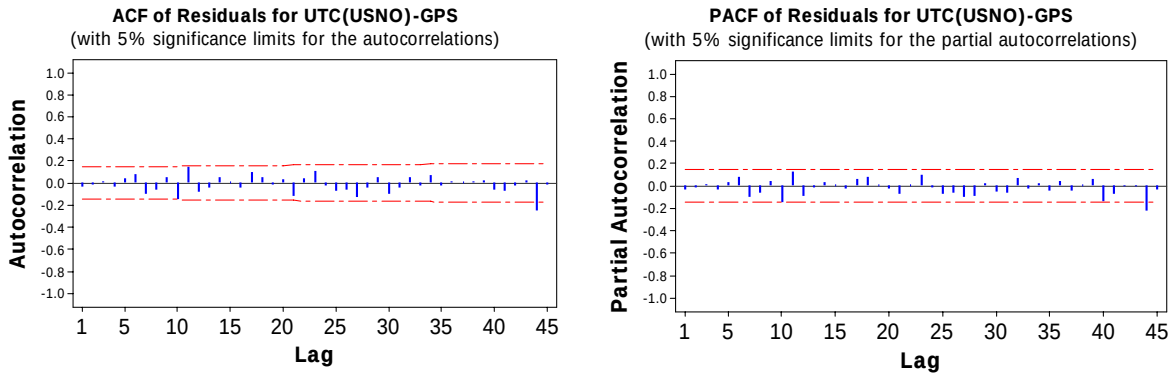

Figure B-23. ACF (left) and PACF (right) of residuals for ARIMA(2,0,1)

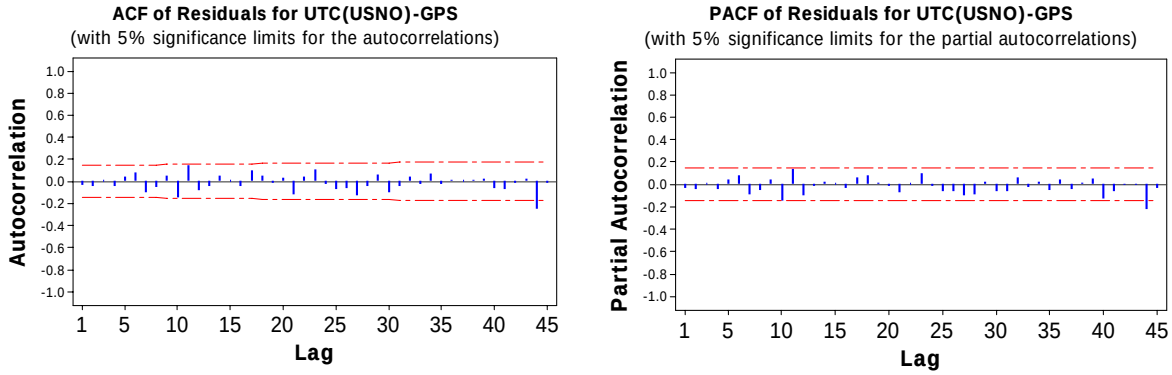

Figure B-24. ACF (left) and PACF (right) of residuals for ARIMA(2,1,2)

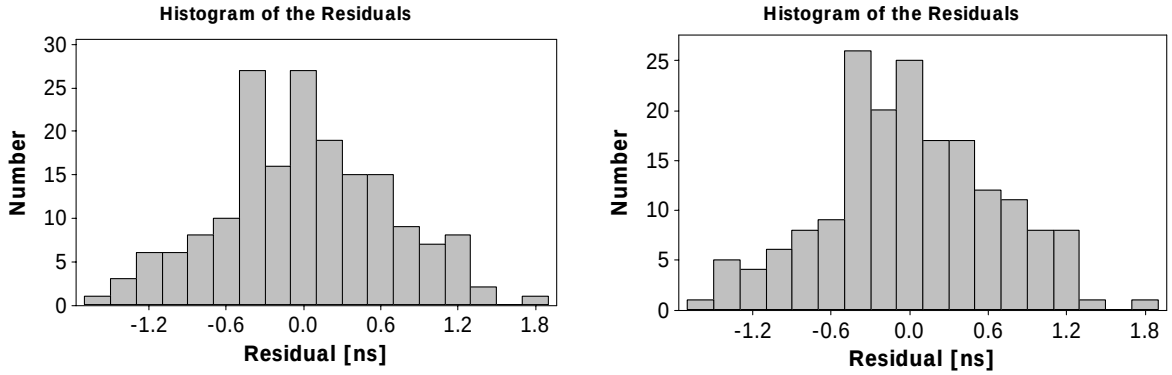

Figure B-25. Histogram of residuals for ARIMA(2,0,1) (left) and ARIMA(2,1,2) (right)

B.2.4 UTC(PTB) – GPS Time

Order of MA model	*RMS of model residuals [ns]*		
	Order of AR model		
	2	***3***	***4***
0	1.991	1.988	1.998
1	1.990	1.999	1.974
2	1.985	1.964	1.951
3	1.997	1.975	1.986

Table B-5 Modeling error for ARIMA(N,0,M) models with PTB data

Order of MA model	*RMS of model residuals [ns]*		
	Order of AR model		
	1	*2*	*3*
0	2.084	2.053	2.052
1	2.066	n/a	2.028
2	n/a	1.957	2.038
3	1.948	1.977	1.955

Table B-6 Modeling error for ARIMA(N,1,M) models with PTB data

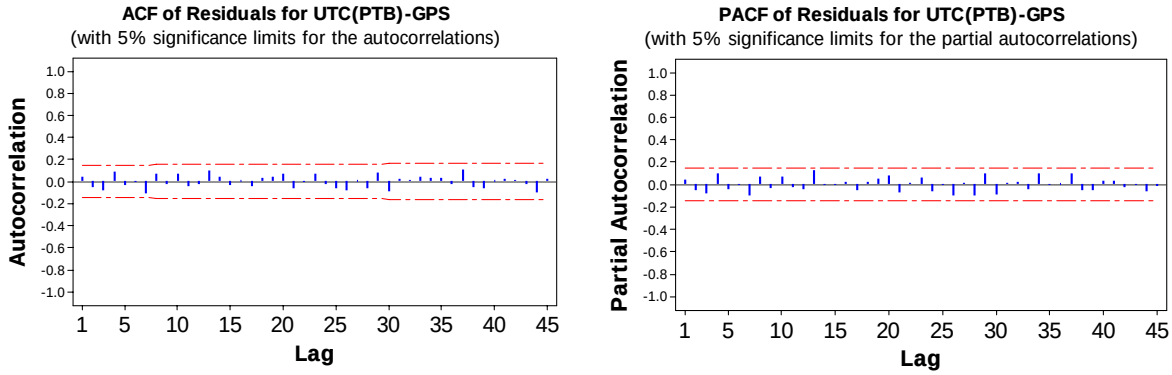

Figure B-26. ACF (left) and PACF (right) of residuals for ARIMA(2,0,0)

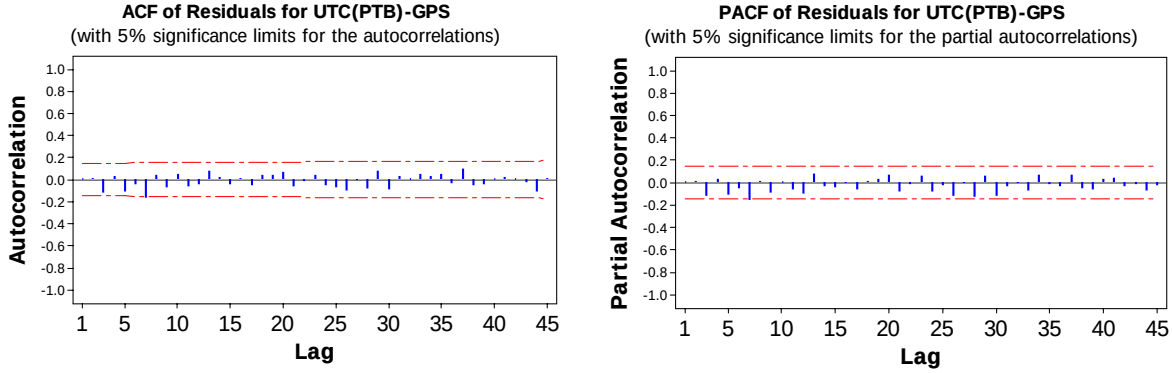

Figure B-27. ACF (left) and PACF (right) of residuals for ARIMA(1,1,1)

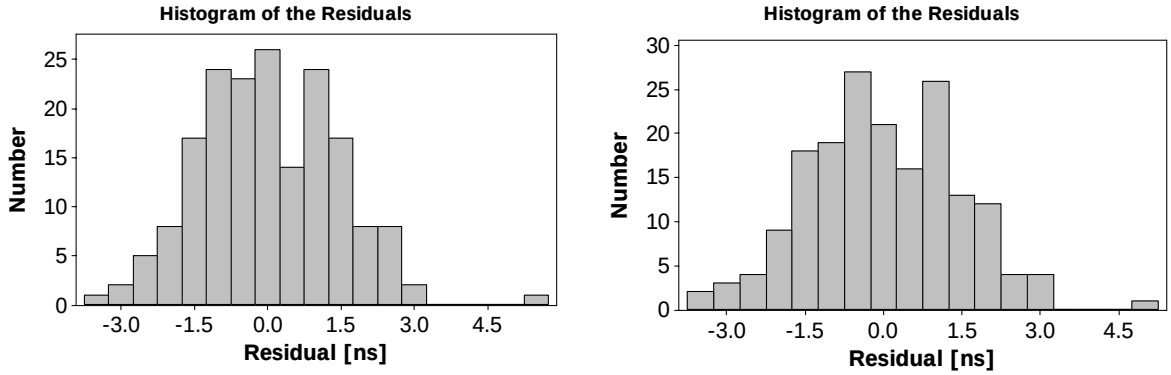

Figure B-28. Histogram of residuals for ARIMA(2,0,0) (left) and ARIMA(1,1,1) (right)

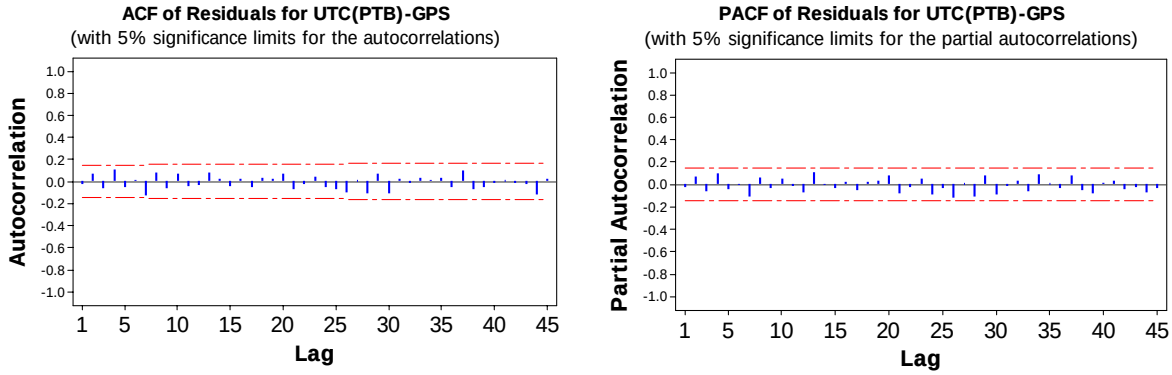

Figure B-29. ACF (left) and PACF (right) of residuals for ARIMA(2,1,2)

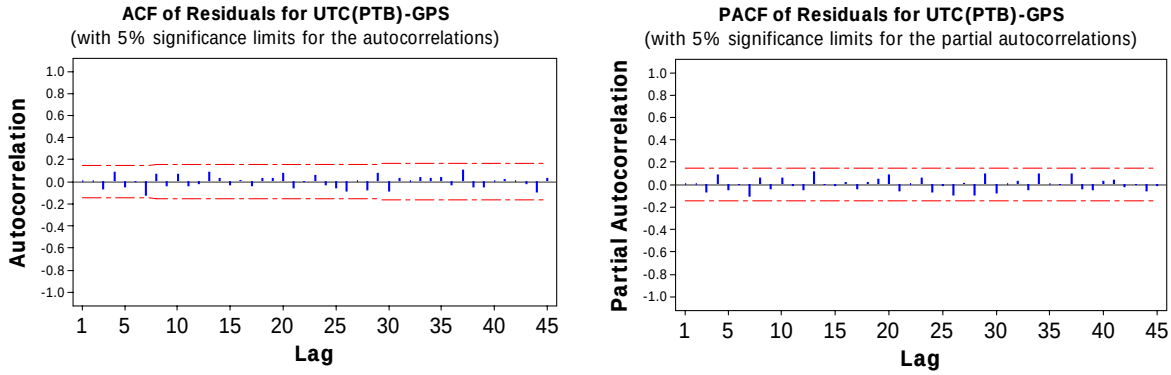

Figure B-30. ACF (left) and PACF (right) of residuals for ARIMA(2,0,1)

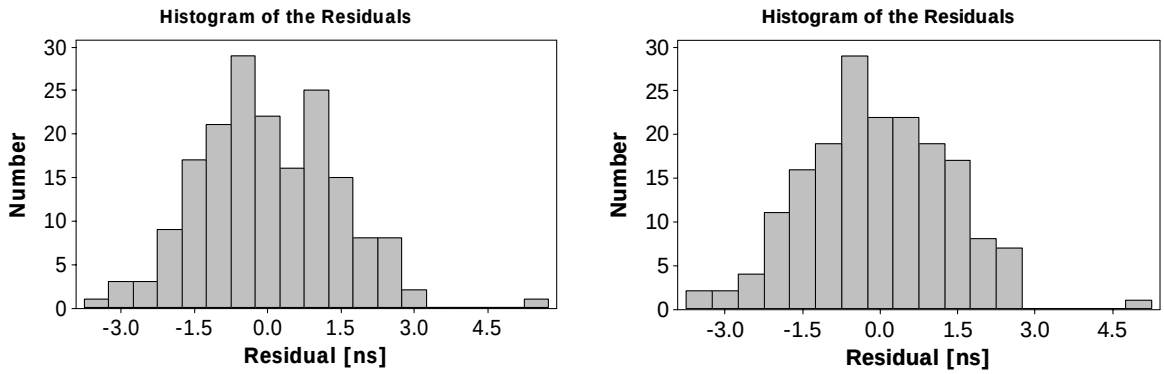

Figure B-31. Histogram of residuals for ARIMA(2,0,1) (left) and ARIMA(2,1,2) (right)

Annex C. Characterization of clock stability

C .1 Clock models: deterministic effects and noises

Relative time deviation x of two clocks running at the same nominal frequency is given by

$$x(t) = \frac{\varphi_1(t) - \varphi_2(t)}{2\pi\nu_0} = \frac{\phi(t)}{2\pi\nu_0} \qquad \text{Eq. C-1}$$

here

ν_0 - nominal frequency,

$\varphi(t)$ - deviation of a particular clock phase from the nominal, and

$\phi(t) = \varphi_1(t) - \varphi_2(t)$ - relative phase deviation.

The instant value of relative frequency deviation (further called just ‚frequency deviation') is defined by

$$y(t) = \frac{dx}{dt} = \frac{1}{2\pi\nu}\frac{d\phi}{dt} \qquad \text{Eq. C-2}$$

As long as time interval between successive measurements τ (also called ‚sample time') has a finite value, the instant value of y cannot be measured directly. In practice, average frequency deviation is used. Average frequency deviation $\bar{y}(t,\tau)$ over time interval $[t_i; t_i + \tau]$ can be computed as follows

$$\bar{y}(t,\tau) = \frac{1}{\tau}\int_{t_i}^{t_i+\tau} y(t)dt = \frac{x(t_i+\tau) - x(t_i)}{\tau} = \frac{\Delta_\tau x(t)}{\tau} \qquad \text{Eq. C-3}$$

Frequency stability measures ADEV, MDEV and TDEV (see Section C .2) can be computed using not absolute but relative time or frequency deviation. In this case, they would characterize the relative stability of two clocks.

Frequency deviation includes not only stochastic but also deterministic part. A liner model is typically used for the deterministic part:

$$y(t) = y_0 + y_1 \cdot t + y_n(t) \qquad \text{Eq. C-4}$$

here y_0 is the initial value of frequency offset, y_1 linear frequency drift, and $y_n(t)$ noise term.

More elaborated models were also investigated (e.g. [Barnes71], [Kartashoff78]), for example, frequency fluctuations due to temperature variations were be considered.

The linear model is still in common use, because measurements over long periods of time are required to estimate parameters of more sophisticated models; estimates of these parameters may be biased due to the nature of clock noise.

In fact, in the presence of flicker noise an estimate of the term y_0 also does not converge to its true value ($\sigma_{y_0} \to \infty$ when $t \to \infty$). Thus, a linear frequency model is a compromise between the accuracy of modeling and required duration of experiment.

Linear model for frequency deviation leads quadratic model for time deviation:

$$x(t) = x_0 + y_0 t + \frac{y_1}{2}t^2 + x_n(t) \qquad \text{Eq. C-5}$$

Usually, x_0, y_0, y_1 are designated as a_0, a_1, a_2 respectively.

C .2 Time domain statistics

C.2.1 Allan variance

$$\sigma_y^2(\tau) = \lim_{N\to\infty} \frac{1}{2(N-1)} \sum_{i=1}^{N-1} (\bar{y}_{i+1} - \bar{y}_i)^2 \qquad \text{Eq. C-6}$$

where

$\tau = k\tau_0$ - averaging period and k is an integer,

τ_0 - sample time,

N - number of averaging periods,

$\bar{y}$ - average frequency over the period τ .

In terms of time measurements

$$\sigma_y^2(\tau) = \lim_{N\to\infty} \frac{1}{2(N-1)\tau^2} \sum_{i=1}^{N-2} \left(\Delta^2 x\right)^2 \qquad \text{Eq. C-7}$$

where x is a time measurement.

Both formulas imply infinite data sets. An approximation of AVAR is used in practice:

$$\sigma_y^2(\tau) \cong \frac{1}{2(N-2)\tau^2} \sum_{i=1}^{N-2} (x_{i+2} - 2x_{i+1} + x_i)^2 \qquad \text{Eq. C-8}$$

Usually, an overlapped version of AVAR is used because it treats available data sets in a more efficient way and improves the confidence of estimates.

AVAR is not able to distinguish white phase noise and flicker phase noise.

C.2.2 Modified Allan variance (MVAR)

MVAR is able to distinguish between white phase noise and flicker phase noise.

$$\sigma_y^2(\tau) = \frac{1}{2\tau^2} \left\langle \left(\Delta^2 \bar{x}\right)^2 \right\rangle \qquad \text{Eq. C-9}$$

where $\bar{x}$ is the phase average.

For practical computation the following approximation of MDEV may be used:

$$\operatorname{mod}\sigma_y^2(\tau) \cong \frac{1}{2(N-3n+1)\tau^2 n^2} \sum_{j=1}^{N-3n+1} \left[\sum_{i=j}^{n+j-1} (x_{i+2n} - 2x_{i+n} + x_i) \right]^2 \qquad \text{Eq. C-10}$$

C.2.3 Time Variance (TVAR)

TVAR is equal to standard variance of time deviations for white phase noise:

$$\sigma_x^2(\tau) = \frac{1}{6} \left\langle \left(\Delta^2 \bar{x}\right)^2 \right\rangle = \frac{\tau^2}{3} \operatorname{mod}\sigma^2(\tau) \qquad \text{Eq. C-11}$$

The following formula is used for the computation of TVAR:

$$\mathrm{mod}\,\sigma_y^2(\tau) \cong \frac{1}{6(N-3n+1)n^2}\sum_{i=0}^{N-3n}\left[\sum_{i=0}^{n-1}\left(x_{i+2n+j} - 2x_{i+n+j} + x_{i+j}\right)\right]^2 \qquad \text{Eq. C-12}$$

C.2.4 Systematic effects and Allan Variance

Systematic effects in clock data affect Allan variance in various ways. [Greenhall88] presents an overview of the effect of deterministic functions at Allan Variance:

- constant time and frequency offsets (terms x_0, y_0) do not effect Allan variance;
- linear frequency drift y_1: $\sigma_y = \frac{|y_1|\tau}{\sqrt{2}}$;
- higher powers of t (n > 2): the Allan Variance does not converge (the limit in Eq. C-6 is $+\infty$). That means that estimated AVAR in this case is not reliable;
- a single step in time data: $\sigma_y = \frac{x_s}{\sqrt{\tau(T-\tau)}}$, where x_s is the magnitude of the step;
- periodic disturbances (e.g. due to daily temperature variations) $\sigma_y = \frac{2}{\tau}x_p \sin^2(\pi\nu\tau)\cdot\begin{cases}\sqrt{2}|\cos\theta|, & if\ 2\pi\nu\tau = \mathrm{int}\\ 1, & otherwise\end{cases}$, here x_p is the amplitude of the disturbance, ν frequency of the disturbance, and θ phase of the disturbance.

In general, it is advisable to remove systematic effects from clock data before computation of Allan Variance. First, time and frequency steps should be detected and estimated by a suitable filter. They should be then repaired by implementing time/frequency corrections to the raw clock data. Second, frequency drift (term y_1 in Eq. C-5) should be estimated (e.g. by a least-squares fit to clock data or using the method of finite differences [Barnes66]) and removed from the raw data.

Remaining systematic effects will affect Allan variance, but it may be thought of as a way to detect these effects.

C .3 Frequency domain statistics

Spectral density is a frequency domain characteristic of stochastic signals. The classical model of spectral density of clock output includes five terms:

$$S_y(f) = h_{-2}f^{-2} + h_{-1}f^{-1} + h_0 f^0 + h_1 f^1 + h_2 f^2 = \sum_{\alpha=-2}^{2} h_\alpha f^\alpha \qquad \text{Eq. C-13}$$

Here $S_y(f)$ is spectral density of frequency fluctuations. The spectral density of phase fluctuations is defined by

$$S_x(f) = \frac{1}{4\pi^2}\sum_{\alpha=-2}^{2} h_\alpha f^\alpha \qquad \text{Eq. C-14}$$

Each term of the model refers to a certain type of noise:

h_2: white phase noise;

h_1: flicker phase noise;

h_0 : white frequency noise or phase random walk;

h_{-1} : flicker frequency noise;

h_{-2} : frequency random walk.

The relationship between spectral density and Allan variance is given in the Table C-1 (e.g. [Kartashoff78]).

$S_y(f)$	$\sigma_y^2(\tau)$	***Type of noise***
$h_2 f^2$	$h_2 \frac{3 f_h}{(2\pi\tau)^2}$	white phase noise
$h_1 f^1$	$h_1 \frac{(6 + 3\ln(2 f_h \pi\tau) - \ln 2)}{(2\pi\tau)^2}$	flicker phase noise
$h_0 f^0$	$h_0 \frac{1}{2\tau}$	white frequency noise or phase random walk
$h_{-1} f^{-1}$	$h_{-1} \cdot 2\ln 2$	flicker frequency noise
$h_{-2} f^{-2}$	$h_{-2} \frac{4\pi^2 \tau}{6}$	frequency random walk

Table C-1 Relationship between spectral density and Allan Variance

Annex D. Atomic clocks: an overview

Atomic clock descriptions provided in Sections D .1, D .2 and D .3 are based on the materials available at the web-site of the U.S. National Institute of Standards (NIST) www.nist.gov/timefreq.

D .1 Rubidium frequency standards

Rubidium standards are the cheapest, the smallest, the most long-living and the most popular of atomic clocks.

Rb87 lamp brings Rb85 buffer gas into a particular energy state. Magnetic field (which is driven by the frequency of a quartz oscillator) applied inside a shielded cavity triggers transition into energy state and increases absorption of the optical beam in the Rb87 buffer gas inside the cavity. The photo detector registers the amount of the passing light and the frequency of the quartz is tuned to maximize the absorption. The maximum is achieved at the Rb87 resonance frequency which is equal to 6,834,682,608 Hz.

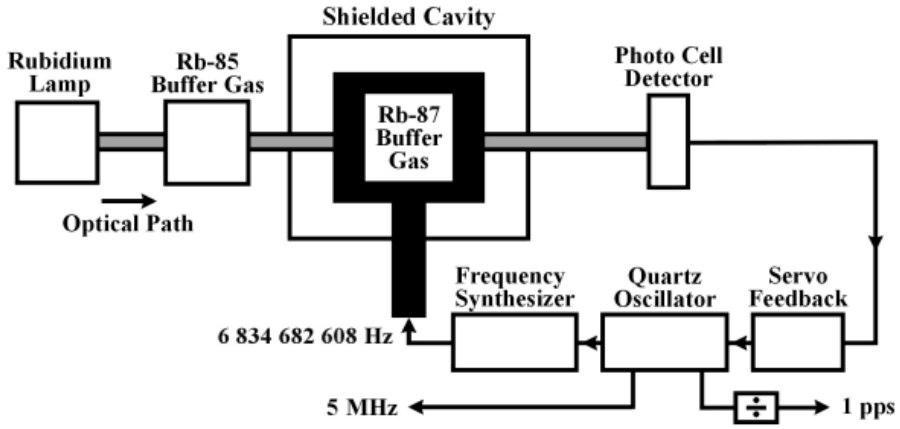

Figure D-1. Commercial Rubidium standard (courtesy NIST)

The typical performance of a commercial Rb standard is presented in Table D-1.

Tau	*ADEV of Temex LCR-900*	*ADEV of Temex LPRO, Options A and S*
1 s	3E-11	1E-11
10 s	1E-11	3E-12
100 s	3E-12	1E-12
1 day	2E-11	2E-12
1 month	5E-11	3E-11

Table D-1 Performance of a high-quality commercial Rubidium standard

The major drawback of Rubidium standards is their high frequency drift and high sensitivity to environmental variation (temperature, humidity etc.).

D .2 Cesium clocks

D.2.1 Commercial Cesium clocks

Commercial Cesium standards rely on the Cesium beam technology (see Figure D-2). Inside the standard oscillator, Cesium is vaporized (through heating in the so called Cesium oven). The vapor passes the state selection magnets which allow only atoms in a particular state to pass it. The magnets also form the atoms into a beam which passes through the vacuum cavity to another pair of magnets. In the cavity the atoms are affected by an additional magnetic field which frequency is driven by a quartz oscillator. In case this frequency matches the resonance frequency of Cesium, the atoms change their energy state. Only these atoms can pass the state detection magnets at the other end of the tube and get to the detector. The frequency of the quartz oscillator is tuned so that the detector output is maximized (i.e. the quartz frequency closely matches the resonance frequency of Cesium).

Performance specification for CAE sums clocks typically used in timing laboratories (Symmetricom 5071A) is presented in Table D-2. Cesium standards exhibit no measurable frequency drift.

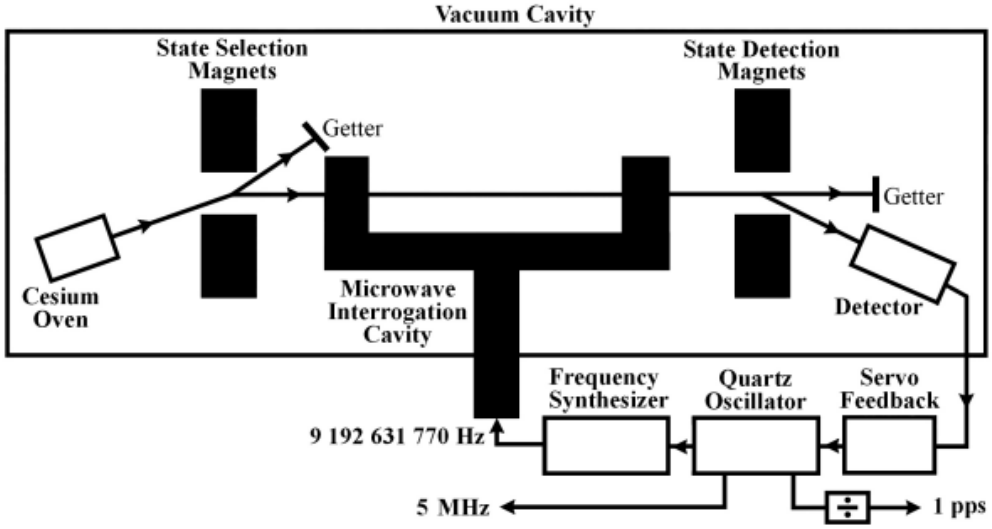

Figure D-2. Commercial Cesium clock (courtesy NIST)

Tau	*ADEV*
1 s	5E-12
10 s	3.5E-12
100 s	8.5E-13
1000 s	2.7E-13
10000 s	8.5E-14
100000 s	2.7E-14
5 days	1E-14
Flicker floor	1E-14

Table D-2 Performance of commercial Cesium standards

D.2.2 Cesium fountain

Cesium fountains are available only at a few laboratories in the world (PTB, USNO, NIST etc.). They serve as the primary frequency standards which represent the SI second. Cesium fountains are used for periodical calibration of TAI frequency.

As in the commercial Cesium clock, in a fountain Cesium is first vaporized. Six infrared lasers are directed at the vapor (see Figure D-3). Their radiation pushes Cesium atoms into a ball and slows then down. As a result, the atoms are cooled down to a few millionths of Kelvin that corresponds to the velocity of a few cm per second. The ball is pushed upward by an impulse of another laser. Then all masers are switched off. The ball flies up about 1 m and then the atoms fall down. The up and down trip takes about 1 second. On the way, magnetic field is applied to the atoms which change their energy.

At the end of the trip, the atoms are “flashed” by another laser. Those of them which have changed their energy states emit photons which are registered by a special detector. The magnetic field in the cavity is tuned to maximize the signal at the detector. The maximum signal corresponds to the magnetic field frequency which is equal to the resonance frequency of Cesium.

Typically, the frequency accuracy of Cesium fountains is better than 1E-15.

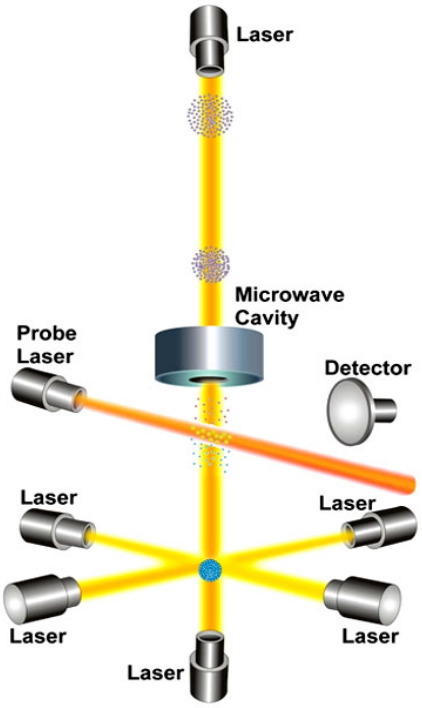

Figure D-3. Cesium fountain (courtesy NIST)

D .3 Hydrogen masers

D.3.1 Active hydrogen masers

Active hydrogen maser is the most expensive of the commercially available atomic clocks. It is also the most stable commercial clock in the short-term. In the long-term, its stability is deteriorated by the frequency drift.

In an active H-maser, gas of hydrogen atoms passes state selection magnets which let only atoms which are at the upper energy level to pass into a tuned vacuum bulb (see Figure D-4). The bulb is placed into a shielded cavity. In the bulb the atoms go into the lower energy state and emit microwaves. The high quality factor bulb cavity confines the microwaves and

re-injects them repeatedly into beam of coming hydrogen atoms. It stimulates further transition between the energy levels and the stimulated emission amplifies the microwaves on each pass through the beam. The emitted frequency is the resonant frequency of the hydrogen 1,420,405,751 Hz. The microwave radiation is captured at the detector in the bulb, and an external quartz oscillator is tuned to the resonance frequency of hydrogen.

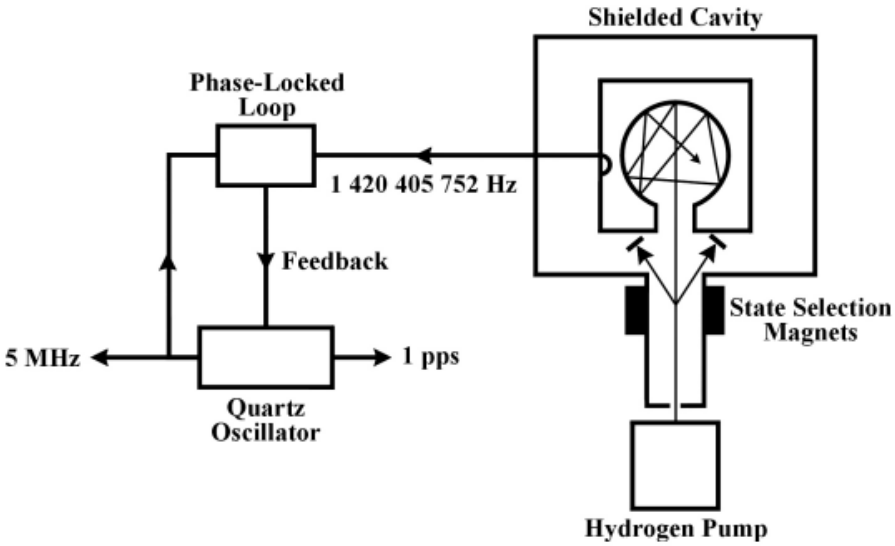

Figure D-4. Active H-maser (courtesy NIST)

The typical performance of an active H-maser is presented in Table D-3.

Tau	*ADEV of Kvarz CH-75A*	*ADEV of T4Science iMaser*
1 s	2E-13	1.5E-13
10 s	3E-14	2E-14
100 s	5E-15	5E-15
1 hour	2E-15	2E-15
1 day	5E-15	-

Table D-3 Performance of active H-masers

The frequency drift varies from 1E-14 (without autotuning) to 5E-16 (with autotuning) per day.

D.3.2 Passive hydrogen masers

Passive hydrogen maser is less expensive, but also less stable than the active one.

As in Cesium standards, magnetic field is used to “state-select” atoms in the hydrogen gas (see Figure D-5). The atoms with the upper energy level further pass into the cavity. The cavity is coated with Teflon to minimize atomic perturbations due to collisions with the cavity walls.

A microwave signal modulated with the resonance frequency of hydrogen is passed through the cavity to induce atomic transitions. As a result, the atoms emit microwaves at the resonance frequency. In active masers, the resonance frequency is detected and utilized directly. In passive masers, the applied modulated microwave signal interacts with the atomic resonance line’s frequency. As a result of phase shift of the carrier frequency and the impact of the AM signal, the modulation frequency appears. This frequency is proportional to the offset of the carrier frequency from the resonance frequency. The AM is further detected and used to tune a quartz oscillator so that the carrier frequency matches the resonance frequency.

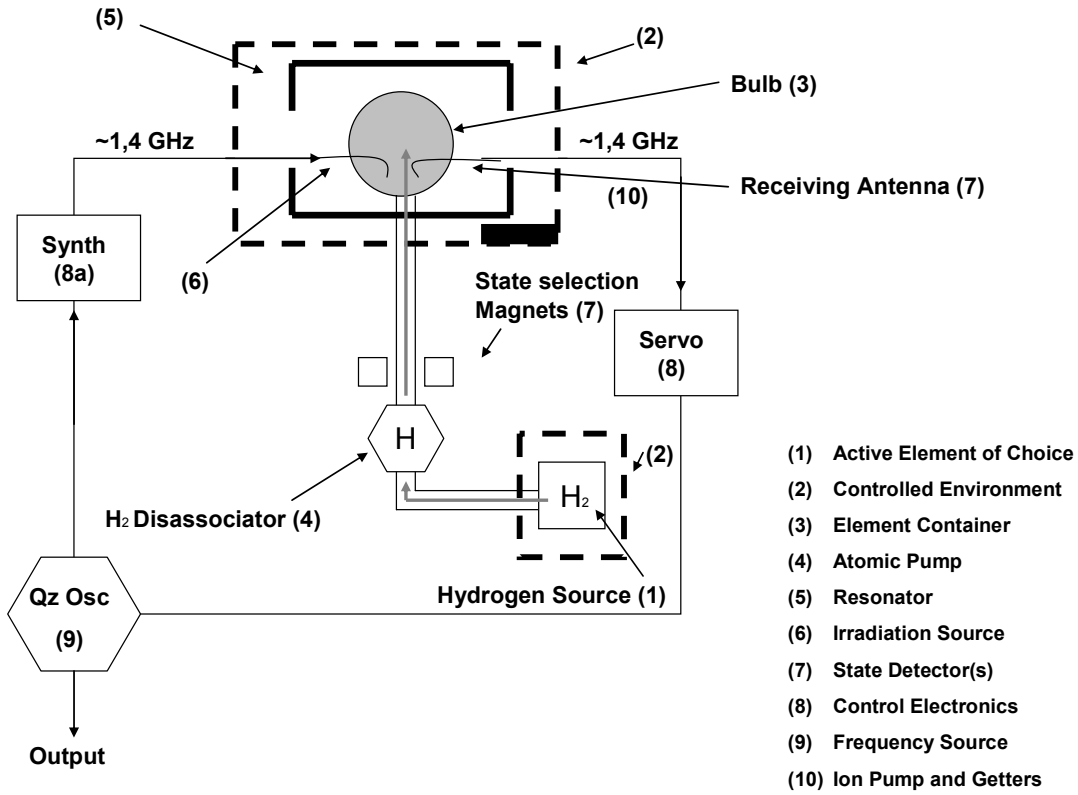

Figure D-5. Passive H-maser

Performance specification for a commercial hydrogen maser is presented in Table D-4.

Tau	*ADEV of Kvarz CH-76A*
1 s	1.5E-12
10 s	5E-13
100 s	2E-13
1000 s	5E-14
1 hour	2E-14
1 day	1E-14

Table D-4 Performance of passive H-masers

The frequency drift of passive H-masers is typically about 3E-15 per day.

D .4 Galileo satellite clocks

D.4.1 RAFS

The frequency stability of Galileo RAFS (second generation) measured during factory tests is presented in Figure D-6. Other important RAFS specifications are summarized in Table D-5 (note that the flicker floor of 3E-14 is the specification of the manufacture, not the Galileo baseline). [Droz03] reports that ESA has also initiated a dedicated program to reduce the flicker floor of RAFS to 2E-14 from originally required 5E-14. The original goal for RAFS time error (TDEV) over 1 day was set to 10 ns [Lucas04].

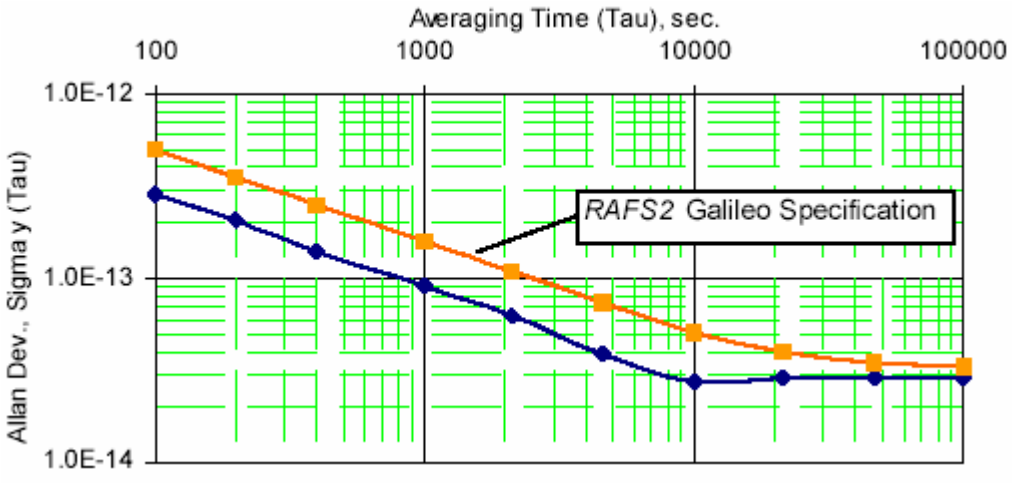

Figure D-6. Frequency stability of RAFS for Galileo [Droz03]

Parameter	*Value*
Frequency accuracy	5E-10
Frequency drift, per year	≤ 3E-10
Allan deviation, 1 s ≤ τ ≤ 10000 s	$\leq 5 \cdot 10^{-12} \times \tau^{-1/2}$
Flicker floor	3E-14
Phase noise	
/Hz @ 1 Hz	-90
/Hz @ 10 Hz	-120
/Hz @ 100 Hz	-130
/Hz @ 1 kHz	-140
/Hz @ 10 kHz	-145
/Hz @ 100 kHz	-145
Temperature sensitivity	≤ 5E-14/°C
Operating temperature range	-5 to +10°C
Qualification temperature range	-15 to +20°C
Volume	2 liters
Mass	3.4 kg
Reliability target over design lifetime	0.9
Design lifetime	12

Table D-5. Galileo RAFS specification [TEMEX03]

D.4.2 Passive H-maser

[Mattoni02] reports test results of prototype passive H-masers for Galileo satellites (SPHM). The measured ADEV of the maser is shown in Figure D-7. The measured frequency drift is reported to be 1.9E-14 per day. The objective for SPHM time error (TDEV) was set to 1 ns over 1 day [Lucas04]. The maser includes magnetic shielding and temperature compensation of its platform. Other important maser parameters are summarized in Table D-6.

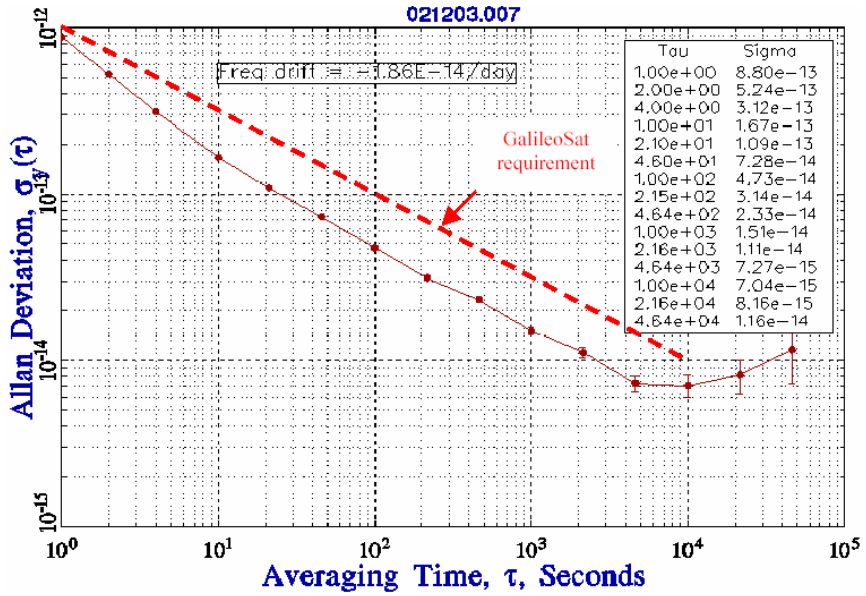

Figure D-7. Frequency stability of passive H-maser for Galileo [Mattoni02]

Parameter	*Value*
Output frequency	10.002857407 MHz
Frequency accuracy	better than 1E-10
Output level	+7 dBm (two outputs)
Frequency drift, per year	≤ 3e-12
Allan deviation, 1 s ≤ τ ≤ 10000 s	$\leq 1 \cdot 10^{-12} \times \tau^{-1/2}$
Temperature sensitivity	≤ 3E-15/°C
Magnetic sensitivity	≤ 2E-14/Gauss
Main Bus voltage sensitivity	≤ 3E-15/V
Power consumption	≤ 5W
Total mass	15 kg (goal)
Qualification temperature range	-15 to +20°C
Orbit (MEO) life	12 years

Table D-6. Galileo passive H-maser specification [Mattoni02]

[Dimarq04] reports additional test results for SPHM (see Table D-7).

Parameter	*Measured value*	*Specification*
Short term stability (@1s)	8.8E-13	≤ 1E-12
Flicker floor	6.8E-15	≤ 1E-14
Random walk	6.1E-15	≤ 1E-14
Drift	1.86E-14/day	≤ 1E-14/day
Time error over 14 hours	1.14E-14	≤ 1.33E-14

Table D-7. Galileo SPHM test results [Dimarq04]

Annex E. Nominal constellations

E .1 Galileo

ID	*Semi-major axis [km]*	*Eccentricity*	*Inclination [°]*	*RAAN [°]*	*Argument of perigee [°]*	*Mean anomaly [°]*
1	29993.707	0	56	0	0	0
2	29993.707	0	56	0	0	40
3	29993.707	0	56	0	0	80
4	29993.707	0	56	0	0	120
5	29993.707	0	56	0	0	160
6	29993.707	0	56	0	0	200
7	29993.707	0	56	0	0	240
8	29993.707	0	56	0	0	280
9	29993.707	0	56	0	0	320
10	29993.707	0	56	120	0	13.33
11	29993.707	0	56	120	0	53.33
12	29993.707	0	56	120	0	93.33
13	29993.707	0	56	120	0	133.33
14	29993.707	0	56	120	0	173.33
15	29993.707	0	56	120	0	213.33
16	29993.707	0	56	120	0	253.33
17	29993.707	0	56	120	0	293.33
18	29993.707	0	56	120	0	333.33
19	29993.707	0	56	240	0	26.66
20	29993.707	0	56	240	0	66.66
21	29993.707	0	56	240	0	106.66
22	29993.707	0	56	240	0	146.66
23	29993.707	0	56	240	0	186.66
24	29993.707	0	56	240	0	226.66
25	29993.707	0	56	240	0	266.66
26	29993.707	0	56	240	0	306.66
27	29993.707	0	56	240	0	346.66
28	29993.707	0	56	0	0	20
29	29993.707	0	56	120	0	20
30	29993.707	0	56	240	0	20

Table E-1 Nominal constellation of Galileo

E .2 GPS

ID	Slot	Semi-major axis [km]	Eccent-ricity	Inclination [°]	RAAN [°]	Argument of perigee [°]	Mean anomaly [°]	Arg. of Latitude [°]	Longitude of acsc node [°]
1	A1	26559.700	0 – 0.02	55 ± 3	272.847	± 180	0	268.126	± 2
2	A2	26559.700	0 – 0.02	55 ± 3	272.847	± 180	40	161.786	± 2
3	A3	26559.700	0 – 0.02	55 ± 3	272.847	± 180	80	11.786	± 2
4	A4	26559.700	0 – 0.02	55 ± 3	272.847	± 180	120	41.806	± 2
5	B1	26559.700	0 – 0.02	55 ± 3	332.847	± 180	160	80.956	± 2
6	B2	26559.700	0 – 0.02	55 ± 3	332.847	± 180	200	173.336	± 2
7	B3	26559.700	0 – 0.02	55 ± 3	332.847	± 180	240	309.976	± 2
8	B4	26559.700	0 – 0.02	55 ± 3	332.847	± 180	280	204.376	± 2
9	C1	26559.700	0 – 0.02	55 ± 3	32.847	± 180	320	111.876	± 2
10	C2	26559.700	0 – 0.02	55 ± 3	32.847	± 180	13.33	11.796	± 2
11	C3	26559.700	0 – 0.02	55 ± 3	32.847	± 180	53.33	339.666	± 2
12	C4	26559.700	0 – 0.02	55 ± 3	32.847	± 180	93.33	241.556	± 2
13	D1	26559.700	0 – 0.02	55 ± 3	92.847	± 180	133.33	135.226	± 2
14	D2	26559.700	0 – 0.02	55 ± 3	92.847	± 180	173.33	265.446	± 2
15	D3	26559.700	0 – 0.02	55 ± 3	92.847	± 180	213.33	35.156	± 2
16	D4	26559.700	0 – 0.02	55 ± 3	92.847	± 180	253.33	167.356	± 2
17	E1	26559.700	0 – 0.02	55 ± 3	152.847	± 180	293.33	197.046	± 2
18	E2	26559.700	0 – 0.02	55 ± 3	152.847	± 180	333.33	302.596	± 2
19	E3	26559.700	0 – 0.02	55 ± 3	152.847	± 180	26.66	66.066	± 2
20	E4	26559.700	0 – 0.02	55 ± 3	152.847	± 180	66.66	333.686	± 2
21	F1	26559.700	0 – 0.02	55 ± 3	212.847	± 180	106.66	238.886	± 2
22	F2	26559.700	0 – 0.02	55 ± 3	212.847	± 180	146.66	345.226	± 2
23	F3	26559.700	0 – 0.02	55 ± 3	212.847	± 180	186.66	105.206	± 2
24	F4	26559.700	0 – 0.02	55 ± 3	212.847	± 180	226.66	135.346	± 2

Table E-2 Nominal constellation of GPS

Annex F. Ensemble time stability

F .1 Weighted average algorithm, satellite clocks with drift

The figures below present simulation results for ensemble time stability with respect to scenarios and failure mode defined in Section 5.3.2.1. The red line in the figures corresponds to the relevant stability requirements. The results were obtained with the weighted average algorithm (see Section 4.1.1) the assuming the frequency drift in satellite clocks is not corrected.

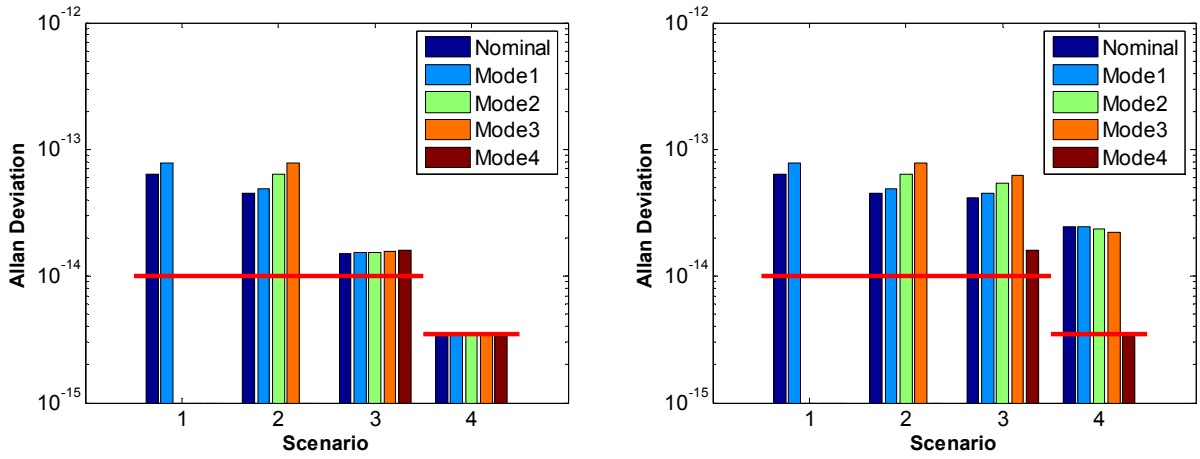

Figure F-1. Ensemble time stability at 100 min (left – optimization time 2 hours, right – 10 days)

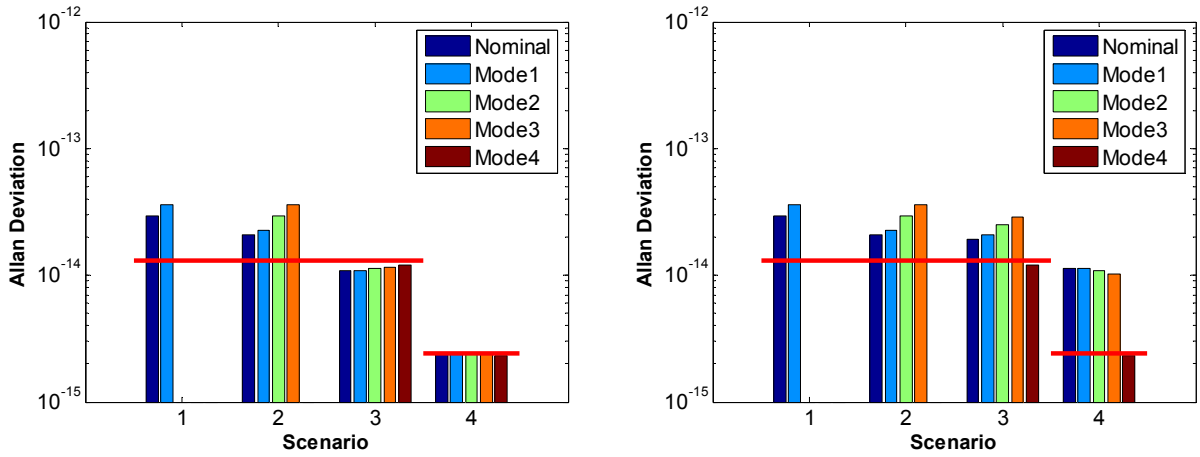

Figure F-2. Ensemble time stability at 8 hours (left – optimization time 2 hours, right – 10 days)

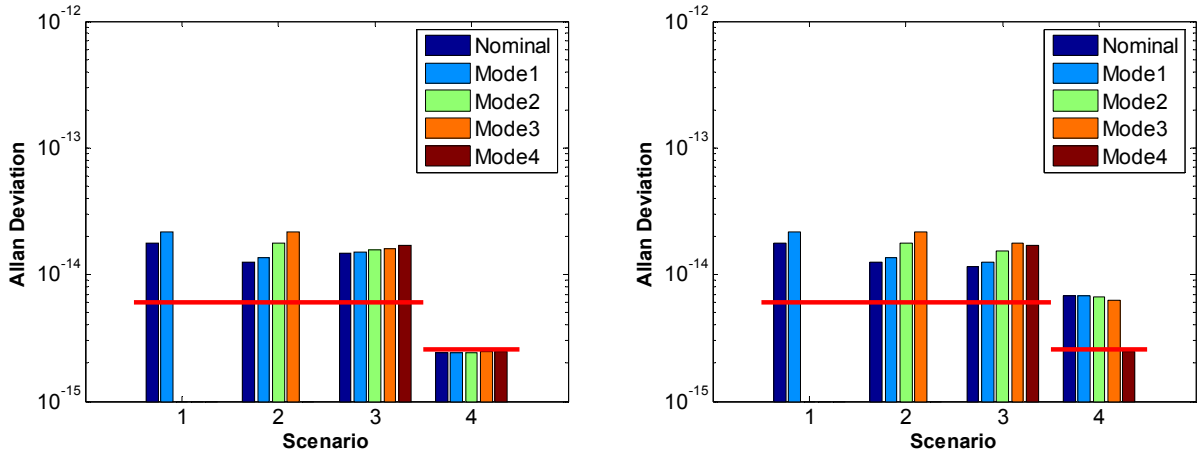

Figure F-3. Ensemble time stability at 24 hours (left – optimization time 2 hours, right – 10 days)

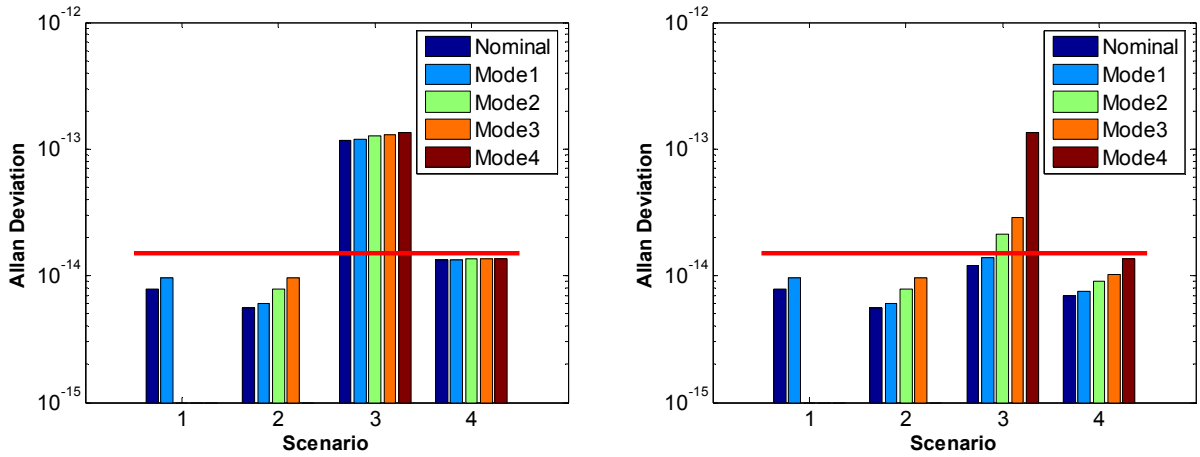

Figure F-4. Ensemble time stability at 10 days (left – optimization time 2 hours, right – 10 days)

F .2 Weighted average algorithm, satellite clocks without drift

The figures below present simulation results for ensemble time stability with respect to scenarios and failure mode defined in Section 5.3.2.1. The red line in the figures corresponds to the relevant stability requirements. The results were obtained with the weighted average algorithm (see Section 4.1.1) the assuming the frequency drift in satellite clocks is corrected.

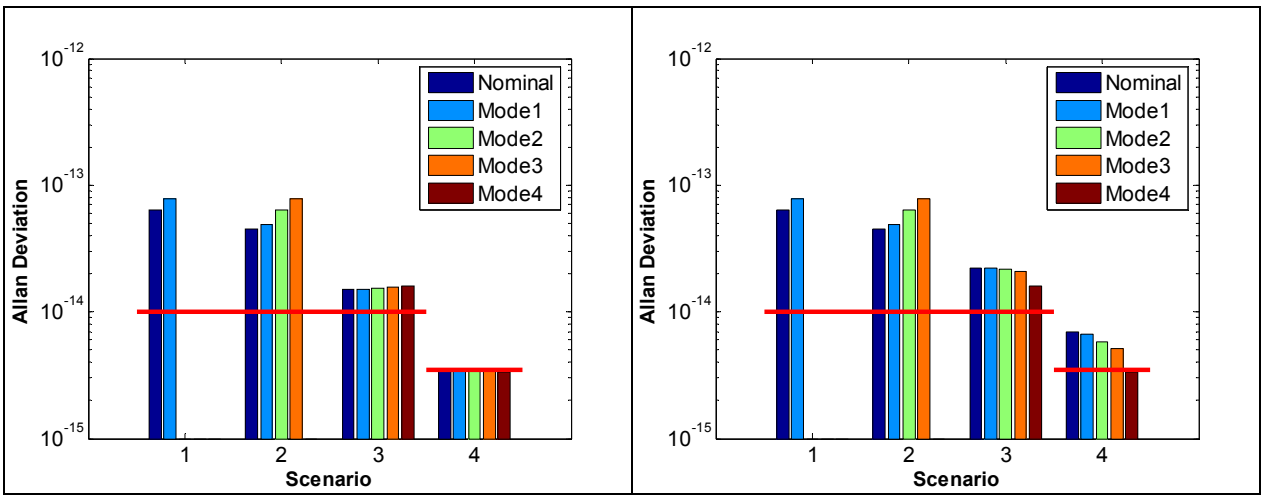

Figure F-5. Ensemble time stability at 100 min (left – optimization time 2 hours, right – 10 days)

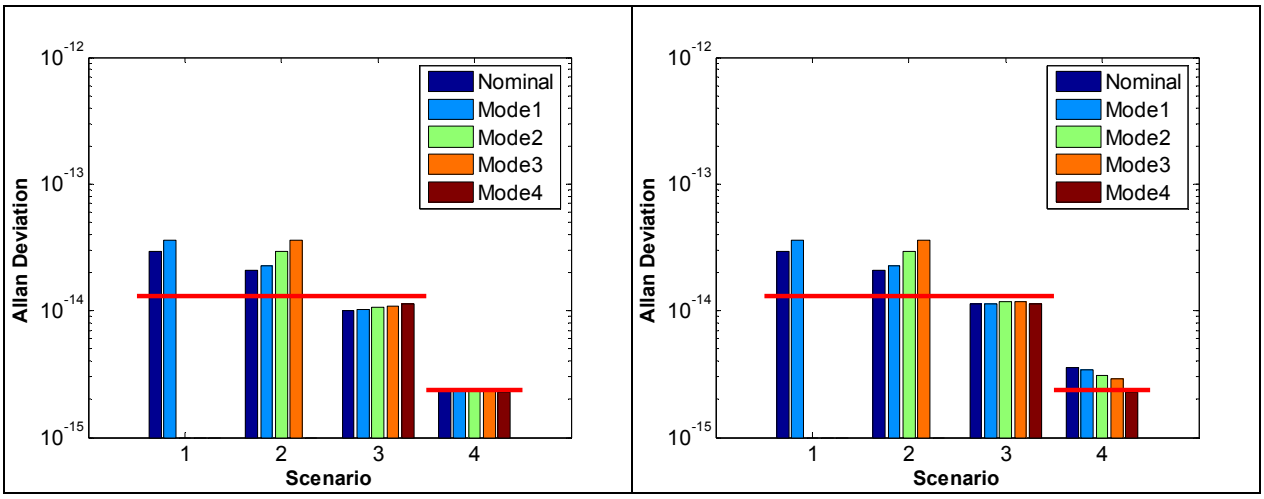

Figure F-6. Ensemble time stability at 8 hours (left – optimization time 2 hours, right – 10 days)

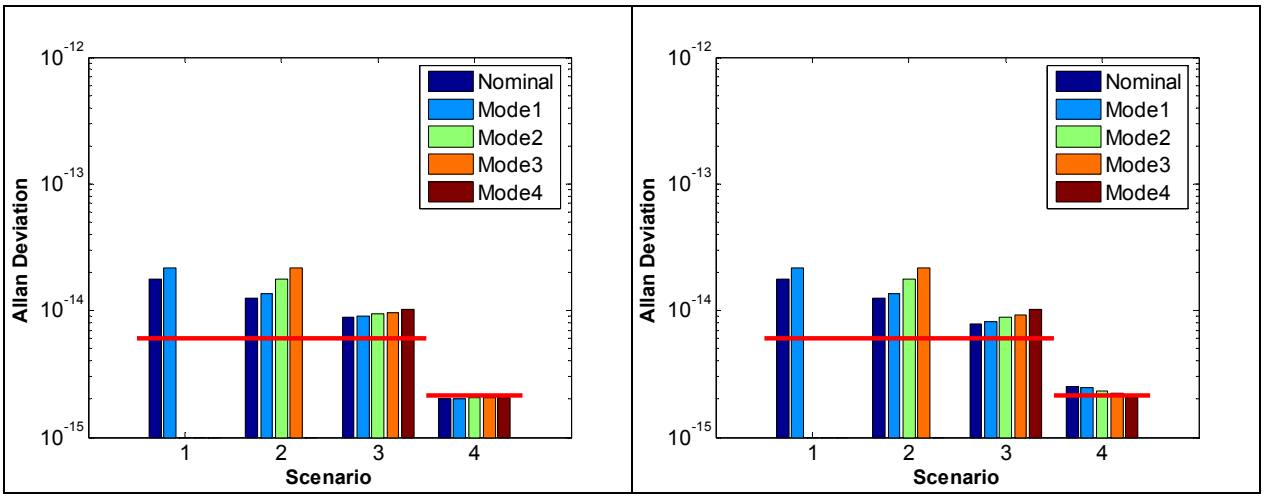

Figure F-7. Ensemble time stability at 24 hours (left – optimization time 2 hours, right – 10 days)

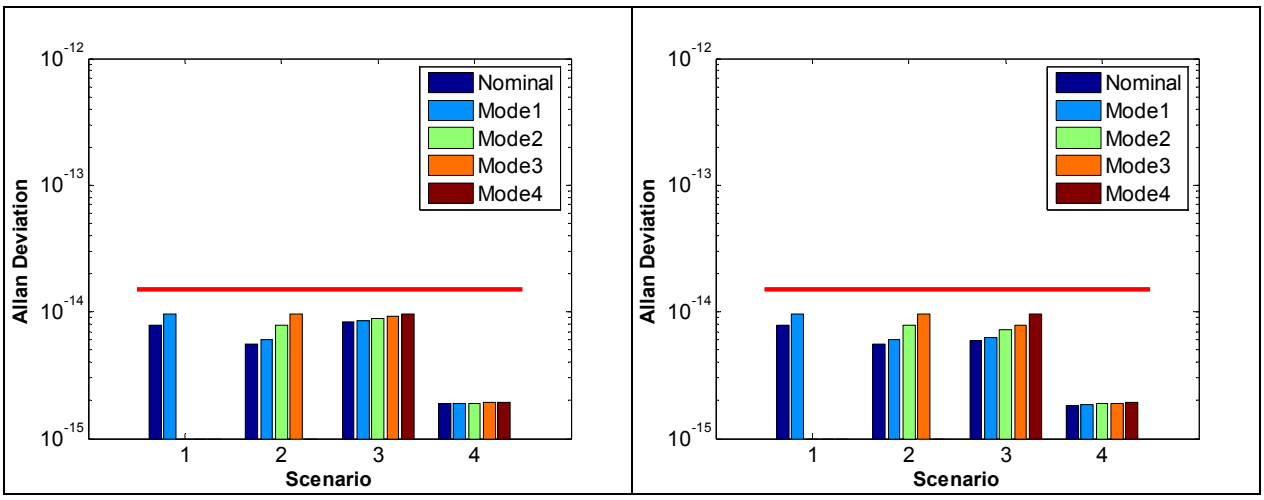

Figure F-8. Ensemble time stability at 10 days (left – optimization time 2 hours, right – 10 days)